Impact of Afferent Inputs on Purkinje Cell Spiking Patterns and Motor Coordination

De impact van afferente input op Purkinje cel vuurpatronen en motor coördinatie

Proefschrift

ter verkrijging van de graad van doctor aan de
Erasmus Universiteit Rotterdam
op gezag van de rector magnificus
Prof.dr. H.G. Schmidt
en volgens besluit van het College voor Promoties

De openbare verdediging zal plaatsvinden op
woensdag 30 maart 2011 om 12.30 uur

door

Aleksandra Maria Badura
Geboren te Piekary Slaskie, Polen

ERASMUS UNIVERSITEIT ROTTERDAM

Promotiecommissie

Promotor: Prof.dr. C.I. de Zeeuw

Overige leden: Dr. T.J.H. Ruigrok
Prof.dr. M.A. Frens
Prof.dr. S.A. Kushner

Copromotor: Dr. M. Schonewille

The work presented in this thesis was performed in the Department of Neuroscience at the Erasmus MC in Rotterdam, The Netherlands and was supported by Prinses Beatrix Fonds

Printed by Off Page

For my parents

TABLE OF CONTENTS

Chapter 1 – Introduction 9

1.1 General

1.2 Cerebellar anatomy and function 11

- 1.2.1 Cerebellar cortex
- 1.2.2 Excitatory input to Purkinje cell
- 1.2.3 Inhibitory afferents to Purkinje cell
- 1.2.4 Compensatory eye movements under floccular control

1.3 Electrophysiology of Purkinje cell 19

- 1.3.1 Simple spikes
- 1.3.2 Complex spikes
- 1.3.3 Behavior of Purkinje cell during motor tasks
- 1.3.4 Plasticity at the synapses

1.4 Main hypothesis concerning cerebellar learning 28

1.5 Scope of the Thesis 29

Chapter 2 – Climbing fiber input

2.1 Disruption of commissural connections in the inferior olive causes more profound impairment than having no cerebellar output at all 41

2.2 Climbing Fiber drives reciprocity of Purkinje cell firing 49

Chapter 3 – Parallel Fiber input. Role of potentiation in Cerebellar Motor Learning 63

Chapter 4 – Role of the inhibition in the cerebellar circuitry

4.1 Molecular layer interneurons mediate consolidation of vestibulo-cerebellar motor learning 81

4.2 Raising Cl^- concentration in cerebellar granule cells affects their excitability and consolidation of vestibulo-ocular phase learning 101

Chapter 5 – Changes in the modulation of Simple Spike responses after motor training 127

Chapter 6 – Materials and Methods 139

Chapter 7 – Discussion 155

Summary 167

Samenvatting 170

Curriculum Vitae 172

List of Publications 173

Portfolio 174

Acknowledgments / Dankwoord 176

CHAPTER 1

INTRODUCTION

1.1 General introduction

The brain is what makes us human. Feelings, memories, complex social interactions, language and movement – all of it originates in the brain. On average, the human brain contains approximately 50–100 billion neurons that communicate with each other through the vast network of 100 – 500 trillion connections called synapses. More than half of the total number of neurons make a structure called the cerebellum. In vertebrates, the cerebellum (Latin for *little brain*) controls movement and monitors its efficiency by collecting sensory information such as visual cues, limb positions and balance. This information is necessary to adequately respond to the environment by controlling and correcting the movements. Historically, since the 18th century when Arne – Charles Lorry showed that the damage to this structure results in loss of motor coordination[1], the cerebellum has been known to be involved in motor coordination. In the 19th century neurophysiologists such as Luigi Rolando and Jean Pierre Flourens revealed that animals with cerebellar damage can still move, but with a loss of coordination and that recovery after the lesion can be nearly complete unless the lesion is very extensive[2]. The milestone for understanding the cerebellum was placed by the research of Camillo Golgi and Satiago Ramon y Cajal in the late 1800s. The work of these anatomists enabled visualization of individual neurons revealing for the first time the structural organization of the brain, including the cerebellum. More than a century later researchers still battle with two main questions. Firstly, how does the cerebellar function contribute and/or results in such a sophisticated level of motor coordination that enables us to do things like playing the violin or ballroom dancing? Secondly, how do we acquire those new motor skills? The cerebellar network seems to be holding the key to answering both of those questions. It has the capacity to process the sensory information and translate it into a motor command.

In this thesis, we describe the effects of alteration in the cerebellar system unraveling the possible role of its afferent inputs.

1.2 Cerebellar anatomy and function

The cerebellum is located at the caudal part of the cerebrum just above the brainstem (**Figure 1**). At the level of large-scale anatomy, the cerebellum consists of a tightly folded layer of cortex, with white matter underneath, several nuclei deeply embedded in the white matter, and a fluid-filled ventricle at the base. The most remarkable feature of the cerebellum is its homogenous and repetitive structure. The organization of this structure varies very little across all vertebrate species.

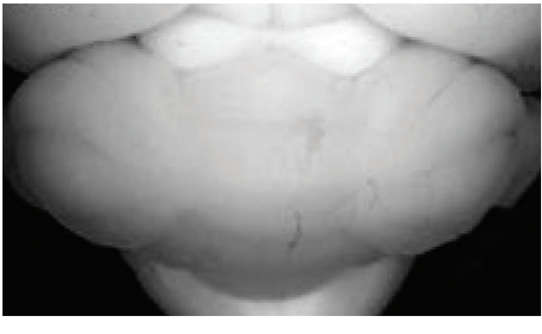

Figure 1. Gross view on the cerebellum of a mouse. Dorsal view on both hemispheres and vermis. Note position of the cerebellum above the brainstem, caudal to the cerebrum and rostral to the spinal cord.

The cerebellum can be divided into different anatomical as well as functional modules gathering information from different modalities[3]. Despite the functional differences the processing of incoming information within each module is very similar. In short each module consists of three parts: climbing fiber input from the inferior olive (IO), the cerebellar cortex and deep cerebellar nuclei (**Figure 2**). This circuitry is known as the olivocerebellar loop where the integration of sensory information takes place at each level. With the exception of the *flocculonodular lobe*, the cerebellar cortex projects to the deep nuclei[4,5]. The *flocculonodular lobe* projects to superior vestibular nuclei and will be discussed separately in the course of this thesis.

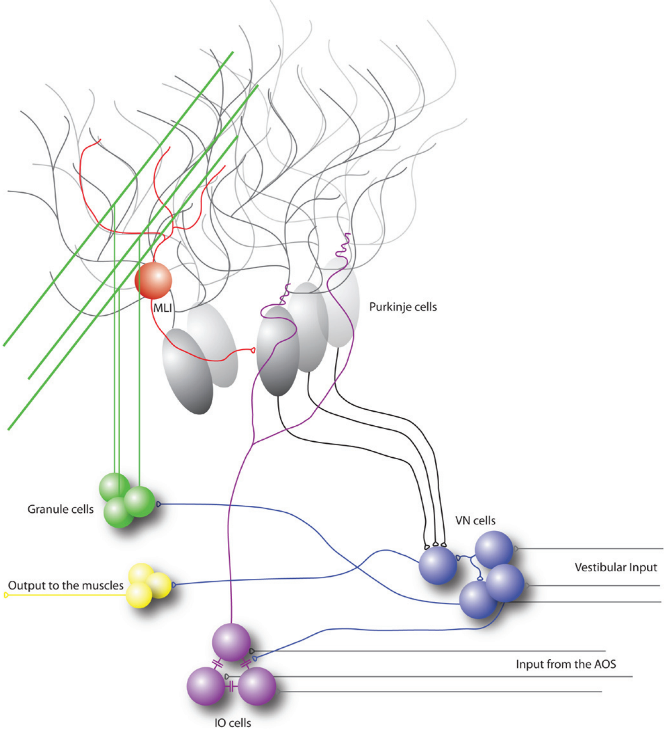

Figure 2. Synaptic organization of a basic cerebellar module involved in the oculomotor pathways. Vestibular input to the vestibular nucleus (VN) caries the signal about the head movement. This signal is then relayed by mossy fibers onto granule cells that innervate Purkinje cells. The inferior olive (IO) receives the information about the retinal slip that is processed at lower levels by the accessory optic system (AOS). Neurons in the IO innervate the Purkinje cells (shown in grey) through climbing fibers. Those two inputs convey on Purkinje cells, which send their output back to VN, forming the excitatory loop. This loop is modulated by a inhibitory side loop in the cortex represented by molecular layer interneuron (MLIs), here in orange.

1.2.1 Cerebellar cortex

The cerebellar cortex is organized into three layers – from outmost to innermost: molecular layer, Purkinje cell layer and granular layer. It contains 7 different types of neurons: Purkinje cells (PC), molecular layer interneurons (stellate and basket cells), Golgi interneurons, granule cells (GC), Lugaro cells and unipolar brush cells[6]. The molecular layer consists of Purkinje cell dendritic trees, stellate and basket cell interneurons, parallel fibers originating from granule cells and end terminals of climbing fibers coming from the IO. The Purkinje cell layer is made solely out of large cell bodies (~30 µm) of Purkinje cells and end terminals of basket cells. The granular layer contains a huge number of densely packed granule cells receiving excitatory input from mossy fibers and unipolar brush cells and inhibitory projections from Golgi interneurons and Lugaro cells (**Figure 3**).

Purkinje cells

The terminal destination of all the somatosensory input to the cerebellum is the Purkinje cell.

They have a very distinctive morphology characterized by a large soma, a flat and extremely branched dendritic tree (see the cover) and a long axon that forms collaterals at its proximal end. The dendritic tree of a Purkinje cell is very unique, it protrudes approximately 250µm wide and 150 µm high into the molecular layer, however it is only 6 µm thick. This feature allows a number of Purkinje cells to align their dendritic trees in long parasagittal stripes. The dendritic tree is divided into 2 primary branches that later divide to secondary, tertiary, quaternary etc. This division has its morphological and physiological consequences. The primary branches form synapses with climbing fiber input and, according to recent findings, express NMDA receptors[7,8], whereas secondary branches express mostly AMPA receptors and make synaptic contacts with parallel fibers. The dendritic protrusions are covered with numerous small spines that make contact with excitatory synapses. Synaptic GABA receptors are situated on the shaft of the dendrites and the Purkinje cell soma and receive inhibitory inputs from molecular layer interneurons. Both the excitatory and inhibitory inputs can modulate the frequency and regularity of Purkinje cell firing. The intriguing characteristics of Purkinje cell firing properties will be further discussed throughout this thesis.

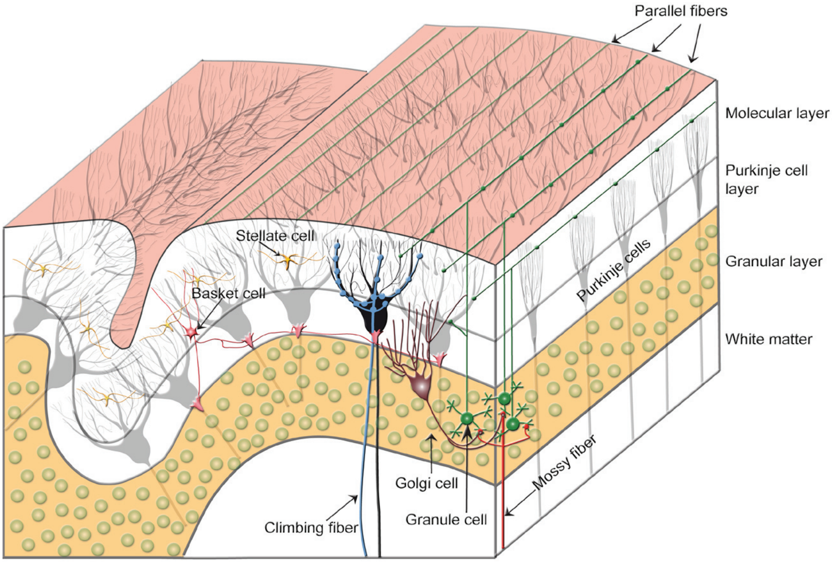

Figure 3. Scheme of cerebellar cortex showing all 3 cortical layers (adapted from Kandel). The biggest cells are Purkinje cells (PC) forming the output from the cerebellum. They are innervated by bundles of parallel fibers called beams that run transversely to PCs innervating them and molecular layer interneurons at the same time. Inhibitory stellate cells make connections on distal parts of dendritic tree. Basket cell axons form a basket-like synapse on the PC soma. Granule cells are inhibited by Golgi cells and make contacts with PCs through their ascending axons and parallel fibers. Mossy fibers originate in the deeper layers (not shown) and form end terminals with granule and Golgi cells called glomerulus. Finally climbing fibers rising from inferior olive innervate PC with one-on-one relationship. They also make synaptic contacts with Golgi cells and indirectly with molecular layer interneurons.

Purkinje cells are the only output from the cerebellar cortex and as such they are responsible for the final state of information processing that is being relayed to cerebellar deep nuclei and vestibular nuclei. The axon terminals of Purkinje cells are all inhibitory and form GABAergic synapses with their target cells[5]. On average one Purkinje cell projects to 30–50 different cerebellar nuclei cells and one cerebellar nuclei cell is innervated by 20–30 different Purkinje cells[9]. The ratio of this convergence is important for information processing. In short it is believed that a single Purkinje cell does not carry sufficient signal to be translated into motor command. Only when an assembly of Purkinje cells relay their signal in a synchronized manner will it result in a meaningful change at the level of cerebellar nuclei[10]. This model will be discussed in depth in chapter 4.

1.2.2 Excitatory input to Purkinje cell

Parallel fibers

In literature, the parallel fiber input onto Purkinje cells is very often interchangeably used with the mossy fiber input. This is confusing and in the light of recent studies[11] incorrect. Parallel fibers are the axons of granule cells that receive the signals from the mossy fibers. Previously it was believed that granule cells are nothing but a relay station simply sending the same signal through their axons onto Purkinje cells[12]. Recently, studies revealed the plasticity mechanism at the level of granule cells[13], which proves that there is a need to distinguish between those two inputs, since the signal send through the parallel fibers is clearly different from the one originating from the mossy fiber.

Mossy fibers originate in the vestibulum, spinal cord and various precerebellar nuclei in the brainstem. In the case of flocculus, mossy fibers arise from 4 main sources[14]: (1) perihypoglosal nucleus, (2) vestibular nuclear complex, (3) medullary reticular formation, (4) pontine reticular formation. Mossy fibers project mostly bilaterally and form excitatory bulbous terminals on dendrites of granule cells. Those synaptic contacts are very specific because they coincide with Golgi cell synapses on granule cells forming a structure called the glomerulus. After the signal from the mossy fiber is processed at the level of granule cells, and transformed into well timed spike–bursts[15], it ascends to Purkinje cells through granule cells axons.

Granule cell axons ascend and protrude into the molecular layer where they make synaptic contacts with the distal parts of Purkinje cell dendrites[16]. Mostly, however the ascending axon splits it a T–shaped fashion at the level of cerebellar cortex forming the parallel fibers[17]. Parallel fibers are approximately 0.6µm thick and protrude through the molecular layer up to a couple of millimeters. They are oriented perpendicularly to the planes of the Purkinje cell dendrites, in total making around 175,000 contacts with the dendritic spines[18]. In contrast to the ascending granule cell axon, a single parallel fiber makes only one or two synaptic contact per dendritic tree but innervates up to 300 Purkinje cells at the same time. Over the course of decades many researchers proved that in adult cerebellum some of the parallel fiber inputs are strengthened whereas others are being silenced[5,6,19,20]. This selective pruning of parallel fiber inputs is dependent on plasticity mechanisms in the Purkinje cell and is believed to play a crucial role in the cerebellar motor learning. In chapter 3 we will try to unravel the importance of long-term potentiation on parallel fiber to Purkinje cell synapse and its role in motor behavior.

Parallel fibers also innervate molecular layer interneurons. Recently, extracellular recordings revealed that receptive fields of interneurons are similar to the receptive fields of mossy fibers terminals in the granule layer directly below the interneuron[21]. That suggests that interneurons, like Purkinje cells, are capable of selecting a desired set of parallel fibers from all the synaptic contact they receive.

Climbing fibers

Purkinje cells receive another major excitatory input from climbing fibers. Climbing fibers are the axons of inferior olive cells that in adult cerebellum cross the midline and ascend upward innervating Purkinje cell dendrites. Each climbing fiber contacts approximately 10 Purkinje cells, however adult Purkinje cell receive input from just one climbing fiber. In early postnatal development up to 4 climbing fibers make synaptic contact with the Purkinje cell, that number of projections is later pruned[22,23]. Histology staining revealed that in the early life the axons of climbing fibers wrap around the soma of the Purkinje cell to later "climb up" their dendritic tree, finally making contacts with primary dendrites[7]. Additionally climbing fibers form collaterals that innervate deep cerebellar nuclei and vestibular nuclei in flocculus. The olivocortical projections are characterized by specific sagittal targeting pattern such that neurons from particular region of the olive project to a very specific sagittal zones of the Purkinje cells[24]. In some cases, olivary axon can reach two different zones – this is the case in the vestibulocerebellum where a single climbing fiber innervates Purkinje cells in the nodulus and flocculus[14]. However, it should be noted that those two different zones could still belong to the same functional module.

Besides projecting to Purkinje cells and sending collaterals to deep cerebellar nuclei neurons, climbing fibers also appear to innervate Golgi cell interneurons and molecular layer interneurons. This last connection has been the topic of heated discussion over the last decade. There is strong evidence to support this notion[21], however still more research is needed to fully understand the nature of the connection between climbing fibers and molecular layer interneurons.

The climbing fiber synapse is one of the most powerful synapses in the mammalian brain. This synaptic connection is so strong because each climbing fiber makes approximately 300 synaptic contacts simultaneously on one Purkinje cell (in the rat)[25]. All of those synapses have a high release probability estimated at approximately 500 active release sites[26]. Activation of this synapse has a central role in a number of hypotheses concerning cerebellar motor learning.

1.2.3 Inhibitory afferents to Purkinje cell - Molecular layer interneurons

Stellate and basket cells, regarded here as molecular layer interneurons (MLIs), are often described separately as two different inhibitory inputs[27], however present studies tend to refer to them as one unit due to shared inputs and similar electrophysiological characteristics[28,29]. Molecular layer interneurons receive the same input as Purkinje cells, namely from the parallel [30] and climbing fibers[31] and therefore theoretically should be able to demonstrate comparable plasticity mechanisms, a hypothesis that is supported by a number of recent studies[28,32,33]. It has been shown that the parallel fiber to molecular layer interneuron synapses can express long term potentiation (LTP) and long term depression (LTD)[34]. It has been theorized that LTP on the parallel fiber to MLIs synapse is climbing fiber dependent due to NMDA receptor involvement[35], whereas LTD of the parallel fiber input to interneurons depends on parallel fiber alone[36]. Intracellular recordings from interneurons following parallel fiber stimulation show a rapid IPSP following an initial EPSP which suggesting that molecular layer interneurons also receive inhibitory inputs from the neighboring MLIs [27,37].

MLIs project their axons onto sagittal band of Purkinje cells creating synapses at their dendritic shafts and cell body; stellate cells that originate from the distal part of molecular layer inhibit the distal part of PC dendritic tree whereas the basket cells that are located in the proximal part of the molecular layer form a basket–like synapse around the soma and axon hillock of the PCs[38,39] (**Figure 4**). In fact the location and size of those cells is the only differentiating factor. MLIs fire spontaneous action potentials at low (~5 Hz in vivo[32]) to moderate (~12 Hz in vitro[40]) frequencies providing the feed forward inhibition onto PCs. It has been shown that MLIs inhibitory input affects the activity of PCs providing a modulatory change in PC firing and that it contributes to phenomena like classical conditioning[41]. Taking those properties under consideration, an interesting question arises: What is the role of those types of cells in motor behavior and learning?

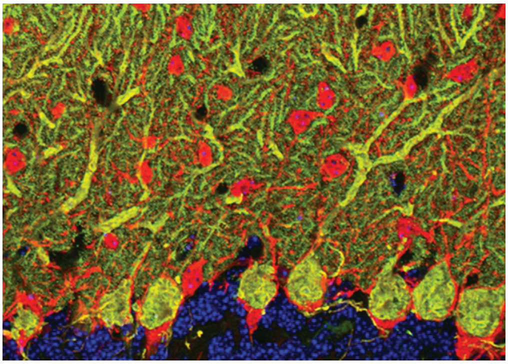

Figure 4. Molecular Layer Interneurons. Immunocytochemistry labeling (Parvalbumin with Calbindin) of stellate and basket cells (in red). Purkinje cells (in green) are surrounded by cell bodies, dendrites and axons of the MLIs. The basket cells form very clear basket-like structures on the somas of Purkinje cells. In blue granular cell layer.

1.2.4 Compensatory eye movements under floccular control

One of the most basic eye movement reflexes are compensatory eye movements. They are designed to stabilize the image on the retina, preventing retinal slip. We use those reflexes in everyday life, when, for example, traveling in a car. Our eyes make small movements adjusting to the view of the moving surroundings without us being aware of it. Since those reflexes are highly cerebellar dependent it is worthwhile to measure them. In mice we can measure two basic reflexes that compensate for the movements of the head (vestibulo–ocular reflex – VOR) or of the surroundings (optokinetic reflex – OKR) (**Figure 5**). During compensatory eye movements vestibular and/or optokinetic sensory input is processed by the cerebellum and transformed into appropriate motor commands to send to the eye muscle.

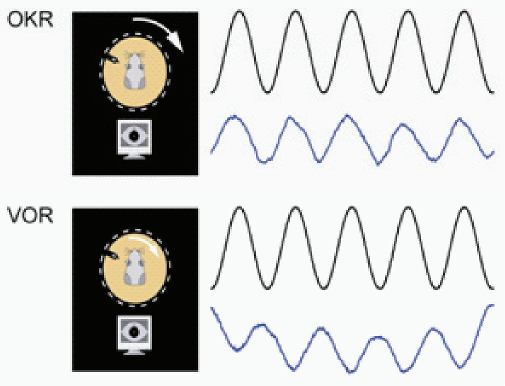

Figure 5. Schematic representation of the experimental setup and the compensatory eye movements in mice. Optokinetic reflex (OKR). The eye movements can be evoked by immobilizing mice and rotating the surrounding in the light. Vestibulo-ocular response (VOR). The eye movements are elicited by rotating the turntable on which the mouse is immobilized. Sinusoidal stimulation (black trace) will result in eye movements (blue trace), which can be traced with an infrared camera allowing for the assessment of gain and phase of the eye movements.

Parameters measured during experimental induction of compensatory eye movements are gain and phase values. Gain is a ratio between amplitude of the eye movement and the amplitude of the stimulus, whereas phase values correspond to the time difference between the eye and the stimulus. In other words, gain allows us to see how big the movement is and phase refers to the position of the eye versus the position of the stimulus and is expressed in degrees[42,43]. Both OKR and VOR are under control of the part of the cerebellum called the flocculus (**Figure 6**). The flocculus receives both visual and vestibular input and is involved in regulation of the performance of the VOR and OKR and also in the adaptation of the VOR[44, 45], which is one of the most studied motor learning paradigms. Recently it has been shown that flocculus in mammals is divided into anatomically and physiologically different zones responding to vertical or horizontal stimulation[4]. Those individual zones receive inputs from different parts of the inferior olive and project to different sets of nuclei controlling both horizontal and vertical eye movements.

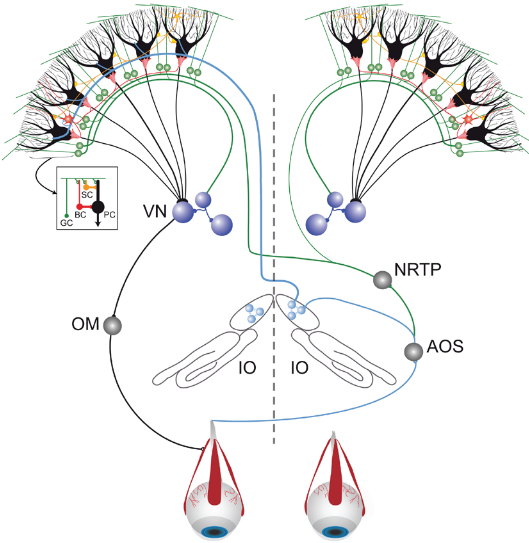

Figure 6. Schematic drawing of a simplified floccular network. Simplified illustration of olivocerebellar circuitry controlling eye movements. Purkinje cells (in black) converge upon neurons in vestibular nuclei (VN) through which they influence the output of the oculomotor neurons (OM) that drive the eye movements. Purkinje cells receive the visual inputs form nucleus reticularis tegmenti pontis (NRTP) through mossy fibers (green) and climbing fibers (blue) originating in the contralateral inferior olive (IO). The parallel fiber (axons of granule cells) innervate Purkinje cells and molecular layer interneurons (basket cells (BC)-red, stellate cells (SC)-yellow), the latter neurons provide feed-forward inhibition on Purkinje cells. AOS indicates accessory optic system.

Optokinetic reflex

The optokinetic reflex is designed to compensate for low velocity disturbances using visual feedback. The output of the OKR system (eye movements) corrects for the somatosensory error signal of the retinal slip, which is at the same time the input of the system. This is why the optokinetic system is often defined as a closed negative feedback loop. At low velocities OKR works best and is able to keep the gain of the eye movements close to 1, meaning that the amplitude of the eye movement is equal to the amplitude of the stimulus. At higher velocities however, the gain declines proving that OKR system acts as a low pass filter [46,42]. The gain and phase of the OKR depend not only on the stimulus velocity but also on the frequency of the stimulus, meaning that the higher the frequency the poorer the response. Those properties of the OKR system make it an excellent “partner system” for vestibulo–ocular system (VOR) that codes best for higher velocities. Animals with fovea also use smooth pursuit eye movements to trace moving objects. This reflex is much faster than OKR, with the ratio between initial jump in the eye velocity compared to the velocity of the stimulus in the range of 0,6. In afoveate species the initial response of the eye is much smaller. (**Figure 5OKR**).

Vestibulo–Ocular Reflex

VOR is triggered by head movements (**Figure 5VOR**). Similar to the OKR, its task is to stabilize the image on the retina. Signals coding for the head position come from the three semi–circular canals (the labyrinth), which detect angular head movements around a vertical and horizontal axis. The canals are situated inside the petrosal bone and are part of the middle ear. They are filled with endolymph that moves around when the head rotates, exciting special receptor cells (hair cells) in the membrane of the labyrinth, which translates the movements into a neuronal signal. The hair cells are also localized in the otolith organs, where they code for the linear acceleration. When hair cells are triggered by endolymph movement they depolarize or hyperpolarize, depending on the direction of the movement, sending signals to the brainstem through the vestibular nerve, projecting to several nuclei. First step of signal integration occurs in the nucleus prepositus hypoglossi (for vertical axis) and interstitial nucleus of Cajal (for both horizontal axes), where the position and velocity components are processed[47]. This information is conveyed onto eye muscles that cause a compensatory movement of the eye ball. The VOR is most reliable at high frequencies.

There are several aspects of VOR that make it potentially prone to errors. First of all, the integration of the position and velocity of the head is not perfect. In the dark the eye will drift back to its original position, which means that this integrator is “leaky”. This drift has a time constant that is species specific (~20s for humans and ~3 seconds for mice[48]). Secondly, VOR functions without the benefit of the feedback, meaning that the eye movements that are generated by this system are not read back into it. Due to this open–loop design the VOR reflex is sensitive for any changes in its internal parameters (for example changes in the size of the eye ball or the strength of the orbital muscles). In order for this system to maintain its accuracy it needs a mechanism that will correct for possible errors and enable the VOR to remain properly calibrated. The cerebellum fulfills this role. By combining the vestibular information with the visual input it provides the VOR with the error–correction system. It has been shown that lesions in cerebellum cause a dramatic change in the time–constant of the VOR[49]. The role of the cerebellum in VOR reflex was further confirmed by studies on *Lurcher* mice, which have a specific mutation causing a gradual loss of Purkinje cells. Adult *Lurcher* mice lack virtually all Purkinje cells, which translates into the loss of cerebellar output and show affected VOR gain[42,50].

To summarize, VOR and OKR complement each other, since OKR works best at low and VOR at high velocities. That means that in a natural environment, when perception of the movements of the surrounding environment are caused by the mouse’s head movements, the low velocities will be compensated by the OKR and high by the VOR. The remaining question is the mechanism of the VOR adaptation. The role of the flocculus in OKR is well established but it is still debated when it comes to the VOR. Nowadays most scientists tend to agree that flocculus (cerebellar cortex) is involved to some extent, however, the discussion whether it is the source of the plasticity changes involved in the learning or whether it computes the signal "online" and passes it on to the vestibular nuclei where the consolidation of motor learning takes place is still ongoing[20,51,52]. In the next section (1.4) theories of cerebellar motor learning will be discussed in detail.

1.3 Electrophysiology of the Purkinje cell

One of the fascinating properties of Purkinje cells is their ability to create spontaneous action potentials in dissociated cells. It has been shown that the source of this intrinsic spiking is the resurgent sodium current that is elicited upon repolarization[53,54]. Purkinje cells are also unique because they elicit two very distinctive types of action potential – simple and complex spikes (**Figure 7**). This specific pattern of spiking, together with certain characteristics of the complex spike, makes Purkinje cells easy to identify in single unit extracellular recordings[55]. It should be noted that intrinsic excitability of Purkinje cells can be up and down regulated by intrinsic plasticity mechanisms, mediated mainly by voltage and calcium activated potassium channels. It has been shown that Purkinje cell intrinsic plasticity lowers the probability for a subsequent LTP induction, affecting the synaptic responses on parallel fiber to Purkinje cell synapse and consequently the Purkinje cell spiking output[56].

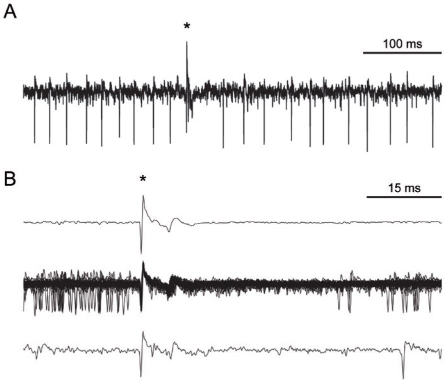

Figure 7. Purkinje cell activity recorded extracellularly in vivo. A) Raw trace of extracellular recording in vivo in awake mouse showing two types of spikes: simple spikes and a complex spike indicated by an asterisk. Note the much higher frequency of simple spikes. B) Complex spike waveform analyzed by MatLab. From the top: average waveform of all complex spikes in the trace; overlay of all complex spikes; single complex spike waveform (raw trace). Both initial sharp sodium spike and wide calcium wave can be seen on the averaged trace**.**

1.3.1 Simple Spikes

Simple spikes (SS) are somatic action potentials generated in the proximal part of the dendrite called the axon hillock [57,58]. It has been shown that it is the intrinsic activity of Purkinje cells that drives the firing of SS[59]. On top of that the excitatory input from the parallel fibers and inhibitory input from the interneurons modulate the occurrence of the SS. The basic firing frequency of SS is quite high, in slices with total blockage of synaptic input and/or in dissociated cultures it reaches approximately 50 Hz [40]. In these conditions Purkinje cells will act as a pacemaker, firing the action potentials very reliably and regularly. There are a couple of mechanisms that are responsible for this intrinsic activity. First, Purkinje cells have specific voltage–gated sodium currents that briefly open upon repolarization of the cells. These resurgent sodium currents[53] play a key role in triggering spontaneous activity of the Purkinje cells. Secondly, potassium currents mediated by Kv3.3 potassium channels have been shown to regulate frequency of the intrinsic firing[59] and thirdly there is evidence that low–voltage activated calcium currents, mediated by so–called T–type "transient" channels, also play a role in spontaneous firing[60,61]. Together those three mechanisms make sure that the membrane of the Purkinje cell gets tonically depolarized. Upon hyperpolarization, the additional mechanism kicks in, namely the I_h current. This current is evoked by opening of cyclic–nucleotide gated channels that conduct sodium, potassium and calcium and restore the resting membrane potential in the cell[62].

The activation of the parallel fiber synapse can trigger a simple spike, although the exact contribution of individual parallel fibers to overall SS firing frequency is still being investigated. Research shows that stimulation of a single granule cell can evoke an EPSC in Purkinje cells in only 10% of the cases[63]. However, in “natural” conditions somatosensory input recruits a whole population of granule cells belonging to the same receptive fields[13], activating whole beams of parallel fibers. That is why during motor behavior simple spike firing frequencies can potentially rise well above the baseline background intrinsic activity and reach values of 200–300 Hz.

Let’s look more closely at what exactly happens in the Purkinje cell when parallel fibers are activated. Upon the arrival of excitatory input from the granule cells, PF presynaptic membrane releases glutamate, which binds to ionotropic and metabotropic glutamate receptors (AMPA and mGluRs, respectively). Activation of AMPA receptors causes a big sodium influx, which leads to fast excitatory postsynaptic potentials (EPSP). Activation of mGluR receptors on the other hand triggers the whole cascade of secondary messengers, namely G–protein–coupled activation of phospholipase C that induces diacylglycerol (DAG) production. This last compound triggers the breakdown of PIP_2 to IP_3. IP_3 binds to receptors on the reticulum and enables release of the Ca^{2+} from the internal calcium stores[64]. This influx of calcium causes slow EPSP and also leads to opening of voltage–gated calcium channels on the spines. The sodium currents initiated by PF stimulation travel passively towards the soma of the Purkinje cell, and trigger the opening of the voltage–gated sodium channels on the axon hillock. These sodium currents can initiate the action potential, later the high voltage–gated calcium channels (mainly P/Q type) open, further depolarizing the Purkinje cell. The last step is the opening of calcium–dependent potassium channels, which causes the efflux of potassium, counteracting the depolarization and preventing excitotoxicity.

SSs are also modulated by inhibitory GABAergic inputs from the molecular layer interneurons (MLIs). The GABAergic input from both stellate and basket cells activates $GABA_A$ receptors on Purkinje cell synapses. This leads to influx of chloride that causes Purkinje cell hyperpolarization, which can be measured as a fast inhibitory postsynaptic potential (IPSP). Release of GABA neurotransmitter also activates metabotropic $GABA_B$ that by G–protein mediated cascade decreases the calcium currents and increases potassium efflux causing hyperpolarization. Blocking the GABA input in slices triggers an increase in Purkinje cell firing frequency. However, we show that when the inhibition is abolished at the developmental level, using transgenic mutants it does not affect the firing frequency but rather the regularity of Purkinje cell firing (see Chapter 4). This inhibitory input is strong enough to decrease the intrinsic SS firing to ~10Hz during for example visual stimulus. This will be discussed in detail in chapter 1.3.4.

Overall, we can say that Purkinje cells have extremely large range of SS firing frequencies that are modulated by intrinsic excitability, excitatory and inhibitory input.

Even though we know a lot about the physiology of the simple spike, the question about its functional implication still remains. The fact that a lot of Purkinje cells converge on one deep cerebellar nucleus/vestibular nucleus cell makes the importance of a single SS questionable. Some researchers believe that it is the overall firing frequency that is crucial for motor behavior, others tend to disagree. In Chapter 4 we provide evidence for the importance of spatiotemporal patterns of SS firing for cerebellar motor learning[10,65]. The regularity of Purkinje cell SS firing seems to be crucial to reliably synchronize/desynchronize the input from a lot of cells converging it into a readable output signal.

1.3.2 Complex spikes

The second type of action potential generated by a Purkinje cell is a complex spike (**Figure 7B**). The waveform of the complex spike has a very unique shape. It starts with a sharp sodium spike and extends to a wide, calcium dependent wave (~20ms) with some spikelets riding on top of it[66]. This shape depicts current changes in Purkinje cell that occur after climbing fiber activity. Below is a brief summary of the most crucial steps of complex spike formation (for extended summary see review by Schmolesky et al.[67]). First, upon arrival of an action potential from the inferior olive climbing fiber synaptic contacts release glutamate which binds to AMPA (and mGluR) receptors causing a robust depolarization. The depolarization is so strong that it triggers a big calcium influx mediated by voltage–gated calcium channels (mainly P/Q and T–type). This calcium wave spreads to the soma and axon hillock where it triggers an opening of voltage–gated sodium channels creating sodium action potentials. There is some debate however whether the sodium action potential is triggered by the dendritic calcium wave. There is evidence that the initial sodium spike not only originates in the soma but it is independent of the dendritic calcium wave[68]. This initial stage of complex spike formation is similar to SS mechanism and the initial sodium spike also shares a lot of SS characteristics[69]. Interestingly, the sodium spike does not propagate into the dendrites[70], most probably due to the complex architecture of the Purkinje cell dendritic tree[71]. The second component of the complex spike is a slow calcium wave, mentioned above. This calcium wave is also referred to as a plateau with visible spikelets "riding" on top of it (**Figure 7B**). There is no argument among the cerebellar researchers community that the depolarization wave is caused by the voltage–gated calcium channels, however there is a lot of debate about the origin of the spikelets. Some claim that they are also caused by the dendritic P/Q and T–type channels accompanied by the de-inactivation of somatic sodium currents[53,67]. Recently however, it has been demonstrated that somatic spikelets originate in the axon hillock as well and are likely to be mediated by sodium and potassium currents[68]. It should be noted that nowadays, there is thought to be a clear distinction between dendritic and somatic spikelets. Dendritic spikelets are speculated to be the direct response of the climbing fiber activation, possibly decoding the state of the olivary oscillations[72] (see next paragraph) and somatic directly coding the output of the Purkinje cell. The third and final phase of the complex spike is a slow repolarization mediated by the calcium–activated potassium channels and a resurgent sodium current followed by a slow afterhypolarization (AHP), which in addition involves the SK and BK channels[73]. When Purkinje cells are recorded *in vivo* each complex spike is followed by a pause in SS firing[55, 74]. This suppression of SSs is called the "climbing fiber pause" and its mechanism is still under debate. There is some evidence for contribution of climbing fiber evoked long term depression (CF–LTD) to this phenomena[67], as well as the dendritic spikelets involvement[68]. It should be noted that recently it has been shown that in adult animals glutamate also binds to NMDA receptors which influences the shape of the complex spike and the number of spikelets[7,8].

The complex spike is triggered by activation of climbing fiber synapses. Climbing fiber input to Purkinje cells arrives from the inferior olive. As previously mentioned, in adult animals one Purkinje cell is innervated by just one climbing fiber. The input from the climbing fiber synapse is powerful enough to overwrite any other synaptic input. This happens due to the fact that a single climbing fiber makes around 1500 synaptic contacts on the Purkinje cell and all of them are constantly at the state of high release probability[75]. The ascending olivary axon crosses the midline and innervates the soma and primary branches of 5 to 10 Purkinje cells in a sagittal band[76]. That means that Purkinje cells that receive contacts from the same olivary cell will be activated synchronously. Because of strong electrotonic coupling between inferior olivary cells via gap junctions it is possible to synchronize the activation of the whole groups of Purkinje cells[77,78]. Due to specific characteristic of olivary cells their spontaneous firing rate of somatic action potentials on average reaches 1 Hz[79,80] and can reach 10 Hz for periods of time[81]. In vivo recordings of Purkinje cells from awake animals showed that complex spike firing frequency is approximately 1 Hz. Therefore, for many decades it was believed that Purkinje cells response to climbing fiber stimulation is all–or–nothing. However, recent findings seem to challenge that concept. It has been shown that axons of the inferior olive cells can fire bursts of spikes at a very high frequency[82]. Also, the action potential bursts in climbing fibers depend on the phase of the subthreshold oscillations in the olivary neurons. Those bursts are recognized by Purkinje cells. There seems to be a relation between bursts in climbing fibers and the number of dendritic spikes elicited by Purkinje cells. More importantly, the climbing fiber bursts can modify the number of spikelets in the complex spike and its duration. It also seems that synaptic plasticity in Purkinje cells can be enhanced by bursting activity of the climbing fibers. It is not exactly known how changes in the number of complex spike spikelets influence the "read out" of this signal at the level of deep cerebellar nuclei. Some studies indicate that each somatic spikelet triggers an action potential in the Purkinje cell axon[68]. If that is true the change in the number of the spikelet could be crucial to the output. Some researchers however, believe that a more important feature of the complex spike is the complex spike pause[83].

The role of the complex spike is still the subject of heated discussion. Traditionally it has been viewed as a "teacher signal" to induce plasticity on parallel fiber to Purkinje cell synapse[6,84]. Others argue that it should be considered to be a "timing device" and link it to inferior olive function[85]. These theories will be covered more extensively in paragraph 1.4. In this thesis I will also try to shed some light on the relationship between complex and simple spikes (Chapter 2).

1.3.3 Behavior of Purkinje cell during motor tasks

Firing patterns of Purkinje cells change dramatically during motor behavior. Sensorimotor information transmitted by the parallel fibers and signals coming from the inferior olive through climbing fibers modulate the firing frequency and temporal patterns of both simple and complex spikes resulting in reciprocal firing configuration (**Figure 8**).

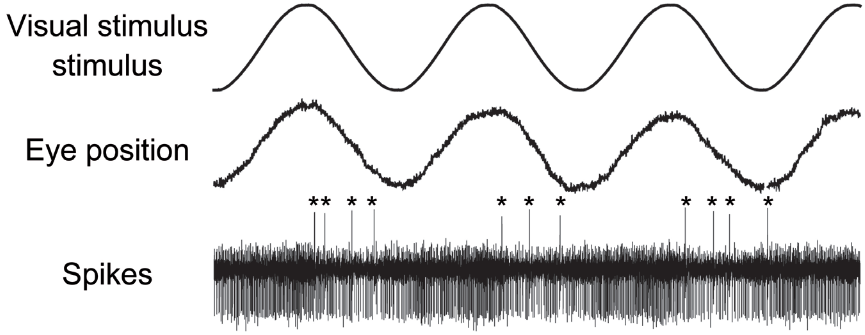

Figure 8. Purkinje cell activity recorded extracellularly in vivo during optokinetic stimulation. Recording of floccular VA cell during visual stimulation. Spike train show the modulation of both simple and complex spikes (asterisks). Ipsilateral rotation of the stimulus (here down slope of the sine) depicts a decrease in simple spike firing rate accompanied by an increase in complex spike frequency.

This phenomenon of reciprocity is particularly evident in the flocculonodular lobe during natural periodic, sensory stimulation and motor control[86,87,88,45,89]. For example, during control of optokinetic responses (OKR), complex spike and simple spike activities in Purkinje cells of the vestibulocerebellum modulate out of phase with respect to each other over a wide range of frequencies [74,88]. It has been shown that during optokinetic stimulation complex spikes are driven by retinal slip[90] encoded by the climbing fiber[88,91]. However it is still unclear what is the origin of complex spike signal during vestibulo–ocular response (VOR)[92]. Simple spike activity during visual stimulus also changes abruptly, oscillating between so called on–phase when the firing frequency can reach ~120Hz and off–phase when firing is depressed down to ~10Hz and less. It was suggested that this depression of simple spikes can be related to hyperpolarized state of the Purkinje cells, called the down state[93,94]. However, recent findings have shown that in awake animals Purkinje cells operate in so–called up state[95], excluding the possibility that changes in membrane potential alone can cause reciprocity. Three other possible sources of reciprocity are: climbing fiber inputs, synchronized parallel fiber signals and, according to recent findings molecular layer interneurons that have the same receptive fields as climbing fibers[17,96]. So far, it has been difficult to pinpoint whether the climbing fiber input controls the reciprocity. Experiments performed in the late 80s and early 90s showed that after lesions of the inferior olive simple spike modulation prevails even if almost all complex spikes are gone[97,98,99]. This theoretically could support the hypothesis that granular cell input is more important for the reciprocity than climbing fiber signals. However, there are two major drawbacks of those experiments. First of all, those experiments were performed in adult animals when, according to the Marr–Albus learning theory[6], climbing fibers already selected appropriate set of parallel fibers (for the detailed description of Marr–Albus theory see paragraph 1.4). Secondly, removing all climbing fiber input results in almost complete loss of the complex spikes making it very hard to draw any definitive conclusions about the nature of complex and simple spike relationship. In chapter 2 we address the issue of reciprocity, taking a new spin on the classical lesion experiments.

It should be noted that all experiments in which we address the Purkinje cell firing patterns and responses to visual and/or vestibular stimulation (in Chapters 2,3,4 and 5) were measured extracellularly in awake animals. In our opinion it is crucial to explore the firing patterns of the Purkinje cells in awake behaving animals. There has been strong evidence that both gas and intravenous anesthesia can strongly affect both sodium and calcium currents, ultimately affecting Purkinje cell firing. For example it has been showed that isoflurane is a potent inhibitor of voltage–gated T–type calcium current[100,101]. Furthermore, it suppresses hyperpolarization–activated depolarizing sodium current[102], significantly hyperpolarizing the cells. A number of *in vivo* experiments have confirmed those findings[103,95]. Intraperitoneal anesthetics such as ketamine have even more profound effects on Purkinje cell firing. Research shows that ketamine depresses the climbing and mossy fiber evoked field potentials in cat cerebellum[104] and inhibits one of the subunits of the $GABA_A$ receptors[105]. In high concentrations ketamine blocks NMDA receptors, which could explains the attenuated MF and CF responses[106].

1.3.4 Plasticity at the synapses

The ability of neurons to process and store the large amount of information lies not only in the "online" computing capabilities of the cells and networks but also (some would even say mainly) in the long lasting changes of the synaptic inputs. Long term potentiation (LTP) as well as long term depression (LTD) are two of the neuronal mechanism that have shown to be involved in learning and memory. Purkinje cells have the necessary molecular machinery to support those synaptic gain changes and indeed many studies have shown that they express both types of synaptic plasticity (**Figure 9**). Throughout the decades studies were focused on the parallel fiber to Purkinje cell synapse (PF–PC), lately however there has been evidence for plasticity changes at the climbing fiber to Purkinje cell site (CF–PC). In addition, a mechanism for long–lasting potentiation has been shown at the molecular layer interneuron to Purkinje cell synapses. Here, all the above mentioned types of synaptic plasticity that occur in the Purkinje cell will be discussed. I would like to emphasize that even though I will characterize molecular mechanisms separately, none of those plasticity changes occur in the vacuum. LTP and LTD at the PF synapse are not only related to each other but they are highly dependent on what happens at the CF synapse[107]. In the past couple of years it has been shown that induction of plasticity depends on more factors than simply the state of the studied synapse. Intrinsic excitability and plasticity of the cell together with delicate balance of phosphatases and kinases are able to shift the "plasticity switch" from potentiation to depression[108]. It should also be noted that under experimental conditions it is difficult to test all the possible ways of LTP and LTD induction. For example, for a couple of decades it was believed that LTD can only be evoked by PF and CF simultaneous activation. In the late 90's however it was proven that given certain conditions PF stimulation alone is able to trigger LTD[109,110]. Also, for many years the cerebellar research community was convinced that there is no role for NMDA receptors in Purkinje cells (or rather that there are simply no functional NMDA receptors). In the past 2 years this well established belief was shaken by Piochon findings[8,7]. One should remember that experiments done in slice conditions, with blockage of synaptic input, do not necessarily reflect all possible conditions of the cell *in vivo*. Therefore it is necessary to approach results obtained in *in vitro* slice preparations with caution.

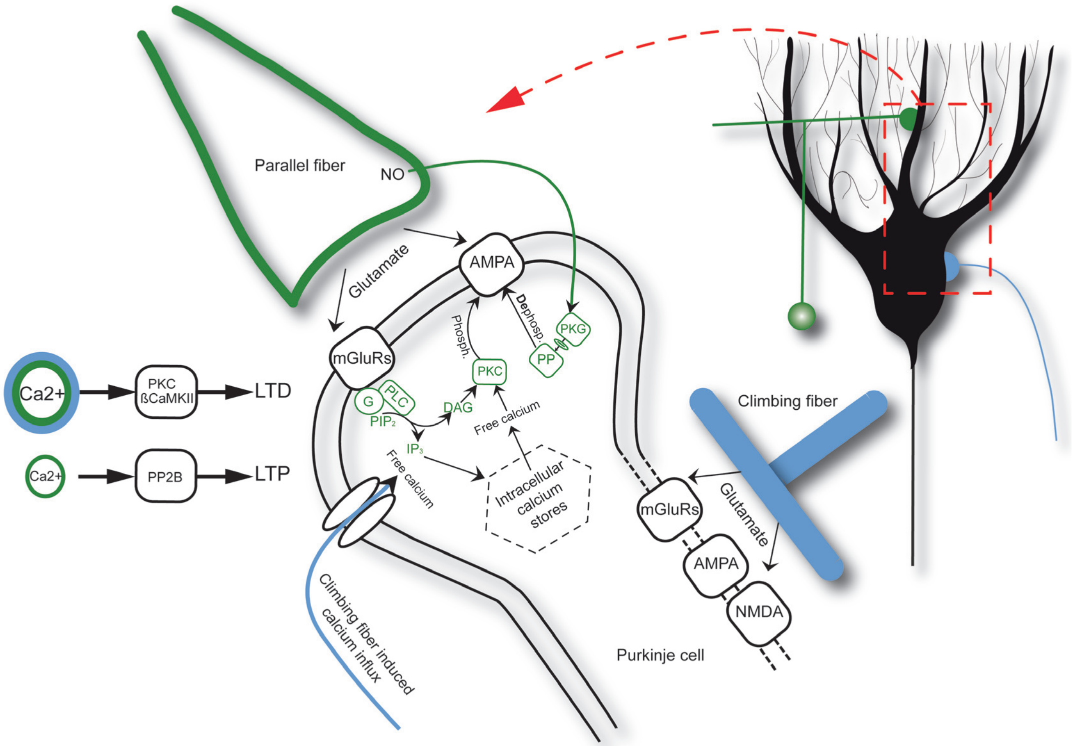
Parallel fiber
NO
Glutamate
AMPA
mGluRs
Phosph.
Dephosp.
PKG
PP
PKC
G
PLC
PIP₂
DAG
Free calcium
IP₃
Free calcium
Intracellular calcium stores
Ca2+
PKC
ßCaMKII
LTD
Ca2+
PP2B
LTP
Climbing fiber induced calcium influx
Climbing fiber
Glutamate
mGluRs
AMPA
NMDA
Purkinje cell

Figure 9. Simplified view on molecular pathways involved in parallel fiber to Purkinje cell plasticity. For clarity reasons parallel and climbing fiber terminals are presented on one compartment of Purkinje cell. LTD is induced by simultaneous climbing fiber (blue) and parallel fiber (green) activation. A large calcium transients resulting from free calcium influx through voltage–gated calcium channels together with release of calcium from intracellular stores mediated by IP3 promote protein kinase C (PKC) activation, which phosphorylates AMPA receptors leading to their internalization. Additionally parallel fiber activation causes presynaptic release of nitric oxide (NO) and results in activation of protein kinase G (PKG). Activation of PKG inhibits protein phosphatases and thus inhibits dephosphorylation of AMPA receptors. On the other hand low calcium transients triggered by parallel fiber stimulation alone promote activation of protein phosphatases 2B (PP2B.) PP2B regulates AMPA receptor insertion.

Parallel fiber long term depression (PF–LTD)

PF–LTD has been one of the most extensively studied plasticity mechanisms in cerebellum. Its role in the cerebellar motor learning was proposed for the first time by Marr and Albus[84]. In 1982 Kano described the mechanism of LTD as being a result of simultaneous parallel and climbing fiber stimulation, suggesting that climbing fiber signals act as a “teacher” selectively weakening PF synapses. Since then a number of molecular mechanisms involved in PF–LTD have been identified. Interestingly, in contrast to, for example, pyramidal cells in hippocampus, Purkinje cells express LTD at high intracellular calcium levels[111]. In order to trigger such a high calcium influx several processes must take place. As described in a previous paragraph, climbing fiber signals trigger a massive calcium influx to soma and proximal dendrites mediated by AMPA receptors and voltage–gated calcium channels. This calcium wave spreads retrogradely to the dendrites activating P/Q and T–type channels. Parallel fiber stimulation also activates AMPA and mGluR1 receptors, which not only triggers an opening of ionic channels but also leads to IP_3 activation. The metabotropic glutamate receptors are socalled G–protein coupled receptors, which means that they act through second messenger pathways. Activation of those receptors causes phospholipase C (PLC) to react with PIP_2, which creates IP_3 and DAG. DAG and calcium released from internal stores (mediated by IP_3) both activate protein kinase C (PKC), which phosphorylates AMPA receptors ultimately leading to their internalization. In short LTD causes a decrease in the number of AMPA receptors at the synaptic membrane. This process is very sensitive to calcium levels and therefore depends on additional calcium influx originating from climbing fiber stimulation[107]. There are several additional players that take part in that process. It has been shown that in addition to glutamate, parallel fibers also release NO, which spreads fast and triggers protein kinase G (PKG) activation[112]. PKG inhibits protein phosphatases that dephosphorylate AMPA receptors. Blocking the dephosphorylation promotes the action of PKC causing AMPA internalization[113]. Recently it has been shown that LTD is also highly dependent on calcium/calmodulin dependent protein kinase II (CamKII). Activation of CamKII is long lasting and appears to regulate the internalization of AMPA receptors, therefore it is crucial for long–term depression. In Purkinje cells one of the CamKII isoforms (βCamKII) is very profoundly expressed. Mice in which βCamKII was deleted show a peculiar phenotype. The LTD induction protocol fails to elicit the long–term depression but it triggers the potentiation instead[108]. Most probably this happens due to above mentioned competition between kinases and phosphatases, specifically the phosphatase PP2B. In the absence of βCamKII, PP2B out–competes other CamKII isomorphs and induces LTP. Notably, LTD can also be modulated by climbing fiber bursts[82]. The generation and impact of the climbing fiber burst was explained in the section dedicated to complex spike generation. As mentioned in the introduction to this paragraph, the very new addition to the LTD picture is the role of NMDA receptors. It has been shown that in adult animals there is a switch from AMPA to NMDA dependent LTD[7]. It is a finding that is quite surprising and definitely needs to be investigated further.

Parallel fiber long term potentiation (PF–LTP)

Contrary to the results obtained in the first *in vitro* experiments performed in the 70's and 80's parallel fiber to Purkinje cell synapse can also be potentiated. In fact, it was demonstrated that LTP and LTD are not two separate mechanisms but they occur interchangeably, depending on the intracellular calcium concentration[107]. Due to the fact that this mechanism was discovered relatively lately there are still a lot of blank spots on the cerebellum LTP map. What is known is that LTP occurs at low calcium concentration, which is opposite to what happens at glutamate synapses in for example hippocampus. In that respect Purkinje cells are unique because they behave contrary to the BCM rule. The BCM theory, named after Elie Bienenstock, Leon Cooper, and Paul Munro, is a theory of learning developed primarily in the visual cortex in 1981. It predicts that a synapse will get potentiated when the input is strong and attenuated at weak input. In Purkinje cells however a robust depolarization caused by simultaneous climbing and parallel fiber stimulation causes LTD whereas the weak stimulation of parallel fiber alone triggers LTP. One of the proteins that are involved in the induction of PF–LTP is protein phosphatase 2B. The idea for a possible role for this protein came from the "inverse" action of CamKII in the cerebellum. In other parts of the brain they are involved in the induction of LTP, however as described before, in the cerebellum they trigger LTD. Since it was known that phosphatases are important for pyramidal cell LTD[114] and given the "reverse mechanism" of plasticity induction in cerebellum, it seemed to be worth investigating what is their role in the cerebellum. In chapter 3 we will discuss in depth the role of PP2B in PF–LTP.

Climbing fiber long term depression (CF–LTD)

For a long time the climbing fiber to Purkinje cell synapse was considered to be invariant. It was believed that upon an activation of the climbing fiber Purkinje cells will always fire a large all–or–nothing action potential, that is independent of the strength of the climbing fiber stimulation[115]. However, in 2000 Hansel and Linden showed that the climbing fiber synapse can also undergo plastic changes[116]. Following a short tetanization of the CF they observed a long term depression of CF–evoked excitatory postsynaptic currents (EPSCs). This change in current translates into reduction of the slow component of the complex spike, which could potentially change the axonal output of the Purkinje cell[67]. The CF–LTD also results in change in afterhyperpolarization (AHP), which in turn can prolong the complex spike pause, changing the action potential firing patterns. The experiments showed that the CF–LTD depends on many factors such as calcium transients, glutamate binding to mGluR1 receptors and PKC activation[116]. Further experiments showed that the CF–LTD is facilitated by corticotropin releasing factor (CRF) signaling, which acts by activating PKC and PKA[117]. Interestingly, the changes is the calcium transients evoked by the CF–LTD affect the polarity of the synaptic plasticity at parallel fiber to Purkinje cell synapse regulating both PF–LTP and PF–LTD[107]. This new role of climbing fiber input further proves that it is an unusual synapse, as it is capable not only to change the strength of the individual parallel fiber synapse but also to influence significantly dendritic calcium currents and dendritic integration and in result change the spike output of the Purkinje cell.

CF induced rebound of inhibition.

Activation of the climbing fiber and subsequent Purkinje cell depolarization causes a long term potentiation of $GABA_A$ synapses[118]. This form of inhibitory LTP is also known as rebound potentiation. It has been shown that after climbing fiber activation $GABA_A$ synapses are sensitized, which results in potentiation of IPSCs. Remarkably, a simultaneous activation of climbing fiber and inhibitory interneuron synapses can suppress the rebound potentiation[119]. Possibly this phenomenon is mediated presynapticaly by glutamate activation of AMPA receptors on interneuron axonal terminals[120]. That means that climbing fiber activation could suppress any coinciding inhibition, facilitating the effect of inhibition following the CF activation. These findings support the importance of interneuron to Purkinje cell synapses. As previously described inhibition has been shown to have a major effect on Purkinje cell spiking. Not only can a single action potential, evoked in inhibitory interneurons, generate delays in Purkinje cell firing, but also tonic inhibitory input can drastically modulate the spike firing pattern in Purkinje cells[40]. The modulatory influence of climbing fiber on interneuron synapse could be crucial for introducing the timed suppression of simple spike firing during different motor tasks that was discussed in paragraph 1.3.3. This hypothesis will be further addressed in chapter 2.

1.4 Three hypothesis concerning cerebellar learning

In the last couple of decades cerebellar research has led to development of many theories on motor learning. Some of them were based strictly on observations whereas others were more abstract. Some aim to describe only one aspect of motor learning, such as for example eye–blink conditioning or VOR adaptation, others look for common substrates for all types of cerebellar related behavior. One of the oldest and probably best known is Marr–Albus theory of cerebellar motor learning. In the early 60s Marr suggested that the climbing fiber acts as a teacher signal calibrating the parallel fiber on Purkinje cell input[6]. A couple of years later Albus extended this theory stressing that in order to establish an accurate pattern recognition the olivary input should silence the parallel fiber input caring inappropriate information from the mossy fibers[84]. The Marr–Albus hypothesis was supported by the work of Ito[69,118] in the beginning of 80s describing the discovery of PF–LTD. Over the past 30 years there has been a lot of debate whether climbing fiber input indeed is the key to understanding how the cerebellum works. It seems that the hypothesis stating that the climbing fiber input is a teacher/error signal has as many supporters[76,121,86,107], as it has enemies[92,51]. There is a common agreement in the cerebellar community that climbing fiber input is essential for weakening parallel fiber input, however some researchers claim that it is not the “source” of changes occurring during motor learning. According to the latter studies PF–LTD is merely one of the synaptic changes in the cerebellar cortex and the actual learning takes place downstream in the deep cerebellar and vestibular nuclei. The model where cerebellum is reduced to the computing device relaying instructive signals downstream was proposed by Miles and Lisberger [122,123] in 1981. Those two theories are in clear opposition to each other since they propose different sites for plasticity and different explanations for changes in Purkinje cells observed during motor tasks. Not too surprisingly the body of work of the last 3 decades provided evidence for and against both of those theories. One of the weakest points of the Marr–Albus hypothesis is the low frequency of CS firing. It seemed implausible that motor commands that have to be readjusted on millisecond basis could be based on signals that occur approximately once per second (1Hz). However, recent findings suggest that CS can carry more signal that simply all–or–nothing response[82] and that climbing fiber can relay the phase of the olivary oscillations providing the phase–dependent changes on the parallel fiber input. Furthermore, there is evidence that climbing fibers may not only influence parallel fiber but also inhibitory interneuron synapses[21,32,120]. Additionally, climbing fiber signals do not only evoke complex spike in Purkinje cells but they also change the levels of intracellular calcium that are crucial for all plasticity occurring in the Purkinje cell[56,107,73,124]. The Miles–Lisberger model on the other hand, has been supported by experiments testing VOR adaptation. In the latter experiments elimination of climbing fiber signals did not abolish acquisition of the VOR adaptation[92] (however it did significantly reduce the amount of acquired learning). The authors conclude that the locus of learning must therefore be lying in brainstem structures. However, Miles–Lisberger model could not be applied to eye–blink conditioning. Chemical lesions to cerebellar cortex and/or cerebellar nuclei clearly showed that there are critical posttraining memory consolidation processes for eye–blink conditioning mediated by the cerebellar cortex[41,125].

In the light of above mentioned results, it becomes abundantly clear that neither of those theories can explain the wide range of motor behavior and learning. Recently a new model was reintroduced. Originally proposed by Fujita in 1982[126], it was based on Marr–Albus theory and described the cerebellum as an adaptive filter. According to this model Purkinje cell would adjust (filter) the input it gets from the granule cells by comparing it to the corresponding desired output signals. Unfortunately, in the early 80s, when Fujita's model was developed, it was believed that parallel to Purkinje cell synapses can only be silenced, which resulted in major computational limitations to this theory. The model being very theoretical could only at the time be applicable to sinusoidal stimulus and therefore was not regarded as valuable. Recently, in the light of evidence for symmetrical bidirectional plasticity at parallel fiber, interneuron plasticity and climbing fiber coding of fast olivary bursts, the adaptive filter model has been resurrected[127]. The detailed description of this model is outside the scope of this thesis so here it will only be briefly summarized. In short, the model states that the cerebellar microcircuit can be mapped onto an adaptive filter structure where mossy fiber inputs are analyzed (mediated by granular and Golgi cells) into parallel fiber component signals, which are then weighted and restructured to form the filter output (Purkinje cell spiking pattern). This filter is adaptive because the weights of the input can be adjusted (LTP and LTD) by a teacher signal carrying an error message (climbing fiber input). What is crucial is that the signal computed by the adaptive filter can be very versatile and depending on the information contained in the error signal it can be used for sensory signal processing, motor control and motor adaptation. This could potentially resolve the long–lasting argument whether cerebellum solely contributes to the control of the motor behavior or whether it is also involved in cognitive processing[128,129]. Even though the adaptive filter theory takes under consideration all recent developments in the cerebellar field it is clear that more experiments are needed to validate it. In chapter 2 we will present data that support this model.

1.5 Scope of the Thesis

The cerebellum plays a key role in regulating motor behavior in learning. Since Purkinje cells are the sole output of the cerebellar cortex it is crucial to understand how different afferent inputs influence their intrinsic firing patterns. In this thesis, we investigate certain aspects of both excitatory and inhibitory connections in the cerebellar cortex.

Chapter 2 explores the importance of commissural connections in the inferior olive that enable the climbing fibers to cross the midline relaying inputs from the contralateral olive. We investigate whether the disruption of the lateralization of the climbing fibers causes more profound impairment than having no cerebellar output at all. In this Chapter we also tackle the question – What is the role of climbing fiber input in reciprocal pattern of Purkinje cell firing during optical stimulation? Our results show that it is the CF input that drives reciprocity of Purkinje cell firing.

Chapter 3 provides new insights into the role of LTP at the parallel fiber to Purkinje cell synapse. Using Purkinje cell specific PP2B knockout mice, we try to answer the question – What is the role of postsynaptic LTP in cerebellar motor control and learning? We show, that ablation of PP2B results in loss of parallel fiber to Purkinje cell LTP. Furthermore, we found that blocking the PF–PC LTP results in profound motor learning deficits and increased simple spike regularity.

In Chapter 4 we turn our interest to the inhibitory input to Purkinje cells. Here we shed light on a long standing query whether interneurons are involved in cerebellar motor learning and if so what phase of the learning process are they crucial for? In two different animal models in which inhibition onto Purkinje cells was ablated we found deficits in long–term VOR adaptation suggesting that the molecular layer interneurons have a profound role in consolidation of motor learning. We also show that the lack of inhibitory input affects the temporal patterns of Purkinje cell simple spike firing, increasing spiking regularity. Moreover, we also found that Golgi cell inhibition of granule cells is important for consolidation of phase but not gain.

In Chapter 5 we investigated whether exposing the animal to a cerebellar learning paradigm has an impact on Purkinje cell spiking patterns. We chose the VOR phase reversal as our long–term adaptation paradigm and studied the firing behavior of Purkinje cells in the flocculus before and after application of the learning protocol. Here we focused on the reciprocal relationship between complex and simple spikes and found that after application of learning paradigm, the amplitude of the simple and complex spike modulation is increased.

Chapter 6 provides a description of the experimental procedures applied in this thesis. Chapter 7 consists of a general discussion of the role of climbing fiber, parallel fiber and interneuron inputs on Purkinje cell in the light of the Marr–Albus theory and the adaptive filter model. Future research directions are discussed in Chapter 7 as well.

References

1. Ito, M. Historical review of the significance of the cerebellum and the role of Purkinje cells in motor learning. *Ann N Y Acad Sci* **978**, 273-88 (2002).
2. Fine, E.J., Ionita, C.C. & Lohr, L. The history of the development of the cerebellar examination. *Semin Neurol* **22**, 375-84 (2002).
3. Ruigrok, T.J., Pijpers, A., Goedknegt-Sabel, E. & Coulon, P. Multiple cerebellar zones are involved in the control of individual muscles: a retrograde transneuronal tracing study with rabies virus in the rat. *Eur J Neurosci* **28**, 181-200 (2008).
4. Schonewille, M. et al. Zonal organization of the mouse flocculus: physiology, input, and output. *J Comp Neurol* **497**, 670-82 (2006).
5. Ito, M. Neural design of the cerebellar motor control system. *Brain Res* **40**, 81-4 (1972).
6. Marr, D. A theory of cerebellar cortex. *J Physiol* **202**, 437-70 (1969).
7. Piochon, C., Levenes, C., Ohtsuki, G. & Hansel, C. Purkinje cell NMDA receptors assume a key role in synaptic gain control in the mature cerebellum. *J Neurosci* **30**, 15330-5.
8. Piochon, C. et al. NMDA receptor contribution to the climbing fiber response in the adult mouse Purkinje cell. *J Neurosci* **27**, 10797-809 (2007).
9. Chan-Palay, V. Cerebellar Dentate Nucleus. *Springer-Verlag, New York* (1977).
10. Wulff, P. et al. Synaptic inhibition of Purkinje cells mediates consolidation of vestibulo-cerebellar motor learning. *Nat Neurosci* **12**, 1042-9 (2009).
11. De Schutter, E. & Bjaalie, J.G. Coding in the granular layer of the cerebellum. *Prog Brain Res* **130**, 279-96 (2001).
12. D'Angelo, E. et al. The cerebellar network: From structure to function and dynamics. *Brain Res Rev*.
13. Ekerot, C.F. & Jorntell, H. Synaptic integration in cerebellar granule cells. *Cerebellum* **7**, 539-41 (2008).
14. Ruigrok, T.J. Collateralization of climbing and mossy fibers projecting to the nodulus and flocculus of the rat cerebellum. *J Comp Neurol* **466**, 278-98 (2003).
15. D'Angelo, E. & De Zeeuw, C.I. Timing and plasticity in the cerebellum: focus on the granular layer. *Trends Neurosci* **32**, 30-40 (2009).
16. Jaeger, D. & Bower, J.M. Prolonged responses in rat cerebellar Purkinje cells following activation of the granule cell layer: an intracellular in vitro and in vivo investigation. *Exp Brain Res* **100**, 200-14 (1994).
17. Ekerot, C.F. & Jorntell, H. Parallel fibre receptive fields of Purkinje cells and interneurons are climbing fibre-specific. *Eur J Neurosci* **13**, 1303-10 (2001).
18. Napper, R.M. & Harvey, R.J. Quantitative study of the Purkinje cell dendritic spines in the rat cerebellum. *J Comp Neurol* **274**, 158-67 (1988).
19. Hansel, C. et al. alphaCaMKII Is essential for cerebellar LTD and motor learning. *Neuron* **51**, 835-43 (2006).
20. Boyden, E.S., Katoh, A. & Raymond, J.L. Cerebellum-dependent learning: the role of multiple plasticity mechanisms. *Annu Rev Neurosci* **27**, 581-609 (2004).
21. Jorntell, H. & Ekerot, C.F. Receptive field plasticity profoundly alters the cutaneous parallel fiber synaptic input to cerebellar interneurons in vivo. *J Neurosci* **23**, 9620-31 (2003).
22. Eccles, J.C., Llinas, R., Sasaki, K. & Voorhoeve, P.E. Interaction experiments on the responses evoked in Purkinje cells by climbing fibres. *J Physiol* **182**, 297-315 (1966).
23. Voogd, J. & Glickstein, M. The anatomy of the cerebellum. *Trends Neurosci* **21**, 370-5 (1998).
24. Ruigrok, T.J. Ins and Outs of Cerebellar Modules. *Cerebellum*.
25. Sugihara, I., Wu, H. & Shinoda, Y. Morphology of single olivocerebellar axons labeled with biotinylated dextran amine in the rat. *J Comp Neurol* **414**, 131-48 (1999).
26. Silver, R.A., Momiyama, A. & Cull-Candy, S.G. Locus of frequency-dependent depression

identified with multiple-probability fluctuation analysis at rat climbing fibre-Purkinje cell synapses. *J Physiol* **510 (Pt 3)**, 881-902 (1998).

27. Eccles, J.C., Llinas, R. & Sasaki, K. The inhibitory interneurones within the cerebellar cortex. *Exp Brain Res* **1**, 1-16 (1966).
28. Jorntell, H., Bengtsson, F., Schonewille, M. & De Zeeuw, C.I. Cerebellar molecular layer interneurons - computational properties and roles in learning. *Trends Neurosci* **33**, 524-32.
29. Bower, J.M. Model-founded explorations of the roles of molecular layer inhibition in regulating purkinje cell responses in cerebellar cortex: more trouble for the beam hypothesis. *Front Cell Neurosci* **4**.
30. Mittmann, W., Koch, U. & Hausser, M. Feed-forward inhibition shapes the spike output of cerebellar Purkinje cells. *J Physiol* **563**, 369-78 (2005).
31. Szapiro, G. & Barbour, B. Multiple climbing fibers signal to molecular layer interneurons exclusively via glutamate spillover. *Nat Neurosci* **10**, 735-42 (2007).
32. Barmack, N.H. & Yakhnitsa, V. Functions of interneurons in mouse cerebellum. *J Neurosci* **28**, 1140-52 (2008).
33. Mittmann, W., Chadderton, P. & Hausser, M. Neuronal microcircuits: frequency-dependent flow of inhibition. *Curr Biol* **14**, R837-9 (2004).
34. Soler-Llavina, G.J. & Sabatini, B.L. Synapse-specific plasticity and compartmentalized signaling in cerebellar stellate cells. *Nat Neurosci* **9**, 798-806 (2006).
35. Rancillac, A. & Crepel, F. Synapses between parallel fibres and stellate cells express long-term changes in synaptic efficacy in rat cerebellum. *J Physiol* **554**, 707-20 (2004).
36. Liu, S.J., Lachamp, P., Liu, Y., Savtchouk, I. & Sun, L. Long-term synaptic plasticity in cerebellar stellate cells. *Cerebellum* **7**, 559-62 (2008).
37. S.L. Palay, S.L. & Chan-Palay, V. The Cerebellar Cortex. *Springer-Verlag, New York* (1974).
38. Bishop, G.A. An analysis of HRP-filled basket cell axons in the cat's cerebellum. I. Morphometry and configuration. *Anat Embryol (Berl)* **188**, 287-97 (1993).
39. Bishop, G.A., Chen, Y.F., Burry, R.W. & King, J.S. An analysis of GABAergic afferents to basket cell bodies in the cat's cerebellum. *Brain Res* **623**, 293-8 (1993).
40. Hausser, M. & Clark, B.A. Tonic synaptic inhibition modulates neuronal output pattern and spatiotemporal synaptic integration. *Neuron* **19**, 665-78 (1997).
41. Attwell, P.J., Ivarsson, M., Millar, L. & Yeo, C.H. Cerebellar mechanisms in eyeblink conditioning. *Ann N Y Acad Sci* **978**, 79-92 (2002).
42. van Alphen, A.M., Stahl, J.S. & De Zeeuw, C.I. The dynamic characteristics of the mouse horizontal vestibulo-ocular and optokinetic response. *Brain Res* **890**, 296-305 (2001).
43. Stahl, J.S., van Alphen, A.M. & De Zeeuw, C.I. A comparison of video and magnetic search coil recordings of mouse eye movements. *J Neurosci Methods* **99**, 101-10 (2000).
44. Lisberger, S.G. & Fuchs, A.F. Response of flocculus Purkinje cells to adequate vestibular stimulation in the alert monkey: fixation vs. compensatory eye movements. *Brain Res* **69**, 347-53 (1974).
45. Raymond, J.L. & Lisberger, S.G. Error signals in horizontal gaze velocity Purkinje cells under stimulus conditions that cause learning in the VOR. *Ann N Y Acad Sci* **781**, 686-9 (1996).
46. Collewijn, H. Optokinetic eye movements in the rabbit: input-output relations. *Vision Res* **9**, 117-32 (1969).
47. Voogd, J., Gerrits, N.M. & Ruigrok, T.J. Organization of the vestibulocerebellum. *Ann N Y Acad Sci* **781**, 553-79 (1996).
48. Robinson, D.A. The effect of cerebellectomy on the cat's bestibulo-ocular integrator. *Brain Res* **71**, 195-207 (1974).
49. Cannon, S.C. & Robinson, D.A. Loss of the neural integrator of the oculomotor system from

brain stem lesions in monkey. *J Neurophysiol* **57**, 1383-409 (1987).

50. Katoh, A., Yoshida, T., Himeshima, Y., Mishina, M. & Hirano, T. Defective control and adaptation of reflex eye movements in mutant mice deficient in either the glutamate receptor delta2 subunit or Purkinje cells. *Eur J Neurosci* **21**, 1315-26 (2005).
51. Raymond, J.L., Lisberger, S.G. & Mauk, M.D. The cerebellum: a neuronal learning machine? *Science* **272**, 1126-31 (1996).
52. Barmack, N.H. et al. Cerebellar nodulectomy impairs spatial memory of vestibular and optokinetic stimulation in rabbits. *J Neurophysiol* **87**, 962-75 (2002).
53. Raman, I.M. & Bean, B.P. Resurgent sodium current and action potential formation in dissociated cerebellar Purkinje neurons. *J Neurosci* **17**, 4517-26 (1997).
54. Raman, I.M. & Bean, B.P. Ionic currents underlying spontaneous action potentials in isolated cerebellar Purkinje neurons. *J Neurosci* **19**, 1663-74 (1999).
55. Thach, W.T., Jr. Somatosensory receptive fields of single units in cat cerebellar cortex. *J Neurophysiol* **30**, 675-96 (1967).
56. Belmeguenai, A. et al. Intrinsic plasticity complements long-term potentiation in parallel fiber input gain control in cerebellar Purkinje cells. *J Neurosci* **30**, 13630-43.
57. Clark, B.A., Monsivais, P., Branco, T., London, M. & Hausser, M. The site of action potential initiation in cerebellar Purkinje neurons. *Nat Neurosci* **8**, 137-9 (2005).
58. Kuruma, A., Inoue, T. & Mikoshiba, K. Dynamics of Ca(2+) and Na(+) in the dendrites of mouse cerebellar Purkinje cells evoked by parallel fibre stimulation. *Eur J Neurosci* **18**, 2677-89 (2003).
59. Akemann, W. & Knopfel, T. Interaction of Kv3 potassium channels and resurgent sodium current influences the rate of spontaneous firing of Purkinje neurons. *J Neurosci* **26**, 4602-12 (2006).
60. Isope, P. & Murphy, T.H. Low threshold calcium currents in rat cerebellar Purkinje cell dendritic spines are mediated by T-type calcium channels. *J Physiol* **562**, 257-69 (2005).
61. Hausser, M. et al. The beat goes on: spontaneous firing in mammalian neuronal microcircuits. *J Neurosci* **24**, 9215-9 (2004).
62. Robinson, R.B. & Siegelbaum, S.A. Hyperpolarization-activated cation currents: from molecules to physiological function. *Annu Rev Physiol* **65**, 453-80 (2003).
63. Isope, P., Franconville, R., Barbour, B. & Ascher, P. Repetitive firing of rat cerebellar parallel fibres after a single stimulation. *J Physiol* **554**, 829-39 (2004).
64. Takechi, H., Eilers, J. & Konnerth, A. A new class of synaptic response involving calcium release in dendritic spines. *Nature* **396**, 757-60 (1998).
65. Hoebeek, F.E. et al. Increased noise level of purkinje cell activities minimizes impact of their modulation during sensorimotor control. *Neuron* **45**, 953-65 (2005).
66. Eccles, J.C., Llinas, R. & Sasaki, K. The excitatory synaptic action of climbing fibres on the purinje cells of the cerebellum. *J Physiol* **182**, 268-96 (1966).
67. Schmolesky, M.T., Weber, J.T., De Zeeuw, C.I. & Hansel, C. The making of a complex spike: ionic composition and plasticity. *Ann N Y Acad Sci* **978**, 359-90 (2002).
68. Davie, J.T., Clark, B.A. & Hausser, M. The origin of the complex spike in cerebellar Purkinje cells. *J Neurosci* **28**, 7599-609 (2008).
69. Ito, M. The modifiable neuronal network of the cerebellum. *Jpn J Physiol* **34**, 781-92 (1984).
70. Stuart, G. & Hausser, M. Initiation and spread of sodium action potentials in cerebellar Purkinje cells. *Neuron* **13**, 703-12 (1994).
71. Vetter, P., Roth, A. & Hausser, M. Propagation of action potentials in dendrites depends on dendritic morphology. *J Neurophysiol* **85**, 926-37 (2001).
72. Hansel, C. Reading the clock: how Purkinje cells decode the phase of olivary oscillations. *Neuron* **62**, 308-9 (2009).

73. Womack, M.D. & Khodakhah, K. Somatic and dendritic small-conductance calcium-activated potassium channels regulate the output of cerebellar Purkinje neurons. *J Neurosci* **23**, 2600-7 (2003).

74. De Zeeuw, C.I., Wylie, D.R., Stahl, J.S. & Simpson, J.I. Phase relations of Purkinje cells in the rabbit flocculus during compensatory eye movements. *J Neurophysiol* **74**, 2051-64 (1995).

75. Dittman, J.S. & Regehr, W.G. Calcium dependence and recovery kinetics of presynaptic depression at the climbing fiber to Purkinje cell synapse. *J Neurosci* **18**, 6147-62 (1998).

76. De Zeeuw, C.I. et al. Microcircuitry and function of the inferior olive. *Trends Neurosci* **21**, 391-400 (1998).

77. Llinas, R., Baker, R. & Sotelo, C. Electrotonic coupling between neurons in cat inferior olive. *J Neurophysiol* **37**, 560-71 (1974).

78. Van Der Giessen, R.S. et al. Role of olivary electrical coupling in cerebellar motor learning. *Neuron* **58**, 599-612 (2008).

79. Llinas, R. & Yarom, Y. Properties and distribution of ionic conductances generating electroresponsiveness of mammalian inferior olivary neurones in vitro. *J Physiol* **315**, 569-84 (1981).

80. Khosrovani, S., Van Der Giessen, R.S., De Zeeuw, C.I. & De Jeu, M.T. In vivo mouse inferior olive neurons exhibit heterogeneous subthreshold oscillations and spiking patterns. *Proc Natl Acad Sci U S A* **104**, 15911-6 (2007).

81. Goossens, J. et al. Expression of protein kinase C inhibitor blocks cerebellar long-term depression without affecting Purkinje cell excitability in alert mice. *J Neurosci* **21**, 5813-23 (2001).

82. Mathy, A. et al. Encoding of oscillations by axonal bursts in inferior olive neurons. *Neuron* **62**, 388-99 (2009).

83. Hong, S. & De Schutter, E. Purkinje neurons: What is the signal for complex spikes? *Curr Biol* **18**, R969-71 (2008).

84. Albus, J.S. A theory of cerebellar function *Mathematical Biosciences* **10**, 25-61 (1971).

85. Welsh, J.P., Lang, E.J., Suglhara, I. & Llinas, R. Dynamic organization of motor control within the olivocerebellar system. *Nature* **374**, 453-7 (1995).

86. Barmack, N.H. & Yakhnitsa, V. Vestibularly evoked climbing-fiber responses modulate simple spikes in rabbit cerebellar Purkinje neurons. *Ann N Y Acad Sci* **978**, 237-54 (2002).

87. Yakhnitsa, V. & Barmack, N.H. Antiphasic Purkinje cell responses in mouse uvula-nodulus are sensitive to static roll-tilt and topographically organized. *Neuroscience* **143**, 615-26 (2006).

88. Simpson, J.I., Wylie, D.R. & De Zeeuw, C.I. On climbing fiber signals and their consequence(s). . *BehBrain Sciences* **19**, 380-394 (1996).

89. Precht, W., Simpson, J.I. & Llinas, R. Responses of Purkinje cells in rabbit nodulus and uvula to natural vestibular and visual stimuli. *Pflugers Arch* **367**, 1-6 (1976).

90. Simpson, J.I., Belton, T., Suh, M. & Winkelman, B. Complex spike activity in the flocculus signals more than the eye can see. *Ann N Y Acad Sci* **978**, 232-6 (2002).

91. Maekawa, K. & Simpson, J.I. Climbing fiber activation of Purkinje cells in the flocculus by impulses transferred through the visual pathway. *Brain Res* **39**, 245-51 (1972).

92. Ke, M.C., Guo, C.C. & Raymond, J.L. Elimination of climbing fiber instructive signals during motor learning. *Nat Neurosci* **12**, 1171-9 (2009).

93. Tal, Z., Chorev, E. & Yarom, Y. State-dependent modification of complex spike waveforms in the cerebellar cortex. *Cerebellum* **7**, 577-82 (2008).

94. Rokni, D. & Yarom, Y. State-dependence of climbing fiber-driven calcium transients in Purkinje cells. *Neuroscience* **162**, 694-701 (2009).

95. Schonewille, M. et al. Purkinje cells in awake behaving animals operate at the upstate

membrane potential. *Nat Neurosci* **9**, 459-61; author reply 461 (2006).

96. Miyashita, Y. & Nagao, S. Contribution of cerebellar intracortical inhibition to Purkinje cell response during vestibulo-ocular reflex of alert rabbits. *J Physiol* **351**, 251-62 (1984).

97. Miyashita, Y. & Nagao, S. Analysis of signal content of Purkinje cell responses to optokinetic stimuli in the rabbit cerebellar flocculus by selective lesions of brainstem pathways. *Neurosci Res* **1**, 223-41 (1984).

98. Montarolo, P.G., Raschi, F. & Strata, P. Are the climbing fibres essential for the Purkinje cell inhibitory action? *Exp Brain Res* **42**, 215-8 (1981).

99. Leonard, C.S. & Simpson, J.I. Simple spike modulation of floccular Purkinje cells during the reversible blockade of their climbing fibre afferents. In: Adaptive processes in visual and oculomotor systems (Keller EL, Zee DS, eds). 429:434. Oxford: Pergamon. (1986).

100. Orestes, P., Bojadzic, D., Chow, R.M. & Todorovic, S.M. Mechanisms and functional significance of inhibition of neuronal T-type calcium channels by isoflurane. *Mol Pharmacol* **75**, 542-54 (2009).

101. Study, R.E. Isoflurane inhibits multiple voltage-gated calcium currents in hippocampal pyramidal neurons. *Anesthesiology* **81**, 104-16 (1994).

102. Chen, X., Shu, S., Kennedy, D.P., Willcox, S.C. & Bayliss, D.A. Subunit-specific effects of isoflurane on neuronal Ih in HCN1 knockout mice. *J Neurophysiol* **101**, 129-40 (2009).

103. Hoebeek, F.E., Witter, L., Ruigrok, T.J. & De Zeeuw, C.I. Differential olivo-cerebellar cortical control of rebound activity in the cerebellar nuclei. *Proc Natl Acad Sci U S A* **107**, 8410-5.

104. Bengtsson, F. & Jorntell, H. Ketamine and xylazine depress sensory-evoked parallel fiber and climbing fiber responses. *J Neurophysiol* **98**, 1697-705 (2007).

105. Hevers, W., Hadley, S.H., Luddens, H. & Amin, J. Ketamine, but not phencyclidine, selectively modulates cerebellar GABA(A) receptors containing alpha6 and delta subunits. *J Neurosci* **28**, 5383-93 (2008).

106. Feuerstein, T.J. [Ketamine inhibits n-methyl-d-aspartate (NMDA) receptor mediated acetylcholine release from rabbit caudate nucleus slices]. *Anaesthesist* **43 Suppl 2**, S48-51 (1994).

107. Coesmans, M., Weber, J.T., De Zeeuw, C.I. & Hansel, C. Bidirectional parallel fiber plasticity in the cerebellum under climbing fiber control. *Neuron* **44**, 691-700 (2004).

108. van Woerden, G.M. et al. betaCaMKII controls the direction of plasticity at parallel fiber-Purkinje cell synapses. *Nat Neurosci* **12**, 823-5 (2009).

109. Hartell, N.A. Strong activation of parallel fibers produces localized calcium transients and a form of LTD that spreads to distant synapses. *Neuron* **16**, 601-10 (1996).

110. Reynolds, T. & Hartell, N.A. An evaluation of the synapse specificity of long-term depression induced in rat cerebellar slices. *J Physiol* **527 Pt 3**, 563-77 (2000).

111. Ito, M. The molecular organization of cerebellar long-term depression. *Nat Rev Neurosci* **3**, 896-902 (2002).

112. Reynolds, T. & Hartell, N.A. Roles for nitric oxide and arachidonic acid in the induction of heterosynaptic cerebellar LTD. *Neuroreport* **12**, 133-6 (2001).

113. Chung, H.J., Steinberg, J.P., Huganir, R.L. & Linden, D.J. Requirement of AMPA receptor GluR2 phosphorylation for cerebellar long-term depression. *Science* **300**, 1751-5 (2003).

114. Isaac, J. Protein phosphatase 1 and LTD: synapses are the architects of depression. *Neuron* **32**, 963-6 (2001).

115. Eccles, J., Llinas, R. & Sasaki, K. Excitation of Cerebellar Purkinje Cells by the Climbing Fibres. *Nature* **203**, 245-6 (1964).

116. Hansel, C. & Linden, D.J. Long-term depression of the cerebellar climbing fiber--Purkinje neuron synapse. *Neuron* **26**, 473-82 (2000).

117. Schmolesky, M.T., De Ruiter, M.M., De Zeeuw, C.I. & Hansel, C. The neuropeptide

corticotropin-releasing factor regulates excitatory transmission and plasticity at the climbing fibre-Purkinje cell synapse. *Eur J Neurosci* **25**, 1460-6 (2007).

118. Kano, M., Rexhausen, U., Dreessen, J. & Konnerth, A. Synaptic excitation produces a long-lasting rebound potentiation of inhibitory synaptic signals in cerebellar Purkinje cells. *Nature* **356**, 601-4 (1992).
119. Kawaguchi, S. & Hirano, T. Suppression of inhibitory synaptic potentiation by presynaptic activity through postsynaptic GABA(B) receptors in a Purkinje neuron. *Neuron* **27**, 339-47 (2000).
120. Satake, S., Saitow, F., Yamada, J. & Konishi, S. Synaptic activation of AMPA receptors inhibits GABA release from cerebellar interneurons. *Nat Neurosci* **3**, 551-8 (2000).
121. Ekerot, C.F. Climbing fibres - a key to cerebellar function. *J Physiol* **516 (Pt 3)**, 629 (1999).
122. Miles, F.A. & Lisberger, S.G. Plasticity in the vestibulo-ocular reflex: a new hypothesis. *Annu Rev Neurosci* **4**, 273-99 (1981).
123. Miles, F.A. & Lisberger, S.G. The “error” signals subserving adaptive gain control in the primate vestibulo-ocular reflex. *Ann N Y Acad Sci* **374**, 513-25 (1981).
124. Ohtsuki, G., Piochon, C. & Hansel, C. Climbing fiber signaling and cerebellar gain control. *Front Cell Neurosci* **3**, 4 (2009).
125. Attwell, P.J., Cooke, S.F. & Yeo, C.H. Cerebellar function in consolidation of a motor memory. *Neuron* **34**, 1011-20 (2002).
126. Fujita, M. Adaptive filter model of the cerebellum. *Biol Cybern* **45**, 195-206 (1982).
127. Dean, P., Porrill, J., Ekerot, C.F. & Jorntell, H. The cerebellar microcircuit as an adaptive filter: experimental and computational evidence. *Nat Rev Neurosci* **11**, 30-43.
128. Bower, J.M. & Parsons, L.M. Rethinking the “lesser brain”. *Sci Am* **289**, 50-7 (2003).
129. Thach, W.T. On the mechanism of cerebellar contributions to cognition. *Cerebellum* **6**, 163-7 (2007).

CHAPTER 2

CLIMBING FIBER INPUT

CHAPTER 2
PARAGRAPH 1

DISRUPTION OF COMMISSURAL CONNECTIONS IN THE INFERIOR OLIVE CAUSES MORE PROFOUND IMPAIRMENT THAN HAVING NO CEREBELLAR OUTPUT AT ALL

*Extract from PLoS Biol***. 2010 Mar 9;8(3):e1000325.**
Renier N, Schonewille M, Giraudet F, Badura A, Tessier-Lavigne M, Avan P, De Zeeuw CI, Chédotal A.

Introduction

The physiological importance of commissures is well established for the forebrain where the consequence of lesions has been extensively studied by Roger Sperry and colleagues in the 1960's. In contrast, the function of hindbrain and spinal cord commissures is largely unknown as no one has yet been able to genetically disrupt the commissural connections in a region specific manner. Here, we investigated the role of the inferior olive axonal commissure by means of deletions of the *Robo3* receptor (a vertebrate roundabout receptor) using the Cre-lox system with the *PTF1a* promotor (*Ptf1a::cre;Robo3*$^{lox/lox}$ mice). We examined the neuro-anatomical and neuro-physiological consequences of these manipulations and their significance in cerebellar motor performance. The olivary axons were rerouted and remained, in contrast to those of controls, largely ipsilateral. However their axon terminals (climbing fibers) reached and innervated their appropriate neuronal targets, namely Purkinje cells and cerebellar nuclei. By using a variety of behavioral tests including eye movement measurements, Rotarod and Erasmus Ladder, we found that mice with a primarily ipsilateral climbing fiber/Purkinje cell projection are strongly ataxic. Interestingly, the selective reduction of the interolivary commissure in the *Ptf1a::cre;Robo3*$^{lox/lox}$ mice also resulted in a stronger locomotion impairment than in the *Lurcher* mutant mice that have no output from the cerebellar cortex. Thus, our results suggest that having only one component of a cerebellar circuitry misrouted may evoke behavioral effects that are functionally worse than having no output at all. To our knowledge, this study is the first to link defects in commissural axon guidance in hindbrain with specific cellular and behavioral phenotypes.

Results

Inferior olivary neurons (IO neurons) are the source of climbing fiber input on cerebellar Purkinje cells. During development, IO neurons migrate tangentially from the rhombic lip towards the floor plate. Upon reaching the floor plate, IO neuron cell bodies stop and only their axons cross it. We showed previously that IO axons are unable to cross the midline in Robo3-/- embryos and, consequently, project to the ipsilateral cerebellum[1]. However, the functional consequence of this ipsilateral rerouting of IO axons was unknown. To attempt to generate mice lacking the interolivary commissure, we crossed Robo3lox/lox conditional knockout with mice in which Cre recombinase was knocked into the Ptf1a (Ptf1-p48) locus (Ptf1a::cre)[2], which encodes a bHLH transcription factor expressed by a majority of IO neuron progenitors. In the resulting Ptf1a::cre;Robo3lox/lox and control mice, the size of the cerebellum and its foliation were similar (**Figure 1D,E and A,B respectively**). Immunostaining with antibodies specific for the different types of cerebellar cortex neurons failed to reveal any differences between mutants and controls (n = 3/3). Furthermore, the morphology and the distribution of Purkinje cells, molecular layer interneurons, and granule cells was unaffected (**Figure 2**), and their climbing fibers arborized normally on Purkinje cell dendrites (**Figure 1C,F**). However, when DiI was injected unilaterally in the cerebellum of newborn controls, it retrogradely labelled IO neurons exclusively on the side opposite to the injection in control mice (4 out of 4 cases; **Figure 1G**), whereas in Ptf1a::cre;Robo3lox/lox mice (8/8 cases; **Figure 1H**) about 67% of the DiI-labelled IO neurons were situated on the side of the injection. However, 33% of the olivary axons still project contralaterally.

Immunolabeling of E13 Ptf1a::cre;Robo3lox/lox embryos (n = 4) with antibodies to Brn3.2, a marker of a large subset of IO neurons, showed that, as previously described in Robo3-/- mice, the ipsilateral IO projection did not result from a migration of IO cell bodies across the midline (**Figure 3**). The use of multiple IO neuron markers (Brn3.2, CaBP, BEN/SC1, CGRP) revealed that the lamellar organization of the IO was perturbed in Ptf1a::cre;Robo3lox/lox mice (**Figure 3**), whereas the mossy fiber inputs and their neuronal sources developed normally (**Figure 2**).

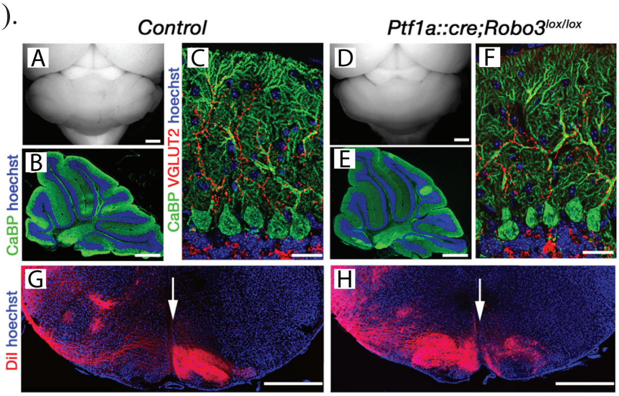

Figure 1. Uncrossed inferior olivary reach their axonal targets. (A to H) These panels show that the cerebellum morphology in the mutants is comparable to that in controls (A to C) and Ptf1a::cre;Robo3lox/lox mice (D to F) and that climbing fibers (the terminal arbors of inferior olivary axons) innervate the cerebellar cortex. (C, F) The size of the cerebellum and its foliation are similar as shown on sagittal sections of P32 control and Ptf1a::cre;Robo3lox/lox mice labelled with anti-calbindin antibodies and hoechst. (C, F) VGLUT2-positive climbing fibers properly innervate CaBP+ Purkinje cell dendrites. (G, H) Coronal sections of P1 mice with unilateral injection of DiI in the cerebellum. The arrow marks the midline. In control (G) DiI-labelled inferior olivary (IO) neurons are exclusively found on the contralateral side, whereas in Ptf1a::cre;Robo3lox/lox mice (H), most IO neurons are traced on the ipsilateral side and their axons don't cross the midline.

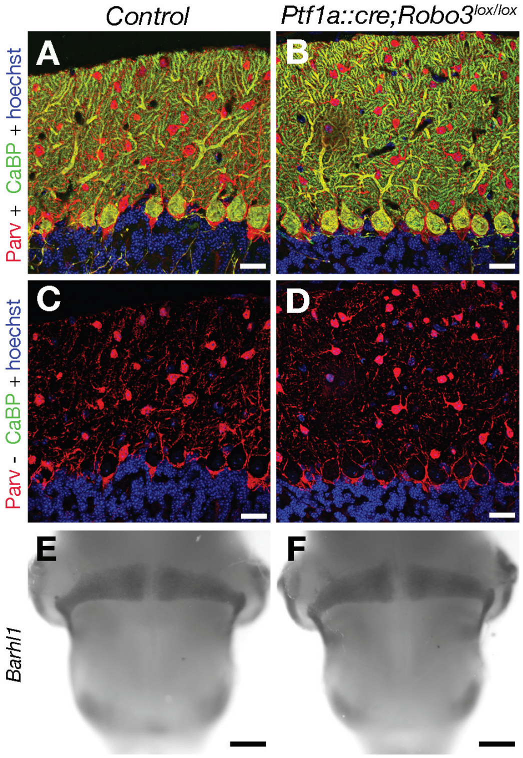

Figure 2. Normal cerebellar cortex and pontine nuclei in Ptf1a::cre;Robo3loxl/ox mice. (A to D) sagittal sections of the cerebellar cortex of P32 Control (A, C) and Ptf1a::cre;Robo3loxl/ox mice (B, D) labelled with antibodies against parvalbumine (Parv) and calbindin (CaBP) and counterstained with hoechst. Purkinje cells coexpress the two proteins whereas molecular layer interneurons only express parvalbumine. C and D were obtained by substraction of the calbindin channel (green) from the parvalbumin channel (red). The morphology of Purkinje cells and the density of molecular layer interneurons are similar. (E, F) are ventral view of whole-mount hindbrain of E15 embryos hybridized with Barhl1 riboprobe. The stream of migrating pontine neurons (arrowheads) is comparable. Scale bars are 25 µm, except E, F: 500 µm

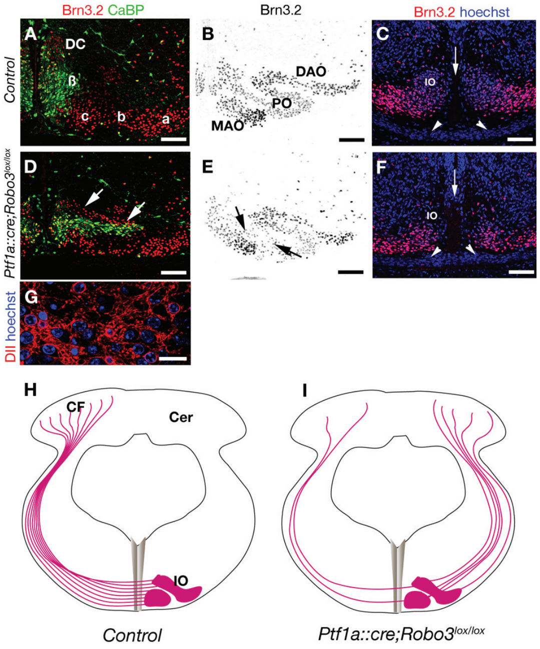
Brn3.2 CaBP
Brn3.2
Brn3.2 hoechst
A
DC
ß
c
b
a
Control
B
DAO
PO
MAO
C
IO
D
Ptf1a::cre;Robo3lox/lox
E
F
IO
G
DiI hoechst
H
CF
Cer
IO
I
Control
Ptf1a::cre;Robo3lox/lox

Figure 3. Phenotype of inferior olivary neurons in Ptf1a::cre;Robo3loxl/ox mice. (A to F) Coronal sections of P0 (A, B, D, E) and E13.5 (C, F) hindbrain at the level of the inferior olive labelled with Brn3.2 (A-F) and Calbindin (A, D). The structure of the inferior olivary nucleus is disorganized in Ptf1a::cre;Robo3loxl/ox mice (compare A and B with D and E) and many of its subdivisions have an abnormal shape. The arrows in (D) show the position of dorsal cap of Kooy (DC in A) and the ß-nucleus (ß in A) neurons, and the arrows in E indicate the disorganized principal olive (PO in B). (C, F) Brn3.2+ IO neurons do not cross the midline (arrow) in either control (C) or Ptf1a::cre;Robo3loxl/ox (F) embryos. The arrowheads point to migrating LRN neurons. (G) is a 1.16 µm thick confocal image of DiI-labelled IO neurons in control P0 mouse with hoechst counterstaining. (H, I) schematic representation of the olivocerebellar projection in control (H) and Ptf1a::cre;Robo3lox/lox mice (I). In control, all IO neurons project across the ventral midline to the contralateral cerebellum (Cer) where their terminal arborization, the climbing fibers (CF), synapse on Purkinje cells. In Ptf1a::cre;Robo3lox/lox mice, most IO axons project into the ipsilateral cerebellar cortex. Scale bars are 100 µm, except G, 20 µm. Abbreviations: MAO, medial accessory olive; DAO, dorsal accessory olive; a, b, c: subnuclei a, b and c of the MAO; DC, Dorsal Cap of Kooy

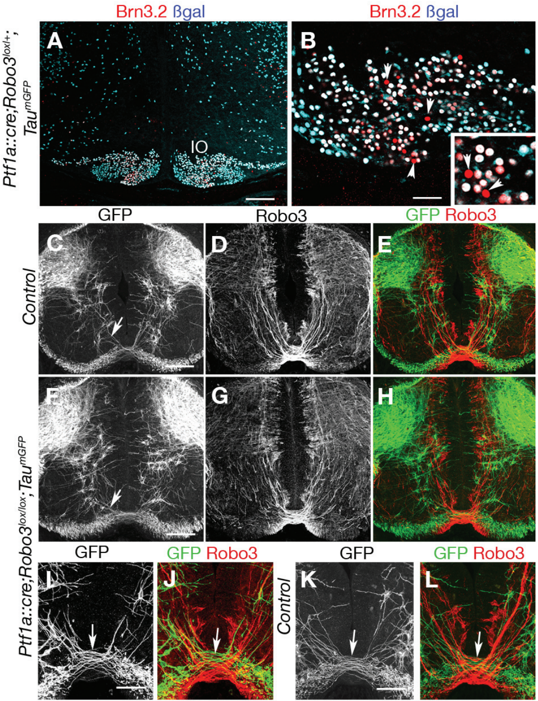
Brn3.2 ßgal
Brn3.2 ßgal
Ptf1a::cre;Robo3lox/+;TaumGFP
A
IO
B
GFP
Robo3
GFP Robo3
Control
C
D
E
F
G
H
Ptf1a::cre;Robo3lox/lox;TaumGFP
GFP
GFP Robo3
GFP
GFP Robo3
I
J
Control
K
L

Figure 4. Analysis of Ptf1a::cre;Robo3lox/lox;TaumGFP mice. (A, B) Coronal sections of the hindbrain at the level of inferior olive of E16 Ptf1a::cre;TaumGFP embryo labelled with anti-ßgal and Brn3.2 antibodies. Some Brn3.2 positive neurons in the inferior olive do not express the ßgal (arrowheads and inset). (C-L) Coronal sections of the spinal cord at the level of the forelimbs in E13 Ptf1a::cre;Robo3lox/+;TaumGFP (C-E, K, L) or Ptf1a::cre;Robo3lox/lox;TaumGFP (F-H, I, J) embryos labelled with anti-GFP and anti-Robo3 antibodies. Most GFP-positive axons are in the dorsal spinal cord and only a small subset of GFP-positive axons (short arrows) cross the floor plate in Ptf1a::cre;Robo3lox/+;TaumGFP (C, K) but don't express Robo3 (E, L). This subset of GFP-Positive commissural axons is still observed in Ptf1a::cre;Robo3lox/lox;TaumGFP embryos (F, J). Scale bars are 100µm except B, I-L 50µm.

To confirm that the ataxic behavior of Ptf1a::cre;Robo3lox/lox mice can primarily be attributed to the ipsilateral rerouting of a majority of olivo-cerebellar axons, we crossed these mice to a Tau-lox-Stop-lox-mGFP-IRES-nls-lacZ knock-in line[3] (here called TaumGFP). Upon Cre recombination in neurons, the Stop cassette is excised leading to the permanent expression of a myristoylated GFP in axons and of ß-galactosidase (ßgal) in nuclei. This strategy made it possible to identify the neurons that expressed Cre recombinase in the

Robo3lox background. In the inferior olive of Ptf1a::cre;Robo3lox/lox E16 embryos (n=3), we found that 87±2% of Brn3.2–positive neurons also expressed ßgal, but 13±2% of the Brn3.2-positive neurons were negative for ßgal (**Figure 4A, B**). This suggests that Cre is not expressed by all IO neurons in the Ptf1a::cre line, and could explain the maintenance of a contralateral contingent of IO axons in Ptf1a::cre;Robo3lox/lox animals (see discussion). To determine if Cre was expressed by spinal cord commissural neurons during midline crossing, we studied ßgal and GFP expression in the spinal cord of E11-E13 TaumGFP embryos (n=3 ; **Figure 4C-L**). We found that in the spinal cord of Ptf1a::cre;Robo3lox/+;TaumGFP E11-E13 embryos, GFP-expressing axons were not immunoreactive for Robo3 and that commissures were not GFP-positive, with the exception of a very small ventral subset of axons (**Figure 4** and not shown). Interestingly, this small subset of GFP axons still crossed the midline in Ptf1a::cre;Robo3lox/lox;TaumGFP embryos (**Figure 4**; n=3 ; see discussion). Moreover, Robo3-immunoreactive commissural neurons did not express ßgal (n=3 animals, data not shown).

The use of additional markers such as TAG-1 and neurofilament confirmed that spinal cord commissures were similar in control and Ptf1a::cre;Robo3lox/lox E13 embryos (**Figure 5**). As shown previously[4], in Ptf1a::cre;Robo3lox/+; TaumGFP E12-E16 embryos we could not detect ßgal expression in the main sources of mossy fiber projection, the pontine neurons, the external cuneatus nucleus or the lateral reticular nucleus (data not shown).

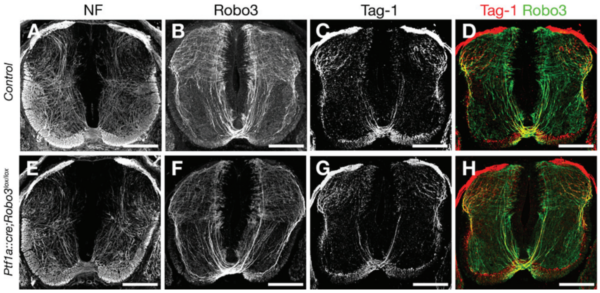

Figure 5. Normal spinal cord commissures in Ptf1a::cre;Robo3loxl/ox embryos. (A to H) are coronal section of the spinal cord of E13 embryos immunolabelled with neurofilament and Robo3 (A, B, E, F) or TAG-1 and Robo3 (C, D, G, H). Commissures are not reduced and still express Robo3 in Ptf1a::cre;Robo3loxl/ox mice. Scale bars are 200 µm.

The Ptf1a::cre;Robo3lox/lox mice were viable, until at least 7 months, but exhibited some profound locomotor deficits from P10 onwards (**Figure 6B**) and an ataxic gait (35/35 cases) that persisted in adulthood. When locomotion was tested on the Rotarod, Ptf1a::cre;Robo3lox/lox mice showed a significant deficit in motor performance (**Figure 6A**). The Ptf1a::cre;Robo3lox/lox mice fell off the Rotarod with significantly shorter latency than controls ($p < 0.001$, Mann-Whitney U-test, $n = 7$ mutants vs 9 controls). The impaired locomotion of our mutants on the rotarod was as strong as in the *Lurcher* mouse, a mouse mutant which is characterized by Purkinje cell degeneration[5]. On the more discriminative Erasmus Ladder[6], the ptf1a::cre;Robo3lox/lox mice show a significant deficit in motor performance (**Figure 6 C,D**). The steptime of these mice is severely impaired (ptf1a::cre;Robo3lox/lox vs. controls $p<0.001$ for all sessions; unpaired Student's t-test) as well as the overall walking pattern (% of failed trials ptf1a::cre;Robo3lox/lox vs. controls $p<0.01$ for all sessions; Mann-Whitney U-test). Interestingly, the motor performance of the ptf1a::cre;Robo3lox/lox mice is also significantly less than that of the *Lurcher* mice (steptime: $p<0.001$ for all sessions; t-test; % of failed trials $p<0.02$ for all sessions; Mann-Whitney U test), which lack virtually all Purkinje cells[7]. These findings indicate that rewiring of the CF projection causes more severe ataxia than the functional loss of the cerebellar cortex, suggesting a pathological dominant negative effect in the ptf1a::cre;Robo3lox/lox mice.

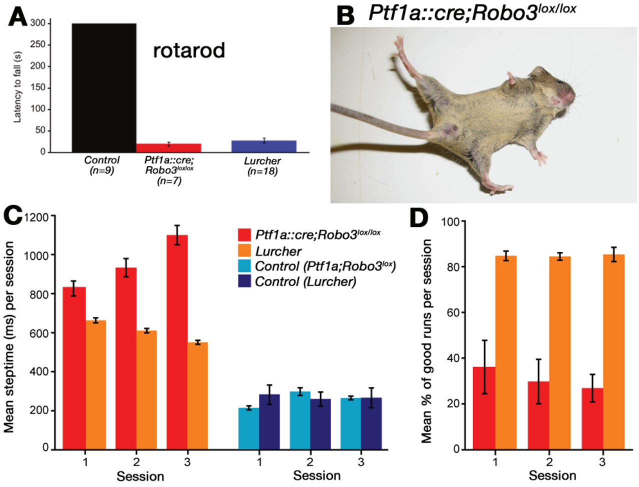

Figure 6. Uncrossed inferior olivary axons cause ataxic gait. (A) Ptf1a::cre;Robo3lox/lox mice are severely ataxic, which is demonstrated a very short latency to fall in the rotarod test (n = 7 mutants vs. n = 9 for controls). (B) image of a 4 month old Ptf1a::cre;Robo3lox/lox mouse displaying an ataxic gait. (C) Ptf1a::cre;Robo3lox/lox mice (red ; n = 6) have longer steptime on the Erasmus Ladder than the controls (blue ; n = 4 ; p<0.001; t-test) as well as the Lurcher mice (orange ; p<0.001; t-test). (D) Ptf1a::cre;Robo3lox/lox mice (red) also showed significantly less successful trials per session than the Lurcher mice (orange) (p=0.02 for session1, p<0.01 for session 2 and 3; Mann-Whitney U test). A trail was defined as successful, if the mice was able to walk on the ladder without disruption (twisting, turning, walking backwards etc.).

Discussion

We show that a *Robo3*-conditional allele can be used to genetically disrupt distinct commissural projections and force axons to project ipsilaterally. Commissure rewiring induces severe and permanent dysfunction of specific neuronal networks. Unlike surgical ablation of a given commissure, this strategy ends up rewiring commissural neurons on the ipsilateral side but does not interrupt the activity of the targeted circuit. We show that, ipsilaterally re-routed axons still connect to their proper targets.

Our results and others[1, 8], suggest that Robo3 expression is required for most, if not all, commissural axons to cross the floor plate throughout spinal cord and hindbrain. The persistence of commissural axons that continue to cross the floor plate in domains expected to express Cre recombinase in the *Robo3* conditional line presented here may be explained in a number of ways. One reason for incomplete rerouting of commissural axons is that Cre recombinase may not be expressed by all r3/r5 neurons, as is the case for inferior olivary neurons in *Ptf1a::cre;Robo3*$^{lox/lox}$ knockout. Secondly, Cre might be expressed too late, after these commissural axons have crossed, an hypothesis we favor to explain the persistence of the ventral subset of commissural axons in the spinal cord of *Ptf1a::cre;Robo3*$^{lox/lox}$ embryos.

Surprisingly, the *Ptf1a::cre;Robo3*$^{lox/lox}$ mice show a severe ataxic gait. In this line, spinal cord commissures and the corticospinal tract (unpublished data) do not seem to be affected and among embryonic precerebellar neurons, Cre recombinase is only expressed by inferior olivary neurons and not by mossy fiber projection neurons. Therefore, we think that the severe reduction of the interolivary commissure is sufficient to impair locomotion. Together, these results suggest that having only one component of a commissural circuit misrouted and uncrossed may be functionally worse than having all of its components affected, or, as the comparison with the *Lurchers* shows, having no output at all.

CHAPTER 2
PARAGRAPH 2

CLIMBING FIBER DRIVES RECIPROCITY OF PURKINJE CELL FIRING

Submitted

Aleksandra Badura, Martijn Schonewille, Zhenyu Gao, Galliano Elisa, Nicolas Renier, Kai Voges, Freek E. Hoebeek, Alain Chédotal, and Chris I. De Zeeuw

Summary paragraph

Purkinje-cells form the sole output of the cerebellar cortex. Unlike most other neurons in the brain[9] they produce two different types of spikes, complex-spikes and simple-spikes[10,11]. The complex-spikes result from activation of the climbing-fibers, whereas the simple-spikes are predominantly triggered by the other main afferent input to the cerebellar cortex, the mossy-fiber – parallel-fiber pathway[11]. The frequencies of these two types of spikes are often modulated reciprocally: an increase in complex-spikes is associated with a decrease in simple-spikes, and vice versa. This reciprocal firing behavior is thought to be essential for coordinated motor behavior[12-14], yet how it is accomplished is still debated[15]. Here, we show that rerouting the climbing-fiber system in *Ptf1a::cre;Robo3*$^{lox/lox}$ mice[16] from a purely contralateral to a predominantly ipsilateral projection reversed the complex-spike modulation during natural optokinetic stimulation. Even though the lateralization of the mossy-fiber system is unaffected in these mutants, the simple-spike modulation also reversed perfectly, leaving the reciprocal firing between complex-spikes and simple-spikes intact. The climbing-fibers enforce this reciprocity at least in part by influencing the connectivity between the parallel-fiber pathway and inhibitory interneurons of the molecular layer, because the phase of the interneuron activity was also reversed, and the peak of the interneuron activity coincided with a trough in the simple-spike firing frequency that was lower than in controls. The movements in *Ptf1a::cre;Robo3*$^{lox/lox}$ mice were severely affected in that their average timing and amplitude were abnormal and that the variability in the timing was increased. Together, these data indicate that by controlling the firing behavior of molecular interneurons and simple-spike activity in Purkinje-cells, the proper timing of the climbing-fiber input is essential for well-coordinated motor performance.

Introduction

The cerebellum has been proposed to operate as a phase lead-lag compensator with learning capabilities[13,17]. It has been hypothesized that the learning may be mediated by an adaptive process in which the climbing-fibers serve as a guide that filters the appropriate information out of a wide diversity of mossy-fiber inputs optimizing motor coordination[18]. If this adaptive filter hypothesis is correct, the climbing-fibers may also be responsible for the phenomenon of reciprocity, which is particularly evident during natural sensorimotor control[12,14]. For example, during control of optokinetic responses (OKR) to sinusoidal stimulation, complex-spike and simple-spike activities in Purkinje-cells of the vestibulocerebellum modulate out of phase with respect to each other[13,15]. So far, it has been difficult to find out whether the climbing-fiber input controls this enigmatic reciprocity, because it has been mind-bugling to manipulate the periodicity of the complex-spike activities without affecting their overall firing frequency, which induces changes in simple-spike firing by itself[15,19-21]. Here, we test the role of the climbing-fiber system in reciprocity control by investigating a mouse mutant (*Ptf1a::cre;Robo3*$^{lox/lox}$ mice), in which the inferior olive, the source of the climbing-fibers, is not blocked, but in which its climbing-fibers project to the ipsilateral, rather than the contralateral side[16]. With this design (**Fig.1a**), we hypothesized, it should be possible to shift the modulation of complex-spike activities without minimizing their overall firing frequency, and subsequently investigate the impact on the modulation of the simple-spikes.

Results

Ptf1a::cre;Robo3$^{lox/lox}$ mice were created by crossing floxed *Robo3* mice with mice that express *Cre* under the *PTF1a* promoter, which is active in olivary neurons[16]. Unilateral injections with retrograde tracers[22] in the flocculus of the vestibulocerebellum in *Ptf1a::cre;Robo3*$^{lox/lox}$ mice (n=6) revealed that 82% of the labeled olivary neurons were located ipsilaterally, against 0% in control mice (n=3) (**Fig.1b-d**). In contrast, lateralization of the mossy-fiber projections was not affected by the mutation (**Fig.1c**).

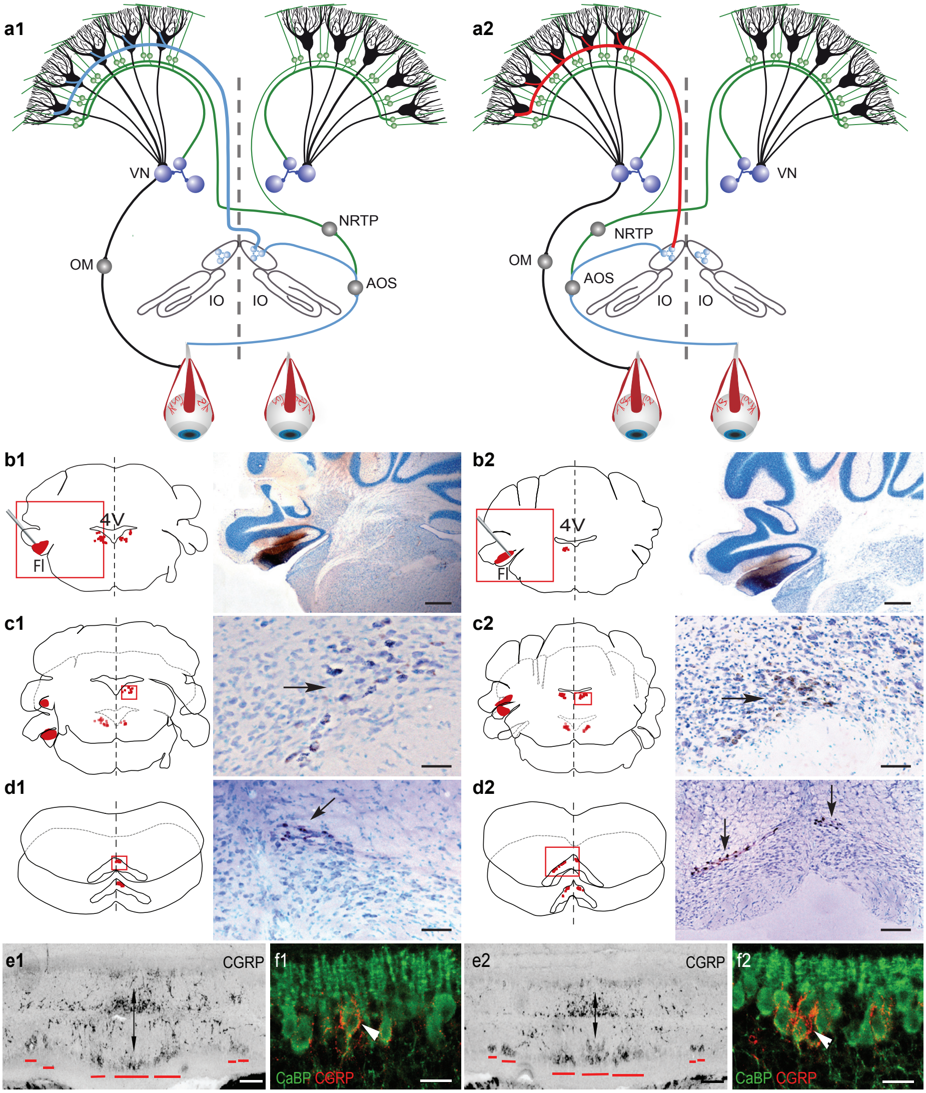

Figure 1. Olivary axons are rerouted from contralateral to ipsilateral in Ptf1a::cre;Robo3$^{lox/lox}$ mice. a1-a2, Schematic illustration of the olivocerebellar circuitry in controls (a1) compared to mutants (a2). b1-b2, Injections of retrograde tracers (cholera toxin B-subunit and gold-lectin) in the flocculus resulted in labeled cell-bodies (arrows) of mossy-fiber sources bilaterally in the vestibular nuclei (c1-c2) (ipsilateral: 59% in control vs. 58% in mutant). d1-d2, In contrast, in the inferior olive the vast majority of labeled cell-bodies (arrows) occurred ipsilaterally (82% in mutants vs. 0% in controls). e1-e2, In the vestibulocerebellar vermis of both controls and mutants symmetrical CGRP+ stripes of climbing-fibers (red lines) were observed. Arrow indicates midline. f1-f2, CGRP+ climbing-fibers (red staining) start to contact cell-bodies of calbindin+ Purkinje-cells (green staining) at P6. Scale bars at b1-b2 indicate 500µm; at c1 50µm; at c2 and d1 100µm; at d2 200µm; at e1-e2 150µm; and at f1-f2 25µm. See Supplementary Table 1 for details.

The ipsilateral climbing-fibers in the *Ptf1a::cre*;*Robo3*$^{lox/lox}$ mice appropriately targeted Purkinje-cells during their development as could be visualized with immunostaining for CGRP and calbindin[23] (**Fig.1e,f; Supplementary Table 1**). Moreover, the vast majority of Purkinje-cells in adult *Ptf1a::cre*;*Robo3*$^{lox/lox}$ mice showed a normal elimination of their surplus in climbing-fiber connections (**Supplementary Fig.1**). Together, these findings indicate that the climbing-fiber projections in *Ptf1a::cre;Robo3*$^{lox/lox}$ mice are successfully rerouted in that they innervate predominantly ipsilateral Purkinje-cells with a normal distribution after a normal development of synaptic contacts in the cerebellar cortex.

When we subjected *Ptf1a::cre;Robo3*$^{lox/lox}$ mice to sinusoidal optokinetic stimulation (**Fig.2a**), the complex-spike activities of their floccular Purkinje-cells[24] modulated robustly at all frequencies tested (0.1-0.8Hz) (**Fig.2b**) and their overall average firing frequency was not significantly different from that in controls (**Supplementary Fig.2d**). While the amplitude of complex-spike modulation was comparable to that in controls, their phase was completely reversed (at all frequencies $p<0.0002$; One-way ANOVA) (**Supplementary Table 2**). The average phase shift ranged from 152° to 181° (**Fig.2b**). The complex-spike activities of a few Purkinje-cells (4 out of 42) in *Ptf1a::cre;Robo3*$^{lox/lox}$ mice responded in line with those of control animals; these cells presumably reflect the small minority of cells that still receive a contralateral climbing-fiber input.

The main question is whether the phase of the simple-spike modulation in *Ptf1a::cre;Robo3*$^{lox/lox}$ mice remained normal, as one might expect from the fact that the lateralization of the mossy-fibers was unaffected. Alternatively, it could shift together with that of the complex-spike activities, as one may predict based on the adaptive filter hypothesis[18]. Clearly, the simple-spike modulation shifted together with that of their complex-spikes at all frequencies demonstrating that the reciprocity stayed intact (**Fig.2c; Supplementary Table 2**); compared to the simple-spike modulation of controls the average phase shift in the mutants ranged from 156° to 180° ($p<0.0001$ for all frequencies; One-way ANOVA). A minority of the Purkinje-cells (4 out of 42) in the *Ptf1a::cre;Robo3*$^{lox/lox}$ mice showed a simple-spike phase that was comparable to that of controls. These simple-spike modulations were observed in exactly the same four Purkinje-cells that showed the control-like complex-spike modulation described above, which re-emphasizes the ubiquitous character of the reciprocity phenomenon in general and the dominant impact of the climbing-fibers. The average peak-to-peak amplitude of simple-spike modulation in *Ptf1a::cre;Robo3*$^{lox/lox}$ mice was significantly higher than that in controls ($p<0.05$ for all frequencies; One-way ANOVA); this difference could be attributed to a change in inhibition rather than excitation, because the average simple-spike firing frequency during the trough of the modulation in the mutants was lower than that in controls ($p<0.03$ for all frequencies; One-way ANOVA), whereas the firing frequencies during the peak of the modulation did not significantly differ (**Fig.3a; Supplementary Table 2**). This increased inhibition also resulted in increased irregularity ($p<0.05$ for all frequencies; One-way ANOVA) (**Supplementary Fig.2d**), which was absent during spontaneous activity. In contrast, the average simple-spike firing frequencies as well as the pause in simple-spike activities after complex-spikes (i.e. climbing-fiber pause) did not differ between *Ptf1a::cre;Robo3*$^{lox/lox}$ and control mice (**Supplementary Fig.2**).

If the climbing-fibers drive the reciprocity by enhancing inhibition of Purkinje-

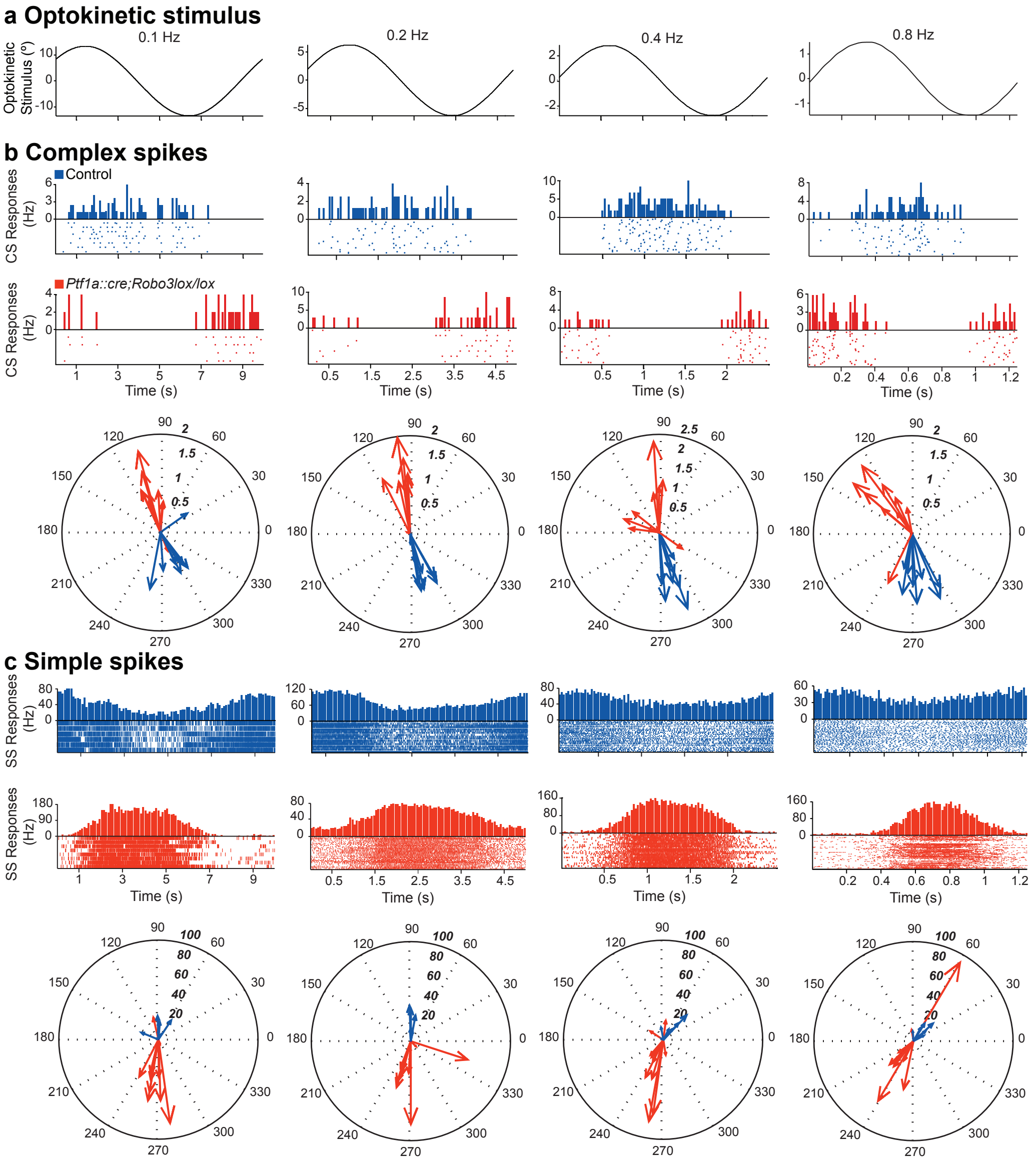

Figure 2. Complex-spike and simple-spike reciprocity is maintained in Ptf1a::cre;Robo3$^{lox/lox}$ mice. a, In vivo extracellular recordings from floccular Purkinje-cells were obtained during optokinetic stimulation at 0.1-0.8 Hz (8°/s peak velocity; all n ≥ 8). b, Representative examples of peri-stimulus time histograms (PSTHs) depicting complex-spike modulation in mutants (red) and controls (blue). Polar plots of complex-spike modulation, with the amplitude of modulation depicted by the radius and the angle indicating the phase of the modulation, demonstrate that the phase of complex-spike modulation is reversed in mutants. c, Corresponding simple-spike PSTHs of Purkinje-cells in b and polar plots reveal that simple-spike modulation in mutants is shifted as well, thereby maintaining the reciprocity. See Supplementary Table 2 for details.

cells, it is parsimonious to hypothesize that the molecular layer interneurons contribute to the phase-shift in simple-spike activity[18,25]; these interneurons inhibit Purkinje-cells[26-28] and their parallel-fiber input may be potentiated by climbing-fiber input[29]. The phase of the activities of molecular layer interneurons (n=7) was indeed also reversed in *Ptf1a::cre;Robo3$^{lox/lox}$* mice. Their phase with respect to the optokinetic stimulus differed on average 155° from that of controls ($p<0.0001$; Student's t-test), meaning that the trough and peak of molecular layer interneuron activity coincided with the peak of the simple-spikes and complex-spikes, respectively (**Fig.3b,c**).

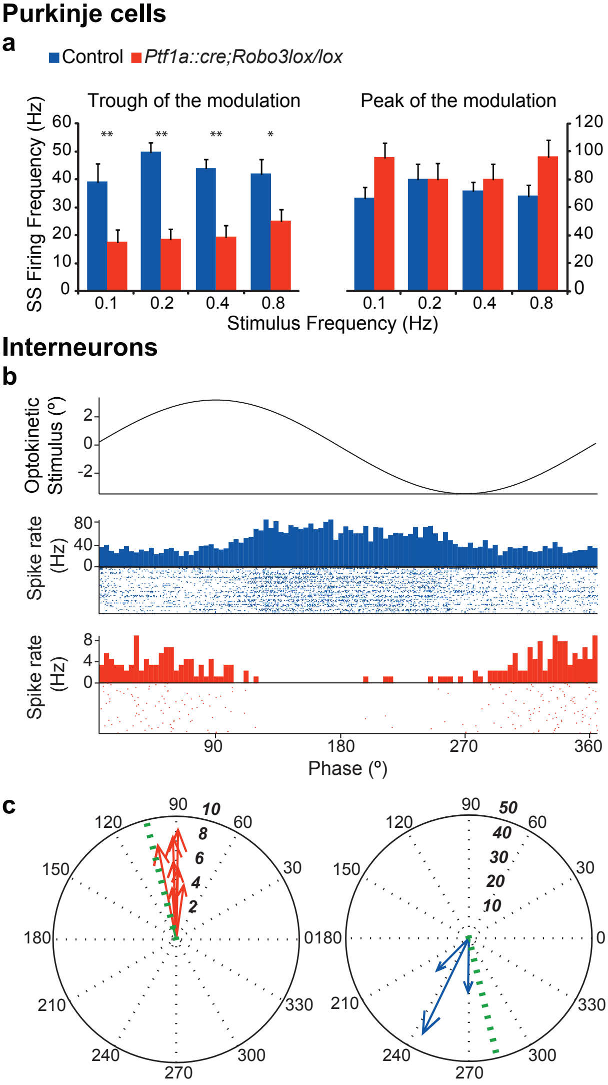

Figure 3 | Inhibition contributes to the phase shift in simple-spike modulation in Ptf1a::cre;Robo3$^{lox/lox}$ mice. a, Compared to controls (blue) simple-spike firing frequency in the mutants (red) was significantly lower at the trough, but not different at the peak of the modulation, suggesting a change in the inhibition of Purkinje-cells. See Supplementary Table 2 for details. b, Representative PSTH of a vertical-axis (VA) floccular molecular layer interneuron in mutant and control during optokinetic stimulation at 0.2 Hz. c, Polar plots confirm that phase of molecular layer interneuron modulation is also reversed in mutants and remains in phase with complex spikes (averaged for 0.2Hz, green dotted line). Error bars denote SEM.

If the phase-shift in molecular layer interneuron activity is controlled by a climbing-fiber-dependent, long-term plastic process such as potentiation of the parallel-fiber to molecular layer interneuron synapse[25,29-30], one expects that the phase-shift in simple-spike activities in *Ptf1a::cre;Robo3$^{lox/lox}$* mice is maintained when the climbing-fiber modulation suddenly disappears. When we stopped the visual climbing fiber modulation of their floccular Purkinje cells by switching off the light during vestibular stimulation, the phase of the simple-spikes modulation indeed remained intact (**Supplementary Fig.3**). Thus, since the phases of simple-spike and complex-spike modulations in *Ptf1a::cre;Robo3*$^{lox/lox}$ mice during vestibular stimulation were comparable to those during the OKR in that they were both reversed compared to those in wild types, these data indicate that the impact of the climbing-fibers on the simple-spike phase lasts longer than the period of visual complex-spike modulation.

Considering that the phase of both complex-spikes and simple-spikes is reversed in *Ptf1a::cre;Robo3*$^{lox/lox}$ mice, one can expect that phase and gain control of their compensatory eye movements is also affected[15]. *Ptf1a::cre;Robo3*$^{lox/lox}$ mice indeed showed significant deficits in the phase of both their OKR and vestibulo-ocular reflex in the light (VVOR) ($p=0.017$ and $p=0.015$; repeated measures ANOVA) as well as in the gain of both reflexes ($p=0.0002$ and $p=0.00001$; repeated measures ANOVA) (**Fig.4**). Moreover, the variability of the OKR and VVOR phase values was also significantly higher than those of controls ($p<0.0001$ and $p=0.0002$, respectively; paired Student's t-test). Thus, motor performance in *Ptf1a::cre;Robo3*$^{lox/lox}$ mice was prominently affected in the paradigms during which the activity of the visual climbing-fibers modulates.

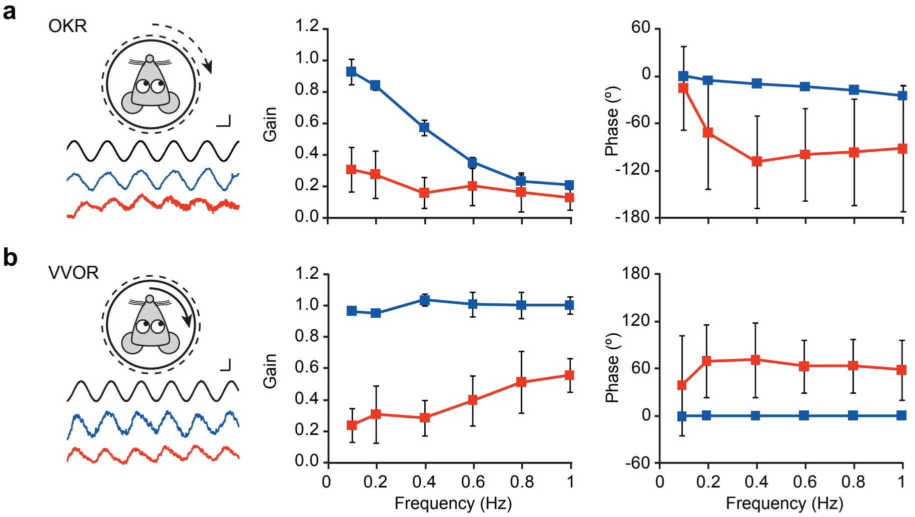

Figure 4 | Compensatory eye movements are impaired in Ptf1a::cre;Robo3$^{lox/lox}$ mice. a, The optokinetic reflex (OKR) is impaired in mutants (n=7, red) as the gain (amplitude) is lower and the phase (timing) is lagging and more variable than those in controls (n=7, blue). b, Similarly, average gain and phase of the visually-enhanced vestibulo-ocular reflex (VVOR) as well as the variability in phase are affected in mutants. The fact that gain is affected more at the lower, visually driven, frequencies, suggests an impaired processing of visual information. Note that error bars indicate SDs

Discussion

The current results show the dominant role of the climbing-fiber input in phase control of simple-spike firing. The reciprocity was maintained in all cells in the *Ptf1a::cre;Robo3*$^{lox/lox}$ mice, even in the few Purkinje-cells that had a preserved contralateral climbing-fiber input. As predicted by the adaptive filter hypothesis[18], the data indicate that the climbing-fibers can select, out of a diverse pool of temporal patterns formed in the granular layer, a subset of parallel-fiber inputs that carry a particular phase. Several of our findings indicate that the underlying mechanisms by which the climbing-fibers form and preserve the reciprocity include induction of potentiation at the parallel-fiber to molecular layer interneuron synapse[25,31]. First, the trough of the simple-spike modulation in the *Ptf1a::cre;Robo3*$^{lox/lox}$ mutants was significantly lower than that in controls, whereas the peaks were not significantly different; since Purkinje-cells are intrinsically active[32,33], it presumably takes an active form of inhibition to reach such low level of simple-spike activities often touching the zero baseline. Second, the phase of the molecular layer interneurons in the *Ptf1a::cre;Robo3*$^{lox/lox}$ was shifted in the proper direction to exert the phase shift in simple-spike activities. Third, the phase shift in simple-spike activities was maintained when the modulation of the visual climbing-fibers was stopped; this preservation of simple-spike modulation points towards an active plastic process such as potentiation of the parallel-fiber to molecular layer interneuron synapse. And finally, blockage of the output of molecular layer interneurons indeed impairs phase reversal learning of the vestibulo-ocular reflex[30].

Even though these arguments favor an important intermediary role of the molecular layer interneurons, we cannot exclude the possibility that other phenomena such as induction of long-term potentiation or long-term depression at the parallel-fiber to Purkinje-cell synapse[34,35], which are associated with the absence and presence of climbing-fiber activity, respectively[36], also contribute to the mechanisms involved in the reciprocity of Purkinje-cell firing. Likewise, tonic GABA release from Bergmann glia cells[37], which may be activated by climbing-fibers releasing corticotropin-releasing factor[38], could in principle also contribute to inhibition and reciprocal firing of Purkinje-cells. All these mechanisms are compatible with the main findings of the current study, which show that the climbing-fibers are likely to play the initiating and dominant role in the phenomenon of reciprocity, and that they allow the olivocerebellar system to operate as a phase lead-lag compensator.

Supplementary Material

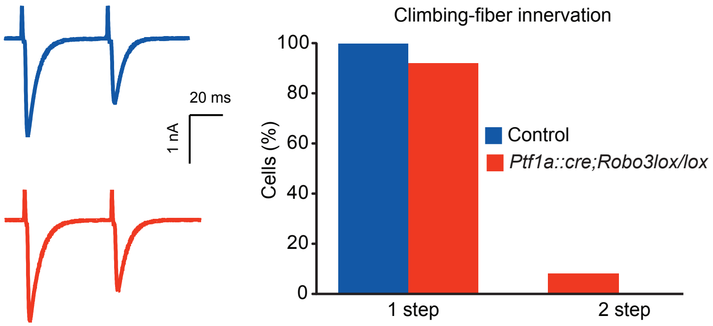

Supplementary Figure 1. Example traces of patch-clamp recordings in acute slices of cerebellar vermis. In Ptf1a::cre;Robo3$^{lox/lox}$ mice (red) stimulation of the granular layer close to the Purkinje-cell soma elicited multiple CF EPSCs in only 1 out of 10 cells, and in 0 out of 11 cells in control animals (blue). Histograms show values as percentage.

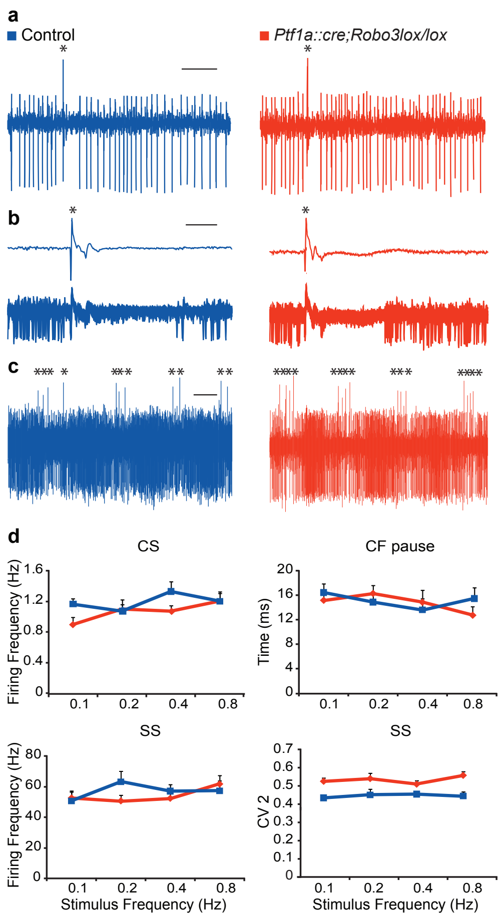

Supplementary Figure 2. Single unit, Purkinje-cell activity in awake mice. a, Raw traces of spontaneous Purkinje-cell activity show simple spikes (negative deflections) and complex-spikes (asterisks). Scale bars depict 100 ms. b, Raw traces of individual complex-spikes. Note that there is no difference in the shape of complex-spikes recorded in Ptf1a::cre;Robo3$^{lox/lox}$ and control mice. Scale bars depict 15 ms. c, Example traces of floccular Purkinje-cell activity recorded during optokinetic stimulation, displaying the typical modulation of complex-spikes and simple-spikes. Scale bars depict 500 ms. d, Complex-spike (CS) and simple-spike (SS) firing frequencies and climbing-fiber (CF) pause during optokinetic stimulation in VA floccular cells of the mutants were not significantly different from those in controls for any of the stimulus frequencies (all $n \geq 8$; complex-spikes: $p = 0.06$ for 0.1Hz, $p = 0.84$ for 0.2Hz, $p = 0.15$ for 0.4Hz, and $p = 0.99$ for 0.8Hz; simple-spikes: $p = 0.79$ for 0.1Hz, $p = 0.11$ for 0.2Hz, $p = 0.48$ for 0.4Hz, and $p = 0.59$ for 0.8Hz; climbing-fiber pause $p = 0.58$ for 0.1Hz, $p = 0.48$ for 0.2Hz, $p = 0.66$ for 0.4Hz, and $p = 0.25$ for 0.8Hz; One-way ANOVA). During modulation, the coefficient of variation for adjacent intervals (CV2) of simple spike activities in the mutants was significantly higher than in controls ($p = 0.002$ for 0.1Hz, $p = 0.05$ for 0.2Hz, $p = 0.05$ for 0.4Hz, and $p = 0.002$ for 0.8Hz; One-way ANOVA). Error bars indicate SEM.

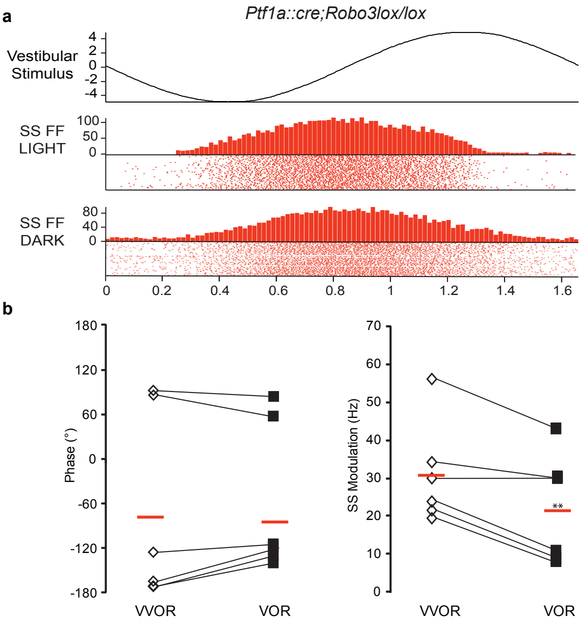

Supplementary Figure 3. Phase shift in simple-spike modulation persists in the absence of complex-spike modulation. a, PSTH of simple-spike activity of a Purkinje cell in Ptf1a::cre;Robo3$^{lox/lox}$ mutant during vestibular stimulation before (VVOR, at 0.6Hz) and after (VOR, at 0.6Hz) turning off the light. The phase of simple spike activity in these cells during vestibular stimulation also significantly shifted compared to that in controls. b, The amplitude of simple-spike modulation ($n = 6$) decreased from VVOR (open signs) to VOR (closed signs), but the phase did not change ($p = 0.009$ and $p = 0.33$, respectively; paired S tudent's t-test). These data indicate that the phase shift in simple-spikes does not depend directly on ongoing visual climbing-fiber modulation, but probably results from a longer process, potentially involving plasticity.

Mean width of the bands

	Medial	Mediolateral	Lateral
Control	225 ± 23 µm	176 ± 24 µm	137 ± 3 µm
Ptf1a::cre;Robo3lox/lox	195 ± 34 µm	165 ± 13 µm	133 ± 10 µm
	T-test = 0.27	T-test = 0.5	T-test = 0.5

Distance of the band from the midline

	Mediolateral	Lateral
Control	150 ± 30 µm	634 ± 40 µm
Ptf1a::cre;Robo3lox/lox	140 ± 6 µm	621 ± 43 µm
	T-test = 0.6	T-test = 0.7

Supplementary Table 1 | Statistics for CGRP+ labeled stripes of climbing-fibers in controls and *Ptf1a::cre;Robo3$^{lox/lox}$* mice. Values for the mean width of the main bands and their distance from the midline.

Complex Spikes

	Modulation amplitude			Phase (°)		
Stimulus (Hz)	Control n = 8 mean ± sem	*PTF1a;Cre::Robo3lox/lox* n≥10 mean ± sem	One way ANOVA	Control n = 8 mean ± sem	*PTF1a;Cre::Robo3lox/lox* n≥10 mean ± sem	One way ANOVA
0.1	0.83 ± 0.05	0.80 ± 0.13	0.84	265 ± 27	118 ± 18	< 0.0002
0.2	0.83 ± 0.12	1.05 ± 0.57	0.35	285 ± 4	121 ± 18	< 0.0001
0.4	1.34 ± 0.15	0.88 ± 0.18	0.08	286 ± 3	146 ± 20	< 0.0001
0.8	1.27 ± 0.11	1.06 ± 0.15	0.33	275 ± 5	135 ± 13	< 0.0001

Simple Spikes

	Modulation amplitude			Phase (°)		
Stimulus (Hz)	Control n = 8 mean ± sem	*PTF1a;Cre::Robo3lox/lox* n≥10 mean ± sem	One way ANOVA	Control n = 8 mean ± sem	*PTF1a;Cre::Robo3lox/lox* n≥10 mean ± sem	One way ANOVA
0.1	14 ± 3	43 ± 6	0.002	97 ± 12	250 ± 15	< 0.0001
0.2	17 ± 4	38 ± 7	0.03	85 ± 2	272 ± 10	< 0.0001
0.4	14 ± 3	34 ± 7	0.05	71 ± 13	225 ± 17	< 0.0001
0.8	14 ± 3	37 ± 8	0.02	58 ± 9	203 ± 21	< 0.0001

	Trough			Peak		
Stimulus (Hz)	Control n = 8 mean ± sem	*PTF1a;Cre::Robo3lox/lox* n≥10 mean ± sem	One way ANOVA	Control n = 8 mean ± sem	*PTF1a;Cre::Robo3lox/lox* n≥10 mean ± sem	One way ANOVA
0.1	39 ± 7	17 ± 5	0.02	66 ± 8	95 ± 11	0.06
0.2	49 ± 4	18 ± 4	< 0.0001	80 ± 11	80 ± 12	0.99
0.4	44 ± 3	19 ± 4	0.001	71 ± 7	79 ± 12	0.57
0.8	41 ± 5	24 ± 4	0.03	68 ± 9	96 ± 12	0.09

Supplementary Table 2 | In vivo spiking characteristics of vertical-axis (VA) floccular Purkinje-cells during modulation. The data indicate means and standard error of the means (SEM) for amplitude of modulation and phase values of complex-spikes and simple-spikes. In addition, values for trough and peak of simple-spike modulation are shown.

References

1. Marillat, V. et al. The slit receptor Rig-1/Robo3 controls midline crossing by hindbrain precerebellar neurons and axons. *Neuron* 43, 69-79 (2004).
2. Kawaguchi, Y. et al. The role of the transcriptional regulator Ptf1a in converting intestinal to pancreatic progenitors. *Nat Genet* 32, 128-34 (2002).
3. Hippenmeyer, S. et al. A developmental switch in the response of DRG neurons to ETS transcription factor signaling. *PLoS Biol* 3, e159 (2005).
4. Yamada, M. et al. Origin of climbing fiber neurons and their developmental dependence on Ptf1a. *J Neurosci* 27, 10924-34 (2007).
5. Cendelin, J., Korelusova, I. & Vozeh, F. The effect of repeated rotarod training on motor skills and spatial learning ability in Lurcher mutant mice. *Behav Brain Res* 189, 65-74 (2008).
6. Van Der Giessen, R.S. et al. Role of olivary electrical coupling in cerebellar motor learning. *Neuron* 58, 599-612 (2008).
7. Wilson, D.B. Histological defects in the cerebellum of adult lurcher (Lc) mice. *J Neuropathol Exp Neurol* 35, 40-5 (1976).
8. Sabatier, C. et al. The divergent Robo family protein rig-1/Robo3 is a negative regulator of slit responsiveness required for midline crossing by commissural axons. *Cell* 117, 157-69 (2004).
9. van Vreeswijk, C. & Sompolinsky, H. Chaos in neuronal networks with balanced excitatory and inhibitory activity. *Science* 274, 1724-6 (1996).
10. Welsh, J.P., Lang, E.J., Suglhara, I. & Llinas, R. Dynamic organization of motor control within the olivocerebellar system. *Nature* 374, 453-7 (1995).
11. Medina, J.F. & Lisberger, S.G. Links from complex spikes to local plasticity and motor learning in the cerebellum of awake-behaving monkeys. *Nat Neurosci* 11, 1185-92 (2008).
12. Graf, W., Simpson, J.I. & Leonard, C.S. Spatial organization of visual messages of the rabbit's cerebellar flocculus. II. Complex and simple spike responses of Purkinje cells. *J Neurophysiol* 60, 2091-121 (1988).
13. De Zeeuw, C.I., Wylie, D.R., Stahl, J.S. & Simpson, J.I. Phase relations of Purkinje cells in the rabbit flocculus during compensatory eye movements. *J Neurophysiol* 74, 2051-64 (1995).
14. Yakhnitsa, V. & Barmack, N.H. Antiphasic Purkinje cell responses in mouse uvula-nodulus are sensitive to static roll-tilt and topographically organized. *Neuroscience* 143, 615-26 (2006).
15. Simpson, J.I., Wylie, D.R. & De Zeeuw, C.I. On climbing fiber signals and their consequence(s). . *BehBrain Sciences* 19, 380-394 (1996).
16. Renier, N. et al. Genetic dissection of the function of hindbrain axonal commissures. *PLoS Biol* 8, e1000325 (2010).
17. Fujita, M. Adaptive filter model of the cerebellum. *Biol Cybern* 45, 195-206 (1982).
18. Dean, P., Porrill, J., Ekerot, C.F. & Jorntell, H. The cerebellar microcircuit as an adaptive filter: experimental and computational evidence. *Nat Rev Neurosci* 11, 30-43.
19. Leonard, C.S. & Simpson, J.I. Simple spike modulation of floccular Purkinje cells during the reversible blockade of their climbing fiber afferents. In Adaptive Processes in Visual and Oculomotor System. Pergamon. Oxford, U. 429-434 (1986).
20. Montarolo, P.G., Palestini, M. & Strata, P. The inhibitory effect of the olivocerebellar input on the cerebellar Purkinje cells in the rat. *J Physiol* 332, 187-202 (1982).
21. Miyashita, Y. & Nagao, S. Analysis of signal content of Purkinje cell responses to optokinetic stimuli in the rabbit cerebellar flocculus by selective lesions of brainstem pathways. *Neurosci Res* 1, 223-41 (1984).
22. Ruigrok, T.J. & Apps, R. A light microscope-based double retrograde tracer strategy to

chart central neuronal connections. *Nat Protoc* 2, 1869-78 (2007).

23. Morara, S., van der Want, J.J., de Weerd, H., Provini, L. & Rosina, A. Ultrastructural analysis of climbing fiber-Purkinje cell synaptogenesis in the rat cerebellum. *Neuroscience* 108, 655-71 (2001).
24. Schonewille, M. et al. Purkinje cells in awake behaving animals operate at the upstate membrane potential. *Nat Neurosci* 9, 459-61; author reply 461 (2006).
25. Jorntell, H., Bengtsson, F., Schonewille, M. & De Zeeuw, C.I. Cerebellar molecular layer interneurons - computational properties and roles in learning. *Trends Neurosci* 33, 524-32.
26. Barmack, N.H. & Yakhnitsa, V. Functions of interneurons in mouse cerebellum. *J Neurosci* 28, 1140-52 (2008).
27. Hausser, M. & Clark, B.A. Tonic synaptic inhibition modulates neuronal output pattern and spatiotemporal synaptic integration. *Neuron* 19, 665-78 (1997).
28. Mittmann, W., Koch, U. & Hausser, M. Feed-forward inhibition shapes the spike output of cerebellar Purkinje cells. *J Physiol* 563, 369-78 (2005).
29. Ekerot, C.F. & Jorntell, H. Parallel fibre receptive fields of Purkinje cells and interneurons are climbing fibre-specific. *Eur J Neurosci* 13, 1303-10 (2001).
30. Wulff, P. et al. Synaptic inhibition of Purkinje cells mediates consolidation of vestibulo-cerebellar motor learning. *Nat Neurosci* 12, 1042-9 (2009).
31. Jorntell, H. & Ekerot, C.F. Receptive field plasticity profoundly alters the cutaneous parallel fiber synaptic input to cerebellar interneurons in vivo. *J Neurosci* 23, 9620-31 (2003).
32. Raman, I.M. & Bean, B.P. Ionic currents underlying spontaneous action potentials in isolated cerebellar Purkinje neurons. *J Neurosci* 19, 1663-74 (1999).
33. Hausser, M. et al. The beat goes on: spontaneous firing in mammalian neuronal microcircuits. *J Neurosci* 24, 9215-9 (2004).
34. Ito, M. Cerebellar long-term depression: characterization, signal transduction, and functional roles. *Physiol Rev* 81, 1143-95 (2001).
35. Schonewille, M. et al. Purkinje cell-specific knockout of the protein phosphatase PP2B impairs potentiation and cerebellar motor learning. *Neuron* 67, 618-28.
36. Coesmans, M., Weber, J.T., De Zeeuw, C.I. & Hansel, C. Bidirectional parallel fiber plasticity in the cerebellum under climbing fiber control. *Neuron* 44, 691-700 (2004).
37. Lee, S. et al. Channel-mediated tonic GABA release from glia. *Science* 330, 790-6.
38. Tian, J.B., King, J.S. & Bishop, G.A. Stimulation of the inferior olivary complex alters the distribution of the type 1 corticotropin releasing factor receptor in the adult rat cerebellar cortex. *Neuroscience* 153, 308-17 (2008).

CHAPTER 3

PARALLEL FIBER INPUT - ROLE OF POTENTIATION IN CEREBELLAR MOTOR LEARNING

Neuron. 2010 August 67, 618-28.

M. Schonewille, A. Belmeguenai, S.K. Koekkoek, S.H. Houtman, H.J. Boele, B.J. van Beugen, Z. Gao, A. Badura, G. Ohtsuki, W.E. Amerika, E. Hosy, F.E. Hoebeek, Y. Elgersma, C. Hansel and C.I. De Zeeuw

Summary

Cerebellar motor learning is required to obtain procedural skills. Studies have provided supportive evidence for a potential role of kinase-mediated long-term depression (LTD) at the parallel fiber to Purkinje cell synapse in cerebellar learning. Recently, phosphatases have been implicated in the induction of potentiation of Purkinje cell activities *in vitro*, but it remains to be shown whether and how phosphatase-mediated potentiation contributes to motor learning. Here, we investigated its possible role by creating and testing a Purkinje cell specific knockout of calcium/calmodulin-activated protein-phosphatase-2B (L7-PP2B). The selective deletion of PP2B indeed abolished postsynaptic long-term potentiation in Purkinje cells and their ability to increase their excitability, whereas LTD was unaffected. The mutants showed impaired *gain-decrease* ánd *gain-increase* adaptation of their VOR as well as impaired *acquisition* of classical delay conditioning of their eyeblink response. Thus, our data indicate that PP2B may mediate indeed potentiation in Purkinje cells and contribute prominently to cerebellar motor learning.

Introduction

At excitatory synapses onto hippocampal or neocortical synapses, protein phosphatases are required for postsynaptic LTD induction, whereas kinases are required for postsynaptic LTP induction[1, 2]. In these regions protein phosphatase 1 (PP1), the activity state of which is indirectly controlled by calcium/calmodulin-activated protein phosphatase 2B (calcineurin or PP2B), has been suggested to act in concert with the α isoform of calcium/calmodulin-dependent kinase II (αCaMKII) to provide a molecular switch regulating the phosphorylation state of AMPA receptors[2, 3]. In contrast, at cerebellar PF synapses onto Purkinje cells LTD induction is PKCα- [4], cGKI- [5] and α/βCaMKII-dependent[6, 7], whereas LTP requires the activation of PP1, PP2A, and calcineurin[8]. Interestingly, changes in LTD and LTP induction can be associated with changes in intrinsic excitability in the hippocampus and cerebellum[9, 10], and calcineurin has indeed been associated differentially with changes in intrinsic excitability in pyramidal cells and Purkinje cells[11]. Thus, cerebellar Purkinje cells operate in general inversely to their hippocampal counterparts in that downstream kinase and phosphatase activity can push the balance towards LTD and LTP, respectively, even though the activity of these enzymes themselves can be regulated by proteins of the opposite category upstream[12, 13].

Over the past decades, attempts to determine the cellular mechanisms underlying cerebellar motor learning have focused virtually exclusively on the impact of LTD[14-17]. Genetic interference with kinase-mediated LTD induction and/or maintenance in Purkinje cells has been reported to be associated with impaired motor learning such as defects in VOR gain adaptation or eyeblink conditioning[5, 6, 15, 18, cf 19]. Some of these studies have encouraged scientists to hypothesize that LTD is specifically responsible for gain *increases* in VOR adaptation[20] and *acquisition* of conditioned eyeblink responses[16, 21] raising the possibility that potentiation might be responsible for gain-*decrease* VOR adaptations and *extinction* of conditioned responses[20]. However, no transgenic mouse mutants have been created yet, which allow us to investigate specifically the possible contribution of potentiation in Purkinje cells. Since calcineurin is required for PF-PC LTP and increases in intrinsic excitability[8], this protein forms an ideal molecular target to genetically manipulate potentiation in Purkinje cells, and to investigate for the first time a potential role of potentiation in cerebellar motor learning. Thus, here we created mutant mice (L7-PP2B), in which calcineurin activity is selectively impaired in Purkinje cells by crossing floxed CNB1 mice (regulatory subunit of calcineurin)[22] with a Purkinje cell specific (L7-)cre-line[23] (Figure 1A), and we subsequently investigated them at the cell physiological and behavioral level.

Results

L7-PP2B mice lack calcineurin but show normal histology

Immunocytochemical analysis of the L7-PP2B mice with antibodies directed against the CNB1 subunit showed that calcineurin is indeed specifically deleted in Purkinje cells (**Figure 1B**). Density analyses showed that PP2B staining intensity was significantly lower in Purkinje cell bodies and primary dendrites ($p = 0.003$ and 0.034, respectively; t-test), but not in granule cells or the neuropil of the molecular layer ($p > 0.6$ for both parameters). Thionine and Golgi stainings revealed that the mutation did not affect the foliation of the cerebellar cortex or the cyto-architecture of Purkinje cells, respectively (**Figure 1C**). Moreover, electron microscopic examinations of calbindin-stained sections of the cerebellar cortex of L7-PP2B mice showed that the number and size of synaptic inputs from PFs onto Purkinje cells were not significantly different from those of littermate controls ($p > 0.26$ for all parameters, i.e. PSD length, PSD area, and density of synapses; t-test) (**Figure 1D**).

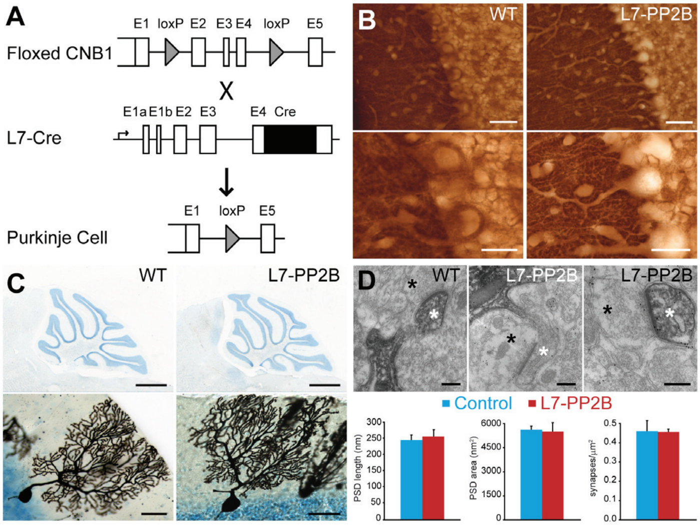

Figure 1. The L7-PP2B mutant: Creation and morphology. A, The L7-PP2B mutant mice were created by crossing a floxed calcineurin line with a L7-Cre line. B, Calcineurin (B subunit) stainings of the cerebellar cortex confirm the selective deletion of PP2B in Purkinje cells in L7-PP2B mice ($n = 4$); note the normal expression of PP2B in the parallel fibers of the molecular layer in which the unstained Purkinje cell dendrites stand out (right panels). C, Thionin (upper panel) and Golgi (lower panel) stainings of sagittal sections of the vermis showed no morphological or cyto-architectural differences between control ($n = 4$) and L7-PP2B mice ($n = 4$)($p > 0.49$; t-test). D, Electron micrographic quantification of parallel fiber contacts with calbindin stained Purkinje cell dendrites in the molecular layer revealed no significant differences between control ($n = 3$) and L7-PP2B mice ($n = 3$) in PSD length, PSD area, and density of synapses ($p > 0.26$ for all parameters; t-test). Scale bars indicate 50 μm (upper panels) and 25 μm (lower panels) in B, 1000 μm (upper panels) and 50 μm (lower panels) in C, and 200 nm (upper panels) in D. Black asterisks indicate parallel fiber terminals, and white asterisks indicate Purkinje cell spines in D.

Moreover, the area covered by the Purkinje cell dendrites as well as the thickness of the different layers of the cerebellar cortex was also unaffected ($p > 0.49$ for both parameters; t-test).

L7-PP2B mice show specific defects in parallel fiber to Purkinje cell plasticity

As predicted by our previous pharmacological *in vitro* studies in cerebellar rat tissue[8], our cell physiological examination of 10-24 week-old L7-PP2B mice indeed showed that LTP induction following parallel fiber stimulation alone was blocked ($p = 0.027$; t-test) (**Figure 2A**). In contrast, LTD induction following paired PF and climbing fiber (CF) stimulation was unaffected in adult L7-PP2B mice ($p = 0.96$; t-test) (**Figure 2C**). In wild type littermates, both LTP and LTD were successfully induced (**Figures 2A and C**). The inability of L7-PP2B mutants to potentiate their parallel fiber input did not depend on the temperature, age or type of induction protocol, while it could be rescued by the addition of active PP2B (data not shown, see supplementary materials in the article). Moreover, EPSPs and intracellular calcium concentrations during the tetanus did not differ (**Figure 2B**), arguing against the possibility that these factors were responsible for the observed deletion of parallel fiber potentiation.

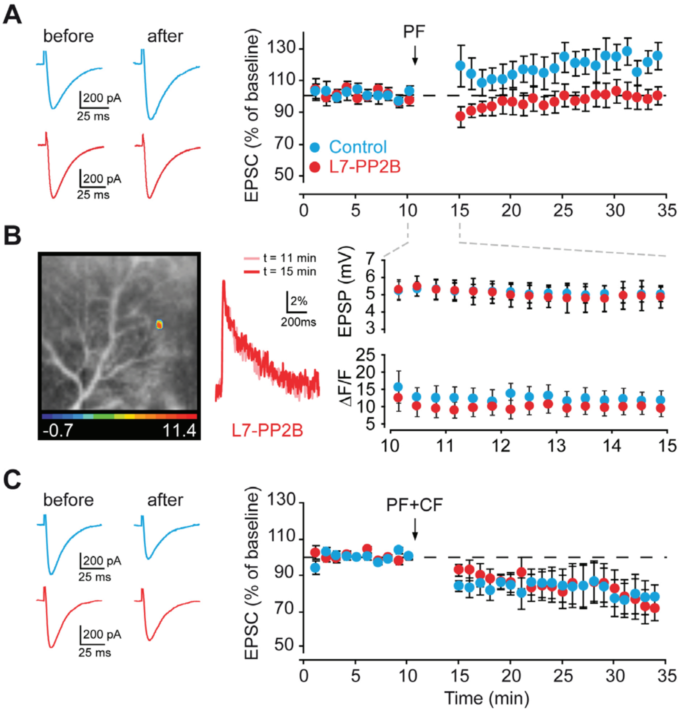

Figure 2. L7-PP2B mice show impaired parallel fiber – Purkinje cell potentiation. A, Induction of LTP at the parallel fiber to Purkinje cell synapse was significantly ($p < 0.03$; t-test) impaired in slices of adult L7-PP2B mice (8 cells from 5 mice) compared to those of controls (7 cells from 6 mice). B, Voltage responses (EPSP, average of 20 stimuli at 1 Hz) and changes in calcium transients (500 ms scans at 0.05 Hz) during the tetanus were not different (both $p > 0.5$; ANOVA for repeated measurements) between controls ($n = 13$ and 5, respectively) and L7-PP2B mice ($n = 10$ and 5). Left, sample image of parallel fiber stimulation induced Ca2+-signal. Middle, example trace of PF-stimulation elicited calcium transients (average of 3). C, Induction of LTD at the parallel fiber to Purkinje cell synapse was not affected ($p = 0.96$; t-test) (7 and 9 cells in 5 mutants and 5 controls, respectively). PF-PC LTP was induced by PF stimulation at 1 Hz for 5 min, while LTD was induced by paired PF and CF stimulation at 1 Hz for 5 min. Traces on the left side show EPSCs before (left) and after (right) induction of plasticity. See also Figure S1-2.

Climbing fiber elimination, paired-pulse ratios and inhibition are not affected in Purkinje cells of L7-PP2B mice

Since the presence or absence of CF activity is critical for the induction of depression and potentiation in Purkinje cells, respectively[24, 25], we also examined whether deletion of calcineurin in Purkinje cells directly affects the developmental elimination of surplus CF inputs, as previously observed for mutant mice lacking PKC[15] or αCaMKII activity[6]. CF elimination in adult L7-PP2B mice (10-24 weeks), however, appeared normal, and is therefore unlikely to have affected synaptic input patterns that could indirectly impair plasticity in Purkinje cells of L7-PP2B mice (**Figure 3A**). Likewise, we did not detect differences in the paired-pulse depression (PPD) ratio at CF synapses and the paired-pulse facilitation (PPF) ratio at PF synapses, respectively (**Figure 3B and C**). In fact, even in the presence of NBQX or lower extracellular calcium the PPF did not differ (**Figure 3C**).

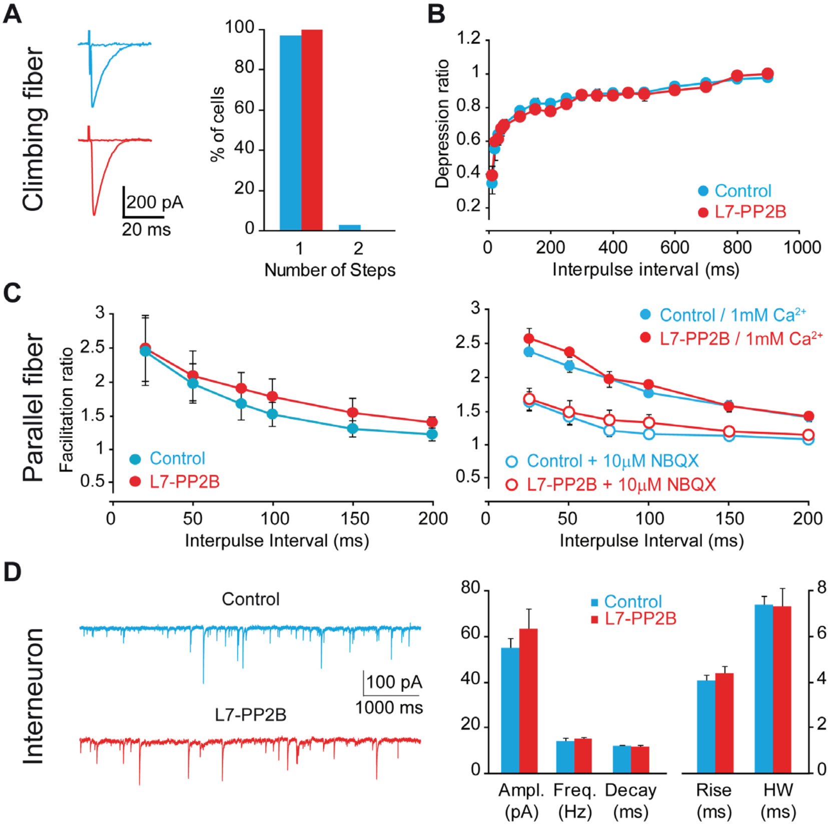

Figure 3. Climbing fiber elimination and basal state of excitatory and inhibitory input to Purkinje cells is unaffected in L7-PP2B mutant mice. A, All-or-none climbing fiber EPSCs were evoked at increasing stimulus intensities. Traces show EPSCs above and below threshold. Climbing fiber elimination is nearly complete in Purkinje cells of both controls and L7-PP2B mutants at 20 10 - 24 wks (33 cells from 12 control mice; 12 cells from 4 mutants). B and C, We did not detect differences in the paired-pulse depression (PPD) ratio at CF synapses (B) and the paired-pulse facilitation (PPF) ratio at PF synapses (C), respectively. PPF ratios were determined for the indicated stimulus intervals in both wild type ($n = 8$) and mutant mice ($n = 5$) and no differences are found ($p = 0.163$; ANOVA for repeated measurements). PPF ratios also did not differ in conditions of lower external calcium ($p = 0.213$; $n = 6$ vs. 6, control vs. L7-PP2B) or in the presence of NBQX ($p = 0.314$; $n = 5$ vs. 8). Insets show sample traces. D, Characterization of sIPSCs revealed no differences in frequency, amplitude, rise time, half width and decay time (all $p > 0.34$; $n = 11$ vs. 6, control vs. L7-PP2B; t-test). Sample traces on the left Error bars indicate SEM**.**

These findings suggest that the observed effects on plasticity were postsynaptic, but they don't allow us to conclude that presynaptic changes were completely absent. Finally, we found no differences in frequency, amplitude, rise/decay time and half width of spontaneous IPSCs in Purkinje cells (**Figure 3D**). Together, these data suggest that the basic synaptic transmission of both excitatory and inhibitory inputs to Purkinje cells is unaffected in L7-PP2B mice.

L7-PP2B mice show defects in intrinsic plasticity of Purkinje cells

In addition to synaptic parallel fiber potentiation, also non-synaptic Purkinje cell intrinsic excitability can be potentiated. This intrinsic potentiation could be readily induced in wild types, but not in the L7-PP2B mutants ($p = 0.007$; ANOVA for repeated measurements) (**Figure 4A**). Notably, we also observed differences in baseline intrinsic excitability. Linear fits of the current-frequency curves showed that the slope of L7-PP2B mice is less steep ($p = 0.002$; t-test) (**Figure 4B)**. This difference suggests that the cells are less excitable, which is confirmed by a lower maximum firing frequency ($p < 0.001$; t-test).

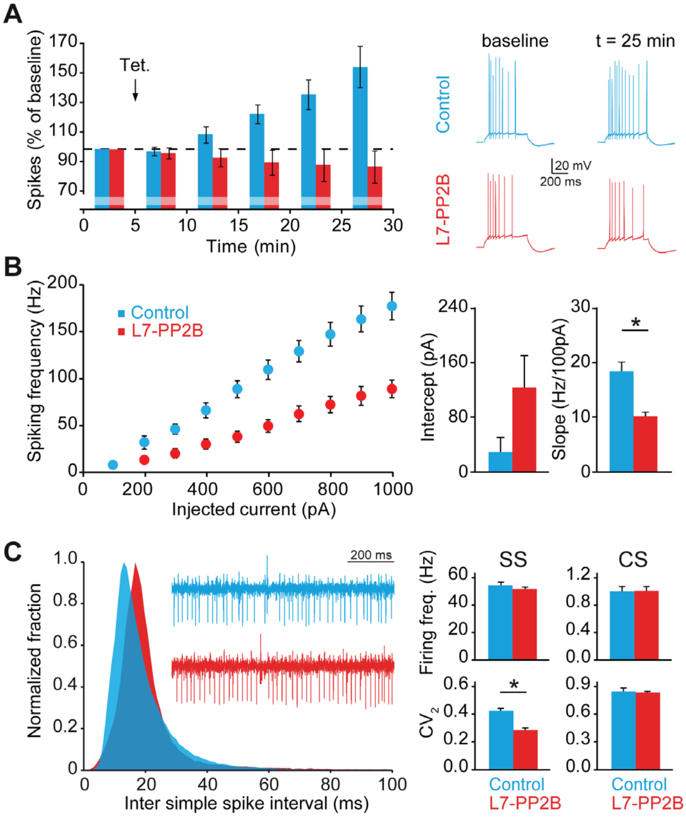

Figure 4. Intrinsic excitability and spiking activity in L7-PP2B mice. A, Following tetanization (150-300 pA at 5 Hz for 3 s) the spike rate evoked with 550 ms depolarizing current pulses of 100-200 pA increased in wild types ($n = 9$), but not in the L7-PP2B mutants ($n = 16$; $p = 0.007$; ANOVA for repeated measurements)(Figure 4A). Right, sample traces before and after induction. B, Basal intrinsic excitability is significantly lower in L7-PP2B mice ($n = 7$ vs. $n = 10$ for controls), quantified by slope ($p = 0.002$; t-test) and intercept with the x-axis ($p = 0.07$; t-test). C, Purkinje activity in vivo is characterized by a sharper inter-simple spike interval distribution (left) and concomitant higher regularity of spiking (i.e. CV2, $p < 0.001$), but the average frequencies of simple spikes and complex spikes were normal (both $p > 0.5$; t-test). Inset shows sample traces. See also Table S1**.**

A lack of PP2B affects regularity but not average firing frequency of simple spike activities in vivo

To test whether the deficits in PF-PC LTP and plasticity of intrinsic excitability affect Purkinje cell activity *in vivo* we performed extracellular recordings in awake mice (n = 25 vs. 30 for control vs. L7-PP2B). Firing frequencies of simple spikes and complex spikes were both normal ($p = 0.94$ and $p = 0.54$, respectively; t-test), but the inter-simple spike interval distribution was sharper with less high-frequency spiking and concomitant higher regularity in L7-PP2B mutants (**Figure 4C**). Thus, the changes in intrinsic excitability and potentiation in L7-PP2B mice correlate with a loss of high-frequency simple spike activity, but do not alter the average firing frequency of Purkinje cells. We therefore conclude that the deficits in potentiation in the L7-PP2B mice may selectively affect their spatiotemporal firing patterns of simple spike activities.

L7-PP2B mice show defects in adaptation of the vestibulo-ocular reflex

In the open field or during footprint analysis L7-PP2B mice did not show obvious signs of ataxia (data not shown, see supplementary materials in the article). To explore their specific capabilities for cerebellar motor learning, we first subjected the mice to compensatory eye movement tests, in particular VOR adaptation tests, which are controlled by the vestibulocerebellum[6, 15, 26] (**Figure 5**). Measurements of basic performance parameters including the gain (amplitude) and phase (timing) of the optokinetic reflex (OKR) and/or VOR showed overall that the motor performance of the L7-PP2B mutants was moderately, but significantly, affected **(Figures 5B-D, Figure S1A-C**). For OKR and VVOR the gain of L7-PP2B mutants were significantly lower than those of wild type littermates (both OKR and VVOR $p < 0.001$; ANOVA for repeated measurements) (**Figure 5B-C**), while their phase values were significantly lagging those of the wild types (OKR $p < 0.01$; VVOR $p < 0.001$; ANOVA for repeated measurements). In contrast, for VOR the gain of L7-PP2B mutants was significantly greater than that of wild type littermates ($p < 0.001$; ANOVA for repeated measurements) (**Figure 5D**), while their phase values were also significantly lagging those of the wild types ($p < 0.01$; ANOVA for repeated measurements) (**Figure S1**). The differences among mutants and wild types during OKR and VVOR were not caused by differences in vision itself, because the latencies of the eye movement responses to the onset of the optokinetic stimuli were unaffected in the mutants ($p = 0.55$, ANOVA for repeated measurements) (**Figure S2**).

A prominent phenotype of the L7-PP2B mice was observed when we subjected the animals to the mismatch learning paradigms. In a two-day visuo-vestibular training paradigm aimed at reducing the gain of the VOR, learning was significantly impaired in the mutants (**Figure 5E**) ($p < 0.0002$ for both days; ANOVA for repeated measurements). In the opposite training paradigm, which was aimed at increasing the gain, the gain values of the mutants even showed a decrease (**Figure 5F**; comparison among mutants and controls $p < 0.000001$ for both days, ANOVA for repeated measurements). Control experiments revealed that this decrease was not due to aspecific effects, because exposure to a normal, non-training paradigm for the same duration did not result in any decrease ($p = 0.83$ and $p = 0.90$ for day 1 and day 2, respectively, ANOVA for repeated measurements) (**Figure 5G**).

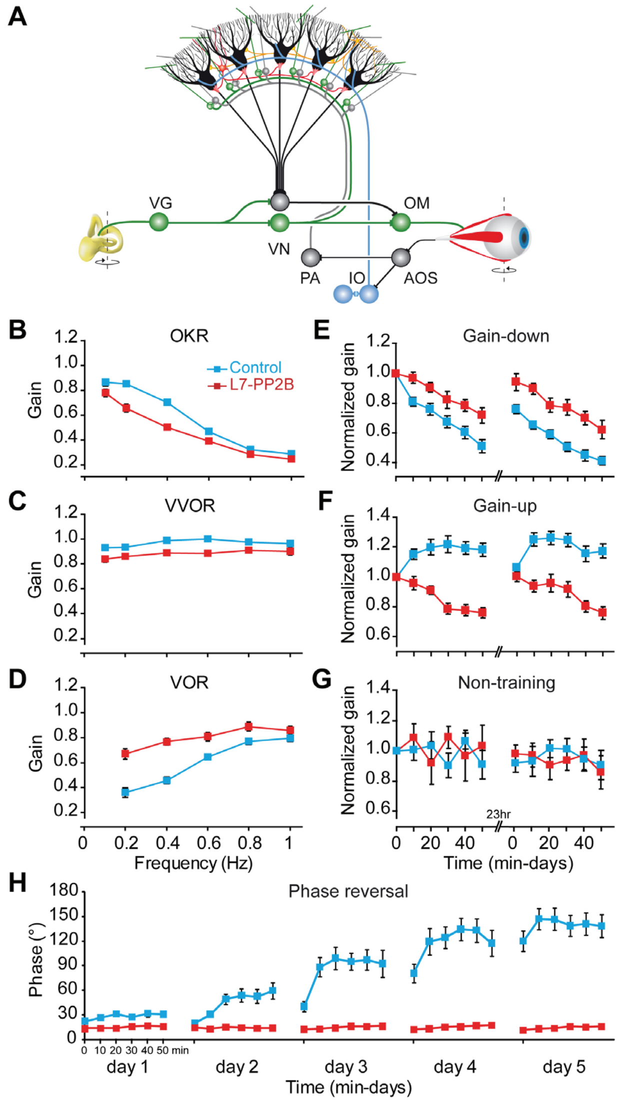

Figure 5. VOR adaptation is affected in L7-PP2B mice. A, Schematic drawing of the vestibulo-cerebellar system. Purkinje cells (black) in the flocculus of the vestibulo-cerebellum converge upon neurons in the vestibular nuclei (VN), through which they can influence the output of the oculomotor neurons (OM) that drive the eye movements. The Purkinje cells are innervated by two main inputs: they receive vestibular and eye movement signals through the mossy fiber - parallel fiber system (represented by green and grey inputs), and retinal slip signals through climbing fibers derived from the inferior olive (IO; blue). The parallel fibers, which all originate from the granule cells, innervate the dendritic trees of the Purkinje cells. VG, AOS and PA indicate vestibular ganglion cells, accessory optic system, and pontine areas, respectively. B, C and D, Motor performance during the optokinetic reflex (OKR), and the vestibulo-ocular reflex in the light (VVOR) and the dark (VOR) revealed moderate aberrations in L7-PP2B mice (n = 15) compared to controls (n = 19) (for OKR, VOR as well as VVOR $p < 0.001$; ANOVA for repeated measurements). E and F, Motor learning in L7-PP2B mice was severely affected; during two days of mismatch training so as to either decrease (E) or increase (F) their VOR gain the L7-PP2B mice (n = 9) learned significantly less than controls (n = 10) ($p < 0.0002$ and $p < 0.000001$ for gain-decrease and gain-increase paradigm, respectively; ANOVA for repeated measurements). Note that gain-increase training resulted in a decrease of the gain in the L7-PP2B mice. G, Without mismatch training stimuli as in E or F, no differences were observed ($p = 0.83$ on day 1 and $p = 0.90$ on day 2; ANOVA for repeated measurements). H, When the L7-PP2B mice (n = 8) were subjected during four consecutive days (days 2 to 5) to a mismatch training paradigm aimed at reversing the phase of their VOR, they learned significantly less ($p < 0.000001$; ANOVA for repeated measurements) than their controls (n = 8). On the day (day 1) preceding this reversal protocol the animals were subjected to the standard in-phase gain-decrease paradigm. Error bars indicate SEM. See also Figure S3-5.

Phase changes are minimal during these gain adaptation paradigms (**Figure S1D-F**), but phase, like gain, can also be adapted. In this respect the ability of the mutants to learn was affected in such a profound way that they were completely unable to adapt their phase during a long-term 5-day phase reversal training paradigm (**Figure 5H)**. In contrast, wild type littermates were able to reverse their phase towards 180 degrees in five consecutive training sessions (5th day, comparison among L7-PP2B mutants and wild type mice; $p < 0.000001$, ANOVA for repeated measurements). Thus, the Purkinje cell-specific PP2B knockout mice were moderately affected in the performance of their basic compensatory eye movements and markedly affected in all forms of VOR adaptation tested.

L7-PP2B mice show impaired eyeblink conditioning

Next, to find out whether the learning deficits in the L7-PP2B mutants are limited to abnormalities in VOR adaptation, which is controlled by the vestibulocerebellum, or whether they reflect a more global deficit in cerebellar motor learning, we also subjected them to a training paradigm that is controlled by a different region of the cerebellum: classical conditioning of eyeblink responses, which in mice is controlled by lobulus simplex in the hemisphere and lobule VI in the vermis[27] (for underlying circuitry see **Figure 6A**). The eyeblink responses of the mice were conditioned using a tone and an air-puff as the conditioned stimulus (CS) and unconditioned stimulus (US), respectively (Koekkoek et al., 2003). After 4 paired training sessions (T-1 to T-4), the L7-PP2B mutants showed significantly less conditioned responses than their wild type littermates (comparison between L7-PP2B mice and wild type littermates at T4: $p < 0.05$, t-test), while this difference was absent during the first training session (at T1: $p = 0.82$, t-test) (**Figures 6B and C**). In fact, the L7-PP2B mutant mice did not show any significant change in percentage of conditioned eyeblink responses over consecutive days of training (e.g. T4 versus T1, $p = 0.52$; one way within subjects ANOVA). The timing of the conditioned responses in the mutants was also affected in that the average peak latency of their CS-alone responses at T4 was significantly shorter ($p < 0.02$; t-test) than that of controls (**Figure 6C**; for peaks in paired trials, see also **Figure 6B**). In contrast, the kinetics of the unconditioned eyeblink responses in the L7-PP2B mutants were indistinguishable ($p > 0.4$ for onset, peak amplitude as well as velocity of UR; t-test) from those in controls (**Figure 6D**). Thus, our eyeblink tests showed that the L7-PP2B mice have a specific impairment in their conditioned responses rather than a general deficit in the motor component of all their eyeblink responses. Together with the VOR gain adaptation tests, we conclude that the L7-PP2B mutants have severe deficits in hallmark features of cerebellar learning functions: The fine-tuning of sensorimotor gains and the fast adaptation of motor output in response to changing behavioral needs.

Discussion

The current study is the first to specifically address the role of potentiation of Purkinje cell activities in cerebellar motor learning. Guided by the original ideas of Albus[28], and Ito[29], virtually all previous studies that were aimed at identifying the molecular and cellular mechanisms underlying cerebellar motor learning focused on depression for review see [16, 29]. These studies provided supportive evidence that kinases such as PKC[15], cGKI[5], CaMKIV[18]

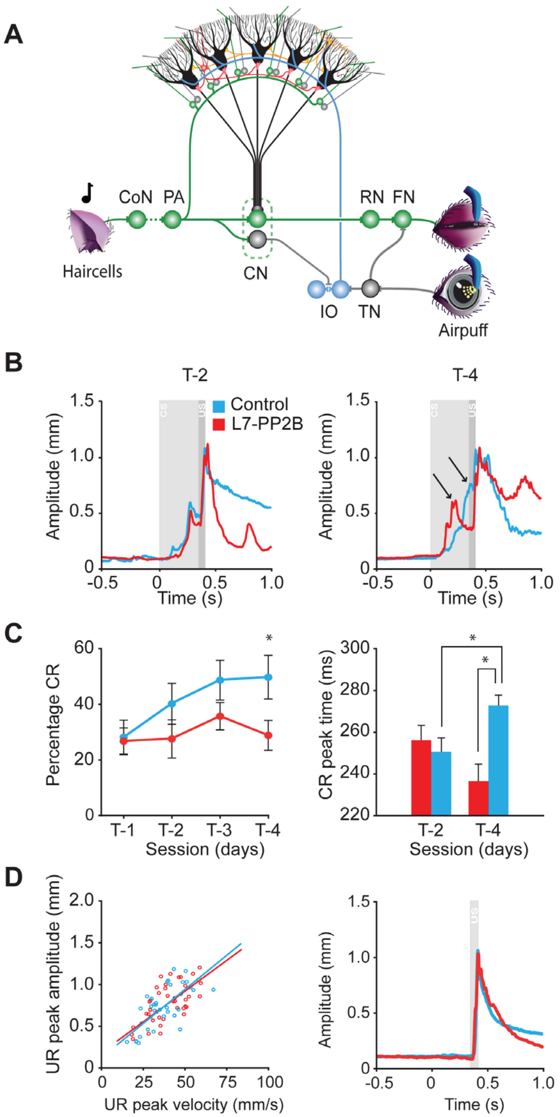

Figure 6. Eyeblink conditioning is impaired in L7-PP2B mutants. A, Neuro-anatomical circuitry involved in eyeblink conditioning. Purkinje cells in the cerebellar cortex form a central site where signal convergence of the unconditioned stimulus (US) and conditioned stimulus (CS) takes place. The US consists of a mild corneal air puff and the CS of an auditory tone. US signals reach the Purkinje cells via the inferior olive (IO) by climbing fibers, while mossy fiber projections from the pontine area (PA) relay the CS. Repeated paired presentation of the CS and US results in conditioned responses (CR), during which the eyelid closes in response to the tone. B, Representative traces of paired CS-US trials from an L7-PP2B knockout (red) and a littermate control (blue) during training sessions T2 and T4. CS onset occurs at time 0, while US follows 325 ms later. Note that the L7-PP2B knockout is not able to improve the timing of the CR (left arrow), whereas the control demonstrates a well-timed CR at T4 (right arrow). C, The percentage of CRs in L7-PP2B knockout mice (n = 9) does not significantly increase over the four training sessions ($p = 0.52$; t-test). Instead, the control littermates (n = 9) demonstrate a clear learning curve ($p < 0.01$; t-test) and at T4 they show significantly more CRs than L7-PP2B knockouts ($p < 0.05$). In addition, the quality of the CR does not improve in L7-PP2B knockout mice. Where controls demonstrate well timed CRs during training session 4 (e.g. T4 versus T2, $p < 0.001$; t-test), L7-PP2B knockout mice do not improve their timing (e.g. at T4 L7-PP2B versus controls, $p < 0.02$; t-test). D, Kinetics of the eyelid responses are not affected in L7-PP2B knockout mice. Onset, peak amplitude and velocity of the eyelid response to the air puff in the mutants do not differ from those of controls ($p > 0.4$ in all comparisons; t-test) indicating that kinetics of the eyelid are the same for both groups. Abbreviations: CN Cerebellar Nuclei; CoN Cochlear Nucleus; FN Facial Nucleus; RN Red nucleus; TN Trigeminal Nucleus. All error bars indicate SEM.

and α/βCaMKII[6, 7] are essential for both LTD at the parallel fiber to Purkinje cell synapse and motor learning. The idea has been put forward that gain-increase adaptations of the VOR may be mediated predominantly by LTD, while gain-decrease adaptations may result from potentiation of Purkinje cells[20]. Likewise, it has been suggested that LTD is required for the acquisition of well-timed conditioned responses[16, cf 19, 21], raising the possibility that the extinction is mediated by potentiation of Purkinje cells. This latter option is supported by the finding that the extinction process requires activation of the GABAergic input to the inferior olive[30], which in principle could reduce climbing fiber activities and thereby shift the balance at the Purkinje cell level from depression to potentiation[25]. Based on these hypotheses, one might have expected that L7-PP2B mice are specifically impaired in learning VOR gain decreases and in extinction of conditioned eyeblink responses. Instead, we observed, next to deficits in gain decreases, profound deficits in VOR gain increases and a virtual absence of phase reversal learning, while the acquisition of conditioned eyeblink responses and their timing were also affected. In fact, the *acquisition* of the conditioning process was such prominently affected that there was no difference in the number of CRs between the last and the first training session making it impossible to estimate a potential contribution of Purkinje cell potentiation to *extinction*. By comparison the behavioral deficits of the potentiation-deficient L7-PP2B mice exceed those of the depression-deficient kinase mutants both during VOR adaptation and eyeblink conditioning[5, 6, 15, 21]. Moreover, a possible functional role for LTP at the parallel fiber to Purkinje cell synapse in our daily motor behavior is further supported by the finding that natural cycles may influence this form of plasticity just like VOR adaptation itself[31]. Thus, Purkinje cell potentiation may not only have been neglected over the past decades, it may even be one of the most dominant players in cerebellar learning.

The approach of the current study has the advantage of simultaneously tackling the two major forms of Purkinje cell potentiation, i.e. PF-PC LTP and PC intrinsic plasticity, in a single animal model and rendering prominent behavioral phenotypes. At the same time, it is not possible to determine to what extent both types of plasticity interact, and which of the two impaired types of potentiation in the L7-PP2B mice is more relevant for which parts of their behavioral phenotypes. Since both types can be induced at physiologically relevant temperatures in wild types, we expect both to contribute, but future studies will have to segregate the two.

Although the kinetics of the unconditioned eyeblink responses in the L7-PP2B mutants were unaffected and therefore unlikely to have contributed to their reduced level of conditioning, we cannot exclude the possibility that the moderate deficits in eye movement performance did contribute to the deficits in VOR adaptation. However, we recently investigated other Purkinje cell specific mutants with comparable performance deficits, and these mutants had no gain learning deficits[26]. Thus, a performance deficit does not necessarily induce a deficit in gain increase and/or gain decrease learning per se.

The robust behavioral phenotypes in our calcineurin-deficient mutants are in line with a recent adaptive-filter model of Porrill and Dean[32]. This model is based on the covariance learning rule, implicating a preponderance of silent PF synapse, which has been experimentally observed[33, 34]. Consequently, their model suggests that LTP is likely to initiate new motor learning, whereas LTD depresses synapses active in the pre-learning situation, a process controlled by the climbing fiber[35]. This way, the cerebellum optimizes the weight of each relevant PF to Purkinje cell synapse given their relative amount of signal and noise. Thus, PP2B-mediated LTP might set the appropriate weights at the PF to Purkinje cell synapses and together with related levels of intrinsic plasticity generate the appropriate spatiotemporal patterns of simple spike activities that are required for cerebellar motor learning. Such an operating scenario could be supported by various other pre- and postsynaptic forms of potentiation at the GABAergic molecular layer interneuron to Purkinje cell synapse[35, 36] allowing temporal pattern formation without affecting the average firing frequency[26]. By combining optimally learned levels of potentiated excitation and feed-forward inhibition Purkinje cells are probably equipped with a push-pull mechanism so as to convey and consolidate appropriately formed patterns of spikes and/or pauses that may be read out in the cerebellar nuclei provided that they occur coherently in ensembles of cells[26, [37-39]. We therefore suggest that potentiation in Purkinje cells complements other forms of cerebellar plasticity in controlling synaptic input strengths and excitability in a dynamic manner, and that the cerebellum uses these plasticity mechanisms to shape the spike activity patterns of the inhibitory Purkinje cell output required for motor learning.

Supplementary Material

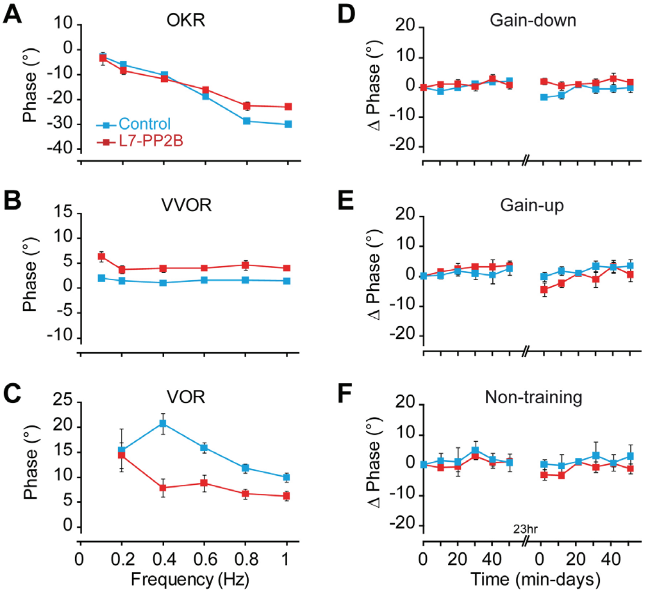

Figure S1. Phase data for compensatory eye movement experiments. A-C, The differences in VVOR and VOR gain, as depicted in Figure 5, are accompanied by differences in phase (OKR, $p = 0.010$; VVOR, $p < 0.001$; VOR, $p = 0.008$). D-F, All (non-) training sessions aimed at changing the gain have only minor effects on the phase. Absolute phase change (Δ phase) was significantly different between control and L7-PP2B mice on the second day of gain-down training ($p = 0.046$; for first day $p = 0.71$)(D), but not on either day for gain-up training (both $p > 0.24$)(E) or control non-training (both $p > 0.21$)(F). For number of animals used, see legends of Figure 5. Error bars indicate SEM.

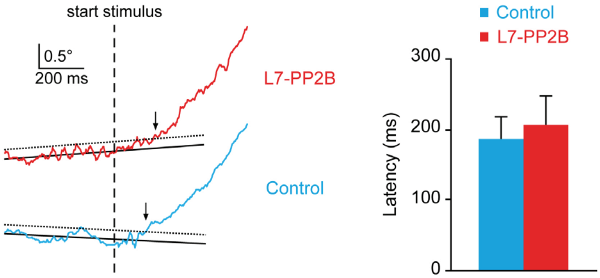

Figure S2. Latency data for OKR. The latency of the eye movement response to the optokinetic stimulus in the L7-PP2B mutants ($n = 7$) was not significantly different from that in the wild types ($n = 7$) ($p = 0.69$, t-test). Traces on the left show samples of individual animals. The moment of onset of the optokinetic response was determined by the crossing of the eye movement trace through the (dotted) line that was 2 SD above the average before the start of the stimulus (dashed line) for at least 10 ms.

References

1. Mulkey, R.M., Herron, C.E. & Malenka, R.C. An essential role for protein phosphatases in hippocampal long-term depression. *Science* **261**, 1051-5 (1993).
2. Lisman, J.E. & Zhabotinsky, A.M. A model of synaptic memory: a CaMKII/PP1 switch that potentiates transmission by organizing an AMPA receptor anchoring assembly. *Neuron* **31**, 191-201 (2001).
3. Malleret, G. et al. Inducible and reversible enhancement of learning, memory, and long-term potentiation by genetic inhibition of calcineurin. *Cell* **104**, 675-86. (2001).
4. Leitges, M., Kovac, J., Plomann, M. & Linden, D.J. A unique PDZ ligand in PKCalpha confers induction of cerebellar long-term synaptic depression. *Neuron* **44**, 585-94 (2004).
5. Feil, R. et al. Impairment of LTD and cerebellar learning by Purkinje cell-specific ablation of cGMP-dependent protein kinase I. *J Cell Biol* **163**, 295-302 (2003).
6. Hansel, C. et al. alphaCaMKII Is essential for cerebellar LTD and motor learning. *Neuron* **51**, 835-43 (2006).
7. van Woerden, G.M. et al. betaCaMKII controls the direction of plasticity at parallel fiber-Purkinje cell synapses. *Nat Neurosci* **12**, 823-5 (2009).
8. Belmeguenai, A. & Hansel, C. A role for protein phosphatases 1, 2A, and 2B in cerebellar long-term potentiation. *J Neurosci* **25**, 10768-72 (2005).
9. Armano, S., Rossi, P., Taglietti, V. & D'Angelo, E. Long-term potentiation of intrinsic excitability at the mossy fiber-granule cell synapse of rat cerebellum. *J Neurosci* **20**, 5208-16 (2000).
10. Lu, Y.M., Mansuy, I.M., Kandel, E.R. & Roder, J. Calcineurin-mediated LTD of GABAergic inhibition underlies the increased excitability of CA1 neurons associated with LTP. *Neuron* **26**, 197-205 (2000).
11. Misonou, H. et al. Regulation of ion channel localization and phosphorylation by neuronal activity. *Nat Neurosci* **7**, 711-8 (2004).
12. Eto, M., Bock, R., Brautigan, D.L. & Linden, D.J. Cerebellar long-term synaptic depression requires PKC-mediated activation of CPI-17, a myosin/moesin phosphatase inhibitor. *Neuron* **36**, 1145-58 (2002).
13. Launey, T., Endo, S., Sakai, R., Harano, J. & Ito, M. Protein phosphatase 2A inhibition induces cerebellar long-term depression and declustering of synaptic AMPA receptor. *Proc Natl Acad Sci U S A* **101**, 676-81 (2004).
14. Aiba, A. et al. Deficient cerebellar long-term depression and impaired motor learning in mGluR1 mutant mice. *Cell* **79**, 377-88 (1994).
15. De Zeeuw, C.I. et al. Expression of a protein kinase C inhibitor in Purkinje cells blocks cerebellar LTD and adaptation of the vestibulo-ocular reflex. *Neuron* **20**, 495-508 (1998).
16. De Zeeuw, C.I. & Yeo, C.H. Time and tide in cerebellar memory formation. *Curr Opin Neurobiol* **15**, 667-74 (2005).
17. Steuber, V. et al. Cerebellar LTD and pattern recognition by Purkinje cells. *Neuron* **54**, 121-36 (2007).
18. Boyden, E.S. et al. Selective engagement of plasticity mechanisms for motor memory storage. *Neuron* **51**, 823-34 (2006).
19. Welsh, J.P. et al. Normal motor learning during pharmacological prevention of Purkinje cell long-term depression. *Proc Natl Acad Sci U S A* **102**, 17166-71 (2005).
20. Boyden, E.S. & Raymond, J.L. Active reversal of motor memories reveals rules governing memory encoding. *Neuron* **39**, 1031-42 (2003).
21. Koekkoek, S.K. et al. Cerebellar LTD and learning-dependent timing of conditioned eyelid responses. *Science* **301**, 1736-9 (2003).
22. Zeng, H. et al. Forebrain-specific calcineurin knockout selectively impairs bidirectional synaptic plasticity and working/episodic-like memory. *Cell* **107**, 617-29 (2001).

23. Barski, J.J., Dethleffsen, K. & Meyer, M. Cre recombinase expression in cerebellar Purkinje cells. *Genesis* **28**, 93-8. (2000).
24. Lev-Ram, V., Wong, S.T., Storm, D.R. & Tsien, R.Y. A new form of cerebellar long-term potentiation is postsynaptic and depends on nitric oxide but not cAMP. *Proc Natl Acad Sci U S A* **99**, 8389-93 (2002).
25. Coesmans, M., Weber, J.T., De Zeeuw, C.I. & Hansel, C. Bidirectional parallel fiber plasticity in the cerebellum under climbing fiber control. *Neuron* **44**, 691-700 (2004).
26. Wulff, P. et al. Synaptic inhibition of Purkinje cells mediates consolidation of vestibulo-cerebellar motor learning. *Nat Neurosci* **12**, 1042-9 (2009).
27. Van Der Giessen, R.S. et al. Role of olivary electrical coupling in cerebellar motor learning. *Neuron* **58**, 599-612 (2008).
28. Albus, J.S. A theory of cerebellar function *Mathematical Biosciences* **10**, 25-61 (1971).
29. Ito, M. Cerebellar long-term depression: characterization, signal transduction, and functional roles. *Physiol Rev* **81**, 1143-95. (2001).
30. Medina, J.F., Nores, W.L. & Mauk, M.D. Inhibition of climbing fibres is a signal for the extinction of conditioned eyelid responses. *Nature* **416**, 330-3. (2002).
31. Andreescu, C.E. et al. Estradiol improves cerebellar memory formation by activating estrogen receptor beta. *J Neurosci* **27**, 10832-9 (2007).
32. Porrill, J. & Dean, P. Silent synapses, LTP, and the indirect parallel-fibre pathway: computational consequences of optimal cerebellar noise-processing. *PLoS Comput Biol* **4**, e1000085 (2008).
33. Chadderton, P., Margrie, T.W. & Hausser, M. Integration of quanta in cerebellar granule cells during sensory processing. *Nature* **428**, 856-60 (2004).
34. Isope, P. & Barbour, B. Properties of unitary granule cell-->Purkinje cell synapses in adult rat cerebellar slices. *J Neurosci* **22**, 9668-78 (2002).
35. Dean, P. & Porrill, J. Adaptive-filter Models of the Cerebellum: Computational Analysis. *Cerebellum* **7**, 567-71 (2008).
36. Jorntell, H. & Ekerot, C.F. Reciprocal bidirectional plasticity of parallel fiber receptive fields in cerebellar Purkinje cells and their afferent interneurons. *Neuron* **34**, 797-806. (2002).
37. Gauck, V. & Jaeger, D. The control of rate and timing of spikes in the deep cerebellar nuclei by inhibition. *J Neurosci* **20**, 3006-16 (2000).
38. De Zeeuw, C.I., Hoebeek, F.E. & Schonewille, M. Causes and consequences of oscillations in the cerebellar cortex. *Neuron* **58**, 655-8 (2008).
39. Telgkamp, P. & Raman, I.M. Depression of inhibitory synaptic transmission between Purkinje cells and neurons of the cerebellar nuclei. *J Neurosci* **22**, 8447-57 (2002).

CHAPTER 4

ROLE OF THE INHIBITION IN THE CEREBELLAR CIRCUITRY

CHAPTER 4
PARAGRAPH 1

MOLECULAR LAYER INTERNEURONS MEDIATE CONSOLIDATION OF VESTIBULO-CEREBELLAR MOTOR LEARNING

Nat Neurosci. 2009 Aug;12(8):1042-9.

Wulff P, Schonewille M, Renzi M, Viltono L, Sassoè-Pognetto M, Badura A, Gao Z, Hoebeek FE, van Dorp S, Wisden W, Farrant M, De Zeeuw CI.

Abstract

Although feedforward inhibition onto Purkinje cells was first documented 40 years ago, we understand little of how inhibitory interneurons contribute to cerebellar function in behaving animals. Using a mouse line (PC-Deltagamma2) in which GABA(A) receptor-mediated synaptic inhibition is selectively removed from Purkinje cells, we examined how feedforward inhibition from molecular layer interneurons regulates adaptation of the vestibulo-ocular reflex. Although impairment of baseline motor performance was relatively mild, the ability to adapt the phase of the vestibulo-ocular reflex and to consolidate gain adaptations was strongly compromised. Purkinje cells showed abnormal patterns of simple spikes, both during and in the absence of evoked compensatory eye movements. On the basis of modeling our experimental data, we propose that feedforward inhibition, by controlling the fine-scale patterns of Purkinje cell activity, enables the induction of plasticity in neurons of the cerebellar and vestibular nuclei.

Introduction

Feed-forward inhibitory microcircuits, in which interneurons and their target principal cells receive common excitatory input, enhance network performance in many brain regions[1,2]. In the hippocampus, feed-forward inhibition, by reducing the time window of synaptic integration, increases the precision of spike timing in CA1 pyramidal neurons[3], and plasticity of feed-forward inhibition is required to maintain the fidelity of information processing[4]. Inthe cerebellum, molecular layer interneurons (stellate and basket cells) control Purkinje cells by powerful feed-forward inhibition[5,6,7,8,9] (see Supplementary Fig. 1 in the online article). Additionally, subsets of Purkinje cells sparsely inhibit each other via axon collaterals[10]. Purkinje cells provide the only output of the cerebellar cortex and project to the cerebellar and vestibular nuclei. They fire complex spikes in response to climbing fiber activity[11], and simple spikes that reflect the integration of intrinsic pacemaker activity with excitatory and inhibitory synaptic inputs from parallel fibers and molecular layer interneurons[8,12,13,14,15].

Although feed-forward inhibition onto Purkinje cells was documented more than four decades ago[5], we still know little about how it contributes to cerebellar function in behaving animals. Fast synaptic inhibition at molecular layer interneuron to Purkinje cell synapses is mediated by $\alpha1\beta2/3\gamma2$-type GABAA receptors[16]. The $\gamma2$ subunit is required to target the receptors to the postsynaptic membrane[17]. Thus, to investigate the role of GABAA receptor-mediated feedforward inhibition we selectively ablated the $\gamma2$ subunit, and thereby synaptic GABAA receptors, from Purkinje cells (PC-$\Delta\gamma2$ mice). The resulting changes in Purkinje cell simple spike activity and motor behaviour implicate molecular layer interneurons as essential regulators of cerebellar signal coding and memory formation.

Results

Purkinje cell-specific removal of synaptic GABAA receptors

To remove GABAA receptor-mediated feed-forward inhibition onto Purkinje cells, we selectively deleted the GABAA receptor $\gamma2$ subunit using the Cre/loxP-system (see Chapter 6 Methods). Cre recombinase, under the control of the L7 promoter, induced a Purkinje cell-specific deletion of the floxed $\gamma2$ subunit gene starting in the second postnatal week[16,18].

Ablation of synaptic GABAA receptors from Purkinje cells caused no anatomical alterations of the cerebellar circuitry (**Fig. 1**).

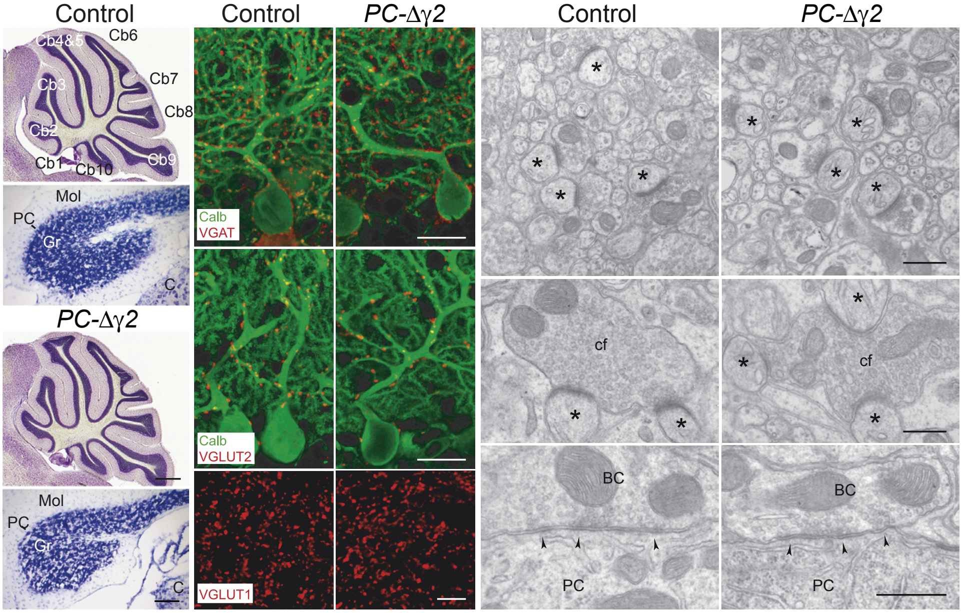

Figure 1. PC-Δγ2 mice show normal cerebellar morphology and synaptic organization. (a, b) Nissl stains of sections through vermis (sagittal) and flocculus (coronal) revealed no differences between control (a) and PC-Δγ2 (b) mice, and the number of Purkinje cells (24.5 ± 2.0 vs 23.9 ± 2.5 cells/1000µm; p = 0.75) and molecular layer interneurons (2.36 ± 0.19 vs 2.28 ± 0.18 cells/1000µm2; p = 0.53) were similar in both groups. Cb1-10, lobules 1-10; Mol, molecular layer; PC, Purkinje cell layer; Gr, granule cell layer, C, cochlear nucleus. (c-e) Immunofluorescence labelling in the flocculus showed no differences in the distribution of GABAergic terminals (vesicular γ-aminobutyric acid transporter; VGAT) (c), climbing fiber terminals (vesicular glutamate transporter 2; VGLUT2) (d) and parallel fiber terminals (VGLUT1) (e). Quantification of puncta per 1000 µm2 revealed no difference (p = 0.27, 0.62 and 0.68, respectively; n = 4). (f-h) Electron microscopy showed no obvious morphological changes of parallel and climbing fiber synapses. (f) Asymmetric synapses between parallel fibers and Purkinje cell spines (asterisks). The density of parallel fiber to Purkinje cell synapses was unchanged (33.0 vs 32.9 synapses/100 µm2 in PC-Δγ2 and control; see Chapter 6 Methods). (g) Asymmetric synapses made by climbing fibers (cf). (h) Symmetric synapses (arrowheads) made by basket cells (BC) onto the cell body of Purkinje cells (PC). Scale bars: (a and b) 250 µm and 50 µm; (c, d) 20 µm; (e) 5 µm; (f) 500 nm; (g) 360 nm; (h) 440 nm.

Patch-clamp recordings in acute slices of cerebellar vermis from adult animals showed spontaneous fast inhibitory postsynaptic currents (sIPSCs) at high frequency in all Purkinje cells (n = 21) from control mice (**Fig. 2a**), which could be blocked by the GABAA receptor antagonist SR-95531 (20µM; data not shown). By contrast, sIPSCs were absent from all Purkinje cells (n = 19) of PC-Δγ2 mice (**Fig. 2b**). In some PC-Δγ2 cells (12 of 19) occasional small, slow-rising currents remained. However, these produced on average less than 2% of the control synaptic charge (**Fig. 2**), and likely reflect spillover of synaptically released GABA onto extrasynaptic α and β subunit-containing receptors[19,20] (see Supplementary Fig. 2 in the online article). Consistent with a complete loss of synaptic GABAA receptors, recordings from PC-Δγ2 mice in the presence of TTX confirmed the absence of miniature IPSCs (mIPSCs) (**Fig. 2c,d**). The loss of synaptic GABAA receptors was restricted to Purkinje cells: mIPSCs in molecular layer interneurons were unaltered in PC-Δγ2 mice (see Supplementary Fig. 3 in the online aricle).

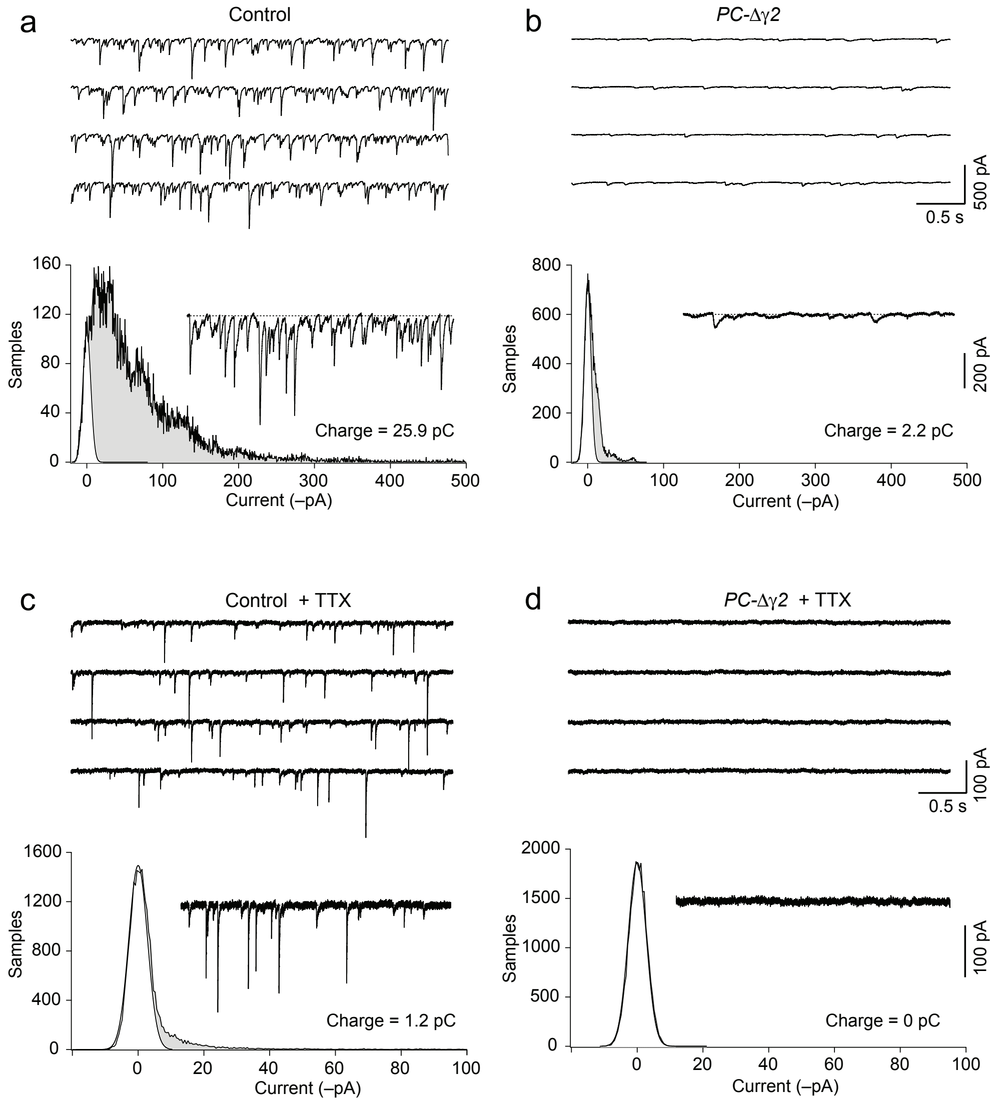

Figure 2. Loss of fast synaptic inhibition from Purkinje cells in PC-Δγ2 mice. (a) Representative contiguous segments of whole-cell recording (−70 mV) from a Purkinje cell of a control mouse. Ionotropic glutamate receptors were blocked with CNQX and d-AP5. Lower panel shows quantification of mean synaptic charge in a different Purkinje cell, with a 2.5 s record of sIPSCs and corresponding all-point amplitude histogram. The left-hand peak (most positive current values), corresponding to the baseline current noise, is fitted with a single-sided Gaussian (white). The peak of the histogram is taken as the zero current value (dotted line in inset). The filled grey area corresponds to all sample points other than those within the baseline noise, and thus represents the current produced by phasic synaptic events. In this cell, the mean synaptic charge was 25.9 pC. (b) Corresponding data from two PC-Δγ2 mice. sIPSCs were seen in all cells from control mice but in none from PC-Δγ2 mice. Slow SR-95531-sensitive currents were seen in ~60% of PC-Δγ2 cells. For the cell shown in the lower panel, phasic charge transfer was 2.2 pC. On average, the charge transfer was reduced from 59.8 ± 18.4 pC in control (n = 8) to 1.0 ± 0.5 pC in PC-Δγ2 cells (n = 15; $p < 0.0002$; Mann-Whitney U-test). (c) and (d) Corresponding data recorded in the presence of TTX. Note the different scaling of the current record and the abscissa of the all-point histogram and the complete absence of mIPSCs in PC-Δγ2 cells.

PC-Δγ2 mice show altered simple spike patterning

Feed-forward inhibition via molecular layer interneurons is rapidly (~ 1 ms) recruited by parallel fiber activation and curtails the parallel fiber-evoked excitatory postsynaptic potential (EPSP) in Purkinje cells[7,21]. To determine how absence of synaptic GABAA receptors affected Purkinje cells response to parallel fiber stimulation, we analyzed the temporal dispersion (jitter) of evoked Purkinje cell simple spikes (**Fig. 3a**). The jitter, quantified as the standard deviation of spike latency in a 10 ms window following stimulation (10V, 100µs), was strongly increased in PC-Δγ2 Purkinje cells (control: 0.81 ± 0.14 ms; PC-Δγ2: 1.80 ± 0.10 ms, $p < 0.0001$, n = 12 and 11, respectively). Acute blockade of GABAA receptors with SR-95531 significantly increased spike jitter in cells from control mice (to 1.45 ± 0.14 ms, p = 0.0011; see also Ref.7), but, as expected, had no effect in PC-Δγ2 cells (1.76 ± 0.10 ms, p = 0.605). We also determined the number of spikes evoked by parallel fiber stimulation (**Fig. 3a, lower panels**). On average, 0.60 ± 0.04 spikes were evoked in the 60 ms following each stimulus in control cells and 0.41 ± 0.05 spikes in PC-Δγ2 cells (n = 17 and 13, respectively; p = 0.0069). This smaller evoked response is consistent with a reduced parallel fiber excitatory input (see Supplementary Fig. 4 in the online article and Discussion). Consistent with the complete loss of GABAA receptor-mediated inhibition in PC-Δγ2 cells, SR-95531 increased the number of evoked spikes only in control cells (0.61 ± 0.05 to 0.76 ± 0.08, n = 11, p = 0.0248; PC-Δγ2 cells 0.41 ± 0.05 to 0.45 ± 0.06, n = 13, p = 0.3199). Thus, loss of molecular layer interneuronmediated feed-forward inhibition in PC-Δγ2 mice results in altered simple spike responses to parallel fiber inputs.

Purkinje cells in cerebellar slices from PC-Δγ2 mice showed a significant increase in simple spike firing regularity compared with controls (**Fig. 3b**). The mean firing rate at room temperature was not different between groups (control 12.3 ± 1.6 vs PC-Δγ2 13.7 ± 0.6 Hz, n = 26 and 9; p = 0.062, Mann-Whitney U-test), but the coefficient of variation (CV; SD/mean) of the inter-spike interval (ISI) was reduced in PC-Δγ2 mice (0.20 ± 0.03 in control vs 0.10 ± 0.01 in PC-Δγ2; p = 0.018, Mann-Whitney U-test). The coefficient of variation of adjacent intervals (CV2; mean value of $2\,|ISIn+1 - ISIn| / (ISIn+1 + ISIn)$; a measure for the regularity of firing on small timescales[22]) also differed. CV2 was 0.19 ± 0.02 in control vs 0.10 ± 0.01 in PC-Δγ2 mice (p = 0.018; Mann-Whitney U-test). Blockade of GABAA receptors with SR-95531 in control Purkinje cells decreased the CV of the ISI (0.20 ± 0.04 vs 0.13 ± 0.02 in SR-95531; p = 0.024, n = 8) to a value comparable to that found in PC-Δγ2 mice (see also Refs. [12,15,23]). As expected, SR-95531 failed to alter the CV of the ISI in cells from PC-Δγ2 mice (0.13 ± 0.02 vs 0.13 ± 0.04, n = 3). Importantly, similar results were obtained at nearphysiological temperature (34-35°C), with no change in mean rate (51.3 ± 9.1 in control vs 50.0 ± 3.5 Hz in PC-Δγ2, n = 9 and 7; p = 0.61; Mann-Whitney U-test), but a significant decrease in the CV (0.14 ± 0.01 in control vs 0.06 ± 0.01 in PC-Δγ2; p = 0.001; Mann-Whitney U-test) and CV2 (0.15 ± 0.02 vs 0.06 ± 0.01; p = 0.0099).

Finally, we examined whether loss of inhibition onto Purkinje cells modified long-term plasticity at parallel fiber to Purkinje cell synapses. Neither parallel fiber LTD nor LTP (see Chapter 6 Methods) were significantly impaired in PC-Δγ2 mice compared with controls (p = 0.624 and p = 0.257, respectively) (**Fig. 3c,d**).

PC-Δγ2 mice display little impairment in motor performance

PC-Δγ2 mice showed no obvious neurological abnormality[16]. To assess cerebellar performance we analyzed compensatory eye movements in male PC-Δγ2 mice (n = 9) and

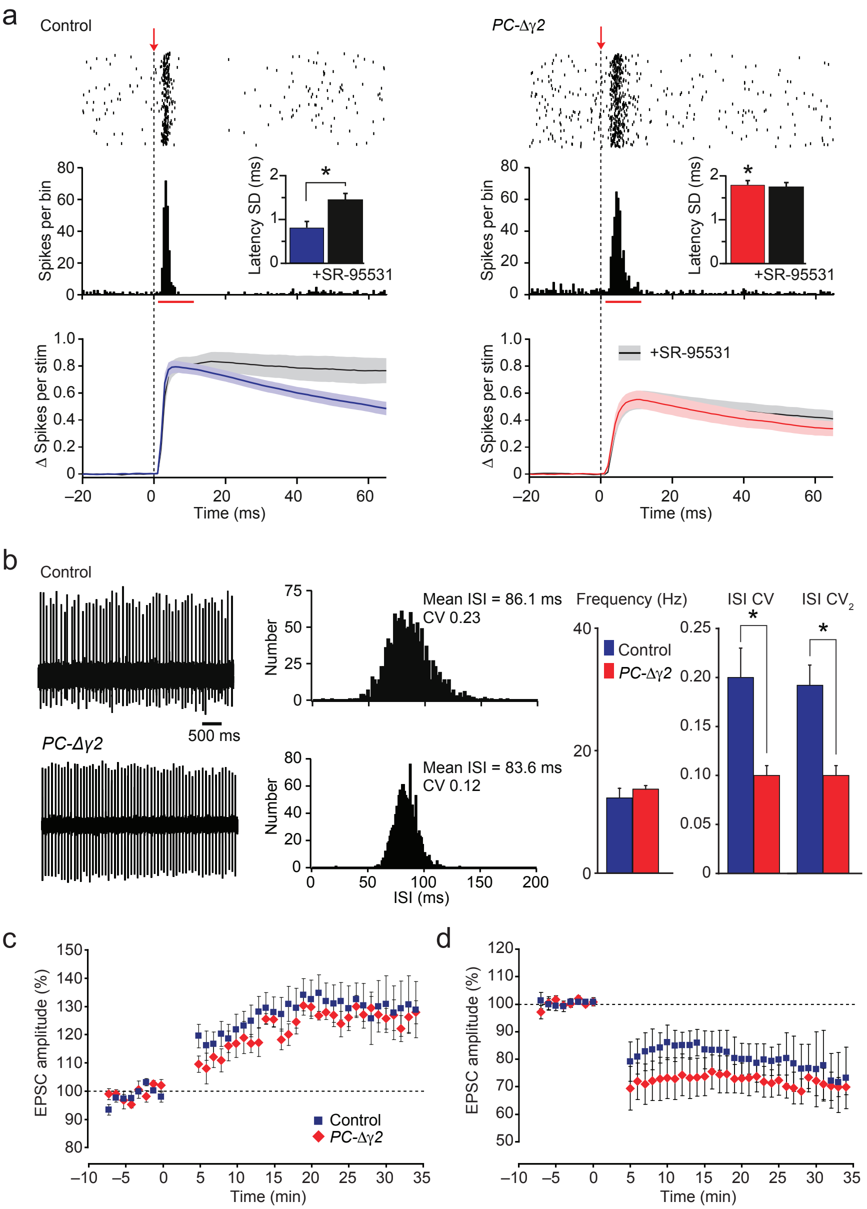

Figure 3. PC-Δγ2 mice display altered parallel fiber-evoked and spontaneous simple spike firing in vitro and unaltered parallel fiber-Purkinje cell LTP and LTD. (a) Simple spikes evoked by parallel fiber activation. Upper and middle panels are raster plots (400 sweeps at 0.5Hz) and corresponding PSTHs (0.5 ms bin-width). Arrows and dashed lines denote stimulation. Insets show SD of spike latency in a 10 ms window (red bars; 12 control, 11 PC-Δγ2 cells). Here, and throughout, error bars denote s.e.m. Jitter was greater in PC-Δγ2 (red) than in control (blue) cells (* $p < 0.0001$). SR-95531 increased jitter in control (* $p = 0.0011$) but not in PC-Δγ2 cells ($p = 0.605$). Lower panels show global averages of baseline-corrected cumulative spike probability (see Chapter 6 Methods). Shaded areas denote s.e.m.; 17 control, 13 PC-Δγ2 cells. Stimulation evoked fewer spikes in PC-Δγ2 cells (averaged between 0 and 60ms, $p = 0.0069$). SR-95531 (40 µM; black line, grey shading) increased spikes in control ($n = 11$; $p = 0.0248$) but not in PC-Δγ2 cells ($n = 13$; $p = 0.3199$). (b) Representative simple spikes (room temperature) and corresponding ISI histograms. Right panels show pooled data (26 control, 9 PC-Δγ2 cells). Mean firing rate was not significantly different. However, the CV and CV2 of ISIs differed significantly (* $p < 0.05$) (see text for details). (c) Pooled data showing parallel fiber-Purkinje cell LTP in control ($n = 7$, blue) and PC-Δγ2 cells ($n = 4$, red); EPSC amplitude was similarly increased in the strains (both $p < 0.005$; control vs PC-Δγ2 $p = 0.257$). (d) Parallel fiber-Purkinje cell LTD was similar in PC-Δγ2 ($n = 5$) and control ($n = 4$) cells (both $p < 0.05$; control vs PC-Δγ2 $p = 0.624$).

littermate controls (n = 8). Mice were exposed to whole-field visual stimuli to determine the amplitude (gain) and timing (phase) of their optokinetic reflex (OKR) and/or tested with turntable stimulation to investigate the same parameters for the vestibulo-ocular reflex in the dark (VOR) and light (visual VOR or VVOR). During OKR, PC-Δγ2 mice showed a relatively small, but significant, deficit, evident as a reduction in gain and a lag in phase compared to controls ($p = 0.018$ and $p = 0.012$, respectively; two-way repeated-measures ANOVA) (see Supplementary Fig. 5a in the online article). During VOR the gain values and phase leads of PC-Δγ2 mice were larger and smaller, respectively, than those of controls ($p = 0.012$ and $p = 0.030$; two-way repeated-measures ANOVA) (see Supplementary Fig. 5b in the online article). By contrast, no significant differences were observed during VVOR ($p = 0.43$ and $p = 0.63$, for gain and phase values, respectively) (see Supplementary Fig. 5c in the online article). Thus, PC-Δγ2 mice show small, but significant, abnormalities in motor performance when visual and vestibular systems are investigated separately, but not when they operate together, as under natural conditions or during visuo-vestibular training.

PC-Δγ2 mice show marked deficits in learning and consolidation

Loss of inhibition onto Purkinje cells had more profound effects on cerebellar motor learning. We studied gain and phase learning by applying a protocol aimed at reducing the gain of the VOR on day 1 (5 × 10 min sinusoidal, in phase drum and table rotation at 0.6 Hz, both with an amplitude of 5°) and subsequently shifting its phase on days 2, 3 and 4 (5 × 10 min sinusoidal in phase drum and table rotation at 0.6 Hz, but with drum amplitudes of 7.5° on day 2 and 10° on days 3 and 4, while the table amplitude remained 5°). Animals were kept in the dark between the recording days. Gain-decrease learning of PC-Δγ2 (n = 9) and control mice (n = 10) on day 1 was similar ($p = 0.11$; two-way repeated-measures ANOVA) (**Fig. 4a,b**). However, when the measurements were resumed the next day, the degree of gain reduction carried forward from the previous day's learning was significantly smaller in PC-Δγ2 mice than in controls ($p = 0.001$) (**Fig. 4b, upper panel**). This consolidation deficit was apparent at a wide range of frequencies (**Fig. 4c, upper panel**). To exclude non-specific effects (habituation during gain-decrease learning) we tested PC-Δγ2 and control mice in non-adapting VOR paradigms; importantly, mice of both genotypes showed no significant decreases in VOR over consecutive days (last gain value of session 1 vs first value of session 2; $p = 0.610$ for controls and 0.551 for PC-Δγ2 mice) (see Supplementary Fig. 6 in the online article).

Deficits in gain consolidation were also seen when the drum rotation amplitude was kept constant (3 × 10 min of sinusoidal in phase drum and table rotation at 0.6 Hz, both with an amplitude of 5°) (Fig. 4d, lower panel). Here too, the initial level of learning was not significantly affected (PC-Δγ2 mice vs controls; $p = 0.61$; n = 6 and 5, respectively), whereas the level of consolidation was significantly reduced (gain day 1→ 2, $p = 0.034$; gain day 2→ 3, $p = 0.046$). Moreover, gain consolidation deficits in PC-Δγ2 mice did not depend on the direction of learning. With a gain-increase paradigm (5 × 10 min sinusoidal out of phase drum and table rotation at 1.0 Hz, both with an amplitude of 1.6°) no significant consolidation was present in the PC-Δγ2 mice (gain day 1→ 2, $p = 0.744$, n = 6; One-Sample t-test). By contrast, consolidation in controls was present and was significantly stronger than in PC-

Δγ2 mice (p =0.002) (**Fig. 4d, lower panel**). Notably, the level of gain increase learning in PC-Δγ2 mice was not significantly different from that in controls (p = 0.800). Thus, deficits in consolidation of learned gain changes, during both gain decrease and increase training paradigms, were not due to differences in baseline performance.

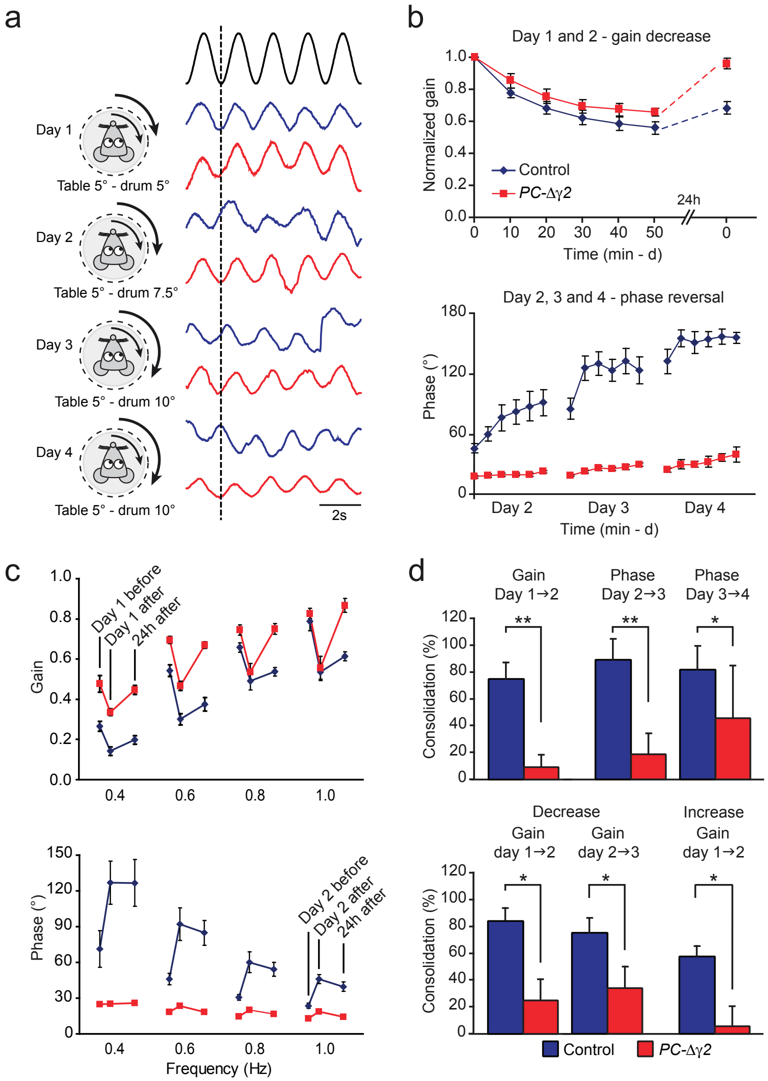

Figure 4. Motor learning is severely affected in PC-Δγ2 mice. (a) Illustration of drum and table rotation during the training paradigm. Traces show sinusoidal drum rotation (black) and examples of eye movement (control, blue; PC-Δγ2, red). Gain and phase parameters were evaluated 5 times at 10 min intervals. (b) On day 1 PC-Δγ2 and control mice showed similar gain reduction (p = 0.11), but the first test on day 2 revealed clear differences (p = 0.001) (upper panel). During phase reversal training, control mice learned better than PC-Δγ2 mice (day 4 p < 0.00001) (lower panel). (c) Differences in gain consolidation and phase reversal occurred over a wide range frequencies. "Day x before" and "Day x after" indicate values before and after training on day "x"; "24hr after" indicates the value on the next day, just before a new measurement. (d) Upper panel: differences in consolidation (percentage change carried forward from the previous day) for gain decrease (day 1 to 2) and phase reversal (day 2 to 3 and day 3 to 4). Lower panel: differences in gain consolidation were also seen with constant in phase drum and table rotation (gain decrease; two histograms on the left), and with constant out of phase drum and table rotation (gain increase; histogram on the right). For the lower panel in (d) data are from 5 control and 6 PC-Δγ2 mice, for all other panels, data are from 10 control and 9 PC-Δγ2 mice. Error bars denote s.e.m.; * and ** p < 0.05 and 0.01.

The adaptation paradigm provided on days 2, 3 and 4 immediately revealed significant deficits in phase learning in PC-Δγ2 mice, starting 10 - 20 min after the initiation of visuo-vestibular training (e.g. at 20 min $p = 0.009$) (**Fig. 4b, lower panel**). These deficits in phase change acquisition were followed by clear differences in consolidation (e.g. from day 2 to day 3 $p = 0.0008$) (Fig. 4d, upper panel). Phase adaptation deficits also occurred at a wide range of frequencies (Fig. 4c, lower panel) and were not caused by visual problems in PC-Δγ2 mice, as eye movement recordings during the adaptation sessions showed that PC-Δγ2 mice were capable of full phase reversal (see Supplementary Fig. 7 in the online article). In short, PC-Δγ2 mice showed a relatively normal capacity for acquisition during gain-decrease and gain-increase motor learning, but a profound deficit in acquisition during phase adaptation learning and a general deficit in consolidation of gain and phase adaptation.

Abnormal temporal patterns of Purkinje cell simple spikes

Since the flocculus controls adaptation of compensatory eye movements[24,25,26] and Purkinje cells provide the sole output of the cerebellar cortex (see Supplementary Fig. 1 in the online article), we analyzed floccular Purkinje cell activity during optokinetic stimulation (**Fig. 5a**). Single units of Purkinje cells that responded optimally to stimulation around the vertical axis were identified by creating tuning curves of their complex spike responses and by identifying a clean climbing fiber pause[26,27]. The average climbing fiber pause in PC-Δγ2 mice and controls was 15.3 ± 0.8 and 18.6 ± 1.3 ms, respectively (55 and 60 PC-Δγ2 and control cells, respectively; $p = 0.029$). The average simple spike firing frequency, phase relative-to-stimulus and modulation amplitude, were similar in PC-Δγ2 and control mice (**Fig. 5b**). However, as predicted by the in vitro recordings, the regularity of Purkinje cell firing was affected. For floccular simple spike activities, the CV of the ISIs was significantly reduced during visual stimulation in PC-Δγ2 mice ($p = 0.008$; PC-Δγ2: $n = 55$, controls: $n = 60$) (**Fig. 5c**). This difference reflected specific changes in temporal patterning, as CV2 was significantly lower in PC-Δγ2 mice ($p < 0.0001$) (**Fig. 5c**; see also Supplementary Fig. 8 in the online article).

If these differences in Purkinje cell firing patterns contribute to consolidation deficits in PC-Δγ2 mice, we would also expect to find them outside periods of optokinetic stimulation. Indeed, both CV and CV2 of ISIs were significantly reduced in the absence of stimulation ($p = 0.022$ and $p < 0.0001$, respectively; PC-Δγ2: $n = 41$, controls: $n = 43$) (**Fig. 5c**). By contrast, the patterns of complex spike activities of Purkinje cells did not differ between PC-Δγ2 and control mice (**Fig. 5a,c**; see also Supplementary Fig. 9 in the online article). Also the antiphasic modulation of complex and simple spikes was unchanged (**Fig. 5a**), arguing against a critical involvement of molecular layer interneurons in this phenomenon[8].

Model and simulations

We interpreted the experimental data from the 4-day gain decrease - phase adaptation routine using a ‘distributed memory’ model (**Fig. 6**). Short-term adaptation is assumed to take place in the cerebellar cortex, and is expressed as adaptation of the phase and gain of modulation of Purkinje cell simple spikes, which in turn modulate the activity of target neurons in the vestibular nucleus; this process underlies the rapid VOR gain adaptation observed in both PC- Δγ2 and control mice. On a longer timescale, the learned Purkinje cell activity

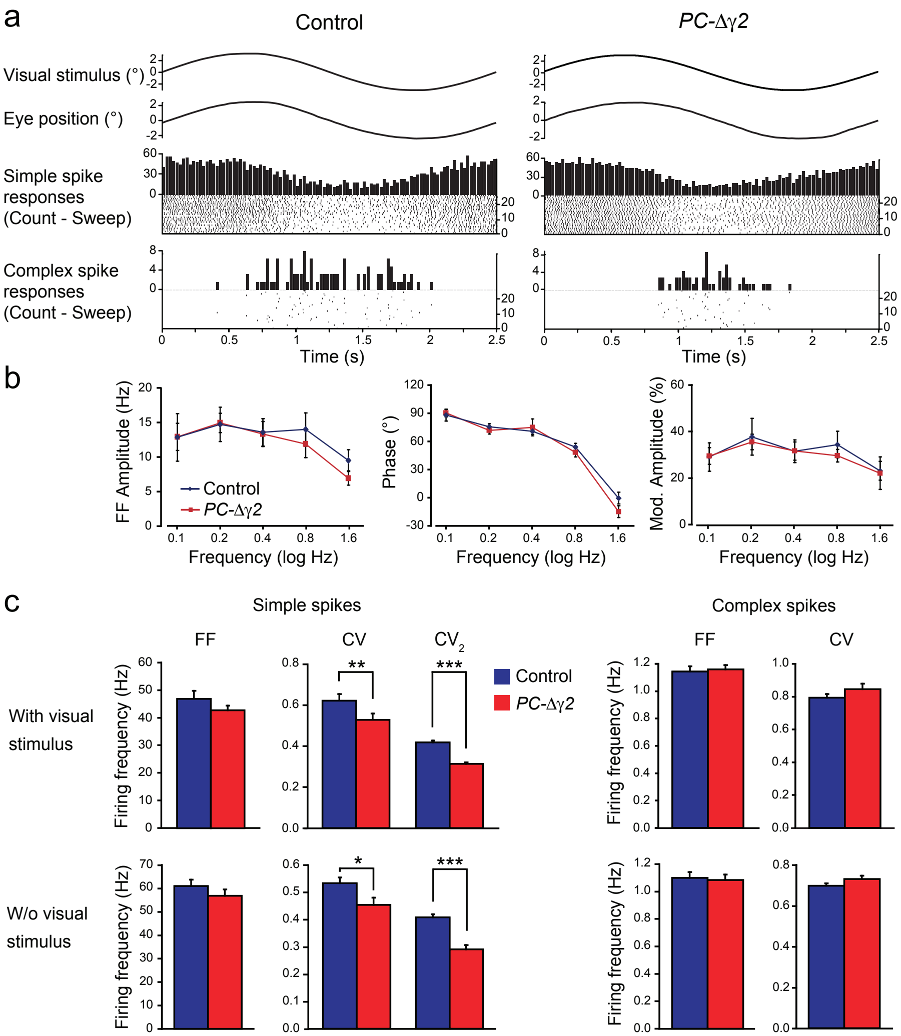

Figure 5. Temporal patterns of simple spike activities of floccular Purkinje cells are specifically affected in PC-Δγ2 mice, both during compensatory eye movement behaviour and during spontaneous behaviour. (a) Representative single unit activity recorded from Purkinje cells in the flocculus of a control and a PC-Δγ2 mouse during fixed velocity (8°/s, 0.2 Hz) OKR stimulation. The visual stimulus and eye position are shown together with histograms of simple spike and complex spike frequencies and corresponding raster plots. (b) Firing frequency, phase relative to stimulus and amplitude of modulation (see Chapter 6 Methods) of floccular simple spike activities during optokinetic stimulation (8°/s, 0.1 - 1.6 Hz) were not significantly different among PC-Δγ2 and control mice. (c) Although average firing frequency of simple and complex spike activity did not differ between PC-Δγ2 and control mice, the coefficient of variation (CV) of simple spikes in PC-Δγ2 mice was significantly reduced in recordings both with and without visual stimuli ($p = 0.008$ and $p = 0.022$, respectively). Also, CV2 values of simple spikes were significantly lower than those of controls in both conditions. Error bars denote s.e.m., * denotes $p < 0.05$, ** $p < 0.01$ and *** $p < 0.0001$.

guides plasticity at the target neurons in the vestibular nuclei[28,29], the polarity of which is presumably regulated by the precise timing of simple spikes relative to input from mossy fiber collaterals[30]. Simultaneously, a partial extinction of the previously learned changes at the level of the Purkinje cells takes place[31]. The memory is thus partially transferred to the target nuclei, potentially underlying long-term consolidation[29,32]. After several days of training, this form of ‘systems-consolidation’ ensures that the cerebellar cortex is no longer responsible for the expression of the learned behavior, but mainly regulates the precise timing (phase). In PC- Δγ2 mice, the altered temporal patterns of Purkinje cell simple spikes could impair the induction of plasticity in the nuclei and thus consolidation.

Given this working hypothesis, we examined whether deficits in VOR gain consolidation and phase adaptation in PC-Δγ2 mice could be replicated in a conceptual model of the idealized VOR circuit (Supplementary Material online). We modeled the modulation of Purkinje cell simple spike firing during head movement as resulting from linear summation of sinusoidal excitatory (parallel fiber) and inhibitory (interneuron) inputs[6]. We assumed the gain and phase of such modulation to be regulated through bidirectional plasticity of the inputs[33]. Purkinje cells and mossy fiber collaterals modulate, by linear summation of their activity, the firing of cells in the vestibular nuclei, which in turn control eye movement. Panels a-f in **Fig. 6** depict an overview of the gains and phases of sinusoidal modulation that can be attained by the elements in the simulation, drawn as positions in a polar plot in which 0° represents modulation in phase with head movement (increased activation during ipsilateral head velocity). The order of the panels follows the signal flow through the vestibulo-cerebellar system from the modeled activation of parallel fibers and interneurons (**Fig. 6a,b**), to the simple spike modulation attainable by appropriate depression and potentiation of these excitatory and inhibitory inputs (**Fig. 6c**), to the modulation of target vestibular nucleus neurons (**Fig. 6d,e**), and ultimately the resulting limits on eye movement (**Fig. 6f**). Due to the absence of inhibition in *PC-Δγ2* mice, the simple spike activation required for adequate modulation of the vestibular nucleus is out of range of the normal plasticity mechanisms in the cerebellar cortex (**Fig. 6c**). In addition, impaired plasticity of the inputs to the vestibular nucleus (**Fig. 6e**) both abolishes consolidation and excludes the possibility of extreme phase adaptations (**Fig. 6f**).

Data from four training sessions, each followed by an overnight period (**Fig. 6g**), were simulated using the upper bounds on sinusoidal modulation as depicted in panels a-f. Adaptation of modulation (**Fig. 6h I and II**) was simulated as an exponential decay from thestart position in the polar plot (defined by the initial gain and phase) towards a new position determined by the experimental paradigm (black horizontal bars in Fig. 6g). As detailed in the Supplementary Material, simulation parameters were chosen to mimic the rate of adaptation observed experimentally. Under these conditions, both control and *PC-Δγ2* Purkinje cells rapidly reached the required modulation during short-term VOR adaptation (**Fig. 6h I**). However, impairments in both VOR gain consolidation and phase adaptation, can be generated if we assume disrupted plasticity in the vestibular nucleus is caused by poor timing of simples pikes. (**Figs. 3, 5, 6h**).

Discussion

Signal coding and plasticity in cerebellar learning

Although inhibitory interneurons in the molecular layer of the cerebellum have been studied extensively[5,6,7,8], their behavioural relevance has remained enigmatic. Here, we show that these interneurons shape the temporal patterns of Purkinje cell simple spikes and suggest that this process could be essential for plasticity and consolidation in the cerebellar and vestibular nuclei.

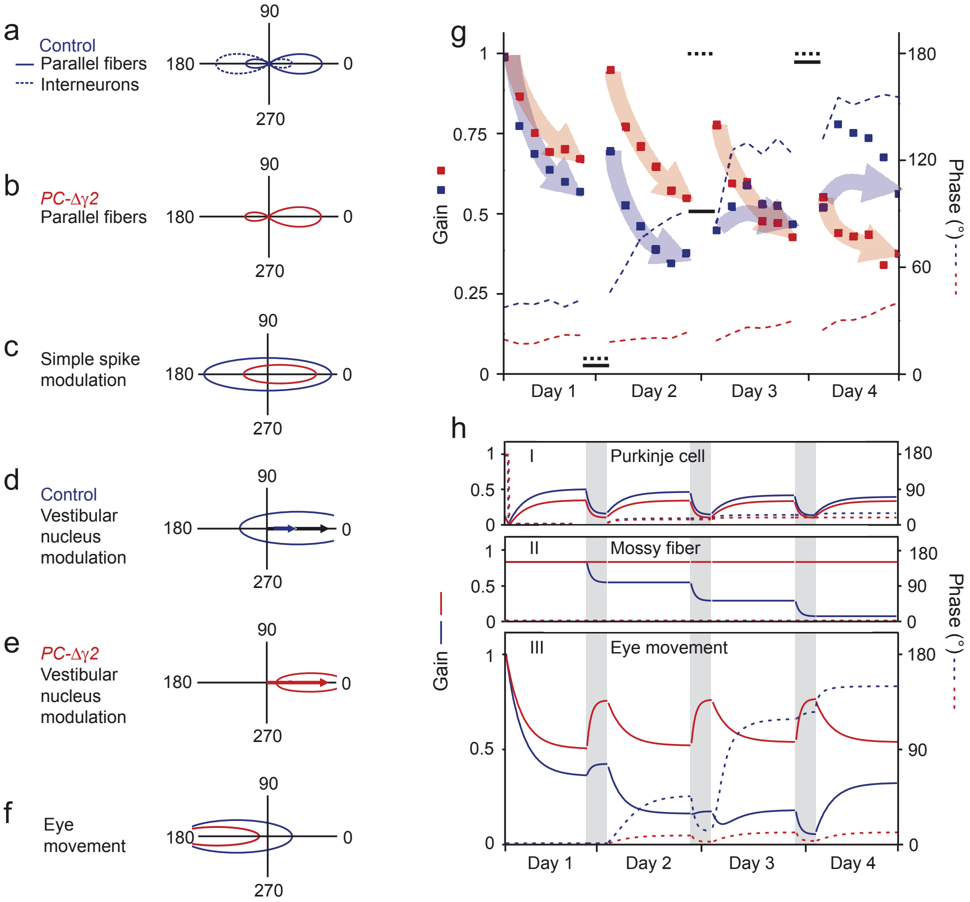

Figure 6. Interpretation of VOR adaptation data using a 'distributed memory' model. (a) Modelled activation of parallel fibers and interneurons plotted in polar coordinates. Most parallel fibers modulate in phase with ipsilateral head movement (0°), while a fraction responds to input from the contralateral horizontal canal (180°). Interneurons are modeled similarly, but with opposite sign representing their inhibitory nature. (b) Same as (a), but for PC-Δγ2 mice lacking inhibition. (c) Maximum simple spike modulation attainable by appropriate depression and potentiation of excitatory and inhibitory inputs shown in (a) and (b) for control (blue) and PC-Δγ2 (red) mice (based on linear input summation). (d) Modulation of target vestibular nucleus neurons attainable by linear summation of mossy fiber inputs (blue arrow, in phase with head movement) and Purkinje cell inputs (panel (c), blue curve) in control mice. The black arrow represents the efficacy of mossy fiber input prior to training. (e) Same as (d), but for PC-Δγ2 mice, where the efficacy of plasticity at the mossy fiber synapses is presumably impaired. (f) Limited simple spike modulation and mossy fiber plasticity restrain eye movements in PC-Δγ2 mice (red curve) as compared to control mice (blue curve). The control curve also covers the area of VOR phase reversal, from out-of-phase with head movement (180° in this figure) to in-phase (0°). (g) Experimental data; squares represent VOR gain and dashed lines represent VOR phase relative to the head (shifted by 180°, for ease of illustration) (see also Fig. 4). For each session, after initial adaptation, the learned Purkinje cell signal determines the new 'desired' phase and gain state for the vestibular nucleus neurons (dashed and solid black bars, respectively). The superimposed blue (control) and red (PC-Δγ2) arrows indicate the direction of change. (h) Simulation of the training paradigm shown in g. During training, Purkinje cells rapidly approach their target modulation (I), reflecting short-term VOR adaptation. Purkinje cell-guided plasticity of mossy fiber input to vestibular nuclei (II) allows control mice to gradually adapt the phase of their VOR during prolonged training (III). In PC-Δγ2 mice, loss of vestibular nucleus consolidation impairs phase adaptation. For simplicity, adaptation in the vestibular nuclei and partial extinction of cortical memory were simulated to occur between training sessions (grey bars).

Floccular Purkinje cells control the adaptation of compensatory eye movements by modulating the activity of vestibular nucleus neurons (see Supplementary Fig. 1 in the online article). To adapt the VOR, two things should happen within the framework of a 'distributed memory' model. First, Purkinje cells should 'learn' the correct simple spike modulation and express it at sufficient gain in order to modulate the vestibular nuclei. Second, the input from the direct vestibular pathway to the vestibular nuclei should be suppressed, as it only allows modulation in phase with ipsilateral head movement. The first of these processes is thought to reflect complementary inhibitory and excitatory actions, with plasticity at parallel fiber to Purkinje cell and parallel fiber to interneuron synapses, both under climbing fiber control[13,24,25]. The second is thought to occur through plasticity at mossy fiber to vestibular nuclei synapses[25,28]. In *PC-Δγ2* mice the temporal fidelity of Purkinje cell firing is disrupted and consolidation of learned VOR adaptations is severely compromised (**Figs. 4 and 6g**). As induction of various forms of plasticity in the vestibular and cerebellar nuclei could depend on the precise timing of inhibitory and excitatory input from Purkinje cells and mossy fiber collaterals (Supplementary online Material), disruption of this timing would impair transfer of plasticity to the nuclei and thus ‘systems consolidation’.

Simple spike trains in Purkinje cells show significantly more temporal patterns than expected from random activation, and these patterns are influenced by natural stimuli[22]. Both the electrical coupling among interneurons and the sagittal orientation of their axons[34,35] (see Supplementary Fig. 1 in the online article) will enhance the effects of feed-forward inhibition by promoting common firing patterns in ensembles of Purkinje cells within individual zones, known to project to the same nucleus[26]. The activity patterns of individual Purkinje cells in an ensemble might thus interact with each other and/or with those of mossy fiber and/or climbing fiber collaterals to facilitate the induction of plasticity in the cerebellar and vestibular nuclei[25,28,36,37]. We therefore propose that the vestibular nuclei are the locus for consolidation (see also Ref. [29,32]). Alternatively, both initial learning and consolidation could occur in the cerebellar cortex and the consolidation signal could be preserved in the average simple spike frequency of a particular Purkinje cell. In fact, changes in simple spike frequencies in the flocculus of monkeys are sufficient to drive changes in eye velocity during trial-by-trial motor learning[38]. To determine the extent to which spatiotemporal patterns of simple spikes contribute to consolidation, and whether this consolidation occurs in the nuclei, future experiments will require simultaneous multi-unit recording from ensembles of Purkinje cells and cerebellar or vestibular nuclei neurons during learning.

Previous studies have identified long-term changes at the parallel fiber to Purkinje cell synapse as a potential plasticity mechanism during cerebellar learning, and some mouse lines with disrupted LTD induction at this synapse indeed show impaired motor learning[39,40,41]. However, neither parallel fiber LTD nor LTP were impaired in *PC-Δγ2* mice. Notably, the motor learning deficits in *PC-Δγ2* mice differed from those seen in mouse lines in which LTD was impaired by blocking PKC, PKG, or alpha-CaMKII activity in Purkinje cells. Furthermore, in the latter mouse lines acute learning was affected more severely than in *PC-Δγ2* mice, whereas learning over multiple days of training was less affected[39,40,41,42].

GABAergic interneurons in the cerebellar cortex have ample possibilities to induce and express plasticity at both the synaptic input and output level[1,9,13,43,44,45]. Simultaneous induction of LTP at molecular layer interneuron and parallel fiber to Purkinje cell synapses is required for associative fear conditioning[9]. In this scenario, the potentiation of GABAergic synapses may balance the LTP of excitatory inputs in a form of scaling to preserve coincidence detection of parallel fiber inputs[7,9]. Loss of this scaling mechanism in *PC-Δγ2* mice might contribute to the observed phenotype.

Inhibition is essential for spike patterning and learning

Although *PC-Δγ2* mice showed marked deficits in cerebellar motor learning, baseline motor performance was only moderately affected. Despite the lack of synaptic GABAA receptors on *PC-Δγ2* Purkinje cells we found their average simple spike frequency to be normal. This could reflect enhancement of another inhibitory input (e.g. GABAB receptors) and/or reduced parallel fiber excitatory input. Whereas GABAB receptor-mediated inhibition of *PC-Δγ2* Purkinje cells was unchanged (see Supplementary Fig. 10 in the online article), we found a significant decrease in AMPA receptormediated EPSC charge transfer after parallel fiber stimulation (see Supplementary Fig. 4 in the online article). This might allow Purkinje cells to maintain their excitability in a normal operational range in the absence of fast inhibition. By contrast, the loss of temporal fidelity in Purkinje cell responses to parallel fiber stimulation and the increase in simple spike regularity in *PC-Δγ2* mice, were comparable to the changes seen after acute pharmacological blockade of GABAA receptors[7,12] (**Figs. 3 and 5**). The cerebellum may thus compensate for the loss of certain functions of molecular layer interneurons, but these interneurons are essential for the temporal control of Purkinje cell activity and for both phase adaptation learning and consolidation of gain adaptations.

Purkinje cell collaterals

By deleting synaptic GABAA receptors from Purkinje cells in *PC-Δγ2* mice we also disrupted any inhibition mediated by recurrent collaterals of Purkinje cell axons[10,46]. However, as GABAergic terminals from basket and stellate cells onto Purkinje cells vastly outnumber those from recurrent collaterals, and as Purkinje-Purkinje contacts in mice appear restricted to young animals[46], the phenotype we observe is most likely caused by the loss of inhibition from molecular layer interneurons. Although it has been proposed that Purkinje cell axon collaterals contribute to fast cerebellar oscillations in adult rats[47], such oscillations have not been recorded in wild-type mice[10].

General functional implications

Studies on learning and memory have focused largely on the role of plasticity at excitatory synapses onto projecting neurons. However, GABAergic interneurons also express plasticity, which increases the computational capacity of their microcircuit[1,2,9]. Here we examined the role of fast synaptic inhibition in cerebellar motor learning using genetic dissection of the circuit and suggest that feed-forward inhibition is essential for specific aspects of procedural learning. Can our findings be extrapolated to other brain regions? Feed-forward inhibition is a common motif throughout the CNS. In the amygdala it mediates extinction learning of conditioned fear responses[48]. In cortical circuits some interneuron types may serve functions similar to those we have identified in the cerebellum. For example, feed-forward inhibitory interneurons in the hippocampus may promote the temporal fidelity of synaptic integration and action potential generation in pyramidal cells necessary for encoding declarative memories[2,3]. Thus, feedforward inhibition might be an operational necessity for memory formation in different brain circuits.

References

1. Smith SL, Otis TS. Pattern-dependent, simultaneous plasticity differentially transforms the inputoutput relationship of a feedforward circuit. *Proceedings of the National Academy of Sciences of the United States of America* 2005;102:14901–14906.
2. Kullmann DM, Lamsa KP. Long-term synaptic plasticity in hippocampal interneurons. *Nature reviews* 2007;8:687–699.
3. Pouille, F.; Scanziani, M. *Science.* Vol. 293. New York, N.Y: 2001. Enforcement of temporal fidelity in pyramidal cells by somatic feed-forward inhibition; p. 1159-1163.
4. Lamsa K, Heeroma JH, Kullmann DM. Hebbian LTP in feed-forward inhibitory interneurons and the temporal fidelity of input discrimination. *Nature neuroscience* 2005;8:916–924.
5. Eccles, JC.; Ito, M.; Szentagothai, J. The cerebellum as a neuronal machine. springer; 1967.
6. Miyashita Y, Nagao S. Contribution of cerebellar intracortical inhibition to Purkinje cell response during vestibulo-ocular reflex of alert rabbits. *The Journal of physiology* 1984;351:251–262.
7. Mittmann W, Koch U, Hausser M. Feed-forward inhibition shapes the spike output of cerebellar Purkinje cells. *The Journal of physiology* 2005;563:369–378.
8. Barmack NH, Yakhnitsa V. Functions of interneurons in mouse cerebellum. *J Neurosci* 2008;28:1140–1152.
9. Scelfo B, Sacchetti B, Strata P. Learning-related long-term potentiation of inhibitory synapses in the cerebellar cortex. *Proceedings of the National Academy of Sciences of the United States of America* 2008;105:769–774.
10. Orduz D, Llano I. Recurrent axon collaterals underlie facilitating synapses between cerebellar Purkinje cells. *Proceedings of the National Academy of Sciences of the United States of America* 2007;104:17831–17836.
11. Davie JT, Clark BA, Hausser M. The origin of the complex spike in cerebellar Purkinje cells. *J Neurosci* 2008;28:7599–7609.
12. Hausser M, Clark BA. Tonic synaptic inhibition modulates neuronal output pattern and spatiotemporal synaptic integration. *Neuron* 1997;19:665–678.
13. Jorntell H, Ekerot CF. Reciprocal bidirectional plasticity of parallel fiber receptive fields in cerebellar Purkinje cells and their afferent interneurons. *Neuron* 2002;34:797–806.
14. Santamaria F, Tripp PG, Bower JM. Feedforward inhibition controls the spread of granule cellinduced Purkinje cell activity in the cerebellar cortex. *Journal of neurophysiology* 2007;97:248–263.
15. Raman IM, Bean BP. Resurgent sodium current and action potential formation in dissociated cerebellar Purkinje neurons. *J Neurosci* 1997;17:4517–4526.
16. Wulff P, et al. From synapse to behavior: rapid modulation of defined neuronal types with engineered GABAA receptors. Nature neuroscience 2007;10:923–929.
17. Schweizer C, et al. The gamma 2 subunit of GABA(A) receptors is required for maintenance of receptors at mature synapses. *Molecular and cellular neurosciences* 2003;24:442–450.
18. Barski JJ, Dethleffsen K, Meyer M. Cre recombinase expression in cerebellar Purkinje cells. *Genesis* 2000;28:93–98.
19. Brickley SG, Cull-Candy SG, Farrant M. Single-channel properties of synaptic and extrasynaptic GABAA receptors suggest differential targeting of receptor subtypes. *J Neurosci* 1999;19:2960–2973.
20. Lorez M, Benke D, Luscher B, Mohler H, Benson JA. Single-channel properties of neuronal GABAA receptors from mice lacking the gamma2 subunit. *The Journal of physiology* 2000;527(Pt 1):11–31.
21. Brunel N, Hakim V, Isope P, Nadal JP, Barbour B. Optimal information storage and the distribution of synaptic weights: perceptron versus Purkinje cell. *Neuron* 2004;43:745–757.

22. Shin SL, et al. Regular patterns in cerebellar Purkinje cell simple spike trains. *PLoS ONE* 2007;2:e485.
23. Walter JT, Alvina K, Womack MD, Chevez C, Khodakhah K. Decreases in the precision of Purkinje cell pacemaking cause cerebellar dysfunction and ataxia. *Nature neuroscience* 2006;9:389–397.
24. Ito M. Cerebellar flocculus hypothesis [letter]. *Nature* 1993;363:24–25.
25. Lisberger SG. Cerebellar LTD: A molecular mechanism of behavioral learning? *Cell* 1998;92:701–704.
26. Schonewille M, et al. Zonal organization of the mouse flocculus: physiology, input, and output. *The Journal of comparative neurology* 2006;497:670–682.
27. Hoebeek FE, et al. Increased noise level of purkinje cell activities minimizes impact of Their modulation during sensorimotor control. *Neuron* 2005;45:953–965.
28. Gittis AH, du Lac S. Intrinsic and synaptic plasticity in the vestibular system. *Current opinion in neurobiology* 2006;16:385–390.
29. Kassardjian CD, et al. The site of a motor memory shifts with consolidation. *J Neurosci* 2005;25:7979–7985.
30. Medina JF, Mauk MD. Computer simulation of cerebellar information processing. *Nature* neuroscience 2000;3(Suppl):1205–1211.
31. Medina JF, Nores WL, Mauk MD. Inhibition of climbing fibres is a signal for the extinction of conditioned eyelid responses. *Nature* 2002;416:330–333.
32. Shutoh F, Ohki M, Kitazawa H, Itohara S, Nagao S. Memory trace of motor learning shifts transsynaptically from cerebellar cortex to nuclei for consolidation. *Neuroscience* 2006;139:767–777.
33. Coesmans M, Weber JT, De Zeeuw CI, Hansel C. Bidirectional parallel fiber plasticity in the cerebellum under climbing fiber control. *Neuron* 2004;44:691–700.
34. Mann-Metzer P, Yarom Y. Electrotonic coupling interacts with intrinsic properties to generate synchronized activity in cerebellar networks of inhibitory interneurons. *J Neurosci* 1999;19:3298–3306.
35. Van Der Giessen RS, Maxeiner S, French PJ, Willecke K, De Zeeuw CI. Spatiotemporal Distribution of Connexin45 in the olivocerebellar system. *The Journal of comparative neurology* 2006;495:173–184.
36. Steuber V, et al. Cerebellar LTD and pattern recognition by Purkinje cells. *Neuron* 2007;54:121–136.
37. Blazquez PM, Hirata Y, Highstein SM. Chronic changes in inputs to dorsal Y neurons accompany VOR motor learning. *Journal of neurophysiology* 2006;95:1812–1825.
38. Medina JF, Lisberger SG. Links from complex spikes to local plasticity and motor learning in the cerebellum of awake-behaving monkeys. *Nature neuroscience* 2008;11:1185–1192.
39. De Zeeuw CI, et al. Expression of a protein kinase C inhibitor in Purkinje cells blocks cerebellar LTD and adaptation of the vestibulo-ocular reflex. *Neuron* 1998;20:495–508.
40. Feil R, et al. Impairment of LTD and cerebellar learning by Purkinje cell-specific ablation of cGMPdependent protein kinase I. *J Cell Biol* 2003;163:295–302.
41. Hansel C, et al. alphaCaMKII Is essential for cerebellar LTD and motor learning. *Neuron* 2006;51:835–843.
42. Boyden ES, et al. Selective engagement of plasticity mechanisms for motor memory storage. *Neuron* 2006;51:823–834.
43. Kano M, Rexhausen U, Dreessen J, Konnerth A. Synaptic excitation produces a long-lasting rebound potentiation of inhibitory synaptic signals in cerebellar Purkinje cells. *Nature* 1992;356:601–604.
44. Duguid IC, Smart TG. Retrograde activation of presynaptic NMDA receptors enhances

GABA release at cerebellar interneuron-Purkinje cell synapses. *Nature neuroscience* 2004;7:525–533.

45. Mittmann W, Hausser M. Linking synaptic plasticity and spike output at excitatory and inhibitory synapses onto cerebellar Purkinje cells. *J Neurosci* 2007;27:5559–5570.
46. Watt AJ, et al. Traveling waves in developing cerebellar cortex mediated by asymmetrical Purkinje cell connectivity. *Nature neuroscience* 2009;12:463–473.
47. de Solages C, et al. High-frequency organization and synchrony of activity in the purkinje cell layerof the cerebellum. *Neuron* 2008;58:775–788.
48. Likhtik E, Popa D, Apergis-Schoute J, Fidacaro GA, Pare D. Amygdala intercalated neurons are required for expression of fear extinction. *Nature* 2008;454:642–645.

CHAPTER 4
PARAGRAPH 2

RAISING CL^- CONCENTRATION IN CEREBELLAR GRANULE CELLS AFFECTS THEIR EXCITABILITY AND CONSOLIDATION OF VESTIBULO-OCULAR PHASE LEARNING

In preparation

Patricia Seja[*], *Martijn Schonewille*[*], *Guillermo Spitzmaul*[*], *Aleksandra Badura*[*], *Ilse Klein, Bill Wisden, Christian A. Hübner, Chris I. De Zeeuw, Thomas J. Jentsch*

Abstract

Cerebellar cortical throughput involved in motor control comprises granule cells and Purkinje cells, both of which receive inhibitory GABAergic input from interneurons. The GABAergic input to Purkinje cells is known to be essential for learning and consolidation of the vestibulo-ocular reflex, but the role of control of excitability of granule cells remains to be elucidated. Here, we disrupted the Kcc2 K-Cl cotransporter specifically in either cell type so as to manipulate their excitability and synaptic inhibition by $GABA_A$-receptor Cl^- channels. In both granule cells and Purkinje cells, Kcc2, but not Kcc3, proved to be the major Cl^- extruder indicated by a roughly twofold increase of $[Cl^-]_i$ upon *Kcc2* disruption. Whereas the reduced Cl^- gradient nearly abolished the GABA-induced hyperpolarization of Purkinje cells, it merely affected the excitability of granule cells, because their resting potential was depolarized owing to a resting Cl^- conductance through GABA- and glycine-receptors. Ablation of Kcc2 cotransporter from granule cells predominantly impaired consolidation of long-term phase learning of the vestibulo-ocular reflex, whereas baseline performance, short-term gain-decrease learning and gain consolidation remained intact. In contrast, a lack of Kcc2 in Purkinje cells caused the known deficits in baseline performance, gain and phase learning, and consolidation. Hence, granule cell excitability plays a hitherto unknown, but specific role in consolidation of phase learning.

Introduction

The cerebellum controls movements through a uniformly patterned neuronal circuitry in the cerebellar cortex (Supplementary Fig. 1). GABAergic Purkinje cells (PCs) provide the only output of the cerebellum. Their spiking pattern is the final integrated response of all the information the cerebellum receives through its mossy and climbing fiber inputs[1]. PCs receive excitatory input at their large dendritic arborizations in the molecular layer directly from climbing fibers, and indirectly from mossy fibers through granule cells (GCs) whose axons form the parallel fiber system. The activity of PCs and GCs is controlled by inhibitory GABAergic interneurons, such as stellate, basket and Golgi cells[2]. These interneurons are also activated by parallel fibers and give rise to a feedback and feedforward inhibition through Golgi cells on GCs, and to feedforward inhibition through stellate cells and basket cells on PCs (Supplementary Fig. 1). In addition, there is lateral inhibition of PCs on other PCs. The role of particularly the inhibition on GC output and eventually motor control remains poorly understood[3]. While feedforward inhibition modulates the timing and pattern of PC activity[4-7], feedback inhibition of GCs is thought to filter their mossy fiber input[3]. So far, the functional roles of specific inhibitory pathways in cerebellar circuits has been probed by elimination of Golgi cells[8] and by genetic disruption of GABA-receptor subunits on PCs[7]. Elimination of Golgi cells produced severe acute motor disorders[8], whereas Purkinje-cell specific disruption of γ2 GABA receptor subunits led to mild impairment of baseline motor performance accompanied by a dramatic deficit in motor learning and consolidation of both amplitude and timing parameters[7].

Here we take a different approach by changing the Cl^- equilibrium potential of the two main cerebellar target cells of synaptic inhibition, GCs and PCs, either singly or in combination. The electrical response of inhibitory $GABA_A$ receptors depends on the difference between the resting membrane potential and the electrochemical equilibrium potential for Cl^-. Neuronal intracellular chloride concentration ($[Cl^-]_i$) is mainly determined by the opposing activities of Cl^--extruding K-Cl cotransporters (KCCs) and Cl^--accumulating Na-K-2Cl cotransporters (NKCCs)[9]. Accordingly, the change from perinatal depolarizing GABA-response to the hyperpolarizing response in the adult CNS (the 'GABA-switch')[10] is correlated with a downregulation of Nkcc1 and an upregulation of Kcc2[11-14]. Kcc2 is neuron-specific and broadly expressed across adult CNS[13]. Although Kcc1 and Kcc3 are also expressed in brain[15-18], their expression is not limited to neurons and it remains unclear whether they play an important role in neuronal Cl^- extrusion[15]. In the cerebellar cortex, Kcc2 is expressed in GCs, PCs and interneurons[13, 19, 20], whereas Kcc3 has only been found on PCs[15, 16]. The neuronal expression of Nkcc1 at early developmental stages generally decreases with time[17, 21], but cerebellar GCs retain substantial Nkcc1 expression levels throughout adulthood[17, 21, 22].

To explore the role of synaptic inhibition in cerebellar function, we specifically disrupted *Kcc2* in GCs and PCs, and *Kcc3* in PCs. This circumvents the perinatal lethality and CNS degeneration of constitutive *Kcc2*[12] and *Kcc3*[15] knock-outs, respectively, and allows the assignment of phenotypes to specific target cells. Whereas this work identifies Kcc2 as the major Cl^- extruder of both GCs and PCs, the effect of *Kcc2* disruption on the GABA-response of either cell was different. It strongly reduced the GABA-induced hyperpolarization of PCs, but surprisingly the voltage-response of GCs remained virtually unchanged. This was owed to a depolarization of $Kcc2^{-/-}$ GCs, whose resting potential was co-determined by Cl^- currents through GABA- and glycine-receptors. Possibly owing to an increased excitability of constitutively depolarized GCs, GC-ΔKCC2 mice were not able to consolidate their phase learning of vestibulo-ocular reflexes. Our work reveals an unexpected role of the $[Cl^-]_i$ of GC in cerebellar plasticity.

Results

Specific deletion of Kcc2 and Kcc3 in cerebellar granule cells and Purkinje cells.

To generate mice that would allow cell-specific deletion of the K^+Cl^--cotransporters Kcc2 and Kcc3, we generated $Kcc2^{lox/lox}$ and $Kcc3^{lox/lox}$ mice in which exons 2-5 and 5-6, respectively, were flanked by loxP sites **(see Methods and Supplementary Figs. 2 and 3).** Western blot analysis showed that $Kcc2^{lox/lox}$ mice expressed Kcc2 at wild-type (WT) levels **(Supplementary Fig. 2c)** and immunohistochemistry revealed no change in its cellular and subcellular localization[12] **(Fig. 1a,e).** Likewise, the expression level of Kcc3 was not changed in $Kcc3^{lox/lox}$ mice (**Supplementary Fig. 3c).**

These 'floxed' mice were crossed with L7/Pcp2::Cre mice[23] or with Δα6::Cre mice[24] to disrupt Kccs specifically in PCs or GC, respectively. The latter mice were intercrossed to delete the respective Kcc gene in both PCs and GCs. For simplicity, the conditional KCC knock-out (KO) mouse models will be named PC-ΔKCC2, GC-ΔKCC2, PC;GC-ΔKCC2, PC-ΔKCC3 and PC-Δ(KCC2+KCC3) for mice lacking expression of Kcc2 and/or Kcc3 in either PC, GC and PC+GC, respectively. Mice with PC- and GC-specific deletion of Kcc2 or Kcc3 displayed normal survival and had no immediately visible phenotype.

We ascertained the cell-specific deletion of *Kcc2* by immunofluorescence. Like in other brain regions, cerebellar expression of Kcc2 increases after birth[13], with adult levels being reached between P20-P30 **(Supplementary Fig. 4a).** When examined around P30, Kcc2 was robustly expressed in the cerebellar cortex **(Fig. 1a,e),** including GCs, granular-layer glomeruli, cell bodies and dendritic trees of PCs, and interneurons in the molecular and granular layers. Kcc2 expression was specifically lost in GCs of GC-ΔKCC2 mice (Fig. 1b,f). PC-ΔKCC2 mice induced deletion of Kcc2 only in PCs **(Fig. 1c,g).** The combination of both Cre-lines deleted Kcc2 from GCs and PCs **(Fig. 1d,h)** while interneurons retained Kcc2 labeling **(Fig. 1c,d, arrows).**

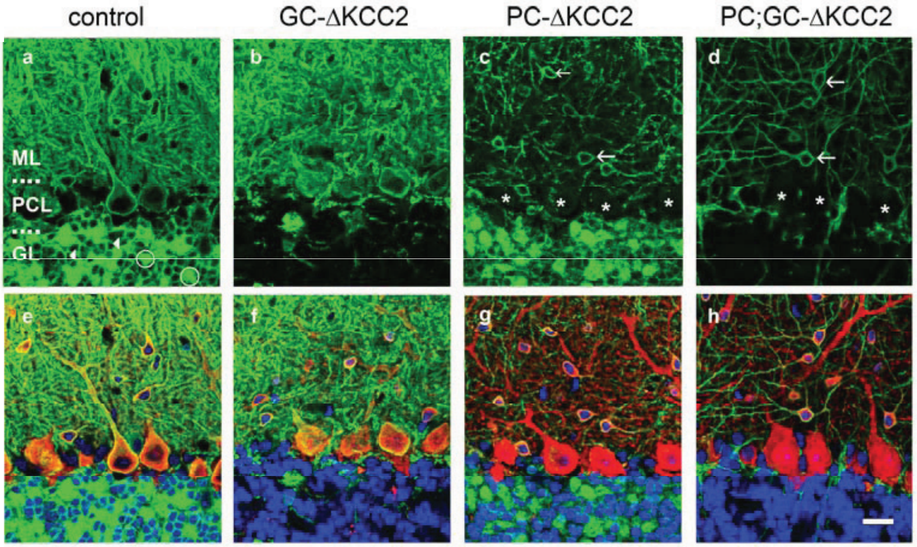

Figure 1. Cell-type specific deletion of Kcc2 in cerebellum. (a-h) Immunofluorescence staining for Kcc2 (green) on sagittal sections of cerebellar cortex for the different mouse genotypes. (a,e) Kcc2$^{lox/lox}$ mice (control). Representative positive granule cells are indicated with arrowheads and granular layer glomeruli with circles. (b,f) GC-ΔKCC2 (Δα6::Cre; Kcc2$^{lox/lox}$) mice with specific deletion of KCC2 in granule cells. (c,g) PC-ΔKCC2 (L7/Pcp2::Cre; Kcc2$^{lox/lox}$) mice with specific deletion of Kcc2 in Purkinje cells (*). (d,h) PC;GC-ΔKCC2 (L7/Pcp2::Cre; Δα6::Cre; Kcc2$^{lox/lox}$) mice with Kcc2 deletion in both Purkinje and granule cells. (e-h) same sections as the corresponding upper panel but co-stained for calbindin (red), a cytosolic marker for Purkinje cells, and TOPRO3 (blue) as nuclear marker. Note persistent expression of Kcc2 in the cerebellar interneurons (arrows, (c,d)). Asteriks in (c,d) indicates Purkinje cell somata. ML, PCL and GL, molecular layer, Purkinje cell layer and granule cell layer, respectively. Scale bar, 20 µm.

Not only the expression of Kcc2 in WT mice, but also its disruption by either L7/Pcp2::Cre or Δα6::Cre progressed with time and was dependent on the cerebellar region (Supplementary Fig. 4). Because we lack Kcc3 antibodies that work reliably in immunocytochemistry, we used *in situ* hybridization to confirm *Kcc3* deletion. It revealed prominent *Kcc3* mRNA expression in PCs that was abolished in PC-ΔKCC3, but not in GC-ΔKCC3 mice **(Supplementary Fig. 5).**

Histological analysis of adult GC-ΔKCC2, PC-ΔKCC2 and PC;GC-ΔKCC2 mice cerebellum showed normal morphology **(Supplementary Fig. 6) a**nd a normal distribution of inhibitory synapses **(Supplementary Fig. 7).** These mice neither showed any morphological deficit at the ultrastructural level **(Supplementary Fig. 8a).** The density of their inhibitory synapses in the granular and molecular layers was indistinguishable from those in controls (p = 0.75, p = 0.22, respectively; One-way ANOVA) **(Supplementary Fig. 8b).** The density of their parallel fiber synapses and the morphology of their Purkinje cell spines also remained normal (p = 0.08 and p = 0.13 compared to controls; One-way ANOVA) **(Supplementary Fig. 8c).**

Kcc2 is the major Cl⁻ extruder of Purkinje cells.

To examine the roles of Kcc2 and Kcc3 in Cl⁻ homeostasis of PCs, we measured GABA-induced Cl⁻ currents using non-invasive gramicidin-perforated patch-clamp technique. In view of the difficulty of patching slices of adult mice, we performed this analysis between P26 and P50 in regions where deletion of Kcc2 was complete **(Supplementary Fig. 4b).**

Short puff application of the $GABA_A$-receptor agonist muscimol strongly hyperpolarized current-clamped PCs from (control) *Kcc2*$^{lox/lox}$ mice. This response was greatly reduced in PC-ΔKCC2 mice **(Fig. 2a).**

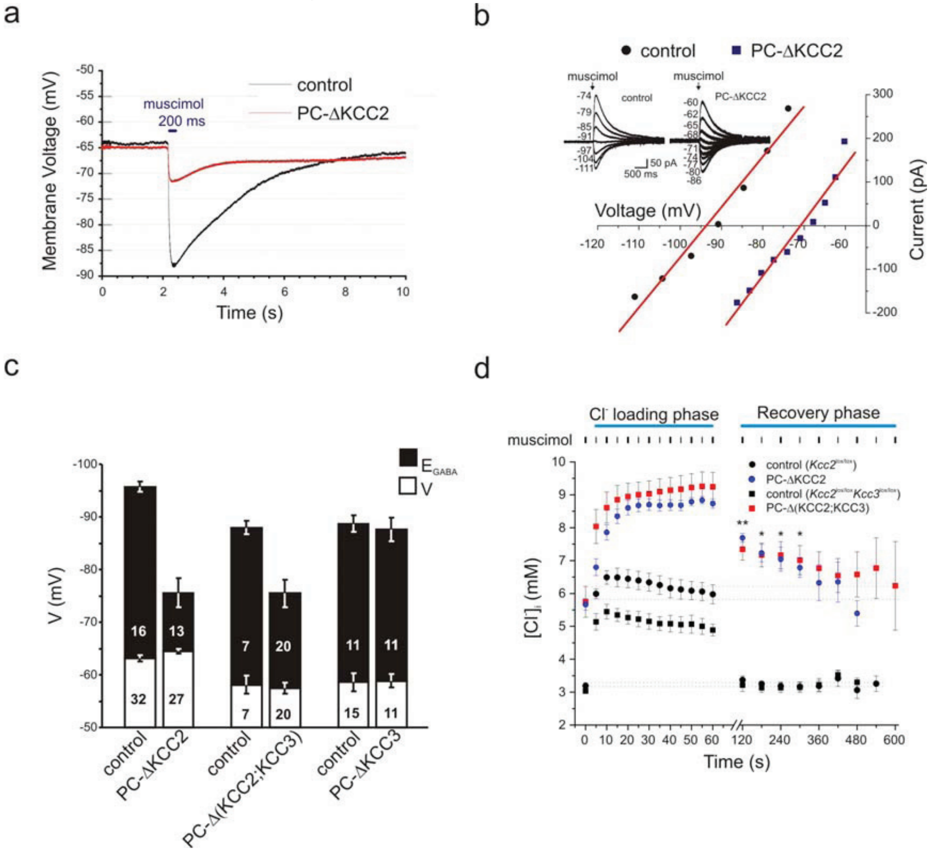

Figure 2. Role of Kcc2 and Kcc3 in setting intracellular Cl⁻ concentration of Purkinje cells. (a), Effect of muscimol on membrane voltage of PCs from control and PC-ΔKCC2 mice. Recordings were obtained in current-clamp (I=0). (b) Determination of E_{GABA}. Maximum current after puff application of muscimol (inset) is plotted against voltage. The intersection of the line (obtained from linear regression) with I=0 gives the Cl⁻ equilibrium potential E_{GABA}. Inset, current responses to puff application of muscimol to PC somata in control (left) and PC-ΔKCC2 (right) mice. Membrane voltages (corrected for series resistance) are shown on the left of traces. (c) Summary of V and E_{GABA} (shown as hatched column above the V column) of different genotypes. 'Floxed' littermates served as paired controls (number of cells measured indicated on bars). (d), Time course of $[Cl^-]_i$ during and after Cl⁻ loading phase for PC-ΔKCC2 mice (blue circles, n=7) and its control littermates (black circle, n=5) and PC-Δ(KCC2+KCC3) mice (red squares, n=6) and its control littermates (black squares, n=5). Plot displays averaged values ± SEM.

Additional disruption of *Kcc3* did not reduce the response further and PC-ΔKCC3 cells responded to muscimol like control PCs (not shown). E_{GABA} was determined from the reversal potential of $GABA_AR$ currents of PCs that were clamped to different potentials and subjected to 30-ms muscimol puffs to their somata **(Fig. 2b, inset).** E_{GABA} of PCs lacking Kcc2 was ~20 mV more positive than in controls (Fig. 2b and Table I), indicating a 2-fold increase in $[Cl^-]_i$ when neglecting the HCO_3^- conductance of GABA-receptors[25] **(Table I).** In PC-ΔKCC3 mice, E_{GABA} was undistinguishable from littermate controls **(Fig. 2c).** In the double conditional KO (PC-Δ(KCC2+KCC3)), E_{GABA} was shifted by ~15 mV to positive voltages **(Fig. 2c)**. Most likely owed to differences in genetic background, this shift was smaller than between PC-ΔKCC2 and their littermates. Control measurements showed that the introduction of loxP sites in the *Kcc2* gene or the expression of the Cre-recombinase did neither alter the resting membrane potential nor E_{GABA} of PCs **(Supplementary Fig. 9a).** The resting membrane voltage V of PCs was not changed by disrupting *Kcc2* or *Kcc3* **(Fig. 2c and Table I).**

We conclude that Kcc2, but not Kcc3, plays a major role in setting resting $[Cl^-]_i$ of PCs. The transport capacity of Cl^- extruders, however, is not directly reflected in steady-state $[Cl^-]_i$. To investigate whether a role of Kcc3 becomes apparent in assays for net Cl^- transport, we examined Cl^-_i extrusion of PCs during and after Cl^- loading[26, 27]. **Depolarizing pulses** were used to drive Cl^- through muscimol-activated GABA-receptors into PCs (see Supplementary Methods and Supplementary Fig. 10). Starting from different resting values (Fig. 2c and Table I), $[Cl^-]_i$ increased rapidly during the loading phase (Fig. 2d). In control mice, $[Cl^-]_i$ quickly reached steady-state and then slightly decreased, possibly owing to an activation of Cl^- extruders (Fig. 2d). By contrast, $[Cl^-]_i$ continued to increase slowly in PCs lacking Kcc2 or both Kcc2 and Kcc3. At the end of an 1-min muscimol washout period, control PCs had fully recovered their resting $[Cl^-]_i$, whereas PCs of either PC-ΔKCC2 or PC-Δ(KCC2+KCC3) mice needed ~4 min to reach their initial $[Cl^-]_i$. Thus, also this test failed to detect a clear contribution of Kcc3 in Cl^- regulation.

Kcc2-mediated Cl^- extrusion contributes to the resting membrane potential in granule cells.

Whereas E_{GABA} of PCs could be obtained by perforated patch measurements, this approach failed with the small GCs. We instead resorted to cell-attached recordings of $GABA_A$-receptor Cl^- currents and voltage-gated K^+ currents[28] to determine the driving force for Cl^- (DF_{GABA})[29] and the membrane voltage V, respectively **(Fig. 3a). As** *Kcc3* expression is not detected in GCs **(Supplementary Fig. 5),** we only analyzed cells from *Kcc2*$^{lox/lox}$ and GC-ΔKCC2 mice.

Single-channel activity of $GABA_ARs$ was detected in approximately 80% of patches from control or GC-ΔKCC2 GCs **(Fig. 3a).** The single channel conductance and apparent mean open time suggested that they mainly correspond to α_6-containing $GABA_ARs$[30]. Their opening could be blocked by including $GABA_A$-receptor blockers picrotoxin or gabazine (100 μM each) in the pipette (not shown). DF_{GABA} was determined as the potential where the single channel currents reversed polarity (at this point $DF_{GABA} = -V_p$). Surprisingly, DF_{GABA} was ~ 7 mV both in the presence and absence of Kcc2 **(Fig. 3a; p>0.05, t-test and Table**

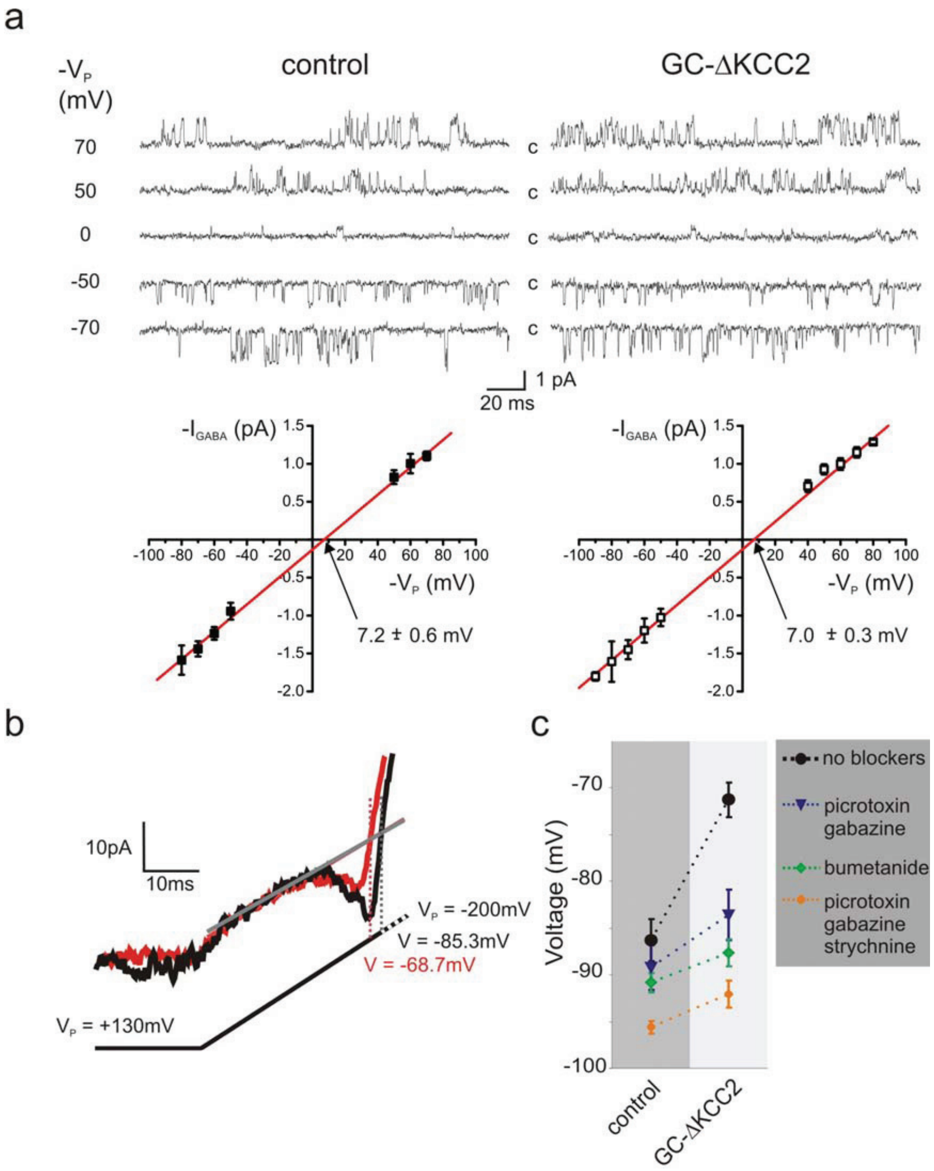

Figure 3. Kcc2 deletion in granule cells alters $[Cl^-]_i$ and the resting membrane potential V. (a), Driving force for Cl^- determined by currents through $GABA_A$ receptors measured in cell-attached patch-clamp recordings with 1 µM muscimol, 20mM TEA, 5mM 4-AP and 1µM strychnine in the pipette. Top, single-channel recordings at different pipette voltages from $Kcc2^{lox/lox}$ (control) and GC-ΔKCC2 GCs. 'c' indicates the closed state. Below, mean single channel currents as function of voltage. Linear regression (line) reveals that Kcc2 deletion does not change the Cl^- driving force (arrow). Single channel conductance and mean open time were similar for both genotypes (18.4 ± 0.3 and 18.3 ± 0.4 pS and 0.40 ± 0.02 and 0.41 ± 0.02 ms for control and GC-ΔKCC2, respectively). (b) V determined from currents through K_V channels measured in cell-attached mode. Representative recordings for a GC-ΔKCC2 (red) and control (black) GC. The intersection of a linear fit to the linear ('leak') current (~ +70 to +20mV) with the recorded outward currents gives V. Below, voltage protocol. (c) V of granule cells from GC-ΔKCC2 mice and control littermates in the absence and presence of blockers for: $GABA_ARs$ (picrotoxin and gabazine, 100 µM each), $GABA_ARs$ + GlyR (100 µM picrotoxin + 100 µM gabazine + 1 µM strychnine) and Nkcc1 (10 µM bumetanide). Data shown are mean ± SEM. Number of experiments: "no blockers" (n=22, control; n=39, GC-ΔKCC2), picrotoxin + gabazine (n=12, control; n=19, GC-ΔKCC2), picrotoxin + gabazine + strychnine (n=9, control; n=11, GC-ΔKCC2) and bumetanide (n=26, control; n=27, GC-ΔKCC2).

I). These values correspond to a slightly depolarizing action of GABA on GCs of either genotype.

To determine V, voltage ramps from +130 to -200mV were applied to cell-attached GC patches to elicit K_v currents[28]. Their reversal potential corresponds to V as the K^+ concentration of the pipette solution (155 mM K^+) closely mimics intracellular [K^+]. Between ramps the pipette was held at +60 mV to avoid inactivation of K_V channels. Currents elicited by voltage ramps showed an initial small 'leak' current followed by an inward current (representing opening of K_V channels) and a robust outward current **(Fig. 3b).** V was determined as the voltage where the extrapolated initial 'leak' current intersected with the K_v current[28] **(Fig. 3b),** giving V = -86.3 ± 2.2 mV (n=22) for control and V = -71.3 ± 1.9 mV (n=39) for GC-ΔKCC2 mice. Hence *Kcc2* disruption depolarizes GCs by about 15 mV. From these values and $E_{GABA}=DF_{GABA}+V$ we deduce that $[Cl^-]_i$ of GCs increased about 2-fold upon *Kcc2* disruption **(Table I).**

The observation that V closely followed the change in E_{GABA} indicated that GCs display a sizeable Cl^- conductance under resting conditions. Because GCs are tonically inhibited by ambient GABA[31], we asked whether blocking $GABA_AR$ Cl^- channels with gabazine and picrotoxin would influence V. Whereas these inhibitors did not significantly change V of control GCs, cells lacking Kcc2 were hyperpolarized to voltages similar to those of controls **(Fig. 3c; p=0.129, t-test).** Additional blockade of GlyRs by 1 μM strychnine hyperpolarized GCs of both control and GC-ΔKCC2 mice to V = -95.6 ± 2 mV (n=9) and V = -92.1 ± 4.9 mV (n=11), respectively **(Fig. 3c).** Thus both $GABA_A$ and GlyRs influence the resting potential of cerebellar granule cells.

Blockade of $GABA_A$- and glycine-receptors strongly hyperpolarized GCs lacking Kcc2, indicating a depolarizing Cl^- efflux and hence a $[Cl^-]_i$ that was above electrochemical equilibrium. Surprisingly, even control cells hyperpolarized when both receptors were blocked, indicating that $[Cl^-]_i$ is above equilibrium even in the presence of Kcc2. A depolarizing Cl^- efflux in WT GCs was also supported by E_{GABA} that was slightly positive to V (-79.1 ± 2.3 vs. -86.3 ± 2.2 mV) **(Table I).** As *in situ* hybridization showed robust *Nkcc1* expression in the granule cell layer **(Supplementary Fig. 11**), we blocked this transporter with 10 μM bumetanide. Thereupon GC-ΔKCC2 granule cells hyperpolarized close to control values **(Fig. 3c)**, identifying Nkcc1 as a major Cl^- loader of those cells. Members of the non-rectifying K2P K^+ channel family, which are highly expressed in GCs[32-34], are most likely responsible for the hyperpolarization of granule cells when GABA- and glycine-receptors were blocked.

In conclusion, the deletion of *Kcc2* in GCs does not change their slightly depolarizing GABA response, which may lead to a shunting inhibition in either genotype. However, the significant depolarization of GCs lacking Kcc2 indicates that they may be more excitable than WT cells.

Spontaneous spiking of Purkinje cells

To investigate whether the disruption of Kcc2 in GCs or PCs affects the electrical output of the cerebellar cortex, we investigated the spontaneous firing of PCs in slice preparations **(Fig. 4).** The frequency of firing was similar between PCs from PC-ΔKCC2, GC-ΔKCC2 and corresponding control littermate mice. However, the regularity of firing, measured as the coefficient of variation of the interspike interval (ISI CV) was significantly reduced in adult mice (>11 weeks) (ISI CV = 0.159 ± 0.015 (n=33) for control and 0.097 ± 0.012 (n=36) for PC-ΔKCC2), indicating a higher firing regularity **(Fig. 4, p<0.05, t-test)**. Interestingly, in GC-ΔKCC2 mice, ISI CV of PC increases with respect to control littermates (ISI CV = 0.096 ± 0.007 and 0.145 ± 0.009 for control (n=50) and GC-ΔKCC2 (n=55), p<0.0001), showing that spontaneous firing events occurs more irregularly **(Fig. 4).**

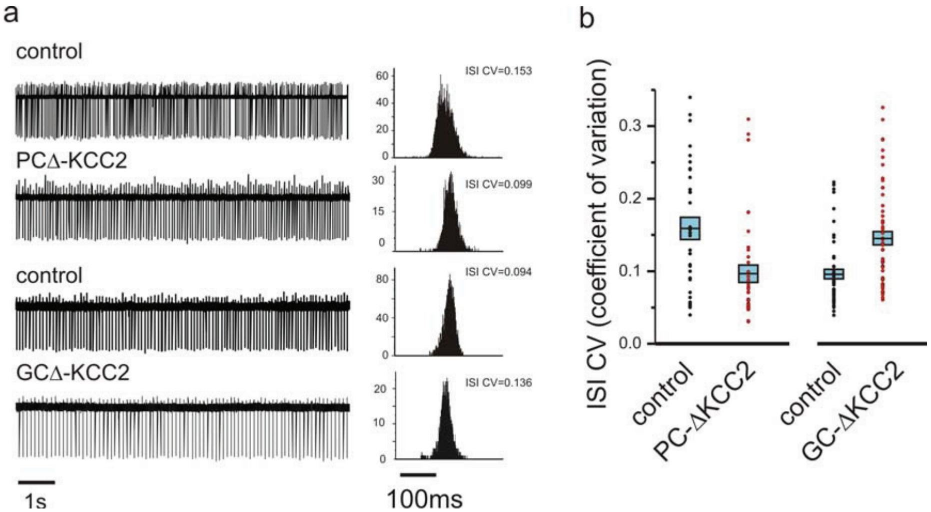

Figure 4. Spontaneous spiking of PCs. (a) Representative simple spike recordings (left) of PCs recorded from PC-ΔKCC2 mice and control littermates (upper traces) and GC-ΔKCC2 mice and control littermates mice (lower traces), and their corresponding ISI histograms (right). (b) The coefficient of variation of interspike interval (CV) for PC-ΔKCC2 mice (n=36), GC-ΔKCC2 mice (n=55) and their respective control littermates (n=33 and n=50). The averages are indicated by black horizontal lines ±SEM (blue boxes). Individual values for each PC are shown as black (control) and red (conditional Kcc2 knockout) circles. Recordings were done at RT with cell attached patch clamp.

Effect of neuron-specific Kcc2 deletion on learning and consolidation.

By eye, GC-ΔKCC2 mice did, just like the other mutants (PC-ΔKCC2 mice and PC;GC-ΔKCC2 mice), not show any overt sign of motor deficits. To further assess their overall cerebellar motor performance we tested their compensatory eye movements (8 male GC-ΔKCC2 mice) and compared them to those of their control littermates (n=8), PC-ΔKCC2 (n=8), and PC;GC-ΔKCC2 mice (n=10) **(Fig. 5).** The GC-ΔKCC2 mice did not show any significant deficit in the gain (amplitude) or phase (timing) of their optokinetic reflex (OKR), their vestibulo-ocular reflex in the dark (VOR), or their vestibulo-ocular reflex in the light (visual VOR or VVOR) (for OKR, VOR and VVOR gain values: p = 1.00, p = 0.99 and p = 0.72, respectively; for OKR, VOR and VVOR phase values: p = 0.85, p = 0.36 and p = 0.14, respectively; repeated measures ANOVA) **(Fig. 5a,b,c).** In contrast, both the PC-ΔKCC2 and PC;GC-ΔKCC2 mice showed a small, but significant, decrease in the gain of their OKR compared to controls (p = 0.015 and p = 0.035, respectively; repeated measures ANOVA), while the PC;GC-ΔKCC2 mice also revealed a significant phase lag during OKR, VOR as well as VVOR (compared to controls p = 0.002, p = 0.006 and p = 0.001, respectively; repeated measures ANOVA).

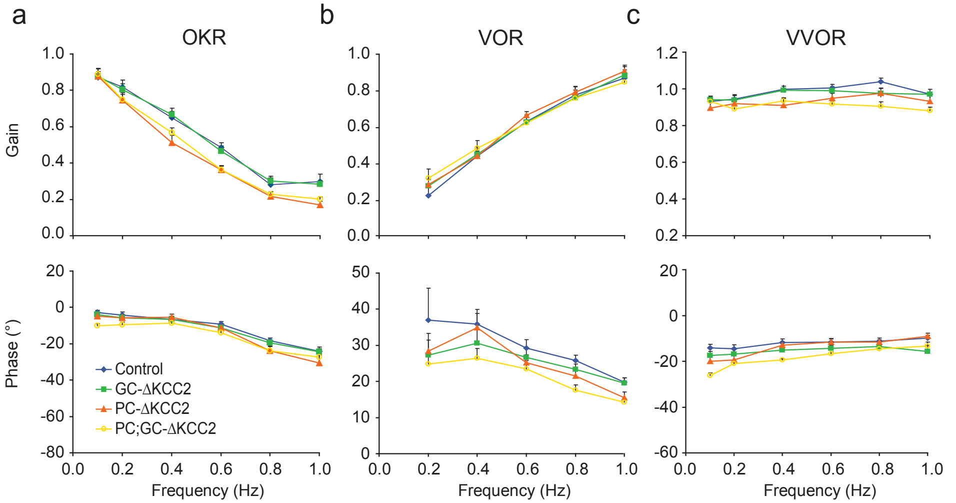

Figure 5. Motor performance in control, GC-ΔKCC2, PC-ΔKCC2 and PC;GC-ΔKCC2 mice. We measured the performance of compensatory eye movements in control mice (n = 8), GC-ΔKCC2 (n = 8) mice, PC-ΔKCC2 mice (n = 8), and PC;GC-ΔKCC2 mice (n = 10). (a) OKR gain was not significantly affected in GC-ΔKCC2 mice (p = 1.00; repeated measures ANOVA), but it was significantly lower in PC-ΔKCC2 mice and PC;GC-ΔKCC2 mice than in controls (p = 0.015 and p = 0.035, respectively; repeated measures ANOVA). The PC;GC-ΔKCC2 mice revealed a significant phase lag during OKR (p = 0.002; repeated measures ANOVA), but the other mutants did not (p = 0.851 for GC-ΔKCC2 mutant, p = 0.241 for PC-ΔKCC2 mutant; repeated measures ANOVA). (b) VOR gain values did not differ among KCC2 conditional KO and control mice (p = 0.992 for GC-ΔKCC2 mice, p = 0.921 for PC-ΔKCC2 mice, p = 0.975 for PC;GC-ΔKCC2 mice controls; repeated measures ANOVA). The PC;GC-ΔKCC2 mice revealed a significant phase lag during VOR (p = 0.006; repeated measures ANOVA), but the other mutants did not (p = 0.361 for GC-ΔKCC2 mutant, p = 0.316 for PC-ΔKCC2 mutant; repeated measures ANOVA). (c) VVOR gain values did not differ among KCC2 mutants and control mice (p = 0.716 for GC-ΔKCC2 mice, p = 0.369 for PC-ΔKCC2 mice, p = 0.074 for PC;GC-ΔKCC2 mice controls; repeated measures ANOVA). The PC;GC-ΔKCC2 mice revealed a significant phase lag during VVOR (p = 0.001; repeated measures ANOVA), but the other mutants did not (p = 0.143 for GC-ΔKCC2 mutant, p = 0.625 for PC-ΔKCC2 mutant; repeated measures ANOVA). Error bars denote SEM.

Next, we investigated the impact of Kcc2 ablation in granule cells on motor learning and consolidation. To this end we subjected the mice to VOR adaptation paradigms that test short-term and long-term learning. Short-term learning was tested by providing mismatch vestibular and visual stimulation that consists of five 10 min sessions with in-phase table and drum rotation at the same amplitude (5 degrees) and frequency (0.6 Hz), effectively inducing a decrease of the VOR gain. The GC-ΔKCC2 mice (n = 9) did not show any deficit during this short-term, gain-decrease learning (p = 0.74; repeated measures ANOVA) **(Fig. 6a).** In contrast, PC-ΔKCC2 (n = 10) and PC;GC-ΔKCC2 mice (n = 10) showed a significant impairment in VOR decrease learning compared to controls (n = 9) (p = 0.003 and p < 0.001, respectively; repeated measures ANOVA). When we measured the VOR the next day after keeping the animals overnight in the dark, the GC-ΔKCC2 mice showed a level of gain consolidation that was comparable to that of controls (i.e. 50 to 60%; p = 0.99 vs. controls; One-way ANOVA) **(Fig. 6b, left panel).** For this parameter too, the PC-ΔKCC2 and PC;GC-ΔKCC2 did show a significant deficit (consolidation levels of about 10% in both cases; p = 0.030 and p = 0.025 vs. controls, respectively; One-way ANOVA) confirming that inhibition provided by the molecular layer interneurons rather than the excitability of granule cells contributes to gain consolidation[7].

Finally, we also subjected the mice to a long-term VOR phase reversal training paradigm, which allows the identification of deficits in the adaptation of timing of movements[7]. For this paradigm the mice are subjected, after an initial day of standard gain-decrease training (see above), to in-phase table stimulation with a fixed amplitude of 5° at 0.6 Hz (days 2, 3, 4 and 5) and drum stimulation with a larger amplitude of 7.5° on day 2 and 10° on days 3, 4 and 5 all at 0.6 Hz, effectively causing a reversal of the VOR phase **(Fig. 6c).** The GC-ΔKCC2 mice were able to significantly modify their VOR phase within 50 minutes of training for each consecutive day ($p < 0.005$ for VOR learning curve on days 2, 3, 4 and 5, Paired Samples Student's t-test). However, starting from day 4 of the training their VOR phase adjustment was impaired when compared to controls ($p = 0.983$ on day 2, $p = 0.088$ on day 3, $p = 0.015$ on day 4 and $p < 0.001$ on day 5 vs. controls; repeated measures ANOVA). This difference can be explained by the fact that the GC-ΔKCC2 mice, in contrast to controls, were not able to consolidate their phase learning overnight (for example from day 3 to 4, 94% of learned responses was consolidated over a night in controls compared to only 6% in the mutants $p = 0.006$; Student's t-test) **(Fig. 6b, right panel).** The PC-ΔKCC2 and PC;GC-ΔKCC2 mice were, in line with their deficits in VOR gain learning and consolidation, unable to reverse the phase of their eye movements ($p < 0.001$ for both mutants vs. controls; repeated measures ANOVA). Together, these data indicate that the excitability of granule cells contributes to phase learning and is necessary for consolidation of phase learning.

Discussion

We investigated the role of GABAergic inhibition in cerebellar function by selectively altering the chloride gradient across membranes of granule cells and Purkinje cells. A rise in $[Cl^-]_i$, as observed with disruption of the Cl^--extruding K-Cl cotransporter Kcc2, is expected to decrease the inhibitory action of GABA. This was indeed observed when *Kcc2* was disrupted in Purkinje cells, but not in granule cells whose resting V depended on Cl^-. Different sets of aspects of cerebellar learning were affected when increasing $[Cl^-]_i$ in granule cells or Purkinje cells.

Intracellular Cl^- homeostasis in cerebellar Purkinje and granule cells

The regulation of cytoplasmic Cl^- concentration is of particular importance for neurons because the electrochemical Cl^- potential determines their response to the neurotransmitters GABA and glycine. In immature neurons, $[Cl^-]_i$ is above electrochemical equilibrium and accordingly opening of GABA- or glycine receptors entails a depolarizing Cl^- efflux that may even be excitatory. It is believed that the early excitatory response to GABA fulfils an important role in brain development[10, 35]. Upon maturation, most CNS neurons develop an inhibitory response to GABA, because increased expression[13, 36] or activation[29, 37] of Cl^- extruding transporters lower their $[Cl^-]_i$. There is broad consensus that the main neuronal Cl^- extruder is the neuron-specific K-Cl cotransporter Kcc2[11, 12]. In parallel with the development of an inhibitory GABA-response and depending on the brain region, Kcc2 expression increases after birth on the mRNA[13] and protein levels as shown here by immunohistochemistry for the cerebellum. The large, roughly twofold increase in $[Cl^-]_i$ we found in Purkinje cells and

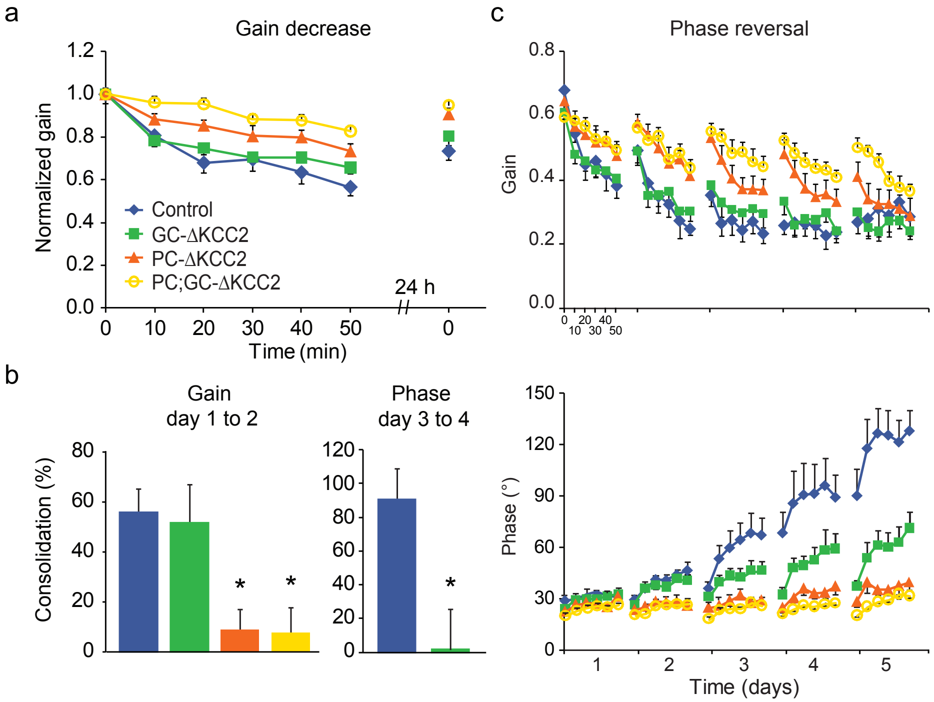

Figure 6. Motor learning and consolidation in control, GC-ΔKCC2, PC-ΔKCC2 and PC;GC-ΔKCC2 mice. We measured various forms of VOR adaptation in control mice (n = 9), GC-ΔKCC2 (n = 10) mice, PC-ΔKCC2 mice (n = 10), and PC;GC-ΔKCC2 mice (n = 10). (a) During short-term VOR gain-decrease learning GC-ΔKCC2 mice did not show any deficit compared to controls ($p = 0.74$; repeated measures ANOVA), whereas PC-ΔKCC2 and PC;GC-ΔKCC2 mice showed a significant impairment ($p < 0.005$ and $p < 0.001$, respectively; repeated measures ANOVA). (b) Likewise, GC-ΔKCC2 mice showed a level of gain consolidation overnight that was comparable to that of controls ($p = 0.99$; One-way ANOVA), whereas PC-ΔKCC2 and PC;GC-ΔKCC2 showed a significant deficit in gain consolidation ($p = 0.030$ and $p = 0.025$ vs. controls, respectively; One-way ANOVA). (c) During long-term VOR phase reversal learning GC-ΔKCC2 mice were able to significantly modify their VOR phase within 50 minutes of training for each consecutive day ($p < 0.005$ for VOR learning curve on day 2, 3, 4 and 5, Paired Samples Student's t-test). However, starting from day 3 of training their VOR phase adjustment was impaired when compared to the controls ($p = 0.983$ on day 2, $p = 0.088$ on day 3, $p = 0.015$ on day 4 and $p < 0.001$ on day 5 vs. controls; repeated measures ANOVA). This difference can be explained by the fact that the GC-ΔKCC2 mice were, in contrast to controls, not able to consolidate their phase learning overnight (for example from day 3 to 4, 94% of learned responses was consolidated over a night in controls compared to only 6% in the mutants ($p = 0.006$; Student's t-test). Due to their deficits in VOR gain learning, the PC-ΔKCC2 and PC;GC-ΔKCC2 mice were also unable to reverse the phase of their eye movements, let alone to consolidate these effects ($p < 0.001$ for both mutants vs. controls in both comparisons; repeated measures ANOVA). Error bars denote SEM.

granule cells after *Kcc2* disruption establishes Kcc2 as the main Cl$^-$ extruder also for these cells.

Unexpectedly, the GABA response of PCs lacking Kcc2 was still slightly hyperpolarizing, implying that their [Cl$^-$]$_i$ remained below its electrochemical equilibrium. Transporters other than Kcc2 that are potentially able to extrude Cl$^-$ include *Kcc*s like Kcc3 and Na$^+$-coupled Cl$^-$/HCO$_3^-$ exchangers that exploit the Na$^+$-gradient for extruding Cl$^-$ against its gradient. The prime candidate was Kcc3 as it is robustly expressed in PC[15]. Although previous work showed that the constitutive disruption of *Kcc3* lowers [Cl$^-$]$_i$ in PCs at P12 – P14, the main role of Kcc3 in neurons may be cell volume regulation[15]. Using mice older than 25 days we found no significant effect of Kcc3 on $[Cl^-]_i$ of PCs even when they lacked Kcc2. Hence the identity the other putative Cl^- extruder of PCs remains unclear.

In contrast to PCs, GCs responded to GABA with a slight depolarization that may cause a shunting inhibition as described previously[38]. Hence $[Cl^-]_i$ of GCs is slightly above electrochemical equilibrium, although Kcc2 is clearly active in these cells as demonstrated by the ~2-fold increase of $[Cl^-]_i$ upon *Kcc2* disruption. Even if GCs would express only Kcc2 and no Cl^- loader, the very negative resting potential of GCs (~-80mV) will strongly reduce or even inverse the driving force for Cl^- exit, since the activity and thermodynamic equilibrium of K-Cl cotransport is voltage-independent. However, the effects of bumetanide and GABA- and glycine-receptor blockers clearly show that also the chloride-loader Nkcc1 as well as a constitutive Cl^- conductance mediated by GABA- and glycine-receptors, respectively, contribute to GC Cl^- homeostasis. It may seem counterintuitive that Cl^- loaders and extruders are active in the same cell, but this situation is not unprecedented and may serve to finely regulate $[Cl^-]_i$, the resting membrane potential and the electrical excitability of GCs.

Effects of Kcc2 disruption on cellular signal transduction

The disruption of *Kcc2* strongly reduced the GABA-induced hyperpolarization of PCs and is therefore expected to decrease the strength of inhibitory synaptic input. The remaining small hyperpolarization and the increased membrane conductance probably still lead to some extent to a shunting inhibition of PCs. However, one should consider that the ability of PCs to extrude Cl^- is strongly reduced in the absence of Kcc2, as revealed by our Cl^- loading experiments. Hence, in particular during repetitive GABA-ergic stimulation at PC dendrites, their may be a considerable increase in cytoplasmic Cl^- that may further reduce synaptic inhibition. Thus, it is not surprising that the impairments in vestibulo-ocular learning and consolidation are virtually identical to those observed with a PC-specific disruption of GABA-receptors[7].

The situation with GCs is more complex and more revealing. We were surprised to find that the electric response to GABA, a slight depolarization, was essentially the same when Kcc2 was lacking. Whereas this may suggest that there may be no effect on synaptic inhibition of GCs, we observed robust effects on the behavioral level. This probably is a consequence of GC depolarization. GCs express non-inactivating α_6 $GABA_AR$ subunits and display tonic inhibition by ambient GABA[38], which may come from their Golgi cell input[38] or from glia where it is released by a channel-like mechanism[39]. The constitutive depolarization probably render GCs more excitable by lowering the threshold to action potential firing or by partially releasing the Mg^{++}-block of their NMDA receptors. Lowering the spiking threshold leads to potentiation of intrinsic excitability of granule cells [40], and the NMDA receptors are implicated in the induction of presynaptic long-term potentiation at the mossy fiber to granule cell synapse[41]. Thus, it is likely that various forms of plasticity are affected in the GC-ΔKCC2 mice, and that, as a consequence, their granule cells indeed produce additional spikes. Interestingly, a higher granule cell output can indeed be associated with an increase in irregularity of Purkinje cell simple spike firing[42] as observed in the current study.

In addition to affecting neuronal excitability by raising $[Cl^-]_i$, disruption of *Kcc2* might also have changed neuronal morphology, because of the presumed role of excitatory

GABA-response in neuronal maturation[10, 35]. Moreover, Kcc2 was reported to interact with the dendritic cytoskeleton to promote spine development in a mechanism that is independent from its ion transport activity[43]. Indeed, spine morphology and synaptic transmission were found to be changed in *Kcc2*$^{-/-}$ neurons in culture[43]. We therefore took great care to determine whether changes in cerebellar morphology might contribute to the behavioral effects observed upon *Kcc2* disruption. We did not find any abnormality at the light or electron microscopic levels and the number and shape of dendritic spines appeared normal.

Impact of cell-specific Kcc2 deletion on vestibulo-cerebellar function.

We found that Purkinje cell specific deletion of Kcc2 cotransporter decreases the efficacy of their inhibitory synaptic input and affects the ability to adjust and consolidate the gain and phase of the eye movements during visuovestibular mismatch training. These findings are in line with a the VOR adaptation deficits that can be observed following Purkinje cell specific ablation of GABA-γ2 receptors [42]. We believe that generation of precise timing of excitatory and inhibitory inputs to Purkinje cells during motor learning is crucial to establish spiking patterns that can be relayed onto the cerebellar nuclei[44,45, 46]. Since the ability of Purkinje cells to reliably respond to synaptic hyperpolarizing input is compromised in our mutants we can suspect that this has a severe impact on the spiking patterns of cerebellar and vestibular nuclei neurons and thereby on eye movement behavior. In contrast, the Kcc2 deletion from granule cells resulted in a selective, but profound disruption of long-term, overnight phase consolidation, while both the gain and phase of the optokinetic and vestibular responses remained intact. We hypothesize that by making GCs more excitable by lowering the threshold to action potential firing, the Purkinje cells receive a corrupted input from parallel fibers that lacks sufficient diversity. This could lead to changes in bidirectional plasticity at the parallel fiber to Purkinje cell synapse, which in turn will affect the output of Purkinje cells.Not too surprisingly, we also found that the PC;GC-ΔKCC2 mutants were the most affected group in that both their baseline motor performance and motor learning were severely compromised. This is probably due to the cumulative effect of decreasing the inhibitory synaptic input to Purkinje cells, while increasing the excitatory parallel fiber activation at the same time.

Impact of granule cell-specific Kcc2 deletion on Purkinje cell output

Inhibition from molecular layer interneurons onto Purkinje cells has little impact on simple spike firing frequency. Instead both chemical[4] and genetic[42] blockade of $GABA_A$ receptors predominantly affect the regularity of firing. Here we used an alternative mechanism to eliminate the hyperpolarizing effect of GABAergic stimulation, by altering the chloride gradient across the membrane. In line with previous results [42]Purkinje cells showed an increase in regularity, indicating that chloride is the main contributor to the GABAergic control of Purkinje cell regularity. Notably, the deletion of KCC2 in cerebellar granule cells had a reverse effect on Purkinje cells, causing them to fire more irregularly. As indicated above, this may be explained by the observed increase in excitability of granule cells, causing an increase in parallel fiber activity that enhances the frequency of both excitatory and inhibitory inputs to Purkinje cells, leading to less regular firing (see model in[42]). An increase in

Purkinje cells irregularity has also been observed in for example the *tottering* mutant, which suffer from a mutation in their voltage gated P/Q-type calcium channels[47]. In those mutants, in which the irregularity in Purkinje cells simple spike firing is more dramatic, the deficits in oculomotor control are also more dramatic even robustly affecting baseline motor performance[47, 48]. It is interesting to observe that a mild increase in simple spike irregularity due to an increased excitability of granule cells results in a more specific phenotype in that particularly consolidation of the phase during reversal learning is affected. As indicated above, we hypothesize that this phenotype is caused by an insufficient diversity of granule cell codings in the temporal domain. If this diversity is insufficient, climbing fiber driven plasticity imposed in the molecular layer cannot be used to efficiently select proper codings carried by the parallel fibers, simply because there may not be a sufficient number of proper parallel fiber codings generated in the granular layer that can be selected from[49].

Supplementary Material

	Granule cell			**Purkinje cell**		
	Kcc2$^{+/+}$	***Kcc2***$^{-/-}$	**Δ**	***Kcc2***$^{+/+}$	***Kcc2***$^{-/-}$	**Δ**
V (mV)	**-86.3 ± 2.2** **(22)**	**-71.3 ± 1.9** **(39)**	**15.0 ± 2.9**	**-63.1 ± 0.6** **(32)**	**-64.5 ± 0.5** **(27)**	**-1.4 ± 0.8**
E_{GABA} (mV)	**-79.1 ± 2.3**	**-64.3 ± 1.9**	**14.5 ± 3.2**	**-94 ± 1** **(16)**	**-75 ± 3** **(13)**	**19 ± 3.2**
DF_{GABA} (mV)	**7.2 ± 0.6** **(11)**	**7.0 ± 0.3** **(15)**	**-0.2 ± 1.2**	**-30.9 ± 1.2**	**-10.5 ± 1.1**	**20.4 ± 1.6**
$[Cl^-]_i$ (mM)	**5.6 ± 1.0**	**10.1 ± 1.5**	**4.5 ± 1.8**	**3.2 ± 0.1**	**6.6 ± 1**	**3.4 ± 1**

Table I. Summary of the effect of Kcc2 deletion on V, E_{GABA}, driving force for GABAergic currents (DF_{GABA}) and intracellular chloride concentration ($[Cl^-]_i$) in granule cells and Purkinje cells. $[Cl^-]_i$ was calculated from E_{GABA} and $[Cl^-]_o$ using the Nernst equation. Values represent arithmetic means ± SEM, with the number of measurements given in brackets. Δ indicates the difference between respective values of *Kcc2*$^{+/+}$ and *Kcc2*$^{-/-}$ mice.

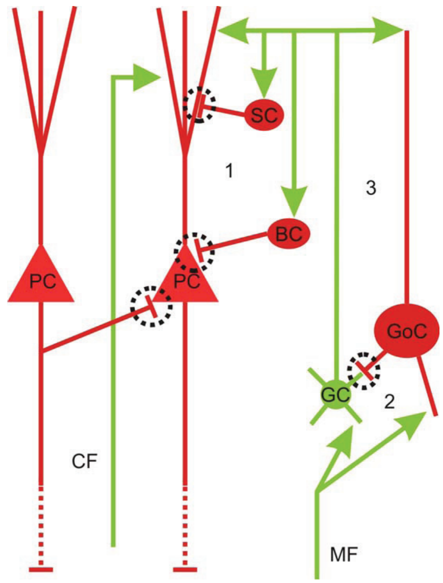

Supplementary Figure 1. Scheme of cerebellar neuronal circuitry. Input into the cerebellum is through mossy fibers (MF) and climbing fibers. GABAergic Purkinje cells (PC) provide the only output. Inhibitory interneurons (stellate cells, SC; basket cells, BC and Golgi cells, GoC) generate feed-forward inhibition on Purkinje cells (PCs) (1) and granule cells (GCs) (2), as well as feed-back inhibition on GCs (3). Dashed circles indicate those synapses, which are expected to be attenuated in ourmouse models. Red color indicates inhibitory neurons and green color indicates excitatory neurons or fibers.

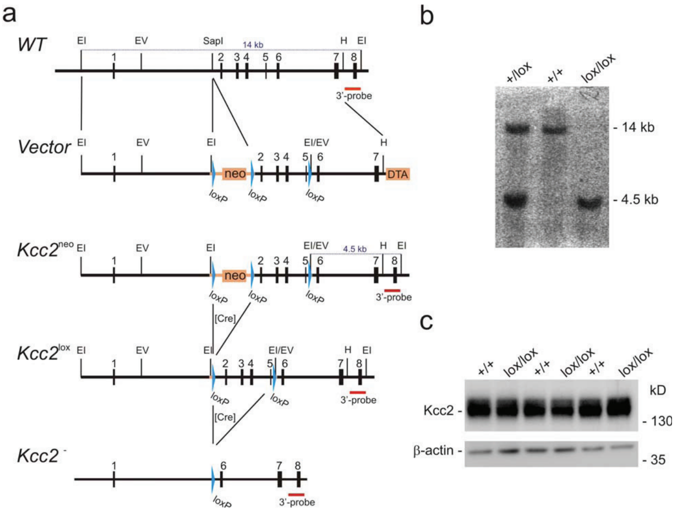
a
WT
EI
EV
SapI
14 kb
H
EI
1
2 3 4 5 6
7 8
3'-probe
Vector
EI
EV
EI
EI/EV
H
neo
DTA
loxP
loxP
loxP
Kcc2neo
4.5 kb
[Cre]
Kcc2lox
Kcc2 -
b
+/lox
+/+
lox/lox
- 14 kb
- 4.5 kb
c
+/+
lox/lox
kD
Kcc2 -
- 130
β-actin -
- 35

Supplementary Figure 2. Generation of Kcc2$^{lox/lox}$ mice. (a) Modification of genomic Kcc2 sequence. At top, partial genomic organization of wildtype (WT) Kcc2 locus (Slc12a5). Below, the targeting vector (vector), primary targeted allele after homologous recombination (Kcc2^{neo}) and the conditional Kcc2^{lox} allele generated after removing the neomycin resistance cassette. Exons are shown as vertical bars, loxP sites as blue arrowheads, neomycin and DTA cassettes as orange rectangles. Indicated restriction enzyme sites are EcoRI (EI), EcoRV (EV), HindIII (H) and SapI. Sizes of restriction fragments are indicated above horizontal blue lines. Transient expression of the Cre recombinase followed by Southern analysis with a 3' probe (red line) was used to select ES cell clones harboring the allele Kcc2^{lox}. (b) Southern blot analysis of EcoRI-digested genomic DNA with the 3'probe reveals a 14 kb WT band and a 4.5 kb Kcc2^{lox} band. (c) Western blot analysis of 20 μg cerebellum membrane protein fractions from WT and Kcc2^{lox} mice with antibodies against Kcc2 and β-actin (loading control) reveals that insertion of loxP sites does not change expression levels of the Kcc2 protein.

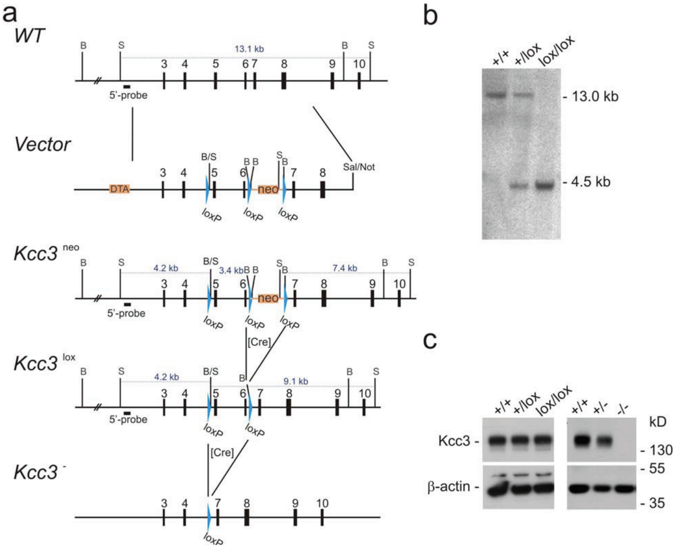
a
WT
B
S
13.1 kb
3 4 5 67 8 9 10
5'-probe
Vector
B/S
B B
S B
Sal/Not
DTA
neo
loxP
Kcc3 neo
4.2 kb
3.4 kb
7.4 kb
[Cre]
Kcc3 lox
9.1 kb
Kcc3 -
b
+/+
+/lox
lox/lox
- 13.0 kb
- 4.5 kb
c
+/+
+/lox
lox/lox
+/-
-/-
kD
Kcc3 -
- 130
- 55
β-actin -
- 35

Supplementary Figure 3. Generation of Kcc3$^{lox/lox}$ mice. (a) Modification of genomic Kcc2 sequence. On top, partial genomic organization of wild-type (WT) Kcc3 locus (Slc12a6). Below, targeting vector (vector), primary targeted allele Kcc3^{neo}, the Kcc3^{lox} allele obtained by Cre-mediated removal of the neomycin resistance cassette, and the constitutive KO allele Kcc3^{-}. Exons are shown as vertical bars, loxP sites as blue arrowheads, neo and DTA cassettes as orange boxes. Restriction sites indicated are SpeI (S), BamHI, (B), SalI, and NotI. Sizes of restriction fragments are indicated above horizontal blue lines. Transient expression of Cre-recombinase followed by Southern analysis with a 5' probe (black box) allowed for selection of ES cell clones harboring the 'floxed' allele Kcc3 ^{lox}. (b) Southern blot analysis of SpeI-digested genomic DNA with the 5' probe reveals a 13.1 kb WT band and a 4.2 kb Kcc3^{lox} band. (c) Western blot analysis of 20 μg brain membrane protein fractions from Kcc3^{lox} and Kcc3^{-} (ref. [1]) lines with an antibody against the Kcc3 amino-terminus and β-actin antibodies (as loading control). Kcc3$^{lox/lox}$ mice displayed WT Kcc3 protein amounts (left), while Kcc3$^{-/-}$ mice lacked the Kcc3 protein completely (right).

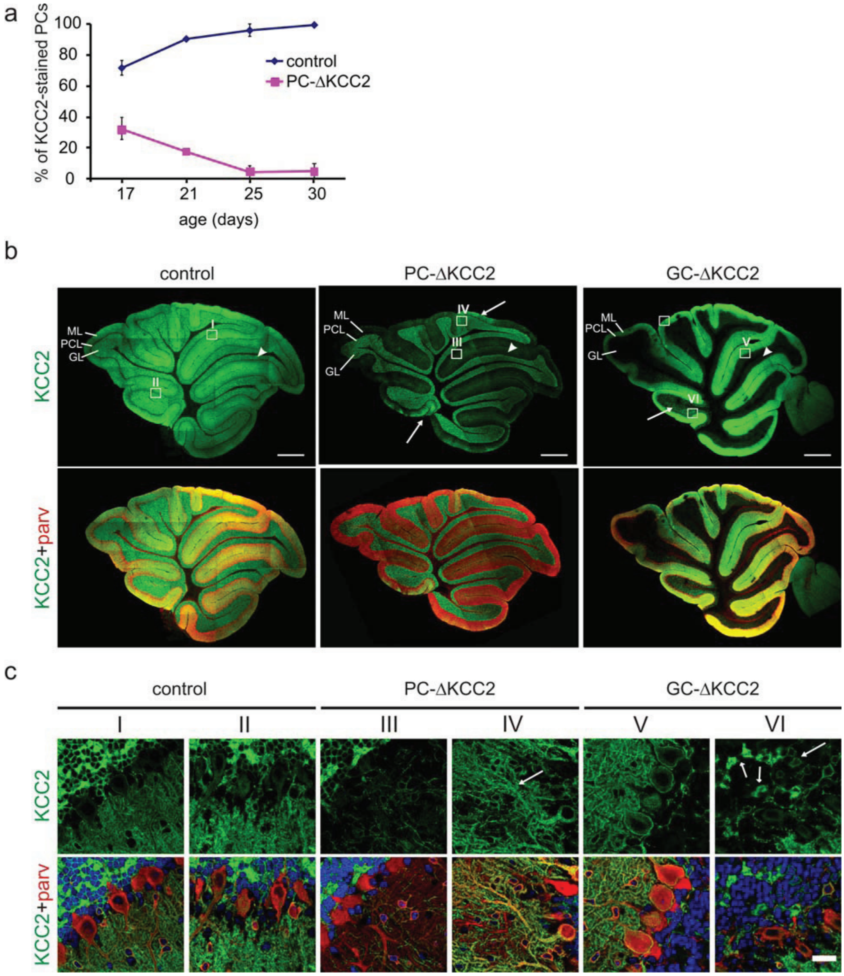
a
% of KCC2-stained PCs
100
80
60
40
20
0
17
21
25
30
age (days)
control
PC-ΔKCC2
b
control
PC-ΔKCC2
GC-ΔKCC2
KCC2
KCC2+parv
ML
PCL
GL
I
II
III
IV
V
VI
c
control
PC-ΔKCC2
GC-ΔKCC2
I
II
III
IV
V
VI
KCC2
KCC2+parv

Supplementary Figure 4. Time course of Kcc2 expression and deletion in PC-ΔKCC2 and GC-ΔKCC2 mice.(a) Progression of Kcc2 expression on Purkinje cells from Kcc2$^{lox/lox}$ (control) and PC-ΔKCC2 mice, averaged over all regions in the vermis. PCs showing somatic membrane staining were counted as positive cells (average ± standard deviation, n = 2, 1, 4 and 2 mice for P17, P21, P25 and P30, respectively (for each genotype). ~200 cells counted per animal) . (b) Pattern of Kcc2 expression at postnatal day 30 (P30) in the cerebella of control (Kcc2$^{lox/lox)}$, PC-ΔKCC2 and GC-ΔKCC2 mice. Sections were stained against Kcc2 (green) and parvalbumin (red). ML, PCL and GL indicate molecular layer, Purkinje cell layer and granule cell layer, respectively. Arrows point to regions were Kcc2 is still present. Arrowheads point at the region where deletion was complete and all patch clamp experiments were done. Scale bar, 500 µm. (c) Higher magnification of 2 different zones (indicated by I-VI) of the cerebella delimited by the white boxes in (b). Scale bar, 20µm.

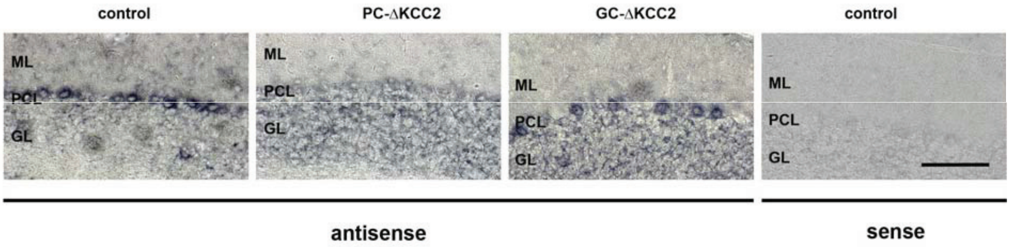

Supplementary Figure 5. Cell-type specific deletion of Kcc3 in the cerebellum. Kcc3$^{lox/lox}$ (control) mice were crossed with Δα6::Cre or L7/Pcp2::Cre to delete Kcc3 specifically in granule and Purkinje cells, respectively. In situ hybridization for Kcc3 mRNA of sagittal sections of cerebellar cortex from control (left), PC-ΔKCC3 (middle) and GC-ΔKCC3 (middle) mice. The probe is directed against sequence of exons 5 and 6 which are flanked by loxP sites in Kcc3$^{lox/lox}$ mice. Strong hybridization of the antisense probe is observed in Purkinje cells of control and GC-ΔKCC3, but not of PC-KCC3 mice. Additional evidence for specificity of the hybridization is provided by only background staining with a sense probe on Kcc3$^{lox/lox}$ (control) cerebellum. Scale bar, 100µm.

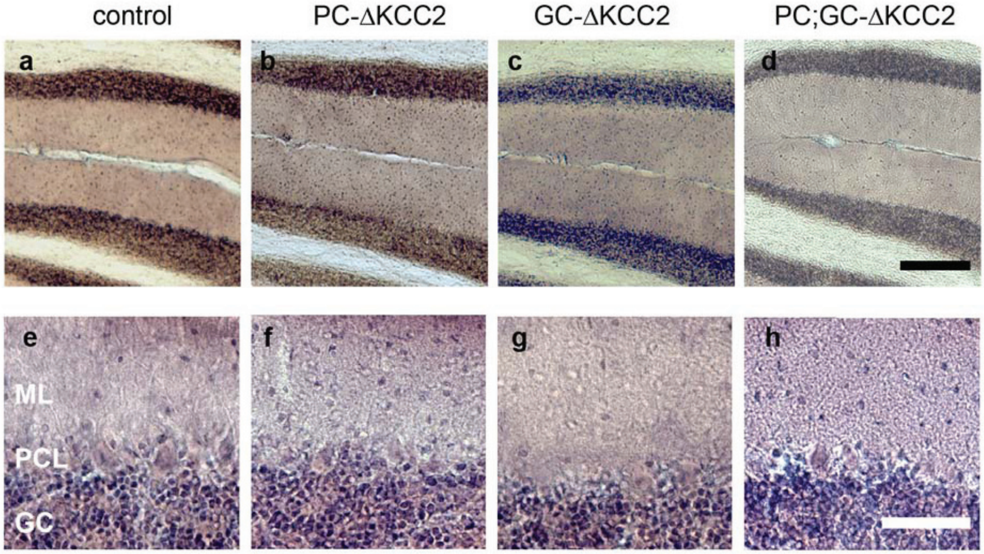

Supplementary Figure 6. Cerebellar architecture is not affected by cell-specific deletion of Kcc2. HE-staining of parasagittal cerebellar sections. Cerebellar folia (a-d) and cortical layers (e-h) of control (Kcc2$^{lox/lox}$; (a,e)), Purkinje cell specific KO (PC-ΔKCC2); (b,f)),; granule cell-specific Kcc2 KO (GC-ΔKCC2 (c,g)) and combined KO (PC;GC-ΔKCC2; (d,h)) reveal normal overall morphology, normal layering of granule cell layer (GL), Purkinje cell (PC) layer and molecular layer (ML), normal layer thickness and normal cell density within layers. Scale bar: a-d, 200 µm; e-h, 50 µm.

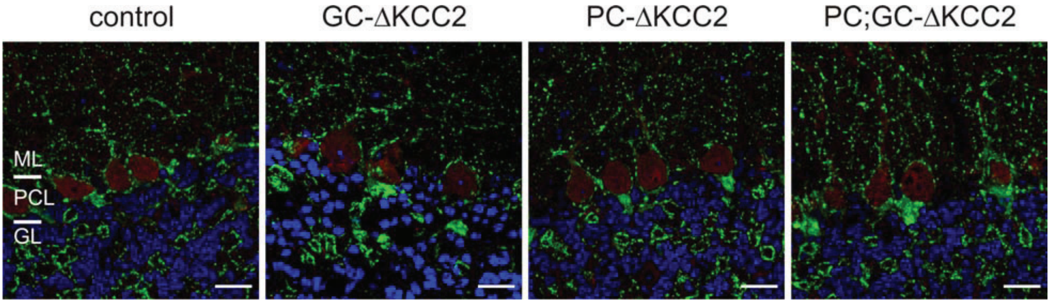

Supplementary Figure 7. Inhibitory synapses in cerebellar cortex appear unchanged upon Kcc2 deletion. Confocal sections of cerebellar cortex stained with VGAT (vesicular GABA transporter, green) as marker for inhibitory synapses for all four genotypes. Staining for parvalbumin is shown in red and blue staining corresponds to nuclei. Scale bar, 20 µm.

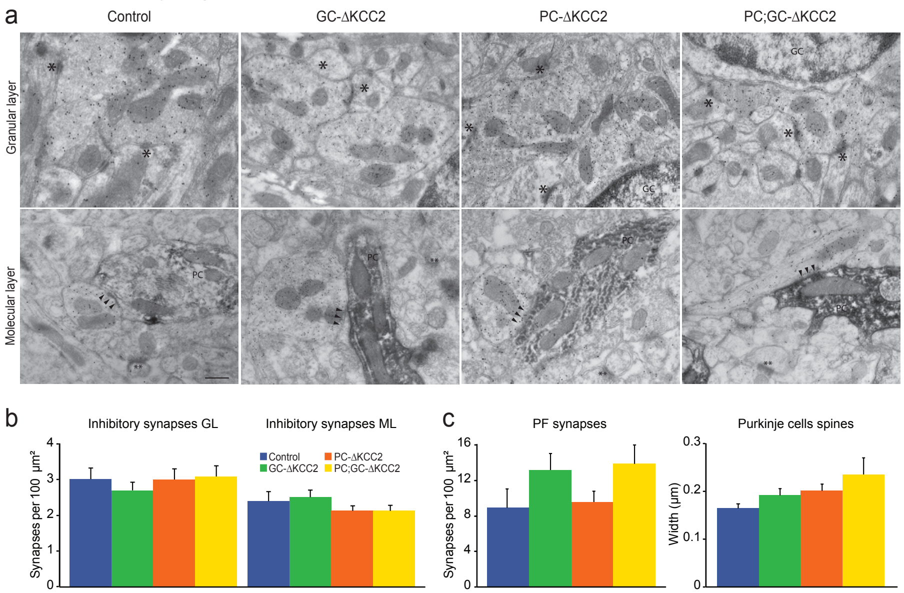
a
Control
GC-ΔKCC2
PC-ΔKCC2
PC;GC-ΔKCC2
Granular layer
Molecular layer
GC
PC
b
Inhibitory synapses GL
Inhibitory synapses ML
Synapses per 100 μm²
0
1
2
3
4
Control
GC-ΔKCC2
PC-ΔKCC2
PC;GC-ΔKCC2
c
PF synapses
Purkinje cells spines
Synapses per 100 μm²
0
4
8
12
16
Width (μm)
0
0.1
0.2
0.3

Supplementary Figure 8. Electron microscopic analysis of the morphological characteristics of the granular layer and molecular layer of control, GC-ΔKCC2, PC-ΔKCC2 and PC;GC-ΔKCC2 mice. (a) Electron micrographs of the granular layer (top panel) and molecular layer (bottom panels) of control mice, GC-ΔKCC2, PC-ΔKCC2 and PC;GC-ΔKCC2 mice (from left to right). Arrowheads indicate symmetric synapses. Big asterisks indicate synapses in glomeruli and small asterisks mark asymmetric synapses in molecular layer. Scale bars indicate 500 nm. (b) The density of inhibitory synapses in the glomeruli of the granular layer in GC-ΔKCC2 mice (n = 4) was indistinguishable from that in controls (n = 4), PC-ΔKCC2 (n = 4) and PC;GC-ΔKCC2 mice (n = 4) (p = 0.89, p = 1.0, and p = 0.99, respectively; One-way ANOVA). The density of inhibitory and excitatory synapses onto Purkinje cells in GC-ΔKCC2 mice was indistinguishable from that in controls, PC-ΔKCC2 and PC;GC-ΔKCC2 mice (p = 0.97, p =0.75, and p = 0.72, respectively; One-way ANOVA). (c) The density of parallel fiber synapses onto Purkinje cell spines in GC-ΔKCC2 mice was indistinguishable from that in controls, PC-ΔKCC2 and PC;GC-ΔKCC2 mice (p = 0.26, p = 0.99, and p = 0.18, respectively; One-way ANOVA). The density of Purkinje cell spines in GC-ΔKCC2 mice was indistinguishable from that in controls, PC-ΔKCC2 and PC;GC-ΔKCC2 mice (p = 0.82, p = 0.61, and p = 0.09, respectively; One-way ANOVA). Error bars depict SEM.

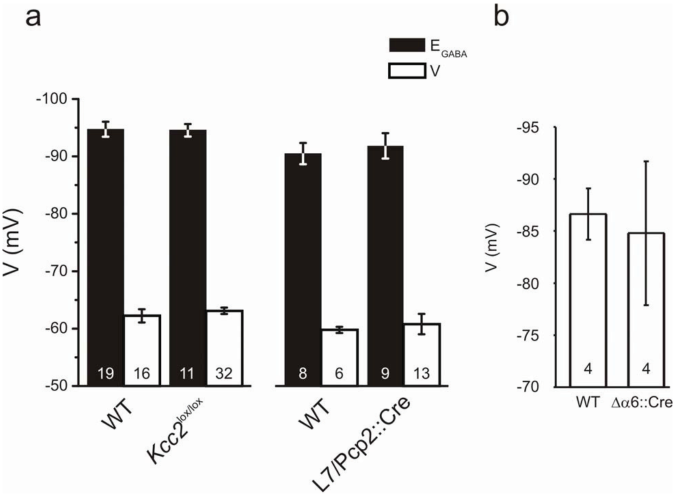

Supplementary Figure 9. Insertion of loxP sites and expression of Cre-recombinase neither change resting membrane potential nor E_{GABA}. (a) Bar diagram comparing V and E_{GABA} of Kcc2$^{lox/lox}$ and L7/Pcp2::Cre mice with WT mice of the respective genetic background. The number of experiments is indicated in columns, error bars show SEM. All recordings were done in gramicidin perforated patch-clamp experiments. V was obtained in current-clamp experiments (I=0) and E_{GABA} was obtained from the current reversal potential obtained by clamping the neuron to different potential and applying muscimol to the soma of PCs as depicted in Fig. 2b (main text). (b) Expression of Cre-recombinase does not change resting membrane potential of cerebellar granule cells. Bar diagram comparing V of α6-Cre mice with control littermates. The number of experiments is indicated in columns, error bars show standard deviation. All recordings were done in cell-attached patch clamp with high K^+ in the pipette.

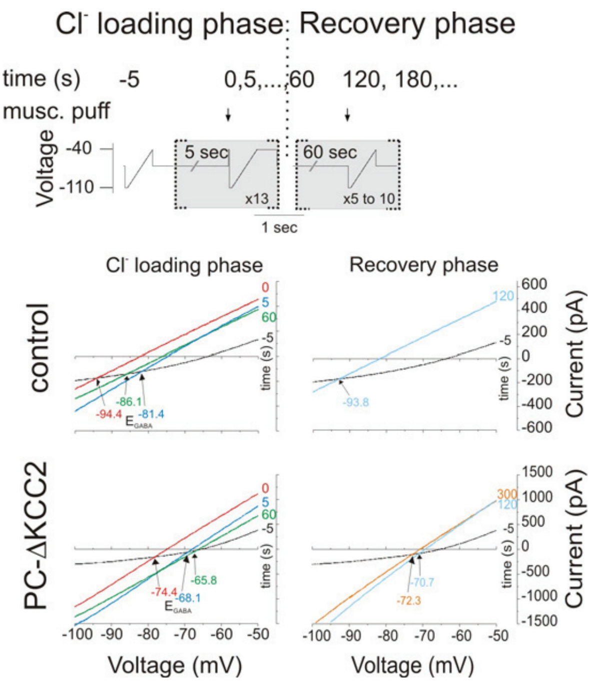

Supplementary Figure 10. Changes in $[Cl^-]_i$ during and after Cl^- loading of Purkinje cells.

Upper panel: A series of voltage ramps (500 ms, from -110 to -40 mV) combined with puff application (50 ms) of 50 µM muscimol (arrows) was used to determine changes in E_{GABA} during the loading phase (60 s duration with puff application at 0.2 Hz, ramp followed by a 400 ms step to -40 mV) and the recovery phase (5 to 10 puff applications every min). The first voltage ramp (t=-5 s) was not combined with muscimol application. Analysis of the recovery phase started 60 sec after the loading phase (t=120 s).

Lower panels: Current responses of PC from control (Kcc2$^{lox/lox}$) and PC-ΔKCC2 (L7/Pcp2::Cre; Kcc2$^{lox/lox}$) mice evoked by voltage ramps during the loading phase (left) and recovery phase (right). Left, superimposed current responses for control (in the absence of muscimol, t=-5 s) and after the first, second and last muscimol application (t=0, 5 and 60 s, respectively). Right, superimposed current responses in the absence of muscimol (t=-5) and the first application of muscimol during the recovery phase (t=120 s) in control mice and the first and fourth muscimol application during the recovery phase (t=120 and 300 s) for PC-ΔKCC2 mice. E_{GABA} was determined as the voltage at the intersection of the initial current (black) and muscimol responses (arrows).

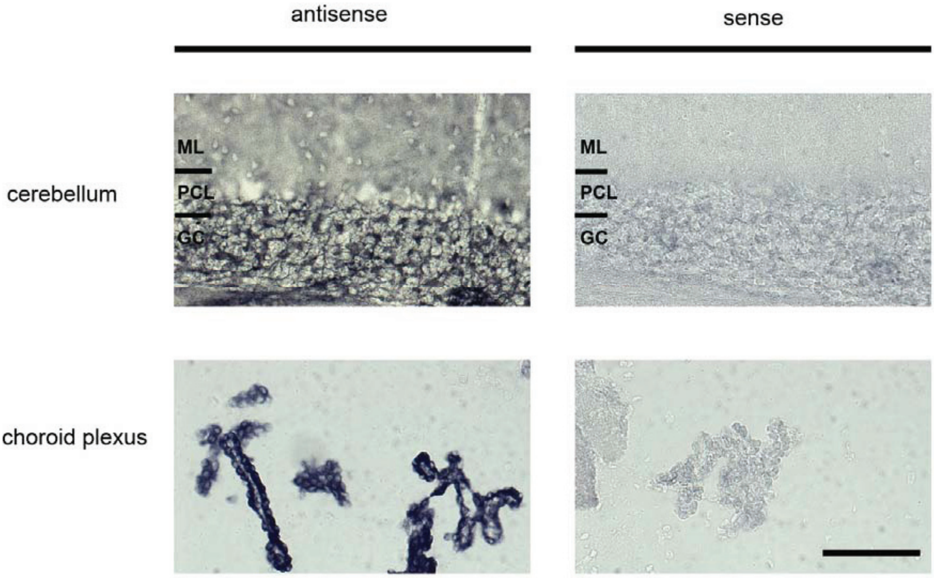

Supplementary Figure 11. Expression of Nkcc1 mRNA in cerebellar granule cells. In situ hybridization for Nkcc1 mRNA of sagittal sections of cerebellar cortex from control mice (C57Bl6). The probe is directed against the sequence of exons 15-19. Hybridization of the antisense probe is observed in granule cells and the choroid plexus. Additional evidence for specificity of the hybridization is provided by only background staining with the sense probe. Scale bar, 100 µm.

References Supplementary Material

1. Boettger, T. et al. Loss of K-Cl co-transporter KCC3 causes deafness, neurodegeneration and rduced seizure threshold. EMBO J 22, 5422-5434 (2003).
2. Jin, X., Huguenard, J. R. & Prince, D. A. Impaired Cl$^-$ extrusion in layer V pyramidal neurons of chronically injured epileptogenic neocortex. J Neurophysiol 93, 2117-2126 (2005).
3. Zhu, L., Lovinger, D. & Delpire, E. Cortical neurons lacking KCC2 expression show impaired regulation of intracellular chloride. J Neurophysiol 93, 1557-1568 (2005).

References

1. Eccles, J.C., Ito, M. & Szentagothai, J. The Cerebellum as a Neuronal Machine (Springer-Verlag, New York, 1967).
2. Hansel, C., Linden, D.J. & D'Angelo, E. Beyond parallel fiber LTD: the diversity of synaptic and non-synaptic plasticity in the cerebellum. *Nat Neurosci* **4**, 467-75 (2001).
3. Gabbiani, F., Midtgaard, J. & Knöpfel, T. Synaptic integration in a model of cerebellar granule cells. *J Neurophysiol* **72**, 999-1009 (1994).
4. Hausser, M. & Clark, B.A. Tonic synaptic inhibition modulates neuronal output pattern and spatiotemporal synaptic integration. *Neuron* **19**, 665-78 (1997).
5. Mittmann, W. & Hausser, M. Linking synaptic plasticity and spike output at excitatory and inhibitory synapses onto cerebellar Purkinje cells. *J Neurosci* **27**, 5559-70 (2007).
6. Santamaria, F., Tripp, P.G. & Bower, J.M. Feedforward inhibition controls the spread of granule cell-induced Purkinje cell activity in the cerebellar cortex. *J Neurophysiol* **97**, 248-63 (2007).
7. Wulff, P. et al. Synaptic inhibition of Purkinje cells mediates consolidation of vestibulo-cerebellar motor learning. *Nat Neurosci* **12**, 1042-9 (2009).
8. Watanabe, D. et al. Ablation of cerebellar Golgi cells disrupts synaptic integration involving GABA inhibition and NMDA receptor activation in motor coordination. *Cell* **95**, 17-27 (1998).
9. Blaesse, P., Airaksinen, M.S., Rivera, C. & Kaila, K. Cation-chloride cotransporters and neuronal function. *Neuron* **61**, 820-38 (2009).
10. Ben-Ari, Y., Khazipov, R., Leinekugel, X., Caillard, O. & Gaiarsa, J.L. $GABA_A$, NMDA and AMPA receptors: a developmentally regulated 'ménage à trois'. *Trends Neurosci* **20**, 523-529 (1997).
11. Rivera, C. et al. The K^+/Cl^- co-transporter KCC2 renders GABA hyperpolarizing during neuronal maturation. *Nature* **397**, 251-5 (1999).
12. Hübner, C.A. et al. Disruption of KCC2 reveals an essential role of K-Cl cotransport already in early synaptic inhibition. *Neuron* **30**, 515-24 (2001).
13. Stein, V., Hermans-Borgmeyer, I., Jentsch, T.J. & Hübner, C.A. Expression of the KCl cotransporter KCC2 parallels neuronal maturation and the emergence of low intracellular chloride. *J Comp Neurol* **468**, 57-64 (2004).
14. Pfeffer, C.K. et al. NKCC1-dependent GABAergic excitation drives synaptic network maturation during early hippocampal development. *J Neurosci* **29**, 3419-30 (2009).
15. Boettger, T. et al. Loss of K-Cl co-transporter KCC3 causes deafness, neurodegeneration and reduced seizure threshold. *EMBO J* **22**, 5422-34 (2003).
16. Pearson, M.M., Lu, J., Mount, D.B. & Delpire, E. Localization of the K^+-Cl^- cotransporter, KCC3, in the central and peripheral nervous systems: expression in the choroid plexus, large neurons and white matter tracts. *Neuroscience* **103**, 481-91 (2001).
17. Mikawa, S. et al. Developmental changes in KCC1, KCC2 and NKCC1 mRNAs in the rat cerebellum. *Brain Res Dev Brain Res* **136**, 93-100 (2002).
18. Wang, C. et al. Developmental changes in KCC1, KCC2, and NKCC1 mRNA expressions in the rat brain. *Brain Res Dev Brain Res* **139**, 59-66 (2002).
19. Williams, J.R., Sharp, J.W., Kumari, V.G., Wilson, M. & Payne, J.A. The neuron-specific K-Cl cotransporter, KCC2. Antibody development and initial characterization of the protein. *J Biol Chem* **274**, 12656-64 (1999).
20. Takayama, C. & Inoue, Y. Developmental localization of potassium chloride co-transporter 2 in granule cells of the early postnatal mouse cerebellum with special reference to the synapse formation. *Neuroscience* **143**, 757-67 (2006).
21. Hübner, C.A., Lorke, D.E. & Hermans-Borgmeyer, I. Expression of the Na-K-2Cl-cotransporter NKCC1 during mouse development. *Mech Dev* **102**, 267-9 (2001).

22. Price, T.J., Hargreaves, K.M. & Cervero, F. Protein expression and mRNA cellular distribution of the NKCC1 cotransporter in the dorsal root and trigeminal ganglia of the rat. *Brain Res* **1112**, 146-58 (2006).
23. Barski, J.J., Dethleffsen, K. & Meyer, M. Cre recombinase expression in cerebellar Purkinje cells. *Genesis* **28**, 93-8 (2000).
24. Aller, M.I. et al. Cerebellar granule cell Cre recombinase expression. *Genesis* **36**, 97-103 (2003).
25. Kaila, K. & Voipio, J. Postsynaptic fall in intracellular pH induced by GABA-activated bicarbonate conductance. *Nature* **330**, 163-5 (1987).
26. Jin, X., Huguenard, J.R. & Prince, D.A. Impaired Cl^- extrusion in layer V pyramidal neurons of chronically injured epileptogenic neocortex. *J Neurophysiol* **93**, 2117-26 (2005).
27. Zhu, L., Lovinger, D. & Delpire, E. Cortical neurons lacking KCC2 expression show impaired regulation of intracellular chloride. *J Neurophysiol* **93**, 1557-68 (2005).
28. Fricker, D., Verheugen, J.A. & Miles, R. Cell-attached measurements of the firing threshold of rat hippocampal neurones. *J Physiol* **517** 791-804 (1999).
29. Tyzio, R. et al. Maternal oxytocin triggers a transient inhibitory switch in GABA signaling in the fetal brain during delivery. *Science* **314**, 1788-92 (2006).
30. Fisher, J.L. The a1 and a6 subunit subtypes of the mammalian $GABA_A$ receptor confer distinct channel gating kinetics. *J Physiol* **561**, 433-48 (2004).
31. Brickley, S.G., Revilla, V., Cull-Candy, S.G., Wisden, W. & Farrant, M. Adaptive regulation of neuronal excitability by a voltage-independent potassium conductance. *Nature* **409**, 88-92 (2001).
32. Aller, M.I. et al. Modifying the subunit composition of TASK channels alters the modulation of a leak conductance in cerebellar granule neurons. *J Neurosci* **25**, 11455-67 (2005).
33. Duprat, F. et al. TASK, a human background K^+ channel to sense external pH variations near physiological pH. *EMBO J* **16**, 5464-71 (1997).
34. Karschin, C. et al. Expression pattern in brain of TASK-1, TASK-3, and a tandem pore domain K^+ channel subunit, TASK-5, associated with the central auditory nervous system. *Molecular and cellular neurosciences* **18**, 632-48 (2001).
35. Ben-Ari, Y. Excitatory actions of GABA during development: the nature of the nurture. *Nat Rev Neurosci* **3**, 728-39 (2002).
36. Ludwig, A. et al. Early growth response 4 mediates BDNF induction of potassium chloride cotransporter 2 transcription. *J Neurosci* **31**, 644-9 (2011).
37. Rinehart, J. et al. Sites of regulated phosphorylation that control K-Cl cotransporter activity. *Cell* **138**, 525-36 (2009).
38. Brickley, S.G., Cull-Candy, S.G. & Farrant, M. Development of a tonic form of synaptic inhibition in rat cerebellar granule cells resulting from persistent activation of GABAA receptors. *J Physiol* **497** 753-9 (1996).
39. Lee, S. et al. Channel-mediated GABA release from glia. *Science* **330**, 790-796 (2010).
40. Armano, S., Rossi, P., Taglietti, V. & D'Angelo, E. Long-term potentiation of intrinsic excitability at the mossy fiber-granule cell synapse of rat cerebellum. *J Neurosci* **20**, 5208-16 (2000).
41. D'Angelo, E., Rossi, P., Armano, S. & Taglietti, V. Evidence for NMDA and mGlu receptor-dependent long-term potentiation of mossy fiber-granule cell transmission in rat cerebellum. *J Neurophysiol* **81**, 277-87. (1999).
42. Wulff, P. et al. Synaptic inhibition of Purkinje cells mediates consolidation of vestibulo-cerebellar motor learning. *Nat Neurosci* (2009).
43. Li, H. et al. KCC2 Interacts with the Dendritic Cytoskeleton to Promote Spine Development. *Neuron* **56**, 1019-33 (2007).
44. Steuber, V. et al. Cerebellar LTD and pattern recognition by Purkinje cells. *Neuron* **54**, 121-

36 (2007).

45. Blazquez, P.M., Hirata, Y. & Highstein, S.M. Chronic changes in inputs to dorsal Y neurons accompany VOR motor learning. *J Neurophysiol* **95**, 1812-25 (2006).

46. McElvain, L.E., Bagnall, M.W., Sakatos, A. & du Lac, S. Bidirectional plasticity gated by hyperpolarization controls the gain of postsynaptic firing responses at central vestibular nerve synapses. *Neuron* **68**, 763-75.

47. Hoebeek, F.E. et al. Increased noise level of purkinje cell activities minimizes impact of their modulation during sensorimotor control. *Neuron* **45**, 953-65 (2005).

48. Stahl, J.S., James, R.A., Oommen, B.S., Hoebeek, F.E. & De Zeeuw, C.I. Eye movements of the murine P/Q calcium channel mutant tottering, and the impact of aging. *J Neurophysiol* **95**, 1588-607 (2006).

49. Gao, Z., Van Beugen, B.J. & de Zeeuw, C.I. Cerebellar Plasticity Dissected into Neuronal Components. (2011, *Submitted*).

CHAPTER 5

CHANGES IN THE MODULATION OF SIMPLE SPIKE RESPONSES AFTER MOTOR TRAINING

In preparation

Badura A, Schonewille M, Voges K., De Zeeuw CI

CHAPTER 6

MATERIALS AND METHODS

All experiments involving animals were conducted in accordance with The Dutch Ethical Committee for animal experiments.

Mouse lines

Ptf1a::cre;$Robo3^{lox/lox}$ *mice*

C57BL/6 mice (Janvier) were used for expression studies. Mice were anesthetized with isofluorane. The day of vaginal plug is embryonic day 0 (E0) and the day of birth corresponds to postnatal day 0 (P0). The *Robo3* conditional knockout mouse line was established at the MCI/ICS (Mouse Clinical Institute -Institut Clinique de la Souris-, Illkirch, France; http://www-mci.u-strasbg.fr). To generate the *Robo3* conditional knockout the targeting vector was constructed as follows. Three fragments of 5.1, 1.1 and 3.7 kb (respectively the 5', floxed and 3' arms) were amplified by PCR using 129S2/SvPas DNA as template and sequentially subcloned in an MCI proprietary vector. This MCI vector has a floxed Neomycin resistance cassette. The linearized construct was electroporated in 129S2/SvPas mouse embryonic stem (ES) cells. After selection, targeted clones were identified by PCR using external primers and further confirmed by Southern blot with 5' and 3' external probes. Two positive ES clones were injected into C57BL/6J blastocysts, and derived male chimaeras gave germline transmission. The *Robo3*-null knockout line was described previously[8]. Briefly, it consists on a knock-in of the *GFP* gene into the first exon of *Robo3*, leading to the expression of the GFP by Robo3-expressing cells. However, the GFP signal is too weak to be seen, without the use of an anti-GFP antibody. The *Hb9::GFP* mice have a transgene containing a 9kb-long region of the Hb9 promoter that drives eGFP expression in all post-mitotic somatic motor neurons[142]. The GFP signal is bright enough to be seen directly. The *Ptf1a::cre* knock-in line was previously described[2]. The Tau^{mGFP} knock-in line was obtained by replacing the coding sequence of the Tau gene by a *lox-Stop-lox-mGFP-IRES-nls-lacZ* cassette[3]. Unless otherwise mentionned, controls were $Robo3^{+/-}$ or $Robo3^{lox/lox}$ animals or double heterozygotes that were always found to be undistinguishable from wildtype mice. All mice were genotyped by PCR.

L7Cre-PP2B mice

Mutant mice in which calcineurin was selectively deleted from Purkinje cells (L7-PP2B mutant) were obtained using the Cre-loxP-system, with loxP sites flanking the regulatory subunit (CNB1) of calcium/calmodulin-activated protein phosphatase 2B (referred to as PP2B-loxP)[60]. Mice heterozygous for PP2B-loxP were crossed with mice heterozygous for both PP2B-loxP and the L7-Cre transgene[95]. Mice of the following genotypes (PP2B-loxP/L7-Cre) were used for the experiments: homozygous/+ (referred to as L7-PP2B) and homozygous/−, wild-type/+ and wild-type/− (littermate controls).

PC-Δγ2 mice

We generated *γ2I77lox* mice by flanking exon 4 of the $GABA_A$ receptor γ2 subunit gene with *loxP* sites[143]. Homozygous *γ2I77lox* mice were crossed with mice heterozygous for *γ2I77lox* and hemizygous for an *L7Cre* transgene[95, 143]. Littermates of the following genotypes were used: *γ2I77lox/γ2I77lox/L7Cre* (*PC-Δγ2*) and *γI77lox/γI77lox* (controls). Mice were genotyped by PCR analysis of genomic DNA using the following primer pairs: γ2lx5′_s (5′-GT CATGCTAAATATCCTACAGTGG-3′) plus γ2lx5′_as (5′-GGATAGTGC ATCAGCAGACAATAG-3′) to test for the *γ2I77lox* allele (213 bp control; 250 bp *γ2I77lox*), and: Cre1 (5′-GACCAGGTTCGTTCACTCATGG-3′) plus Cre2 (5′-AGGCTAAGTGCCTTCTCTACAC-3′) to test for the *Cre* transgene (250 bp *L7Cre*).

Kcc2$^{lox/lox}$ mice

To generate *Kcc2*$^{lox/lox}$ mice, a partial genomic clone of murine *Kcc2* gene (*Slc12a5)* was isolated from a 129/Sv mouse genomic library in λFixII (Stratagene). A loxP site was inserted into intron 5 by PCR, and a neomycin resistance (NEO) cassette flanked by loxP sites into a blunted genomic SapI restriction site between exons 1 and 2 (Supplementary Fig. 1a). A diphtheria toxin A (DTA) cassette was added to the 3' end of the targeting construct as negative selection marker (Supplementary Fig. 1a). The linearized vector was electroporated into R1 ES cells. The NEO cassette was removed from correctly targeted clones by transfection with a plasmid expressing Cre-recombinase. Correct clones were identified by Southern analysis (Supplementary Fig. 1b) and injected into C57Bl6 blastocysts that were implanted into foster mothers. Male chimeras carrying the *Kcc2*^{lox} allele were bred with C57Bl6 females to finally yield *Kcc2*$^{lox/lox}$ mice.

For *Kcc3*$^{lox/lox}$ mice we started from partial genomic clones of murine *Slc12a6* from a 129/Sv mouse genomic library in λFixII (Stratagene). A loxP site plus additional SpeI and BamHI site were inserted into the KasI restriction site of intron 4, and an AscI-fragment containing a 'floxed' neomycin resistance (NEO) cassette into a newly added MluI site between BstBI and EcoRI in intron 6 (Supplementary Fig. 2a). A diphtheria toxin A (DTA) cassette was added to the 5' end. The generation of *Kcc3*$^{lox/lox}$ mice followed essentially the procedure described above for *Kcc2*$^{lox/lox}$ mice.

Kcc2$^{lox/lox}$ and *Kcc3*$^{lox/lox}$ mice were crossed with L7/Pcp2::Cre mice[95] and Δα6::Cre mice[96] to delete *Kcc* in Purkinje cells and granule cells, respectively. Animals were kept on a mixed genetic background and littermates were used as controls.

Behavioral tests

Rotarod Training

Mice (8–30 weeks old) were placed on the cylinder of a rotarod apparatus (model 7650, Ugo Basile Biological Research Apparatus, Varese, Italy) that rotated at four turns per minute and the time the mice spent on top of the cylinder was recorded. After 300 s the recording was ended. The animals were tested twice and between the sessions there was a 60 min break during which the mice rested in their cages. Mean values of the two trials were calculated for each animal. The Mann–Whitney test was used for statistical analyses ($p < 0.05$ was considered significant).

Erasmus Ladder

The Erasmus ladder is a fully automated system designed to screen motor performance and motor learning. It consists of a horizontal ladder that is composed of 2 x 37 rungs (pressure sensors) and is situated between two sheltered boxes equipped with pressurized air outlets. In order to test motor performance mice (8–30 weeks old) were placed in one of the shelters. After a randomized delay of 9-12 second the light was turned on in the box, automatically followed after 3 seconds by air puff from the pressurized air outlet, encouraging the mice to leave the shelter and walk across the ladder to the shelter on the other side, where the procedure was repeated. The paw placement and overall steptime (the time needed to transfer the paw from one sensor to the other) was recorded for each trial in real time using the pressure sensors. One trial was defined as a crossing from one shelter to another. A trial was regarded successful, if the mice walked with a consistent pattern, touching the pressure sensors with all paws and with no disruption such: as rearing, twisting, and turning around. One session consisted of at least 20 trails.

Eye movement recordings

Mice (8–30 weeks old) were surgically prepared under general anesthesia with isoflurane/

O2. A pedestal was attached with two nuts to the frontal and parietal bones using Optibond (Kerr) and Charisma (Heraeus Kulzer). The temperature of the animal and the depth of the anesthesia were constantly monitored, and if necessary, the mice received analgesic treatment after the surgery (temgesic/buprenophine subcutaneous injection 0.015 mg/kg). After 3 days of recovery the animals were placed in a restrainer with the pedestal fixed to a metal bar. The restrainer was fixed onto the turntable, which was surrounded by a cylindrical screen (diameter 63 cm) with a random-dotted pattern surrounding the turntable (diameter 60 cm). Prior to experiments the animals received one training session (1 hour in the restrainer) in order to habituate to the experimental settings. Eye movements (OKR and (V)VOR) were evoked by rotating the screen and/or turntable at different frequencies (Ac servo-motors, harmonic drive AG). The positions of table and drum were recorded by potentiometers and stored for off-line analysis. Eye movements were recorded, as previously described[144,145], with the use of an infrared CCD camera fixed to the turntable (240 Hz, ISCAN Inc.). Two table-fixed infrared emitters (maximum output 600 mW, dispersion angle 7°, peak wavelength 880 nm) illuminated the eye during the recording, and a third emitter was aligned horizontally with the camera's optical axis so as to produce a corneal reflection (CR). The eye movement calibrations were computed as previously described[117, 131], and subsequently the mice were submitted to baseline measurements and training sessions for 5 consecutive days. Gain and phase learning capabilities were studied by applying protocols for two consecutive days that were aimed either at reducing the gain of the VOR by subjecting the mice to 5 × 10 min periods of sinusoidal in phase drum and table rotation at 0.6 Hz (both with an amplitude of 5°) or at increasing the gain by subjecting them to out of phase drum and table stimulation at 1.0 Hz (both with an amplitude of 1.6°). Phase reversal was tested by applying an in phase stimulation on day 1 and subsequently reversing the phase on days 2, 3, 4, and 5 by subjecting the animals to 5 × 10 min periods of sinusoidal in phase drum and table rotation at 0.6 Hz, but with drum amplitudes of 7.5° (days 2) and 10° (days 3, 4, and 5), while the amplitude of the turntable remained 5°. The animals were kept in the dark in between all recording days. After the experiments the animals were euthanized by cervical dislocation under isoflurane anesthesia. Gain and phase values of the eye movements were calculated offline using custom-made Matlab routines (The MathWorks, Natick, MA, USA)[3,5]. Consolidation was calculated by dividing the minimal gain or phase change carried onwards to the next day by the maximal change achieved during the initial day.

Eyeblink conditioning

Mice, aged 11-30 wks, were anesthetized, surgically prepared and investigated with the use of MDMT as described before[59]. A magnet was glued to the lower eyelid and a GMR sensor chip was placed over the upper eyelid such that the axis of sensitivity was aligned with the north-south axis of the magnet. The eyelid responses of the wild type mice and L7-PP2B mutants were conditioned to a tone as the CS (10 kHz, gradually increased over 25 ms to 73 dB) during daily training sessions of 8 blocks of 8 trials. The blocks consisted of 1 US-alone trial, 6 paired trials, and 1 CS-alone trial, and the trials were separated by a random intertrial interval in the range of 20 to 40 s. In paired group the onsets of the CS and US were separated by an inter-stimulus interval of 350 ms.

Ultrastructural examination

Chapter 2

Histology and Immunocytochemistry

Embryos and mice were processed as described previously[146]. Tissue sections and wholemount embryos were hybridized with digoxygenin-labelled riboprobes as described previously[146].

The following primary antibodies were used: mouse anti-CaBP (1:2000, Swant), mouse anti-Neurofilament (1:1000, gift from Virginia M.-Y. Lee, Philadelphia, PA, USA), mouse anti-Islet1 (1:100, Developmental Studies Hybridoma Bank, University of Iowa, USA), mouse anti-Parvalbumin (1:1000, Swant), mouse anti-Robo3 (1:200, R&D ; which recognizes the N-term domain of Robo3), guinea pig anti-VGLUT2 (1:1000, Millipore), rabbit anti-Hb9 (1:1000, Abcam), rabbit anti-CGRP (1:1000, Peninsula), rabbit anti-GFP (1:300, Invitrogen), rabbit anti-Tag1 (1:3000, gift from Dr Domna Karagogeos, University of Crete Medical School, Heraklion, Greece), rabbit anti-CaBP (1:5000, Swant), rabbit anti-ßGal (1 :1000, Cappel), goat anti-mouse Alcam (1:200, R&D), goat anti-Brn3.2 (1:200, Santa-Cruz), goat anti-Robo3 (1:300, R&D), goat anti-ChAT (1:400, Millipore), chicken anti-GFP (1:800, Abcam). The following secondary antibody were used: Donkey anti-Goat, anti-Mouse, anti-Rabbit and anti-Guinea pig coupled to CY3 or CY5 (1:600, Jackson Laboratories), Donkey anti-Goat, anti-Mouse, anti-Rabbit and anti-Chicken coupled to Alexa Fluor 488 (1:600, Invitrogen). Sections counterstained with hoechst 33258 (10 µg ml^{-1}, Sigma) were examined with a fluorescent microscope (DM6000, Leica) coupled to a CoolSnapHQ camera (Roper Scientific) or a confocal microscope (FV1000, Olympus).

For double CTb and gold-lectin labeling the tissue was processed as previously described[22]. In short after 5-7 days post-injection the animals were deeply anesthetized with pentobarbital and perfused with 4% paraformaldehyde and 0.1% glutaraldehyde. After the perfusion the brains were extracted, post-fixed, embedded in 10% gelatin and sectioned transversally at 40µm on a freezing microtome. Free floating sections were then processed for anti-CTb immunocytochemistry[147]. Visualization of gold-lectin labeling was enhanced with silver intensification. Sections were subsequently serially mounted on the chrome-gelatinized glass slides, air dried, counter stained with thionin, cleared with xylene and coverslipped with Permount (Fisher Scientific). For morphological studies of IO neurons and confirmation of CF targeting onto specific cerebellarmicrozonesP7 Animals were perfused intracardiacly with a 4% PFA, 0,12M phosphate solution. Brains were dissected, cryoprotected in a 10% sucrose, 0,12M phosphate solution and frozen at -40°c in isopentane. 20µm cryostat sections were immunostained in a PBS Triton 0,25%, gelatin 2g/L (from pork skin) solution with rabbit anti-CGRP (1:1000, Peninsula) and mouse anti-CaBP (1:5000, Swant), and revealed with donkey anti-rabbit-CY3 (1:600, Jackson Immunoresearch) and donkey anti-mouse-Alexa488 (1:600, Invitrogen).

In situ hybridization

Antisense riboprobes were labelled with digoxigenin-11-D-UTP (Roche Diagnostics) as described previously[146] by in vitro transcription of cDNAs encoding Robo3[1], Barhl1[148], Slit1-Slit3[146], Netrin1[149] and Shh[150]. A mouse Robo3 cDNA specific for exons 12-14 was amplified by PCR with the following primers : 5'-CGGAATTCTGGTATTCAGTGATGACCCC-3' and 5'-GCTCTAGAACAGCAGCCTATCTAGGCCA-3' and cloned into pBluescript vector. The anti-sense probe was synthetised in vitro by digesting the construct with XbaI and using T7 RNA polymerase. Control sense probe yielded no signal.

DiI tracing

4% PFA fixed embryos or postnatal animals were injected with small crystals of DiI (Molecular Probes) using glass micropipets. Injected brains were kept at 37°C for one (aVCN-MNTB and VI-III commissures) to three weeks (olivocerebellar projection). Brains were cut in 100 µm sections with a vibratome (Leica) and counterstained with hoechst.

Quantifications

Di-labelled IO neurons were counted as follows: on every section containing the inferior olive, 4 confocal optic planes were acquired (2 on the contralateral side and 2 on the ipsilateral side) and only the cells showing a circle shaped DiI-labeling were counted positive (Figure 3, Chapter 2 Paragraph 1). The percentage of ipsilateral and contralateral neurons represents the number of ipsilateral or contralateral-labelled neurons divided by the total number of traced neurons on both sides.

The percentage of (ßgal- ; Brn3.2+) olivary neurons was calculated as the ratio of (ßgal- ; Brn3.2+) on (ßgal+ ; Brn3.2+) neurons. Immunolabelled nuclei were counted on 20µm sections of E16 inferior olives (1 section out of 5 was considered from 3 embryos).

Chapter 3

Immunocytochemistry and Electron Microscopy

Immunocytochemistry of L7-PP2B was performed on free-floating 40 µm thick frozen sections from 3- to 5-month-old mice, employing a standard avidin-biotin-immunoperoxidase complex method (ABC, Vector Laboratories) with PP2B as the primary antibody and diaminobenzidine (0.05%) as the chromogen[44].

For electron microscopy, sections were stained for calbindin immunocytochemistry with rabbit anti-calbindin antibody (Swant), osmicated, embedded in Durcupan, and processed for electron microscopy[53]. Electron micrographs and other photographs were stored and analyzed using Adobe PhotoShop (San Jose, CA). Surface areas and thickness of layers for light microscopic data were determined using Neurolucida software (Microbrightfield). For electron microscopy 16 micrographs were taken randomly in each mouse from the molecular layer at a magnification of 19,000 and the density of parallel fiber to Purkinje cell synapses and the morphology of the PSDs was determined using MetaVue 4.6 (Metavue Corporation).

Chapter 4 paragraph 1

Immunocytochemistry and Electron Microscopy

Adult mice were anaesthetized by intraperitoneal injection of ketamine/xylazine and perfused with 4% paraformaldehyde in phosphate-buffered saline (PBS; pH7.4). Cerebella were cryoprotected in sucrose (10%, 20% and 30% in PBS) and cut into 16µm coronal sections with a cryostat. Following blocking in normal goat serum (10% in PBS with 0.5% Triton X-100), sections were incubated with antibodies against calbindin (1:10000; Swant), anti-VGAT (1:3000), anti-VGLUT1 (1:1000), or anti-VGLUT2 (1:500; all Synaptic Systems). Sections were rinsed and incubated with secondary antibodies conjugated to Alexa 488 (Molecular Probes) or Cy3 (Jackson Immunoresearch). Sections were examined with a laser scanning confocal microscope (Zeiss LSM5 Pascal). Stacks of 5-15 sections spaced by 250-350nm were acquired (pinhole: 1 Airy unit). Quantification of VGLUT2-positive puncta was done on segmented images spanning the molecular layer; 8 confocal fields (13225 μm^2/field) were counted per animal (n = 4). For VGLUT1 and VGAT, images acquired at a magnification of 8.1×10^{-3} μm^2/pixel (512 × 512 pixels) were segmented using a threshold that maximized the selection of immunofluorescent puncta over background. The number and density of puncta were calculated with ImageJ software (http://rsbweb.nih.gov/ij/). For VGLUT1 and VGAT, 6 and 8 fields (2125 μm^2/field) were counted per animal (n = 3 and 4, respectively). To quantify the number of Purkinje cells, a line was placed through the Purkinje cell layer and all calbindin-positive cells on the line were counted (4 sections per animal, n = 4). The density of molecular layer interneurons was calculated in 3-6 fields (5000 μm^2/field) of 3-5 Nissl-stained sections per animal (n = 4).

For electron microscopy, adult mice of the various genotypes were perfused with 4% paraformaldehyde and 2.5% glutaraldehyde (vol/vol) in phosphate buffer (0.1 M, pH 7.4). Their cerebella were postfixed in the same solution overnight, and the tissue was processed as described previously[151]. Ultrathin sections (40 µm) were stained with DAB-Calbindin (pre-immuno) and Goldstaining[7] (GABA post-immuno). From tissue blocks each mouse, 16 electron micrographs were taken randomly from the granular cell layer as well as from the molecular layer at a magnification of 19,000 to compare the morphology and density of inhibitory terminals, the density of parallel fiber to Purkinje cell synapses, and the morphology of Purkinje cell spines. The images were stored on an HDD for later off-line analysis (MetaVue 4.6). GABA gold staining was analyzed as described previously[66].

Chapter 4 paragraph 2

Antibodies

Antibodies against Kcc2 were raised in rabbits against Kcc2 peptides (J14 N-terminal: peptide CEDGDGGANPGDGNP [84]; J21 C-terminal: peptide KNEREREIQSITDESC) and affinity-purified. Both antibodies were tested on Western Blot using WT and *Kcc2*$^{-/-}$ protein lysates and gave specific results. Other primary antibodies were mouse anti vesicular inhibitory amino acid transporter (VGAT, Synaptic systems), mouse anti calbindin 28kd (Sigma), rabbit anti calbindin D9k (Swant) and mouse anti parvalbumin (Swant).

Secondary antibodies were Alexa 488-conjugated goat anti-mouse (Molecular Probes), Alexa 488-conjugated goat anti-rabbit (Molecular Probes), Alexa 555-conjugated goat anti mouse (Molecular Probes) and Alexa 555-conjugated goat anti rabbit (Molecular Probes). Nuclei were fluorescence labeled using ToPro-3 (Molecular Probes).

Histology and Immunohistochemistry.

Deeply anesthetized mice were transcardially perfused with cold 0.1 M PB, pH 7.4, followed by 4% paraformaldehyde (PFA) in 1x PBS. Brains were rapidly dissected and postfixed for a few hours on ice. For histological analysis (HE staining), 7µm brain section were prepared from paraffin embedded fixed brains. For immunohistochemistry and immunofluorescence, respectively, fixed brains were equilibrated in 30% sucrose /0.1 M PB, pH 7.4, and 50 µm sagittal floating sections were cut using a freezing microtome (Leica, SM 2000 R). Immunohistochemistry was as described previously[84]. Confocal fluorescence microscopy used a Leica SP2 CSM and 40x objective with and without digital zoom.

In situ hybridization

Sense and antisense RNA probes were generated with T7 and SP6 RNA polymerase, respectively, from a linearized Kcc3 mouse cDNA subclone (nucleotides 146-1056) and labelled with DIG-11-UTP (DIG RNA Labelling Mix, Roche), followed by purification with RNAeasy Kit. *In situ* hybridisation on sagittal cryosections of mouse brains was performed as described previously (Braissant and Wahli 1998).

Calcium Imaging

Patch-clamp recordings were made from Purkinje cells as described above with a calcium indicator dye added to the solution (Oregon Green BAPTA-2, 200 µM). After patch formation the calcium dye was allowed to passively diffuse into the distal dendrites for a minimum of 30 min. Once the entire dendritic tree was visible, the stimulus electrode was positioned at a remote dendritic site to avoid congruent climbing fiber activation. To standardize recordings between both groups, PFs were stimulated to elicit EPSCs of approximately 300 pA. Fluorescence recordings were performed using a NeuroCCD-SMQ camera (80 × 80 pixels) and NeuroPlex software (both RedShirtImaging, Decatur, GA) for data acquisition. The fluorophore was excited using a 100W Xenon arc lamp (Cairn Research Ltd, Faversham, UK). During the tetanus-protocol (PF-stimulation for 5 min at 1 Hz) the elicited calcium-signals were monitored every 20 s. Data was acquired at 2 kHz for sweep durations of

500 ms. Fluorescence changes were normalized to resting levels and expressed as the ratio $\Delta F/F$ (t) = [F(t)-F]/F, where F(t) is the fluorescence value at time t, and F is the averaged fluorescence obtained during the baseline period preceding the stimulus application. To correct for dye-bleaching, an exponential curve was fitted to the recording and subtracted. After acquisition, recordings were filtered using a Gaussian low-pass filter with a cut-off at 150 Hz. The region of interest was set such that it gave the maximal response.

In Vitro Electrophysiology

Chapter 2

Three 4-5 months old homozygous animals and three of their wild type littermates were anaesthetized with isoflurane and decapitated. The cerebellarvermis was isolated, glued to the stage of a Vibratome (Leica, Germany) and rapidly immersed in oxygenated ice-cold slicing medium containing in mM: 230 Sucrose, 5 KCl, 1 $CaCl_2$, 1.25 NaH_2PO_4, 2 $MgSO_4$, 26 $NaHCO_3$ and 10 d-Glucose; perfused with 95% O_2 / 5% CO_2. Sagittalcerebellar slices (250 µm thick) were prepared and placed at room temperature in ACSF (containing in mM: 124 NaCl, 5 KCl, 2 $CaCl_2$, 1.25 NaH_2PO_4, 2 $MgSO_4$, 26 $NaHCO_3$ and 15 d-Glucose; bubbled with 95% O_2 / 5% CO_2) for > 2 hours before the experiment started. Purkinje cells were visualized using an upright microscope (Axioskop 2 FS plus, Carl Zeiss, Jena, Germany) equipped with a 40X water immersed objective. Whole-cell patch-clamp recordings were performed using an EPC-10 amplifier (HEKA Electronics, Lambrecht, Germany). Electrodes were filled with a Cesium based intracellular solution containing in mM 4 $MgCl_2$, 130 $CsMeSo_4$, 0.2 EGTA, 4 NaATP, 0.4 NaGTP, 10 Hepes, 10 Na-phosphocreatine, 1 QX-314, pH 7.25-7.35; osmolarity ~290.

For extracellular stimulation, a patch electrode filled with ACSF was positioned in the bath so that it touched the surface of the slice in the granular layer close to the recorded Purkinje cell to stimulate the climbing fiber. Climbing fibers EPSCs amplitude and pair-pulse depression were tested at room temperature using double test pulses with 50ms stimulus interval. Considering the all-or-none nature of climbing fiber responses, multiple climbing fiber innervations can be tested by increasing the stimulation intensity and quantifying the number of discrete steps in the response amplitude. For every cell we stimulated at different intensities systematically moving the pipette in the portion of the granular layer close to the cell. Series and input resistances (RS and RI, respectively) were monitored by applying 10 mV hyperpolarizing current step, and afterward Rs was compensated in order to have a residual value lower than 10 MΩ. The experiments were performed in presence of bath-applied 10 mMpicrotoxin to block inhibitory synapses. All chemicals were purchased from Sigma. Data were amplified, filtered and stored for off-line analysis (Pulse software, HEKA, Germany).

Chapter 3

Sagittal slices of the cerebellar vermis of 10- to 24-week-old mice (adult) or p16 – p21 mice (young) were kept in ACSF containing (in mM): 124 NaCl, 5 KCl, 1.25 Na_2HPO_4, 2 $MgSO_4$, 2 $CaCl_2$, 26 $NaHCO_3$, 20 D-glucose, and picrotoxin (100 µM), bubbled with 95% O_2 and 5% CO_2 (all drugs are purchased from Sigma-Aldrich, unless stated otherwise). Whole-cell patch-clamp recordings were performed at room temperature or physiological temperatures (as indicated in the text) using an EPC-10 amplifier (HEKA Electronics, Germany). The patch pipettes were filled with intracellular solution containing (in mM): 120 K-gluconate, 9 KCl, 10 KOH, 3.48 $MgCl_2$, 4 NaCl, 10 HEPES, 4 Na_2ATP, 0.4 Na_3GTP, and 17.5 sucrose (pH 7.25). Test responses were evoked at a frequency of 0.05 Hz with the use of patch pipettes filled with ACSF at 1–4 µA for 500 µs (LTP) or 700 µs (LTD). Holding potentials in the range of −60 to −75 mV were chosen to prevent spontaneous spike activity, and cells were switched to current-clamp mode for tetanization. PF-LTD was induced by paired PF and CF stimulation at 1 Hz for 5 min in current-clamp mode, while PF-LTP was induced by PF stimulation alone at 1 Hz for 5 min unless indicated otherwise[46]. For the experiments on intrinsic excitability and plasticity recordings were performed in current-clamp mode, again using an EPC-10 amplifier (HEKA Electronics). Intrinsic excitability was monitored during the test periods by injection of brief (550 ms) depolarizing current pulses (100–200 pA) adjusted to evoke 5–15 spikes. Intrinsic plasticity was induced by tetanization of the Purkinje cell with 150–300 pA current pulses at 5 Hz for 3 s. The spike count was taken as a measure of excitability. Input resistance (Ri) was measured by injection of hyperpolarizing test currents (200 pA; 100 ms) and was calculated from the voltage transient toward the end of current injection. Recordings were excluded if the series or input resistance varied by >15%.

To test whether CF elimination was delayed in L7-PP2B mice, we recorded CF-EPSCs in voltage-clamp mode in 10- to 24-week-old animals, while increasing the stimulus intensity and counting the number of all-or-none steps in the EPSC amplitude. The paired-pulse ratios at CF and PF synapses, respectively, were examined in voltage-clamp mode, by applying stimulus pairs at varying intervals. The paired-pulse ratio was calculated as the ratio of EPSC 2/EPSC 1. Inhibitory transmission was examined by recording spontaneous IPSCs using an internal solution (pH 7.3) containing (in mM): 150 CsCl, 15 CsOH, 1.5 $MgCl_2$, 0.5 EGTA, 10 HEPES, 4 Na_2ATP, and 0.4 Na_3GTP. Purkinje cells were voltage clamped at −70 mV at 34 ± 1°C in the presence of 10 μM NBQX (Tocris Cookson, Bristol, UK).

Chapter 4 paragraph 1

Mice (10 – 25 weeks old) were anaesthetized with isoflurane (IVAX Pharmaceuticals) and parasagittal slices (250-300 μm) were cut from the cerebellar vermis/paravermis (HM 650V; Microm International GmbH) as previously described[143]. Slices were transferred to a submerged recording chamber and perfused (1.5-2.5 ml/min) with an 'external' solution containing (in mM): 125 NaCl, 2.5 KCl, 2 $CaCl_2$, 1 $MgCl_2$, 25 $NaHCO_3$, 1.25 NaH_2PO_4, and 25 d-glucose; pH 7.4, when bubbled with 95% O_2 and 5% CO_2. Patch-clamp recordings were made with Axopatch-200A or -200B amplifiers (Molecular Devices Corporation) from Purkinje cells visualized under infrared differential interference contrast optics (Zeiss Axioscop or Olympus BX51 WI). Whole-cell and single-channel currents were recorded at room temperature (25 ± 1°C). Simple spike activity was recorded at both room and near-physiological temperature (34 ± 2°C), in loose cell-attached mode with external solution in the recording pipette. Firing was recorded in voltage- or current-clamp with the pipette current set to zero[27].

For whole-cell and loose cell-attached recordings, pipettes were pulled from thin-walled borosilicate glass tubing (1.5 mm o.d., 1.17 mm i.d; G150TF-3; Warner Instr. Inc.). For patch recordings, thick-walled borosilicate glass tubing (1.5 mm o.d., 0.86 mm i.d; GC-150F; Harvard Apparatus Ltd) was used. Pipettes were coated with Sylgard resin (Dow Corning 184) and fire polished to give a final resistance of 2-6 MΩ (whole-cell and loose cell-attached) or 10-15 MΩ (single-channel). The internal solution contained (in mM): CsCl, 140; NaCl, 4; $CaCl_2$, 0.5; N-2-hydroxyethylpiperazine-N′-2-ethanesulphonic acid (HEPES), 10; ethyleneglycol-bis (β-aminoethylether)-N,N,N′,N′-tetraacetic acid (EGTA), 5; Mg-ATP, 2; pH 7.3 with CsOH. Ionotropic glutamate receptors were blocked with 10μM d-AP5 and 5μM 6-cyano-7-nitroquinoxaline-2,3-dione (CNQX). mIPSCs were recorded in the presence of 0.5-1 μM tetrodotoxin (TTX).

Parallel fiber-evoked responses were recorded in loose cell-attached mode during molecular layer stimulation (glass pipette containing external solution placed in fixed position ~100-150 μm from the recorded Purkinje cell soma). Stimuli of 5-10 V and 100 μs duration were delivered at 0.5 Hz (Digitimer DS2 isolated stimulator). Recordings were made in the absence of drugs. The effect of $GABA_A$ receptor blockade was tested using SR-95531 (40 µM). In all cases tested, NBQX completely blocked evoked responses (data not shown). Long-term plasticity at parallel fiber-Purkinje cell synapses was examined as previously described[44]. 200 µm thick parasagittal slices were cut in ice-cold ACSF (containing in mM: 124 NaCl, 5 KCl, 1.25 Na_2PO_4, 2 $MgSO_4$, 2 $CaCl_2$, 26 $NaHCO_3$ and 15 d-glucose, bubbled with 95% O_2 and 5% CO_2). Experiments were made at room temperature with $GABA_A$ receptors blocked (100 µM picrotoxin). Whole-cell patch-clamp recordings of Purkinje cells were performed using an EPC-10 amplifier (HEKA electronics). Pipette resistance was 4-5 MΩ when filled with intracellular solution containing (in mM): 120 K-gluconate, 9 KCl, 10 KOH, 3.48 $MgCl_2$, 4 NaCl, 10 HEPES, 4 Na_2ATP, 0.4 Na_3GTP and 17.5 sucrose (pH 7.25). LTP was induced by parallel fiber stimulation at 1 Hz for 5 min in current-clamp mode and measured by test responses recorded in voltage-clamp mode. LTD was induced using combined parallel and climbing fiber stimulation[44]. All drugs were obtained from Tocris Bioscience, Ascent Scientific or Sigma.

Chapter 4 paragraph 2

Brains were removed from decapitated mice (P25 - 21 weeks) and placed into cold “low Ca^{2+}” artificial CSF (ACSF) containing the following (in mM): 119 NaCl, 2.5 KCl, 0,5 $CaCl_2$, 1.3 $MgSO_4$, 1 NaH_2PO_4, 26 $NaHCO_3$, and 11 glucose, which was gassed continuously with 95% O_2/5% CO_2 (carbogen). Brains were cut sagittaly in 200µm thick slices with a vibratome (Leica). After equilibration in ACSF at RT for at least 90min, slices were placed into a recording chamber and continuously superfused with carbogen-gassed ACSF at 22–24°C. PCs and GCs were identified with DIC-infrared video microscopy by their location and shape. Gramicidin-perforated patch-clamp recordings were performed from PCs and cell-attached patch-clamp from GCs. ACSF for perfusion contained (in mM): 119 NaCl, 2.5 KCl, 1.3 $MgSO_4$, 1 NaH_2PO_4, 26 $NaHCO_3$, 2.5 $CaCl_2$ and 11 glucose and was gravity fed to a rate of 2 ml/min controlled with a flow valve (Warner Instruments, Vacuum/Solution Flow Valves, FR-50). Drugs used: 1 µM TTX, 50 µM D-(-)-2amino-5-phophonopentanoic acid (D-AP5) (Tocris N° 0106), 10 µM 6-Cyano-7-nitroquinoxaline-2,3-dione (CNQX) (Tocris N° 0190), 100 µM picrotoxin (Tocris N° 1128), 20 µM bicuculline (Sigma N° B6889) and 100 µM gabazine (SR-95531, Sigma N° S106). Pipette resistances were 2-6 MΩ. For perforated patch-clamp, pipette solution consisted of (in mM): 140 KCl, 5 $MgCl_2$, 10 HEPES and 5 EGTA, pH 7.3. Gramicidin was added to a final concentration of 5 to 50 µg/ml. The tip of the pipette was filled with gramicidin-free solution and backfilled with gramicidin solution. Usually it took 10 to 45 min for gramicidin to lower the series resistance to <20 MΩ, at which point experiments were started. Potentials were corrected off-line for series resistance. Resting membrane potential V was determined with a MultiClamp 700B amplifier (Molecular Devices) in current-clamp mode with I=0. GABA reversal potential (E_{GABA}) of PCs was measured in voltage clamp mode. The membrane was clamped to voltages from -140mV to -40mV in steps of 5-10mV. During these steps 100 µM GABA was applied focally to the neuron by pressure application (30 ms, 4-6 psi, Pressure System IIe, Toohey Company) from a pipette (2-4 MΩ) with the tip located close to the soma. In some experiments we used muscimol (20-50 µM) instead of GABA. Recordings were obtained and analyzed with pClamp 10.0 (Axon). For cell attached recordings in PCs, pipettes with a resistance of 2-3MΩ were filled with ACSF. No blockers were added.

For single-channel recordings of GCs, pipette solution consisted of (in mM): 120 NaCl, 5 KCl, 0.1 $CaCl_2$, 10 $MgCl_2$, 20 TEA-Cl, 5 4-AP, 10 glucose and 10 HEPES, pH 7.4. Picrotoxin, gabazine, bicuculline, GABA or muscimol were added in various combinations.

For recording K_v currents in cell attached voltage-clamp mode[152], pipettes with a resistance of 4-6MΩ were filled with a high K^+ solution consisting of (in mM): 120 KCl, 11 EGTA, 1 $CaCl_2$, 2 $MgCl_2$, 10 HEPES, 20 glucose, pH 7.25 with 35 mM KOH (final K^+ concentration 155 mM), 310 mOsmol.

In Vivo Electrophysiology

Chapter 2

In vivo electrophysiology and floccular injections

Mice (15–40 weeks old) were surgically prepared under general isoflurane anesthesia by mounting a pedestal as described above. After that procedure the occipital bones were exposed and a craniotomy was made in the left occipital bone. An acrylic cement chamber was built around the craniotomy and the chamber was sealed with bone wax. After 3 days of recovery mice were submitted to experimental procedures. For the extracellular Purkinje cell activities the animals were placed in the restrainer fixed onto the turntable (diameter 63 cm) with a cylindrical screen with a random-dotted pattern surrounding the turntable (diameter 60 cm). The turntable was equipped with an electrode manipulator, which guided the borosilicate glass electrodes (2µm tip diameter), filled with 2M NaClsolution, into the brain. The extracellular signals were recorded either from the flocculus of the cerebellar cortex[12]. The cells were recorded at rest without stimulation or during optokineticor vestibular stimulation (see the eye movement methods). Signals were filtered, amplified (Cyberamp 380, Axon Instruments, UK), digitized (Power 1401, CED, Cambridge, UK) and stored for the off-line analysis. Purkinje cells were identified by their complex spike firing. Single unit recordings were confirmed by the short pause in simple spike firing following each complex spike (climbing fiber pause)[153].Tuning curves of complex spikes were made to determine the optimal axis of stimulation. Only cells that responded optimally to stimulation around the vertical axis were used in this study. Cells were recorded during optokinetic stimulation of frequencies ranging from 0.1 to 0.8 Hz. In 9 mutant and 3 control animals, at the end of the experiment the recording electrode was exchanged for a pipette (15-18µm tips) containing 5 µl of 1% cholera toxin B-subunit (CTb), an antero- and retrograde tracer[147]. The CTb injection was made using an anodal current of 4µA, pulsed 7 seconds on, 7 seconds off for the duration of 5 minutes[22]. After the CTb injections were made the pipette was replaced by another electrode (~20µm tips) containing approximately 1µl of gold-lectin conjugate of bovine serum albumin with wheat germ agglutinate and 10 nm gold sol (Aurion, Wageningen, NL), a retrograde tracer[22]. The electrode was positioned in the flocculus and injections were made with pressure pulses, using a custom madepressure device. Following the injections the brain was covered with gramicidin-containing ointment at sealed with bone wax. After 72 hours the animals were sacrificed, perfused and their brains were processed for histology.

Chapter 3,4 and 5

Mice (15 – 40 weeks old) were surgically prepared under general anesthesia by mounting a pedestal as described above[117]. A recording chamber was built around craniotomies in left and right occipital bones. Extracellular Purkinje cell activity was recorded using borosilicate glass electrodes (OD 2.0 mm, ID 1.16 mm, 2 M NaCl, 4-8 MΩ). Electrodes were advanced by a hydraulic micro-drive (Narishige). Recordings were made from left and right Crus I and II, paramedian lobule, and (para)flocculus (recordings during optokinetic and vestibular stimulation were from floccular Purkinje cells). Purkinje cells were identified by the brief pause in simple spike activity following each complex spike. The raw signal was amplified, filtered (CyberAmp, CED), digitized (CED) and stored for off-line analysis. Following each recording session the brain was covered with gramicidin-containing ointment and the chamber was sealed with bone wax.

Data and Statistical analysis

Off-line analysis of the eye movements and Purkinje cell activity was performed using custom-made Matlab (MathWorks) routines as described before[131,117]. The mean maximum and minimum spike rates were calculated from 10 bins (bin size 3.6 degree) preceding and 10 bins following the peak (90 degree) and trough (270 degree) of the fitted sine wave in the peri-stimulus phase histograms. For data representation the Means and Standard Error of Mean (SEM) were calculated. For *in vitro* off-line analysis we used Patch Master (HEKA Electronics, Lambrecht, Germany). The histological material was analyzed with a Leica DMR light microscope equipped with a DC 300 digital camera. Labeled neurons in the IO and VN were plotted serially from aone out of four series of sections using an Olympus microscope equipped with a Lucivid_ miniature monitor, and using Neurolucida TM software (Microbrightfield, Colchester, VT, USA).The reconstructions of drawings and photo panels were constructed in Adobe Photoshop CS3 Version 10.0 and brightness, contrast and color balance was corrected. Immunocytochemical quantifications were performed as previously described[16].

Unless mentioned in the text, results are presented as Means and Standard Error of Mean (SEM). For statistical analyses repeated measures two-way ANOVA, One-way ANOVA, Students t-test, Paired Samples Students t-test and Turkey HSD post-hoc tests were used to determine significant difference and where data were non-normally distributed (Shapiro-Wilk test), the Mann-Whitney *U*-test. Statistics were carried out with SPSS 11 (SPSS Inc.).

Models and simulations

A phenomenological model of an idealized VOR circuit was created to elucidate the potential role of vestibular nuclei in a phase adaptation paradigm. Elements in the VOR circuit were characterized by the gain and phase of their sinusoidal modulation, which define the coordinates of a position on a polar plot. Plasticity rules were employed phenomenologically, as exponential decay of the modulation along a trajectory in a polar plot, with the target gain and phase (new position in the polar plot) defined by the vestibular mismatch. Equations were solved numerically using Matlab.

References

1. Sabatier, C. et al. The divergent Robo family protein rig-1/Robo3 is a negative regulator of slit responsiveness required for midline crossing by commissural axons. *Cell* 117, 157-69 (2004).
2. Wilson, J.M. et al. Conditional rhythmicity of ventral spinal interneurons defined by expression of the Hb9 homeodomain protein. *J Neurosci* 25, 5710-9 (2005).
3. Kawaguchi, Y. et al. The role of the transcriptional regulator Ptf1a in converting intestinal to pancreatic progenitors. *Nat Genet* 32, 128-34 (2002).
4. Hippenmeyer, S. et al. A developmental switch in the response of DRG neurons to ETS transcription factor signaling. *PLoS Biol* 3, e159 (2005).
5. Zeng, H. et al. Forebrain-specific calcineurin knockout selectively impairs bidirectional synaptic plasticity and working/episodic-like memory. *Cell* 107, 617-29 (2001).
6. Barski, J.J., Dethleffsen, K. & Meyer, M. Cre recombinase expression in cerebellar Purkinje cells. *Genesis* 28, 93-8 (2000).
7. Wulff, P. et al. From synapse to behavior: rapid modulation of defined neuronal types with engineered GABAA receptors. *Nat Neurosci* 10, 923-9 (2007).
8. Stahl, J.S., van Alphen, A.M. & De Zeeuw, C.I. A comparison of video and magnetic search coil recordings of mouse eye movements. *J Neurosci Methods* 99, 101-10 (2000).
9. van Alphen, A.M., Stahl, J.S. & De Zeeuw, C.I. The dynamic characteristics of the mouse horizontal vestibulo-ocular and optokinetic response. *Brain Res* 890, 296-305 (2001).
10. Hoebeek, F.E. et al. Increased noise level of purkinje cell activities minimizes impact of their modulation during sensorimotor control. *Neuron* 45, 953-65 (2005).
11. Goossens, H.H. et al. Simple spike and complex spike activity of floccular Purkinje cells during the optokinetic reflex in mice lacking cerebellar long-term depression. *Eur J Neurosci* 19, 687-97 (2004).
12. Koekkoek, S.K. et al. Cerebellar LTD and learning-dependent timing of conditioned eyelid responses. *Science* 301, 1736-9 (2003).
13. Marillat, V. et al. Spatiotemporal expression patterns of slit and robo genes in the rat brain. *J Comp Neurol* 442, 130-55 (2002).
14. Ruigrok, T.J. & Apps, R. A light microscope-based double retrograde tracer strategy to chart central neuronal connections. *Nat Protoc* 2, 1869-78 (2007).
15. Ruigrok, T.J., Teune, T.M., van der Burg, J. & Sabel-Goedknegt, H. A retrograde double-labeling technique for light microscopy. A combination of axonal transport of cholera toxin B-subunit and a gold-lectin conjugate. *J Neurosci Methods* 61, 127-38 (1995).
16. Marillat, V. et al. The slit receptor Rig-1/Robo3 controls midline crossing by hindbrain precerebellar neurons and axons. *Neuron* 43, 69-79 (2004).
17. Li, S., Qiu, F., Xu, A., Price, S.M. & Xiang, M. Barhl1 regulates migration and survival of cerebellar granule cells by controlling expression of the neurotrophin-3 gene. *J Neurosci* 24, 3104-14 (2004).
18. Serafini, T. et al. The netrins define a family of axon outgrowth-promoting proteins homologous to C. elegans UNC-6. *Cell* 78, 409-24 (1994).
19. Charron, F., Stein, E., Jeong, J., McMahon, A.P. & Tessier-Lavigne, M. The morphogen sonic hedgehog is an axonal chemoattractant that collaborates with netrin-1 in midline axon guidance. *Cell* 113, 11-23 (2003).
20. Hansel, C. et al. alphaCaMKII Is essential for cerebellar LTD and motor learning. *Neuron* 51, 835-43 (2006).
21. De Zeeuw, C.I. et al. Expression of a protein kinase C inhibitor in Purkinje cells blocks cerebellar LTD and adaptation of the vestibulo-ocular reflex. *Neuron* 20, 495-508 (1998).
22. de Zeeuw, C.I., Holstege, J.C., Ruigrok, T.J. & Voogd, J. Ultrastructural study of the GABAergic, cerebellar, and mesodiencephalic innervation of the cat medial accessory olive: anterograde tracing combined with immunocytochemistry. *J Comp Neurol* 284, 12-35 (1989).
23. Andreescu, C.E. et al. Estradiol improves cerebellar memory formation by activating estrogen receptor beta. *J Neurosci* 27, 10832-9 (2007).
24. Belmeguenai, A. & Hansel, C. A role for protein phosphatases 1, 2A, and 2B in cerebellar

long-term potentiation. *J Neurosci* 25, 10768-72 (2005).
25. Hausser, M. & Clark, B.A. Tonic synaptic inhibition modulates neuronal output pattern and spatiotemporal synaptic integration. *Neuron* 19, 665-78 (1997).
26. De Zeeuw, C.I., Wylie, D.R., DiGiorgi, P.L. & Simpson, J.I. Projections of individual Purkinje cells of identified zones in the flocculus to the vestibular and cerebellar nuclei in the rabbit. *J Comp Neurol* 349, 428-47 (1994).
27. Renier, N. et al. Genetic dissection of the function of hindbrain axonal commissures. *PLoS Biol* 8, e1000325 (2010).

CHAPTER 7

DISCUSSION

In this thesis we investigated the impact of afferent inputs to cerebellar cortex on Purkinje cell spiking patterns and motor coordination using a wide variety of genetically manipulated mice. By examining the electrophysiological properties of Purkinje cells and motor behavior of the mutant mice, we determined that while all alterations to Purkinje cell inputs cause impairment of cerebellar related motor behavior, each alteration has its unique consequences on Purkinje cell spiking properties and motor performance. In our studies we mainly focused on one aspect of motor behavior, namely compensatory eye movements, which due to their well described circuitry are the perfect model for studying cerebellar tasks. Our results suggest that the neurons in the cerebellar network relay crucial information by reading and creating specific spatiotemporal patterns of complex and simple spike activities rather than by increasing or decreasing their average firing rate. We also think that work presented in this thesis supports the notion of cerebellum acting as an adaptive filter. Being aware of the limitations posed by the use of genetically engineered mice we propose a battery of future experiments that will hopefully shed more light on the contribution of Purkinje cells to cerebellar motor learning and memory formation.

Dissecting the circuitry - Purkinje cell inputs under investigation

This thesis focuses on both excitatory input to Purkinje cells mediated by climbing and parallel fibers as well as inhibitory input which comes from molecular layer interneurons[1, 2]. While climbing fiber input always triggers an action potential (i.e. complex spike) in the Purkinje cell[3] the parallel fibers and molecular layer interneurons have a more modulatory function on the Purkinje cell intrinsic spiking (i.e. simple spikes) causing a well timed decrease or increase in spiking intervals respectively[4, 5]. In the light of findings presented in this thesis, I would like to shortly discuss the role of those three inputs in cerebellar functioning.

Climbing fiber input

Ever since the late 60’s, when Eccles described the potent climbing fiber to Purkinje cell synapse, there has been countless studies on this specific connection[6-13]. From the earliest investigations scientists in the cerebellar field believed that it might hold the key to unraveling the process of cerebellar motor learning. The one-on-one relationship (meaning that each Purkinje cell is innervated by only one climbing fiber), the zonal organization of the climbing fibers corresponding to different receptive fields and finally the all or nothing response upon activation of the synapse triggering an unusually huge influx of calcium to the Purkinje cell made the climbing fiber a great candidate for being a key player in the cerebellar cortex. For decades activation of climbing fiber has been thought to carry a teacher signal which is able to shape the other synaptic inputs[1, 14]. While some studies supported this notion there has been a number of results opposing this theory[15, 16]. In the light of our recent findings however it seems unreasonable to argue against the importance of climbing fibers in cerebellar learning. We have recently learned that climbing fibers are able to transmit bursts of spikes at very high frequency reliably relaying the spiking and oscillatory phase of the olivary cells.[17, 18]. Climbing fiber activation has not only proven to be responsible for determining the direction of plasticity on the parallel fiber synapse by changing intracellular calcium levels in Purkinje cell[19, 20], but also has the ability to acutely overwrite any other synaptic input to Purkinje cell remaining at the same time plastic[21]. Our results add to this long list of remarkable climbing fiber synapse properties. Firstly, we show that impaired wiring of climbing fiber axons has fatal consequences to the motor behavior resulting in profound ataxia (Chapter 2.1). When we investigated the *Ptf1a::Robo3^{loxlox}* mouse we found that rerouting most olivary axons, from the contralateral to the ipsilateral side causes more severe motor deficits than having no output at all from the cerebellar cortex (as it happens in the *Lurcher* mice[22]). Secondly, our results show how crucial the climbing fiber is to reciprocal simple and complex spike firing during motor behavior. Our results clearly demonstrate that it is the climbing fiber that dictates the phase of not only complex spike modulation but that it is able to overwrite normal simple spike modulation, shifting its phase with accordance to complex spike modulation(Chapter 2.2). This finding was on its own striking since it potentially could put an end to longstanding discussion about the origin of reciprocity (I will discuss that in details in the next paragraph). Even more surprising were the results suggesting that the climbing fiber acts on simple spike modulation by changing the timing of spiking in molecular layer interneurons. However, this is in accordance with the notion presented in several recent papers that underline the impact of climbing fibers on molecular layer interneurons[5, 23, 24]. It seems that climbing fiber activity indeed plays a key role in cerebellar physiology and therefore has earned its title as the “star” of cerebellar circuitry.

Parallel fiber input

Similar to climbing fiber input, the parallel fiber excitatory pathway has been studied extensively in the past couple of decades. With the discovery of parallel fiber long term depression (PF-LTD)[1, 10, 25-27] it became obvious that selective silencing of parallel fibers could be a potential learning mechanism through which Purkinje cell could adjust their synaptic. This hypothesis has been the subject of very heated discussions and throughout the years research has provided arguments supporting[26, 28] as well as falsifying this notion[29]. The discovery of parallel fiber long term potentiation (PF-LTP)[19, 30] provided new insights into the role of parallel fiber synapse and gave scientists a new pathway to look at. Nowadays it seems obvious that it is the bidirectional plasticity at the parallel fiber synapse that provides the capacity for Purkinje cells to adapt[19]. Obviously we were curious to see what happens when PF-LTP is taken out of this equation. We selectively deleted the phosphatase 2B[30] in Purkinje cells in mutant mice and found that indeed it abolished PF-LTP resulting in a profound behavioral phenotype (Chapter 3). The mice’s ability to adapt their VOR reflex was almost completely abolished. This might suggests that PF-LTP is more crucial to cerebellar motor learning than PF-LTD, however we think that this is not the case. Rather it is the homeostatic balance between the LTP and LTD that seems crucial for proper Purkinje cell functioning. Also, the phosphatase 2B could be involved in the induction of rebound potentiation (the potentiation of GABAergic inhibition onto Purkinje cells by concurrent climbing fiber stimulation)[31]. We therefore cannot exclude that the observed phenotype in our PF-LTP deficient mutants is partially dependent on the disrupted inhibition from the molecular layer interneurons rather than from excitation coming from the parallel fibers.

It should be noted that even though this thesis is focused on Purkinje cell physiology we are aware that learning might occur also upstream and downstream from Purkinje cells. There has been strong evidence for plasticity in granule cells[32] and we hypothesize that for some motor behavior it is the integration that takes place at the level of granule cell that is substantial for motor learning. When we selectively deleted potassium-chloride cotransporter 2 (Kcc2) from granule cells we found that mice with that alteration were no longer able to consolidate the phase of the vestibulo-ocular response during the VOR adaptation (Chapter 4.2). This surprising finding could potentially be an argument for a role of granule cells in cerebellar motor learning. However, we should not forget that by changing the excitability of granule cells the Purkinje cell firing patterns and plasticity may change as well (due to higher excitation received from the parallel fibers). Naturally this hypothesis needs to be more extensively studied in the future.

Molecular layer interneurons

In the light of the recent finding it is puzzling that molecular layer interneurons and more general the inhibition in the cerebellar cortex have been neglected for such a long time. It is even more surprising given that the input from molecular layer interneurons was experimentally proven to have an impact on simple spike firing patterns in the late 90's[33]. There have been several studies that explored this subject, but to our knowledge experiments presented in Chapter 4 are the first example of a genetic deletion of molecular layer inhibition onto Purkinje cells. It has been shown before that pharmacological blockage of inhibition causes disturbances in Purkinje cell firing patterns[34]. We went a step further and showed that abolishing the inhibitory action of molecular layer interneurons in mice (either by eliminating the functional $GABA_A$ receptor or by deletion of Kcc2 contransporter in Purkinje cells) leads to minor performance problems and major learning deficits (Chapter 4.1 and 4.2). Our findings strongly support the hypothesis stating that molecular layer interneurons are crucial during motor learning.

At first glance it seems that climbing fiber, parallel fiber and molecular layer interneuron inputs act independently on Purkinje cell and in consequence on motor behavior and coordination. This is however not the case. We have strong evidence supporting the hypothesis that climbing fiber contributions to cerebellar physiology are much greater than that of the parallel fiber and molecular layer interneurons: 1) Climbing fiber excitation acts as a plasticity switch on the parallel fiber to Purkinje cell synapse: combined climbing and parallel fiber activity induce high intracellular calcium concentration[35] leading to endocytosis of AMPA receptors[36] and in consequence to LTD[27], whereas low level of calcium triggered by parallel fiber input alone, in the absence of climbing fiber signal, leads to the induction of LTP; 2) Climbing fiber activation coinciding with molecular layer interneuron signaling induces rebound potentiation in Purkinje cells that can further strengthen the depression at the parallel fiber synapse[37, 38]; 3) Receptive fields of parallel fibers and molecular layer interneurons are climbing fiber specific[39, 40], meaning that climbing fiber activity can change the receptive field of both parallel fibers and interneurons, most probably through bidirectional parallel fiber plasticity and long term potentiation at the molecular layer interneuron synapse[41] respectively; 4) Rerouting the climbing fiber input from contra- to ipsilateral results in more severe ataxia than any other manipulation of the cerebellar circuitry (Chapter 2.1); and 5) Climbing fiber induced complex spike activity can overwrite the simple spike modulation (Chapter 2.2).

Obviously these examples of climbing fiber dominance do not mean that parallel fibers and interneurons play no role in cerebellar motor behavior. Motor performance and motor learning can only be achieved if all above mentioned pathways work in unison to create appropriate spatiotemporal patterns of complex and simple spikes.

Complex and simple spike firing patterns and their reciprocal relationship

Purkinje cells are substantially different from other principal neurons (like in hippocampus or cerebral cortex[42]) in that they are intrinsically active, generating persistent spiking activities[43,44]. They are also unique because they generate two different types of spikes: simple and complex spikes[1,2,45,8, 46]. Together, complex and simple spikes compose the output of the Purkinje cell that will be relayed onto cerebellar nuclei and in the case of vestibulocerebellum onto vestibular nuclei.

Complex spikes properties

Complex spikes are induced by climbing fiber stimulation[47]. The strength of the climbing fiber on Purkinje cell synapse is unusually large due to a widespread synchronous depolarization spreading from approximately 500 presynaptic release sites upon single climbing fiber activation[48, 49]. This allows a climbing fiber to relay not only single action potential but also high frequency bursts[17]. This reliable transmission of the signal from climbing fibers allows the complex spike activities in the Purkinje cells to follow the temporal and spatial pattern of olivary cell activities[12, 18, 50]. In Chapter 2.2 we show that changing the input of the climbing fibers from contra- to ipsilateral results in phase shift in complex spike occurrence. It proves that complex spikes reliably follow the somatosensory information received from olivary neurons (in the case of *PTF1aCre::Robo3l^{oxlox}* mutant mice this information is gathered from the ipsilateral side of the olive hence the change in the phase of complex spike activity).

Simple spikes patterns

As mentioned above, Purkinje cells are intrinsically active[43], which means that in the absence of any synaptic input (even in the dissociated cultures[51]) they fire simple action potentials (i.e. simple spikes) at the frequency of approximately 50Hz. This intrinsic peacemaking activity is highly regular and stable. It is the synaptic input from granule cells and molecular layer interneurons that increase and decrease the simple spike firing frequency respectively[52]. However, the synaptic input to Purkinje cells does more than simply controlling the average firing frequency. The excitatory and inhibitory inputs shape the precise temporal patterns of simple spike firing[5, 38]. As shown in Chapter 3 and 4.1 the changes in inter simple spike interval (ISSI) distributions have profound effect on motor performance and learning. In both mutant mice (PF-LTP deficient mice described in Chapter 3 and mice without synaptic inhibition onto Purkinje cells investigated in Chapter 4.1) we observed an increase in simple spike regularity (measured by calculating simple spike CV_2, which was significantly lower in both mutant mice). The necessity for Purkinje cells to display a certain level of simple spike firing irregularity can be explained by the anatomy of cerebellar circuitry. Since approximately 10-100 Purkinje cell converge on one cerebellar nuclei cell[53] it seems logical that Purkinje cells need to synchronize their input in order to reliably relay the information further downstream. As proposed by the model in Chapter 4.1 (Figure 6) synchronization of simple spike activities is only possible when certain amount of irregularity is introduced into simple spike firing patterns. It has been shown in the past studies that too much noise is also not beneficial for sufficient information transfer – Purkinje cells of *tottering* mice (which exhibit profound motor impairment) show highly irregular simple spike firing patterns[54]. All together these data emphasize the significant role of optimal tuning of spatiotemporal simple spike firing patterns in motor performance and learning.

Interactions of complex and simple spikes during compensatory eye movements

In most parts of the cerebellum Purkinje cells the simple spikes have the tendency to modulate out of phase with complex spike activities[11, 55]. In the vestibulocerebellum this phenomenon of reciprocity is particularly prominent and has been hypothesized to control compensatory eye and head movements[56-58]. In this thesis we carefully investigated the simple and complex spike reciprocity and found that it is dependent on climbing fiber activity (Chapter 2.2). We also present evidence that climbing fibers impose this reciprocal firing of complex and simple spikes potentially via molecular layer interneurons (hypothesis supported by a number of studies[23, 24, 33]). In Chapter 5 we show that that once consolidated, phase reversal training is correlated with higher amplitude of simple spike modulation, but not with changes in simple spike firing frequency or regularity. The observed strengthening of simple spike modulation can be weakly correlated to stronger inhibition at the trough of the modulation as well as stronger excitation at its peak. These results provide additional evidence for reciprocity being not the epiphenomenon triggered by the motor activity but actively shaping the behavior during compensatory eye movements.

Surprisingly, most theories of cerebellar learning neglected the potential functions of spatiotemporal spiking patterns. This thesis clearly shows that any alteration to afferent inputs to Purkinje cells leads to a change in the spatiotemporal firing pattern and in consequence to disrupted motor behavior (**Table 1**). Of course this does not mean that the read out of changes in average firing frequency is without meaning. We assume that both of those mechanisms are important depending on the state of the sensorimotor task. For example the precise simple spike patterning (mediated by feed-forward inhibition) may be crucial for the consolidation during adaptation of vestibulo-ocular reflex (Chapter 4.1), while motor performance could rely more on changes in the modulation amplitude of simple and complex spike activities[56,(Chapter 5)].

Table 1. Summary of cerebellar mouse mutants described in this thesis

	Simple spike						Complex spike					Behavior			
Mutations	FF	CV	CV2	CF pause	Modulation amplitude	Modulation phase	FF	CV	Modulation amplitude	Modulation phase	CF elimination	Performance	Acute learning (1 day)	Long-term learning (>3 days)	Consoli-dation
PTF1aCre:: Robo3lox/lox	n	↑	↑	n	↑	shifted	n	n	n	shifted	n	severly imp	n.m.	n.m	n.m
L7-Cre x CNB1lox/lox	n	↓	↓	n	?	?	n	n	?	?	n	imp	imp	imp	n.m
L7-Cre x gamma2lox/lox	n	↓	↓	↑	n	n	n	n	n	n	?	imp	n	imp	imp
L7-Cre x KCC2lox/lox	?	?	?	?	?	?	?	?	?	?	?	n (only OKR imp)	imp	imp	gain imp
A6-Cre x KCC2lox/lox	?	?	?	?	?	?	?	?	?	?	?	n	n	imp	phase imp
A6/L7-Cre x KCC2lox/lox	?	?	?	?	?	?	?	?	?	?	?	imp	imp	imp	n.m

n - normal,↑ - higher,↓ - lower, imp - impaired, n.m. - not measurable

Plans for the future

To further establish hypotheses presented in this discussion, various experiments have to be performed in the future. Most of the work presented in this thesis (with the exception of Chapter 5) has been done in cell specific mutant mice (Chapter 2 ,3 and 4), which poses a serious difficulty in interpreting the results due to a possible involvement of compensatory mechanisms. Which probably are more pronounced when changes are affecting specific proteins (Chapter3), channels (Chapter 4.1) or cotransporters (Chapter 4.2) rather than when the circuitry has been rerouted such as in the mutants used in the study presented in Chapter 2. In the case of "software" changes (when a cellular mechanism is being tampered with) it is reasonable to suspect that the cell can "protect" its homeostasis by up or down–regulating other pathways. This could account for the mild performance phenotype in LTP deficient mice as well as in mice with GABA_A receptor ablation. We hypothesize that acute disruption of those mechanisms would result in much more profound deficits. Introduction of inducible Purkinje cell specific knockouts could help us to fully understand the importance of specific molecular pathways on cerebellar functions. It would be very interesting to acutely switch on and off whole populations of neurons (for example molecular layer interneurons) and study the effects of this type of alterations on the cerebellar motor behavior. This could be potentially achieved by introduction of optogenetic methods. For example, using halorhodopsin selectively expressed in molecular layer interneurons we could finally get a clear answer to the contribution of the latter neurons to motor performance and learning.

Still there are a lot of answers that could be obtained by studying wildtype mice. Definitely more experiments are needed to further investigate the changes in simple spike modulation following cerebellar motor learning. Based on the results presented in Chapter 5, where we measured Purkinje cell activity in "naïve" vs "reversed" mice (animals exposed to 5 day long learning paradigm aimed at reversing the phase of the eye movements), we could think of a number follow up experiments: it would certainly be very interesting to investigate whether the amplitude of modulation goes back to baseline when animals are left in the light and if so, how much time it would take for Purkinje cells to readjust their spiking patterns; we would also like to record molecular layer interneurons in both C57BL/6 and mutant mice to correlate their activity with observed changes in the depth of inhibition during an off-phase stage of modulation. It would also be interesting to further investigate this issue in L7gamma2 mice (Chapter 4.1). Preliminary results obtained on these mutant mice show much higher variation of their simple spike firing patterns (changes in CV_2) but more experiments are needed to draw conclusions about the phase and amplitude of simple spike modulation.

In order to investigate if and how the spatiotemporal spiking patterns encoded by Purkinje cells relayed downstream it is inevitable to perform combined recordings from deep cerebellar and/or vestibular nuclei and Purkinje cells in awake behaving animals.

Reference

1. Marr, D. A theory of cerebellar cortex. *J Physiol* **202**, 437-70 (1969).
2. Eccles, J.C., Ito, M. & Szentagothai, J. The cerebellum as a neuronal machine. (1967).
3. Eccles, J.C., Llinas, R., Sasaki, K. & Voorhoeve, P.E. Interaction experiments on the responses evoked in Purkinje cells by climbing fibres. *J Physiol* **182**, 297-315 (1966).
4. De Schutter, E. Using realistic models to study synaptic integration in cerebellar Purkinje cells. *Rev Neurosci* **10**, 233-45 (1999).
5. Mittmann, W., Koch, U. & Hausser, M. Feed-forward inhibition shapes the spike output of cerebellar Purkinje cells. *J Physiol* **563**, 369-78 (2005).
6. Maekawa, K. & Simpson, J.I. Climbing fiber activation of Purkinje cells in the flocculus by impulses transferred through the visual pathway. *Brain Res* **39**, 245-51 (1972).
7. Simpson, J.I. & Alley, K.E. Visual climbing fiber input to rabbit vestibulo-cerebellum: a source of direction-specific information. *Brain Res* **82**, 302-8 (1974).
8. McDevitt, C.J., Ebner, T.J. & Bloedel, J.R. The changes in Purkinje cell simple spike activity following spontaneous climbing fiber inputs. *Brain Res* **237**, 484-91 (1982).
9. Demer, J.L., Echelman, D.A. & Robinson, D.A. Effects of electrical stimulation and reversible lesions of the olivocerebellar pathway on Purkinje cell activity in the flocculus of the cat. *Brain Res* **346**, 22-31 (1985).
10. Ito, M. Long-term depression as a memory process in the cerebellum. *Neurosci Res* **3**, 531-9 (1986).
11. Simpson, J.I., Wylie, D.R. & De Zeeuw, C.I. On climbing fiber signals and their consequence(s). . *BehBrain Sciences* **19**, 380-394 (1996).
12. Jorntell, H., Ekerot, C., Garwicz, M. & Luo, X.L. Functional organization of climbing fibre projection to the cerebellar anterior lobe of the rat. *J Physiol* **522 Pt 2**, 297-309 (2000).
13. Winkelman, B. & Frens, M. Motor coding in floccular climbing fibers. *J Neurophysiol* **95**, 2342-51 (2006).
14. Ekerot, C.F. Climbing fibres - a key to cerebellar function. *J Physiol* **516 (Pt 3)**, 629 (1999).
15. Raymond, J.L., Lisberger, S.G. & Mauk, M.D. The cerebellum: a neuronal learning machine? *Science* **272**, 1126-31 (1996).
16. Ke, M.C., Guo, C.C. & Raymond, J.L. Elimination of climbing fiber instructive signals during motor learning. *Nat Neurosci* **12**, 1171-9 (2009).
17. Mathy, A. et al. Encoding of oscillations by axonal bursts in inferior olive neurons. *Neuron* **62**, 388-99 (2009).
18. Hansel, C. Reading the clock: how Purkinje cells decode the phase of olivary oscillations. *Neuron* **62**, 308-9 (2009).
19. Coesmans, M., Weber, J.T., De Zeeuw, C.I. & Hansel, C. Bidirectional parallel fiber plasticity in the cerebellum under climbing fiber control. *Neuron* **44**, 691-700 (2004).
20. Ohtsuki, G., Piochon, C. & Hansel, C. Climbing fiber signaling and cerebellar gain control. *Front Cell Neurosci* **3**, 4 (2009).
21. Schmolesky, M.T., Weber, J.T., De Zeeuw, C.I. & Hansel, C. The making of a complex spike: ionic composition and plasticity. *Ann N Y Acad Sci* **978**, 359-90 (2002).
22. Van Alphen, A.M., Schepers, T., Luo, C. & De Zeeuw, C.I. Motor performance and motor learning in Lurcher mice. *Ann N Y Acad Sci* **978**, 413-24 (2002).
23. Barmack, N.H. & Yakhnitsa, V. Functions of interneurons in mouse cerebellum. *J Neurosci* **28**, 1140-52 (2008).
24. Jorntell, H., Bengtsson, F., Schonewille, M. & De Zeeuw, C.I. Cerebellar molecular layer interneurons - computational properties and roles in learning. *Trends Neurosci* **33**, 524-32.
25. Ito, M. Neural design of the cerebellar motor control system. *Brain Res* **40**, 81-4 (1972).
26. Hansel, C. et al. alphaCaMKII Is essential for cerebellar LTD and motor learning. *Neuron*

51, 835-43 (2006).
27. Hansel, C. & Linden, D.J. Long-term depression of the cerebellar climbing fiber--Purkinje neuron synapse. *Neuron* **26**, 473-82 (2000).
28. De Zeeuw, C.I. et al. Expression of a protein kinase C inhibitor in Purkinje cells blocks cerebellar LTD and adaptation of the vestibulo-ocular reflex. *Neuron* **20**, 495-508 (1998).
29. Schonewille, M. et al. Re-evaluating the role of LTD in Cerebellar Motor Learning. *Neuron* (2011, *In press*).
30. Belmeguenai, A. & Hansel, C. A role for protein phosphatases 1, 2A, and 2B in cerebellar long-term potentiation. *J Neurosci* **25**, 10768-72 (2005).
31. Kano, M., Rexhausen, U., Dreessen, J. & Konnerth, A. Synaptic excitation produces a long-lasting rebound potentiation of inhibitory synaptic signals in cerebellar Purkinje cells. *Nature* **356**, 601-4 (1992).
32. Ekerot, C.F. & Jorntell, H. Synaptic integration in cerebellar granule cells. *Cerebellum* **7**, 539-41 (2008).
33. Hausser, M. & Clark, B.A. Tonic synaptic inhibition modulates neuronal output pattern and spatiotemporal synaptic integration. *Neuron* **19**, 665-78 (1997).
34. Miyashita, Y. & Nagao, S. Contribution of cerebellar intracortical inhibition to Purkinje cell response during vestibulo-ocular reflex of alert rabbits. *J Physiol* **351**, 251-62 (1984).
35. Jorntell, H. & Hansel, C. Synaptic memories upside down: bidirectional plasticity at cerebellar parallel fiber-Purkinje cell synapses. *Neuron* **52**, 227-38 (2006).
36. Wang, Y.T. & Linden, D.J. Expression of cerebellar long-term depression requires postsynaptic clathrin-mediated endocytosis. *Neuron* **25**, 635-47 (2000).
37. Kano, M., Fukunaga, K. & Konnerth, A. Ca(2+)-induced rebound potentiation of gamma-aminobutyric acid-mediated currents requires activation of Ca2+/calmodulin-dependent kinase II. *Proc Natl Acad Sci U S A* **93**, 13351-6 (1996).
38. Mittmann, W. & Hausser, M. Linking synaptic plasticity and spike output at excitatory and inhibitory synapses onto cerebellar Purkinje cells. *J Neurosci* **27**, 5559-70 (2007).
39. Ekerot, C.F. & Jorntell, H. Parallel fibre receptive fields of Purkinje cells and interneurons are climbing fibre-specific. *Eur J Neurosci* **13**, 1303-10 (2001).
40. Jorntell, H. & Ekerot, C.F. Reciprocal bidirectional plasticity of parallel fiber receptive fields in cerebellar Purkinje cells and their afferent interneurons. *Neuron* **34**, 797-806 (2002).
41. Jorntell, H. & Ekerot, C.F. Receptive field plasticity profoundly alters the cutaneous parallel fiber synaptic input to cerebellar interneurons in vivo. *J Neurosci* **23**, 9620-31 (2003).
42. Markram, H., Lubke, J., Frotscher, M., Roth, A. & Sakmann, B. Physiology and anatomy of synaptic connections between thick tufted pyramidal neurones in the developing rat neocortex. *J Physiol* **500 (Pt 2)**, 409-40 (1997).
43. Hausser, M. et al. The beat goes on: spontaneous firing in mammalian neuronal microcircuits. *J Neurosci* **24**, 9215-9 (2004).
44. Raman, I.M. & Bean, B.P. Ionic currents underlying spontaneous action potentials in isolated cerebellar Purkinje neurons. *J Neurosci* **19**, 1663-74 (1999).
45. Gilbert, P.F. & Thach, W.T. Purkinje cell activity during motor learning. *Brain Res* **128**, 309-28 (1977).
46. Watanabe, E. Neuronal events correlated with long-term adaptation of the horizontal vestibulo-ocular reflex in the primate flocculus. *Brain Res* **297**, 169-74 (1984).
47. Eccles, J.C., Llinas, R. & Sasaki, K. Intracellularly recorded responses of the cerebellar Purkinje cells. *Exp Brain Res* **1**, 161-83 (1966).
48. Eccles, J., Llinas, R. & Sasaki, K. Excitation of Cerebellar Purkinje Cells by the Climbing Fibres. *Nature* **203**, 245-6 (1964).
49. Dittman, J.S. & Regehr, W.G. Calcium dependence and recovery kinetics of presynaptic

depression at the climbing fiber to Purkinje cell synapse. *J Neurosci* **18**, 6147-62 (1998).

50. Apps, R. & Garwicz, M. Anatomical and physiological foundations of cerebellar information processing. *Nat Rev Neurosci* **6**, 297-311 (2005).

51. Raman, I.M. & Bean, B.P. Resurgent sodium current and action potential formation in dissociated cerebellar Purkinje neurons. *J Neurosci* **17**, 4517-26 (1997).

52. Miyashita, Y. & Nagao, S. Analysis of signal content of Purkinje cell responses to optokinetic stimuli in the rabbit cerebellar flocculus by selective lesions of brainstem pathways. *Neurosci Res* **1**, 223-41 (1984).

53. Palkovits, M., Mezey, E., Hamori, J. & Szentagothai, J. Quantitative histological analysis of the cerebellar nuclei in the cat. I. Numerical data on cells and on synapses. *Exp Brain Res* **28**, 189-209 (1977).

54. Hoebeek, F.E. et al. Increased noise level of purkinje cell activities minimizes impact of their modulation during sensorimotor control. *Neuron* **45**, 953-65 (2005).

55. Bosman, L.W. et al. Encoding of whisker input by cerebellar Purkinje cells. *J Physiol* **588**, 3757-83.

56. De Zeeuw, C.I., Wylie, D.R., Stahl, J.S. & Simpson, J.I. Phase relations of Purkinje cells in the rabbit flocculus during compensatory eye movements. *J Neurophysiol* **74**, 2051-64 (1995).

57. Schonewille, M. et al. Zonal organization of the mouse flocculus: physiology, input, and output. *J Comp Neurol* **497**, 670-82 (2006).

58. Yakhnitsa, V. & Barmack, N.H. Antiphasic Purkinje cell responses in mouse uvula-nodulus are sensitive to static roll-tilt and topographically organized. *Neuroscience* **143**, 615-26 (2006).

SUMMARY/SAMENVATTING

Even though the cerebellum accounts for only 20 per cent of the overall brain mass it contains almost 70 percent of the neurons. This thesis focuses on one type of neurons present in the cerebellum, namely Purkinje cells. The mesmerizing morphology and enigmatic physiology of Purkinje cells makes them one of the most interesting cells in the central nervous system. Here we made an attempt to investigate how excitatory and inhibitory inputs influence Purkinje cell spiking activities and what is their relevance to motor performance and learning. We studied the role of afferent inputs to Purkinje cell using a wide variety of genetically engineered mice subjected to cellular physiology techniques and a number of behavioral tests. We focused our research questions mainly on floccular Purkinje cell activity and correlated the results with compensatory eye movements evoked by vestibular and/ or visual stimulation (Chapters 2.2, 3, 4.1 and 5) . We chose this paradigm due to the well documented involvement of the flocculus in the eye movements. To reliably quantify motor learning we studied one of the most pronounced and frequently studied forms of motor memory: vestibulo-ocular reflex (VOR) adaptation (Chapter 3, 4.1, 4.2 and 5).

We first focused on one of the most prominent excitatory input signal to cerebellar cortex, namely climbing fiber activity and corresponding Purkinje cell spiking responses (Chapter 2). In Chapter 2.1 we describe the importance of commissural connections in the inferior olive that enable the climbing fibers to cross the midline relaying inputs from the contralateral olive. Our results show that the disruption of the lateralization of the climbing fibers causes more profound impairments than having no cerebellar output at all. Chapter 2.2 gives a detailed description of the impact of the climbing fibers on pattern of Purkinje cell firing during optical stimulation. Data presented in this chapter argues for complex spike dominance in the reciprocity phenomenon proving that it is the climbing fiber input that drives reciprocity of Purkinje cell firing.

We then turn our interest to the other excitatory input to Purkinje cells – the parallel fibers (Chapter 3). Here we focused on the role of long term potentiation at the parallel fiber to Purkinje cell synapse (PF-LTP). By selectively removing the protein phosphatases 2B (PP2B) from the Purkinje cells we managed to block PF-LTP. The ablation of PP2B results in profound motor learning deficits and increased simple spike regularity. This finding challenges the long-standing theory about the importance of long term depression at the parallel fiber synapse (PF-LTD) since this mechanism is unaffected in our mutant mice.

Next, we explore a relatively neglected area in the cerebellar research, namely the role of the inhibitory input to Purkinje cells (Chapter 4.1). We investigated the impact of molecular layer interneurons (MLIs) on motor learning and Purkinje cell firing patterns using 2 different animal models, in which inhibition onto Purkinje cells was ablated. In both mutant mice (Chapter 4.1 and 4.2) we found severe deficits in long–term VOR adaptation suggesting that the molecular layer interneurons have a profound role in consolidation of motor learning. We also show that the lack of inhibitory input affects temporal patterns of Purkinje cell simple spike firing, increasing spiking regularity. Moreover, we found that Golgi cell inhibition of granule cells is important for consolidation of phase but not gain (Chapter 4.2).

Finally we investigated the impact of cerebellar learning on Purkinje spiking patterns (Chapter 5). We exposed mice to VOR phase reversal training and studied the firing behavior of Purkinje cells in the flocculus before and after application of the learning protocol. We show that application of long–term adaptation paradigm results in changes in the reciprocal relationship between complex and simple spikes in that the amplitude of the simple spike modulation is increased.

Overall, experiments presented in this thesis represent a considerable step towards understanding how excitatory and inhibitory pathways in cerebellar cortex influence Purkinje cell firing patterns and contribute to motor performance and learning. Ultimately our results could contribute to better understanding of the general cerebellar learning mechanisms and provide basis for future study of cerebellar circuitry and function.

Alhoewel de massa van het cerebellum maar 20 procent van het hele brein bedraagt, bevat het bijna 70 procent van alle neuronen. In dit proefschrift ligt de nadruk op één type neuron in het cerebellum: De Purkinje cel. De betoverende vorm en raadselachtige fysiologie maken de Purkinje cell tot één van de meest interessante cellen in het centrale zenuwstelsel. In dit proefschrift wordt onderzocht hoe excitatoire (stimulerende) en inhibitoire (remmende) invloeden op de Purkinje cel samenhangen met het vuurgedrag van de Purkinje cell en uiteindelijk met beweging en het leren van bewegingen. De rol van de input op de Purkinje cel is onderzocht met een reeks genetisch gemodificeerde muizen die onderworpen zijn aan cel-fysiologische metingen en een aantal gedragstesten. Ons onderzoek was vooral gericht op Purkinje cellen in de flocullus. De activiteit van deze cellen kan gecorreleerd worden met compensatoire oogbewegingen opgewekt met vestibulaire (evenwicht) en visuele stimuli (Hoofdstuk 2.2, 3.4, 4.1 en 5). Om betrouwbaar het leergedrag te kunnen quantificeren, hebben we één van de duidelijkste en meest bestudeerde vormen van motor geheugen bestudeerd: Vestibulo-oculaire reflex (VOR) adaptatie (Hoofdstuk 3, 4.1, 4.2 en 5).

Eerst hebben we ons gericht op klimvezel activiteit, een van de meest invloedrijke excitatoire signalen naar de cerebellaire cortex, en de reactie daarop van de Purkinje cel (Hoofdstuk 2). In hoofdstuk 2.1 beschrijven we het belang van verbindingen tussen de hersenhelften die er voor zorgen dat de klimvezels vanuit de onderste olijfkern de middenlijn kunnen oversteken en signalen kunnen afgeven aan de overliggende (contralaterale) cerebellaire schors. Onze resultaten laten zien dat het verstoren van deze verbinding, waardoor de klimvezels niet oversteken, een grotere verstoring van bewegingen teweegbrengen dan volledige afwezigheid van het cerebellum. Hoofstuk 2.2 geeft een gedetailleerde beschrijving van de impact van klimvezels op patronen van Purkinje cel vuurgedrag tijdens visuele stimulatie. De data in dit hoofdstuk pleiten voor een dominante rol van de klimvezel input in de reciproke relatie tussen complex spikes (van de klimvezel) en simpel spikes.

Hierna richten we onze aandacht op de andere excitatoire invloed op de Purkinje cel: De parallel vezels (Hoofdstuk 3). De nadruk in dit hoofdstuk ligt op de versterking van de synaps tussen de parallel vezel en de Purkinje cel (PF-LTP). Door het eiwit fosfatase 2B (PP2B) selectief uit de Purkinje cellen te verwijderen in een muis konden we PF-LTP blokkeren. Dit resulteerde in een ernstige verstoring van het leren van bewegingen en een toename in de regelmatigheid van simple spike activiteit in Purkinje cellen. Deze vinding trekt de klassieke theorie, dat het leren van bewegingen afhangt van het verzwakken van verbindingen tussen de parallel vezel en de Purkinje cel (PF-LTD), in twijfel aangezien dit mechanisme onaangeroerd is gebleven in onze mutante muizen.

Vervolgens hebben we gekeken naar een relatief verwaarloosd onderdeel binnen cerebellair onderzoek: de rol van inhibitoire invloed op de Purkinje cel (Hoofdstuk 4.1). De impact van moleculaire laag interneuronen (MLIs) op het leren van bewegingen en Purkinje cel vuurgedrag hebben we onderzocht door gebruik te maken van twee verschillende dier modellen waar de invloed van MLIs op Purkinje cellen is uitgeschakeld. In allebei de mutanten (Hoofdstuk 4.1 en 4.2) hebben we een ernstig defect geconstateerd in lange-termijn VOR adaptatie, wat suggereert dat de MLIs een belangrijke rol spelen in de consolidatie van het aangeleerde. We laten ook zien dat de Purkinje cellen regelmatiger vuren door de afwezigheid van inhibitie. Bovendien laten we zien dat de inhibitie van Golgi cellen op korrelcellen belangrijk is voor de opslag van de fase (tijdcomponent), maar niet van de amplitude (grootte) van de oogbeweging (Hoofdstuk 4.2).

Ten slotte hebben we de invloed van cerebellair leren op Purkinje cel vuurgedrag onderzocht (Hoofdstuk 5). We hebben Purkinje cel activiteit gemeten in de flocculus van muizen voor en nadat deze dieren waren blootgesteld aan VOR fase-omkeer training. We laten zien dat deze training veranderingen teweeg brengt in de reciproke relatie tussen simpel en complex spikes, waarbij de amplitude-variatie van simpel spike modulatie vergroot wordt tijdens training.

Uiteindelijk kunnen we met deze experimenten een goede stap voorwaarts zetten in ons begrip van hoe excitatoire en inhibitoire invloeden op de Purkinje cel bijdragen aan bewegingen en het leren van bewegingen. De hier gepresenteerde resultaten kunnen bijdragen aan een beter begrip van mechanismen van cerebellair leren en ze kunnen als basis dienen voor verdere studies naar de werking van het cerebellum en haar circuits.

Personal Information

Name :	Aleksandra Maria Badura
Date and place of birth:	14.11.1982, Piekary Śląskie, Poland

Education

2007 - present	Ph. D. Student at Erasmus MC in Rotterdam, The Netherlands.
2001 - 2006	Master degree in Applied Psychology, Jagiellonian University, Poland.
1997 - 2001	High School in Bytom, Poland.

Experience in research

2007 - present	Ph. D. Student at Erasmus MC in Rotterdam. Promotor Prof. Dr. C.I. De Zeeuw. Field: Cerebellar research.
July - November 2006	Junior Researcher position in NICI at Radboud University in Nijmegen. Epilepsy research studies in Wag/rij rats. Coordinator: Dr. C.M. van Rijn.
January - Mai 2006	Student Assistant position in NICI at Radboud University in Nijmegen. Epilepsy research studies in Wag/rij rats. Coordinator: Dr. E.L.J.M. van Luijtelaar.
October - December 2005	Sleep-wake research at Radboud University in Nijmegen (Biological Psychology Department NICI). Research performed under supervision of Prof. A.M.L. Coenen.

Additional Information

Dutch animal experimentation certificate (Artikel 9); Chair of Jump The FENS Committe (Student Party during 7th FENS Forum for European Neuroscience)

List of Publications

Badura A, Martijn Schonewille M, Gao Z, Galliano E, Nicolas Renier N, Voges K, Hoebeek FE, Alain Chédotal A, and Chris I. De ZeeuwC.I. *Climbing Fiber drives reciprocity of Purkinje cell firing.* Submitted

Seja P, Schonewille M, Spitzmaul G, **Badura A**, Klei I, Wisden B, Christian A. Hübner C.A., Chris I. De Zeeuw C.I., Jentsch T.J. *Raising Cl^- concentration in cerebellar granule cells affects their excitability and consolidation of vestibulo-ocular phase learning.* In preparation

Badura A, Schonewille M, Voges K., De Zeeuw CI. *Changes in the modulation of Simple Spike responses after motor training.* In preparation

Schonewille M, Belmeguenai A, Koekkoek SK, Houtman SH, Boele HJ, van Beugen BJ, Gao Z, **Badura A**, Ohtsuki G, Amerika WE, Hosy E, Hoebeek FE, Elgersma Y, Hansel C, De Zeeuw CI. *Purkinje cell-specific knockout of the protein phosphatase PP2B impairs potentiation and cerebellar motor learning.* Neuron. 2010 Aug 26;67(4):618-28.

Renier N, Schonewille M, Giraudet F, **Badura A**, Tessier-Lavigne M, Avan P, De Zeeuw CI, Chédotal A. *Genetic dissection of the function of hindbrain axonal commissures.* PLoS Biol. 2010 Mar 9;8(3):e1000325.

Van Rijn CM, Gaetani S, Santolini I, **Badura A**, Gabova A, Fu J, Watanabe M, Cuomo V, van Luijtelaar G, Nicoletti F, Ngomba RT. *WAG/Rij rats show a reduced expression of CB receptors in thalamic nuclei and respond to the CB receptor agonist, R(+)WIN55,212-2, with a reduced incidence of spike-wave discharges.* Epilepsia. 2010 Feb 3

Wulff P, Schonewille M, Renzi M, Viltono L, Sassoè-Pognetto M, **Badura A**, Gao Z, Hoebeek FE, van Dorp S, Wisden W, Farrant M, De Zeeuw CI. *Synaptic inhibition of Purkinje cells mediates consolidation of vestibulo-cerebellar motor learning.* Nat Neurosci. 2009 Aug;12(8):1042-9.

Ngomba RT, Ferraguti F, **Badura A**, Citraro R, Santolini I, Battaglia G, Bruno V, De Sarro G, Simonyi A, van Luijtelaar G, Nicoletti F. *Positive allosteric modulation of metabotropic glutamate 4 (mGlu4) receptors enhances spontaneous and evoked absence seizures.* Neuropharmacology. 2008 Feb;54(2):344-54.

General courses

2008	Biomedical English Writing and Communication, Rotterdam, The Netherlands
2007	Linear Control Systems in the Oculomotor System, Rotterdam , The Netherlands
2006	Dutch animal experimentation certificate (Artikel 9 cursus), Nijmegen, The Netherlands

Scientific Meetings

2010	40th Society for neuroscience Annual Meeting, San Diego, USA (poster presentation)
2010	7th FENS Forum of European Neuroscience, Geneva, Switzerland (poster presentation)
2009	39th Society for neuroscience Annual Meeting, Chicago, USA
2008	6th FENS Forum of European Neuroscience, Geneva, Switzerland (poster presentation)
2008	15th Annual ONWAR PhD meeting, Zeist, The Netherlands (poster presentation)
2007	Retraite of the Helmholtz Institute, Bergen, the Netherlands (oral presentation)

Teaching and Organizational skills

2007- 2010	Teaching assistant, eye and ear anatomy course for medical students
2010	Chair of Jump The FENS Committee (Student Party Committee during 7th FENS Forum for European Neuroscience)

Writing a PhD thesis should be considered an extreme sport. It requires physical and mental skills to cope with sleep deprivation, frustration that comes with failed experiments and rejected manuscripts and social alienation due to constant lack of free time. However it also gives one the opportunity to experience the rush of adrenaline and feeling of accomplishment with every successful project and a chance to meet amazing, driven people who chose the same carrier path. There is also one more thing that a PhD student has in common with sportsmen – publishing your booklet, just like crossing the finish line means that there has been the whole team of people working alongside for your success. Here, I would like to thank people, who made this booklet a reality for their help and support as well as making the past couple of years an unforgettable journey.

First, I would like to thank my promotor Prof. dr Chris I. De Zeeuw. Dear Chris, you changed my life path when you accepted me as an AIO. Your energy and passion for neuroscience have given me the motivation to do my job. Thank you for always encouraging me to search for the answers and be a better scientist. You have been a great advisor and mentor and this PhD thesis could never have been written without your help. I am also very grateful for your friendship and I am sure that this thesis will not be the end of our cooperation.

I would like to thank my co-promotor Martijn who taught me everything I know about electrophysiology. Thank you for taking time to guide me during the experiments and for your help in writing this thesis. It was a privilege to be your paranimf and now to have you in my thesis committee. I will miss our scientific and non-scientific discussions – especially now since the "Schonewille lab" got a new coffee machine ☺

Next to my two advisors I would like to thank the rest of my thesis committee for agreeing to participate in my promotion and for spending time on reading my thesis: Tom, for your valuable comments, advice and anatomical expertise I'd like to thank you. I will always remember the number of synaptic contacts at the climbing fiber to Purkinje cell synapse; Maarten for always being ready to discuss scientific and non-scientific issues, thank you for trusting me in organizing a party for 2500 people – it was great to be part of something as big as the FENS meeting; Steven, for kindly agreeing to review my work; Gerard, for your comments and questions, which always motivated me to give my best at any presentation at the department; Jerry, for your discussions, difficult questions and your friendship; Alain, for our fruitful collaboration.

I would also like to thank people who have been so important for my scientific carrier prior to my time at the Neuroscience Department in Rotterdam. To the supervisor of my master thesis, Prof. dr Ryszard Przewlocki, you opened my eyes to science and helped me to make one of my biggest dreams come true: to go abroad to do research. You got me in touch with Prof. dr Ton Coenen at the Radboud University in Nijmegen who agreed to supervise the research for my master thesis. Dear Ton, thank you for all your kindness and patience in explaining the basis of electrophysiology to such a rooky as I was. Thanks to your help I was not only able to conduct the experiments for my master thesis but also to extend my stay in Netherlands to conduct studies on rats with absence epilepsy. Gilles and Tineke – I have learned so much from both of you. It was while I was involved in our studies on epilepsy that I realized that this is exactly what I would like to do for a living. Thank you for all the time

we spent together in and outside of the lab I am very proud that my work contributed to 2 beautiful publications. Here I would also like to thank my Radboud colleagues and friends: Saskia, Hans, Pascal, Irina, Richard, Jeroen, Matthias, Rebecca – you made my stay in Nijmegen so enjoyable it was hard for me to leave!

I am very lucky to have two of my good friends as my paranimfs: Paolo, you are a great companion inside and outside of the lab. Thank you for your help – without you there would be no party! Lau, my dear friend, your friendship is invaluable to me. After all you're one of a few people who laughs at my 11th "stelling". I wish both of my paranimfs lots of luck with finishing their PhDs!

There are many people at the department that I would like to thank. Let me start with Erika and Elize - your guidance and expertise in the histology lab was essential to my PhD education. Special "thank you" goes to Elize for all the hours spent at the EM, our chitchats and movie nights. Dear Hans, thank you for all technical support and above all for the great atmosphere you bring into the lab. You were always ready to help me with my little "setup dramas" (even though I'm Polish, not Italian ☺).

I would like to thank my roommates from lab Ee1257. Kai, I am very happy that you joined our group last year. My "Matlab master" – thank you for all work discussion, data analysis and also for all the fun we had outside of the lab. Esther, you're a stabilizing factor in our room – always friendly and quiet ☺ Rogerio, my "gekke amigo", with you in the lab it could never get boring! Thank you for the joy and excitement you bring to work, but moreover for being my friend. I could not forget about my ex-roommates – two fantastic Italian girls: Tiziana and Claudia. I miss both of you!

Only writing this acknowledgements did I realize how big Chris's group really is. All of the members deserve a big "thank you" on my behalf and here I would like personally thank some of them: Freek, for the scientific input you gave me in the lab and all the drinks we had at the conferences; Gao, for our discussions and help with the *PTF1a* project. Good luck with your defense!; Elisa, for the work on the *PTF1a* project, conversations, understanding and delicious snacks ☺; Mandy and Petra, for your the help with genotyping and our great chitchat/gossip times; Bas, for always being ready to help me with my laptop problems and for your cheerful attitude and friendliness; Henk Jan, for great times at the conferences, I could always count on you to hit the dance floor with me!; Cullen, thanks for proof reading my thesis and taking care of my cat while I was away; Marcel (de Jeu), for the scientific input and our totally non-scientific discussions and Sheena, for your great company at many lunches. Here, I would also like to say "thank you" to the NIN team – Stijn, Beerend and Jornt, thank you and see you guys in July!

Among other current and ex members of the Neuroscience Department I would like to personally thank: Casper and Ype, for your input during my oral presentations, I have always valued your opinions; members of the "Casper's lab" for all the fun we've had and all the beers we shared in the past years. Myrrhe, Phebe, Nanda, Marijn, Kah Wai, Esther and Bjorn (who in my head will forever stay a part of your lab) – I could always count on you to join me for "one more drink" after our Friday borrels. Special "thanks" goes to Max for the jokes, great discussions and teaching me that even a scientist should NOT try to prove all her theories experimentally ☺; Dick for the fun we had while teaching medical students; Vera,

for the great times inside and outside of the lab; Ru, for the beers, dinners, funny and serious conversations and above all for the "arrrrrrr" moments; John for all philosophical discussion; Tom, for being merciful to my tonsils; Marcela, for sharing a room with me in Chicago and the fun we had there; Jos and Stefan for our conversations; Thijs, Caroline, Susan, Jaga, Nils and Stathis for the great times we had and all the beers we drank; Minetta and Laura, for your help with managing my mice colony; Joel, for giving me an opportunity to speak polish from time to time and making me smile; Aram for the trips to Ikea and swimming pool and finally to Alexander (and Mieke) for your friendship and quality time we spend in the lab/ski resorts/beach/bars ☺.

A big "thank you" to Kenneth and Annette for your cheerfulness and help with taking care of financial issues. Dear Edith, Loes and Suzan, thank you for taking care of the bureaucratical side of a PhD defense (special thanks to Edith for the delicious cookies!).

A very special thanks goes to some very special ladies. Sara, Jeannete, Eva, MJ and Samantha - I feel so grateful for getting to know each one of you and developing this beautiful friendship that we have. My sweet Sara, you showed me that the heart of an Iranian girl beats in the same rhythm as a Polish one. Jeannette, you taught me how to combine research with passions and hobbies. Eva, thank you for always remembering to call and ask how things are going with me. MJ, you've known me the longest and been with me throughout all my ups and downs – I am so happy we both found what we've been looking for. Samantha, I will always remember the trips we made (including the last crazy road trip in California!), the parties we went to and the tequila shots we drank but most of all your patience and commitment in wiping all my tears throughout the years. Ladies – thank you for the parties, late-night phone calls, trips and dinners. You will always have a special place in my heart. Big hugs and kisses to all of you!

To my "polish gang" – thank you for making my life so much more entertaining! Madzia, Staska, Piter, Jola – all of my old roommates, you have been with me through good and rough periods. Thank you for making life abroad so much easier and happier. Alicja, Meg, our trip to Copenhagen was unforgettable – we have to repeat that! Za wszystkie imprezy, nocnych polakow rozmowy i za to, ze jestecie ludzmi z ktorymi mozna "konie krasc" Dziekuje!!

Most importantly I would like to thank my parents for their patience, support and unconditional love. Kochani rodzice, to wam dedykuje moja prace doktorska. Dziekuje wam za to, ze zawsze wspieraliscie mnie, nawet jesli szlo to w parze z nasza rozlaka. Kocham was i mam nadzieje ze jestescie ze mnie dumni.

And "last but not least" I'd like to thank a person who can always bring a smile to my face, who always is there for me and who kept me from going totally nuts during this last couple of months of my PhD. Daan, you are the most important person in my life and I simply can't find words to express how happy you have made me. I want you to know that no matter where we'll end up – you will always come first.